PERFORMANCE ANALYSIS OF COGNITIVE RELAY NETWORKS USING SPECTRAL- AND ENERGY-EFFICIENT SCHEMES

Ph.D. Thesis

by

SOURABH SOLANKI

DISCIPLINE OF ELECTRICAL ENGINEERING

INDIAN INSTITUTE OF TECHNOLOGY INDORE

FEBRUARY 2019

PERFORMANCE ANALYSIS OF COGNITIVE RELAY NETWORKS USING SPECTRAL- AND ENERGY-EFFICIENT SCHEMES

A THESIS

Submitted in partial fulfillment of the

requirements for the award of the degree

of

DOCTOR OF PHILOSOPHY

by

SOURABH SOLANKI

DISCIPLINE OF ELECTRICAL ENGINEERING

INDIAN INSTITUTE OF TECHNOLOGY INDORE

FEBRUARY 2019

INDIAN INSTITUTE OF TECHNOLOGY INDORE

CANDIDATE'S DECLARATION

I hereby certify that the work which is being presented in the thesis entitled "**PERFORMANCE ANALYSIS OF COGNITIVE RELAY NETWORKS USING SPECTRAL- AND ENERGY-EFFICIENT SCHEMES**" in the partial fulfillment of the requirements for the award of the degree of DOCTOR OF PHILOSOPHY and submitted in the DISCIPLINE OF ELECTRICAL ENGINEERING, Indian Institute of Technology Indore, is an authentic record of my own work carried out during the time period from July 2015 to January 2019 under the supervision of Dr. Prabhat Kumar Upadhyay, Associate Professor, Indian Institute of Technology Indore, India.

The matter presented in this thesis has not been submitted by me for the award of any other degree of this or any other institute.

Signature of the student with date
(SOURABH SOLANKI)

This is to certify that the above statement made by the candidate is correct to the best of my knowledge.

Signature of Thesis Supervisor with date
(Dr. PRABHAT KUMAR UPADHYAY)

Sourabh Solanki has successfully given his Ph.D. Oral Examination held on ....

Signature of Chairperson (OEB) Date:	Signature of External Examiner Date:	Signature of Thesis Supervisor Date:
Signature of PSPC Member #1 Date:	Signature of PSPC Member #2 Date:	Signature of Convener, DPGC Date:

Signature of Head of Discipline
Date:

ACKNOWLEDGEMENTS

I take this opportunity to acknowledge my heartfelt gratitude to all those who have directly or indirectly helped me throughout my PhD. First and foremost, I thank God Almighty for giving me the strength, knowledge, and enlightenment to undertake this research work. Then, I would like to express my deep sense of respect and gratitude to my supervisor and mentor, Dr Prabhat Kumar Upadhyay, for his invaluable guidance, sustained inspiration, and kind support towards my thesis work. He has given me all the freedom to pursue my research, and provided helpful career advice and suggestions, extending beyond academic boundaries, whenever needed. He has always been my source of inspiration during my stay at IIT Indore and will be, all my life.

Next, I would like to sincerely thank my comprehensive evaluation of research progress committee members Dr Amod C. Umarikar and Dr Santosh K. Sahu for their interesting discussions and suggestions towards my research. I am thankful to all the faculty members and the staffs at IIT Indore for their cooperation throughout my thesis work.

My appreciation also goes to all the members of the Wireless Communications Research Group (WiCom) for creating a friendly and conducive environment. It was my privilege to share the lab with Vinay Bankey, Vibhum Singh, and Chandan Kumar Singh. I am immensely grateful to my seniors Dr Pankaj K Sharma, Dr Devendra S. Gurjar for providing their help and valuable suggestions both technically and non-technically during my work. I am extremely thankful to Dr Amit K. Jain, Dr Sandeep Kumar, and Shishir Maheshwari for making a wonderful company and for sharing all the casual and valued moments which helped me during the hardship of this work. Special thanks go to my friends Sheetal Dole and Pankaj Rathore for all the cheerful talks and encouragement, and also for their caring nature. I am also thankful to my ex-roommates Satyartha Sharma and Kapil Swarnakar and to my juniors Ashwini Tiwari and Anish K. Singh for being great friends and for sharing the magic moments of my life at IIT Indore.

I would like to thank the Ministry of Human Resource Development (MHRD), Government of India and IIT Indore for providing financial assistance. I would also to thank Science & Engineering Research Board (SERB), Department of Science and Technology (DST), Government of India for providing me with the international travel support for attending the overseas conference. I will also thank the finance, administration, academic, and R&D sections for all the necessary support.

Above all, the most valued gratitude is expressed for my mother, Usha Solanki, my father, Karan Singh Solanki, my brother, Surendra Singh Solanki, and my sweet sister, Priyanka, for their unbounded love, endless support, and faith in me, without which I would have not been able to achieve the greatest milestone of my life.

Lastly, I want to thank everyone who were part of this journey and has, in one way or another, helped me to successfully complete this research work.

Sourabh Solanki

Dedicated to
my family

ABSTRACT

Over the past few years, the wireless communication technologies have witnessed the rapid evolution to enrich the quality of our day-to-day life. This evolution may eventually necessitates the efficient utilization of limited spectral resources. In this regard, cognitive radio technology has received tremendous research interest owing to its capability for improving spectrum utilization efficiency in wireless networks. This dynamic spectrum access technology enables the unlicensed secondary users (SUs) to share the licensed spectrum of primary users (PUs) under certain constraints. With such quality-of-service restrictions from the PUs, it becomes challenging to improve the performance of SUs. For this, cooperative relaying techniques have been integrated with the cognitive radio technology to improve the overall system performance and reliability. Another important aspect of the future networks is energy efficiency. On that front, the energy harvesting (EH) techniques have been suggested for the design of energy-efficient wireless systems. To address the design objectives of the future networks, this thesis comprehensively analyzes the performance of relay-aided cognitive radio networks, referred to as cognitive relay networks (CRNs), by exploring various spectral- and energy-efficient schemes.

Firstly, we consider a resource sharing CRN (RSCRN) with two-way PUs' communication. In this analytical system design, besides assisting the transmission of SUs, the relay also provides an aid for the bi-directional PUs' transmission. To further enhance the performance of SUs, the secondary system employs an opportunistic user scheduling with multiple destinations. For the performance assessment of this system, we derive novel closed-form expressions of outage and average error probabilities considering Nakagami-m fading channels. Our results illustrate that, leveraging two-way relaying for primary transmissions, the proposed RSCRN offers higher spectral efficiency. Moreover, by exploiting inherent multiuser diversity, reliability of SUs' communication can be significantly improved. We further investigate the performance of an underlay two-way CRN (TWCRN) with direct link in the presence of PU's interference. Hereby, we propose an adaptive link utilization scheme (ALUS) that can exploit both direct and relay links with appropriate diversity combining methods to improve the performance of SUs. For this system, we derive tight closed-form expressions for the outage probability of secondary communications for two different relaying strategies viz., fixed relaying and incremental

relaying. We also conduct asymptotic analysis to examine the diversity order of the considered system. Our results reveal that the full diversity for secondary system can be achieved as long as the primary interference remains limited, otherwise the performance remarkably deteriorates.

Next, we analyze the performance of cognitive multi-relay network (CMRN) in the presence of hardware and channel imperfections under different operating conditions. Herein, we consider the hardware impairments (HIs) invoked by the non-ideal secondary transceivers and residual interference originating from channel estimation errors (CEEs). From our analysis, we find that the detrimental impact of HIs can potentially cap the fundamental capacity of the system for the high-rate applications. We also observe that, due to CEEs, the system could not exploit the diversity, resulting in irreducible outage floors. Based on our investigations, we provide useful insights into the tolerable level of HIs for designing the practical systems. We also compare the robustness of two classical relaying schemes, i.e., amplify-and-forward and decode-and-forward, for the considered CMRN against HIs.

To improve the energy efficiency of cognitive radio networks, we employ a radio-frequency based EH technique in CRNs. Specifically, we consider a non-linear EH-based overlay CRN (EHCRN) where an energy-constrained secondary node acts as a cooperative relay to assist the transmission of PU. In return for the benign cooperation, the secondary node enjoys access to the PU's spectrum for its own information transfer. For this overall setup, we investigate the system performance by deriving the expressions for outage probability of the primary and secondary networks over Rayleigh fading channels. Further, we attempt to harness the combined advantages of multiuser diversity and cooperative diversity to improve the performance of primary network. Thereafter, we propose an improved EH-based relaying scheme which is shown to substantially enhance the performance of considered EHCRN.

Above all, this thesis addresses various technical aspects and challenges for realization of CRNs and eventually provides useful insights into the practical system design. All the theoretical developments, proposed schemes, and strategies hereunder are primarily aimed at improving the spectral efficiency, energy efficiency, and reliability of the CRNs for their possible applications in the future networks.

CONTENTS

LIST OF FIGURES

List of Symbols

- Basic arithmetic and calculus notations have standard definitions.

Elementary & Special Functions

Notation	Definition
$\Gamma(x)$	Gamma function
$\Upsilon(x, y)$	lower incomplete Gamma function
$\Gamma(x, y)$	upper incomplete Gamma function
$\mathcal{K}_{\upsilon}(x)$	modified Bessel function of the second kind of order υ
$G^{m,n}_{p,q}\left[\cdot\middle\vert\begin{smallmatrix}\cdot\\\cdot\end{smallmatrix}\right]$	Meijer's G-function
$\mathcal{W}_{u,v}(\cdot)$	Whittaker function
$\log_i(\cdot)$	logarithm to base i

Probability & Statistics

Let X be a random variable, and $\mathcal{A}$ be an arbitrary event.

Notation	Definition
$\mathbb{E}(\cdot)$	expectation
$f_X(\cdot)$	probability density function (PDF) of X
$F_X(\cdot)$	cumulative distribution function (CDF) of X
$\Pr[\mathcal{A}]$	probability of $\mathcal{A}$
$X \sim \mathcal{CN}(\mu, \sigma^2)$	X is complex normal distributed with mean μ and variance σ^2

Miscellaneous

Notation	Definition
$\lvert \cdot \rvert$	absolute value
$\triangleq$	equality by definition
$n!$	factorial of n
$\mathcal{C}^n_r = \binom{n}{r} = \frac{n!}{r!(n-r)!}$	binomial coefficient
$\arg\max\limits_i b_i$	index i corresponding to the largest b_i
$\arg\min\limits_i b_i$	index i corresponding to the smallest b_i
$\min(b_1, b_2)$	minimum of scalars b_1 and b_2
$\max(b_1, b_2)$	maximum of scalars b_1 and b_2

List of Abbreviations

5G	Fifth-Generation
AF	Amplify-and-Forward
ANC	Analog Network Coding
AWGN	Additive White Gaussian Noise
CDF	Cumulative Distribution Function
CSI	Channel State Information
CEE	Channel Estimation Error
CRN	Cognitive Relay Network
DF	Decode-and-Forward
EH	Energy Harvesting
EVM	Error Vector Magnitude
HIs	Hardware Impairments
i.i.d	Independent and Identically Distributed
i.ni.d	Independent and Non-Identically Distributed
IoT	Internet-of-Things
IP	Information Processing
IQ	In-Quadrature-Phase
LTE	Long Term Evolution
MABC	Multiple Access Broadcast
MIMO	Multiple-Input Multiple-Output
MMSE	Minimum Mean Square Error
MRC	Maximal Ratio Combining
OWR	One-Way Relaying
PDF	Probability Density Function
PS	Power-Splitting
PU	Primary User
QoS	Quality-of-Service
RF	Radio-Frequency
SC	Selection Combining
SINR	Signal-to-Interference-Plus-Noise Ratio
SNR	Signal-to-Noise Ratio
SNDR	Signal-to-Noise-and-Distortion Ratio
SU	Secondary User

SWIPT	Simultaneous Wireless Information and Power Transfer
TDBC	Time Division Broadcast
TRAI	Telecom Regulatory Authority of India
TS	Time-Switching
TWR	Two-Way Relaying

CHAPTER 1

INTRODUCTION

We have been witnessing the escalating growth in the mobile data traffic since last decade. And this ever increasing traffic presumably grows 1000-fold by the year 2020. Such proliferation may eventually necessitates the efficient utilization of scarce spectrum resources for the fifth-generation (5G) and beyond wireless networks. Moreover, with the evolution of a large number of new applications, the demand for spectrum is expected to rise even more in the forthcoming years. Owing to the limited availability of radio spectrum and its rising demands, accommodating new applications and users in the radio spectrum has become a challenging task for regulatory bodies (Telecom Regulatory Authority of India (TRAI) in India). These problems are not just because of increasing demands for the spectrum, but also because of its inefficient utilization [1]. In fact, when spectrum is allocated to users for different applications, it has been observed that a larger portion of the assigned spectrum is used irregularly, i.e., some frequency bands in the spectrum are unused[1] most of the time, some other frequency bands are occupied partially, and the other remaining bands are used heavily. To counteract this problem, cognitive radio technology has received tremendous research interest owing to its capability for improving spectrum utilization efficiency in wireless networks [2]. This dynamic spectrum access technology enables the unlicensed users, also called secondary users (SUs), to share the spectrum licensed to primary users (PUs) as long as the quality of service (QoS) requirements of PUs are not compromised.

In addition to the inefficient spectrum utilization problem, the inherited fading in the wireless channel limits the service reliability and coverage of the wireless ap-

[1]The unused band at a particular time and specific geographic location is termed as spectrum hole or white space.

plications. Therefore, it is difficult for the traditional point-to-point communication system to ensure reliable transmission, wide coverage, and high throughput. To overcome this problem, cooperative relaying [3] has been proposed as a potential paradigm to mitigate the effects of fading.

On the other hand, due to exploding mobile traffic, the energy consumption of the wireless networks is also rising. Due to increase in energy consumption, the emission of green house gases also increases. Currently, the information and communication technologies account for around 2-4% of the carbon footprint generated by human activity. This trend is speculated to increase further in the forthcoming years. One of the ways to reduce the power consumption is to efficiently use the available energy resources. As such, the energy efficiency is one of the key aspects to be considered for the deployment of future networks. Recently, energy harvesting (EH) technologies have been emerged as a viable solution to improve the energy efficiency of wireless networks and to increase the lifetime of network nodes. Energising the network nodes via EH techniques has been regarded feasible, thanks to the low-power requirements of electronics and smart devices. Moreover, the number of interconnected low-power wireless devices is expected to rise many-fold by 2020 owing to the roll-out of Internet-of-Things (IoT). Thus, powering these low-power devices through EH techniques will drastically improve the energy efficiency of wireless networks.

To realize the spectral- and energy-efficient design of wireless networks, we focus on three key-enabling technologies which are briefly described as follows:

1.1 Cognitive Radio

To counteract the spectrum under-utilization problem, cognitive radio technology was introduced by Mitola [4]. This dynamic spectrum access technique allows the SUs to share the spectrum licensed to PUs, while ensuring the QoS requirements of PUs. In a cognitive radio network, the access to the licensed spectrum can be provided by using three main paradigms, i.e., underlay, overlay, and interweave [5].

Underlay Approach: In underlay approach, cognitive or SUs use the radio spectrum simultaneously with the PUs. Hereby, the SUs are allowed to share the spectrum resources under strict interference constraints (also called interference temperature limit) from the primary receiver. Underlay approach enjoys the flexibility for the transmission at all time and is not necessarily be synchronized with the PUs. However, the SUs need to obtain the channel state information (CSI) of the pertaining links towards PUs for controlling their transmission power. Owing to the constrained power at SUs, in this paradigm, improving the performance of SUs is critical and challenging.

Overlay Approach: In overlay approach, both PUs and SUs simultaneously share the spectrum while improving or maintaining the transmission of the PUs by using sophisticated and appropriate methods of cooperative communication, signal processing and coding. For instance, spectrum sharing can be facilitated by incentivizing PUs through the cooperation of SUs.

Interweave Approach: In this approach, SUs opportunistically utilize the white spaces of spectrum for transmission without causing any interference to the PUs communication. The major disadvantage of this approach is that the SUs are required to sense the spectrum hole before transmission and, therefore, is highly sensitive to the primary traffic behavior and spectrum sensing errors. This approach may not be suitable for the dense networks due to the lack of availability of spectrum holes.

For applying the cognitive radio techniques, IEEE 802.22 standard [6] has been developed for wireless regional area networks using white spaces in TV spectrum. In addition to IEEE 802.22, standard IEEE 802.11af [7] has also been introduced to allow wireless local area network operation in TV white spaces.

1.2 Cooperative Relaying

Cooperative relaying has been regarded as an effective approach to combat the effect of multi-path fading in wireless communications. It can be broadly classified into two categories, viz., fixed relaying and adaptive relaying.

1.2.1 Fixed Relaying

In this, the channel resources are distributed between source and relay in a fixed manner. Such protocols are easy to implement but they have drawback of low bandwidth efficiency. Fixed relaying includes commonly adopted amplify-and-forward (AF) and decode-and-forward (DF) protocols.

Amplify-and-Forward Relaying: In AF relaying protocol, the relay simply amplifies the signal received from its source and transmits it further to the destination. Here, amplification is done essentially to combat the effect of the fading between the source and relay channel. In this process, the noise at the relay also get amplified by the relay, which is main drawback of this protocol. However, reduced hardware complexity is advantageous over its DF counterpart.

Decode-and-Forward Relaying: DF relaying is also known as regenerative relaying. In DF relaying protocol, relay decodes the signal received from its source, then re-encodes it and transmits to the destination. While doing this, there is a possibility that relay decodes the signal incorrectly and forwards it, resulting in an error propagation. In such case, the decoding at the relay becomes meaningless. Error correction codes are one way to reduce error in the decoded signals. Another solution to the problem is adaptive relaying.

1.2.2 Adaptive Relaying

Adaptive relaying includes an incremental relaying protocol which relies upon the limited feedback from the destination terminal. In this, the cooperation from the relay is invoked only when the direct transmission fails. And, once the cooperation is triggered, its operation becomes similar to the fixed relaying. Hereby, firstly, the source node transmits its information to the destination as well as to the relay node. Then, depending on the quality of the received direct link signal, receiver node decides whether relaying transmission is required or not by sending a single-bit feedback to the relay. If the source-destination signal-to-noise ratio (SNR) is sufficiently high, the feedback indicates success of the direct transmission, and the relay does nothing. Whereas, when it is not, then the feedback requests that the relay forwards the received signal from the source. Adaptive relaying is found to be more spectral-efficient compared to fixed relaying.

Depending on the data flow direction, relaying operation can be further categorized into one-way relaying and two-way relaying.

1.2.3 One-Way Relaying

Fig. 1.1 presents a basic one-way relaying scheme wherein the information transmission from S_1 to S_2 is accomplished using the cooperation from a relay node R. Hereby, the information transfer takes place in two orthogonal transmission phases owing to the half-duplex operation of the nodes. Specifically, in first phase, S_1 transmits its information to S_2 and R. In second phase, relay forwards the received information to S_2 by employing any relaying protocol as discussed in Section 1.2.

As the information flow from S_1 to S_2 requires two time phases, the bi-directional information exchange between S_1 and S_2 would need four time phases which makes one-way relaying relatively less spectral-efficient compared with two-way relaying. Cooperative one-way relaying networks have already been adopted in modern wireless standards such as LTE and WiMAX (IEEE 802.16j [8], [9] and IEEE 802.16e [10]).

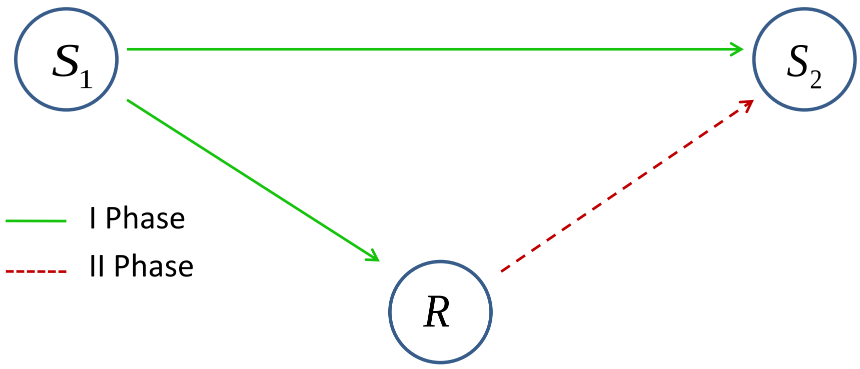

Figure 1.1: One-way relaying.

1.2.4 Two-Way Relaying

Two-way relaying protocol utilizes either two or three time phases for the bi-directional information exchange. There are two major protocols for two-way relaying, namely two-phase multiple access broadcast (MABC) [11] and three-phase time division broadcast (TDBC) [12]. In MABC protocol, as shown in Fig. 1.2, nodes S_1 and S_2 communicate bi-directionally using a relay R in two successive time phases, namely multiple access (MAC) and broadcast (BC). Note that, in MABC protocol, it is

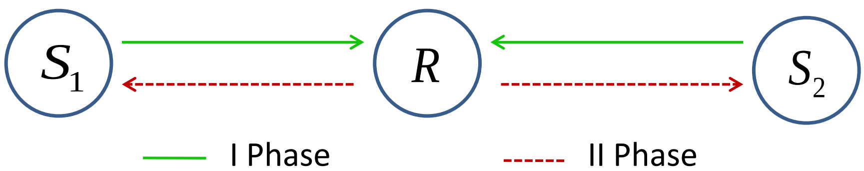

Figure 1.2: MABC protocol.

not possible to exploit the available potential direct link due to half-duplex nature of nodes. Therefore, MABC protocol poses critical concerns for the reliability and performance of bi-directional systems. To exploit the available direct link, another two-way relaying protocol called TDBC has been introduced. As shown in Fig. 1.3, in TDBC protocol, the bi-directional information exchange takes place in three-time phases.

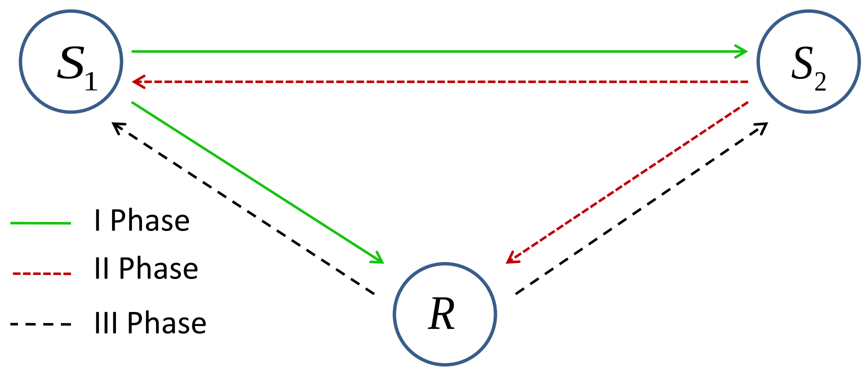

Figure 1.3: TDBC protocol.

1.3 Radio-Frequency Energy Harvesting

Over the past few years, EH has emerged as a promising technology for the design of energy-efficient systems. To this end, the simultaneous wireless information and

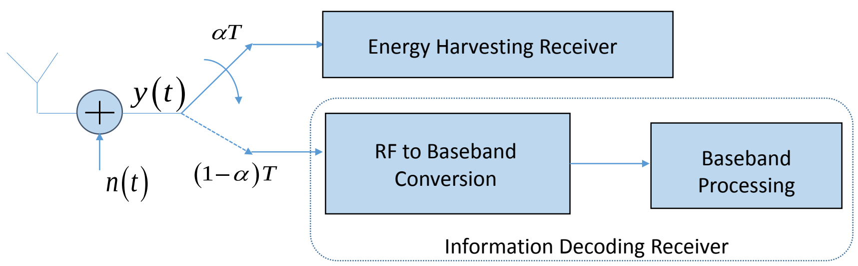

Figure 1.4: TS-based receiver architecture.

power transfer (SWIPT) scheme has been regarded as an effective approach to scavenge the energy from the ambient radio-frequency (RF) signals [13]. The SWIPT scheme is based on the fact that energy and information can be simultaneously carried through RF signals. In this, the EH node gathers the transmitted energy (RF radiation) and stores it in a battery by converting it into the direct current (DC) using appropriate circuitry. However, it is difficult for a receiver to concurrently process the information and harvest energy from the received RF signals. For this, two practical receiver architectures viz., time-switching (TS) and power-splitting (PS), have been introduced. In the TS-based receiver architecture, time is switched between information processing (IP) and EH. While in the PS-based architecture, a part of the received power is used for the EH and the remaining one for the IP.

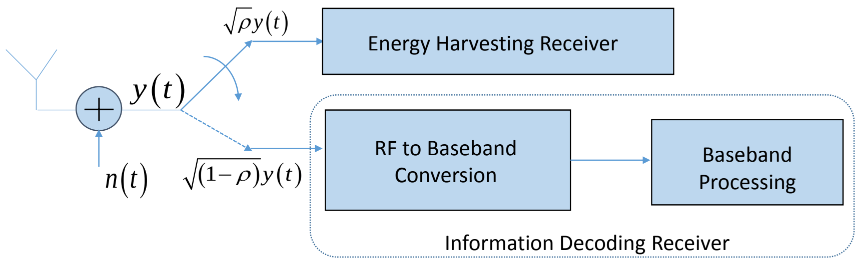

Figure 1.5: PS-based receiver architecture.

1.4 Motivation and Objectives

In this section, we present the motivation and objectives behind the research work in this thesis.

1.4.1 Motivation

Spectral efficiency and energy efficiency are two important design objectives for future wireless networks, i.e., 5G and beyond [14]. To improve the spectral efficiency, cognitive radio is a promising technology which can eliminate the spectrum underutilization problem. However, in the cognitive radio networks, SUs are allowed to transmit under the various constraints which eventually limits their performance. In addition, the interference from the transmissions of PUs is also detrimental for the performance of SUs. As a consequence, enhancing the performance of SUs becomes critical and challenging. In this direction, several efforts have been made in the existing literature to improvise the performance of SUs. Among others, integration of cooperative relaying techniques in the cognitive radio networks has been shown to dramatically improve the performance of the SUs. Subsequently, such wireless networks, namely cognitive relay networks (CRNs), have been extensively studied in the literature considering either one-way or two-way relaying protocols [15]-[22]. Two-way relaying is deemed more spectral-efficient when compared with its one-way counterpart [23]. As such, the majority of existing works have focused on allocation of the available relay resources to secondary system only. Though few works have considered the sharing of relay resources in CRNs, they employ less spectral-efficient one-way relay functionality for the primary transmission [24]-[26]. In addition, the exploitation of a potential direct link in two-way CRNs has been ignored which, otherwise, could be useful for harnessing the benefits of cooperative diversity. Furthermore, the incorporation of a more spectral-efficient scheme, viz., incremental relaying, has also been overlooked in the literature. Moreover, most of the existing works on two-way CRNs have focused on obtaining instantaneous CSI pertaining to the links between secondary transmitters and primary receivers to constrain the SUs' transmit power. However, acquiring instantaneous CSI is typically difficult and may invoke additional complexity. In contrast, the average CSI seems more viable as it can be determined using transmission distance, frequency of radio waves, etc.

On another front, most of the existing studies on CRNs assumed ideal hardware at the network nodes for its performance analysis. However, in practice, RF transceivers are inflicted with various hardware imperfections e.g., in-quadrature-phase (IQ) imbalances, amplifier non-linearities, and phase noises [27]. Although hardware impairments (HIs) are typically mitigated by using compensation algorithms, the residual impairments always persist. As a result, a non-ideal transceiver induces undesirable distortions in the transmitted and received signals which limit the system capacity primarily in the high-rate applications. Besides HIs, the performance of cooperative relay systems may also get impaired by imperfect CSI due to channel estimation errors (CEEs) [28]. Therefore, it is important to analyze the joint impact of these hardware and channel imperfections on the performance of CRNs under various realistic scenarios.

The other design objective of energy efficiency is very important for the cognitive radio networks. In this regard, cooperative relaying techniques have shown to improve the energy efficiency of the wireless networks [29]. Therefore, CRNs can be considered more energy-efficient compared with the conventional point-to-point cognitive radio networks. To further ameliorate the energy efficiency of CRNs, various efforts have been made in the literature to employ the EH techniques to power the network nodes. As such, majority of the existing works focused on the performance analysis of EH-based underlay CRNs [30]-[35]. Nevertheless, in underlay CRNs, SUs have to limit their transmit power in compliance with the interference temperature limit stipulated by the PUs. Consequently, the performance of the secondary system is significantly affected. On the contrary, in the overlay CRNs, there is no such restriction over the transmit power at the SUs. As such, very few works have employed the EH techniques in overlay CRNs for the performance assessment [36]-[41]. However, all these studies adopted the linear model of EH, but since the EH circuit consists of various non-linear elements viz., capacitors, inductors, and diodes, the conventional linear model may not be appropriate to obtain the practical design insights.

1.4.2 Objectives

The aforementioned research voids have motivated us to achieve the following objectives towards the design of future wireless networks:

- To explore the possibility of the resource sharing in two-way CRNs and then to investigate the performance of the considered network.
- To devise the schemes for the two-way CRNs which can efficiently exploit the available direct and relaying links for harnessing the benefits of cooperative diversity.
- To analyze the joint impact of hardware and channel imperfections on the performance of CRNs in realistic fading scenarios.
- To design and analyze the practical non-linear EH-based CRNs for their possible applications in the future networks.

With above-stated objectives, this thesis presents the comprehensive analysis of CRNs while considering various realistic aspects to offer valuable design insights for the possible applications of CRNs in the future networks.

1.5 Thesis Outline and Contributions

Given the importance of efficiently utilizing the available spectrum and energy resources for wireless networks, we aim to comprehensively analyze the performance of CRNs by using various spectral- and energy-efficient schemes. The current chapter introduces the reader to the background of the work, outlines the research objectives and their motivation, and discusses various technologies involved in this thesis work. The main contributions from the other chapters are summarized as follows:

- In Chapter 2[2], we investigate the performance of a resource sharing CRN

[2]The contributions of this chapter are presented in the following papers:

1. S. Solanki, P. K. Sharma, and P. K. Upadhyay, "Cognitive relay sharing for two-way primary transmissions under Nakagami-m fading channels," in *Proc. International Conference on Signal Processing and Communications (SPCOM)*, Indian Institute of Science (IISc) Bangalore, India, June 2016.
2. S. Solanki and P. K. Upadhyay, "Performance analysis of cognitive relay sharing systems with bi-directional primary transmissions under Nakagami-m fading," *IET Communications*, vol. 11, no. 8, pp. 1199-1206, June 2017.

(RSCRN) wherein two PUs exchange the information bi-directionally. The overall transmission in the considered RSCRN takes place using an AF-based MABC protocol. Herein, besides assisting the transmission of SUs, the relay also provides an aid for the bi-directional communication between PUs. In addition to that, the secondary system employs an opportunistic user scheduling with multiple destinations to further ameliorate the performance of secondary network. Here, by considering Nakagami-m fading channels, we derive novel closed-form expressions of outage and average error probabilities for both primary and secondary systems. Based on the derived expressions of outage probability, we also quantify the average system throughput. Our results illustrate that, leveraging two-way relaying for primary transmissions, the proposed RSCRN offers higher spectral efficiency. Moreover, by exploiting the advantages of multiuser cooperation, reliability of SU communication can be improved significantly. Finally, we validate our theoretical developments using Monte Carlo simulations.

- In Chapter 3[3], we investigate the performance of an underlay two-way CRN (TWCRN) with direct link using TDBC protocol in the presence of PU's interference. Herein, relying on the practicability and low-complexity of statistical CSI, the secondary transmissions are in compliance with the fading-averaged interference constraints imposed by the primary receiver. We study an adaptive link utilization scheme (ALUS) that can exploit both direct and relay links with appropriate diversity combining methods to improve the performance of SUs. Based on ALUS, we evaluate and compare the performance of two DF-based relaying strategies viz., fixed relaying and incremental relaying. For this system framework, we derive the tight closed-form expressions for the outage probability of secondary communications for both the considered relaying strategies. We further conduct asymptotic high signal-to-interference-plus-noise ratio (SINR) analysis to examine the achievable diversity order of

[3]The contributions of this chapter are presented in the following papers:

1. S. Solanki, P. K. Sharma, and P. K. Upadhyay, "Average interference-constrained cognitive two-way relaying with efficient link utilization," in *Proc. IEEE International Conference on Communications (ICC)*, Kuala Lumpur, Malaysia, May 2016.
2. S. Solanki, P. K. Sharma, and P. K. Upadhyay, "Adaptive link utilization in two-way spectrum sharing relay systems under average interference-constraints," *IEEE Systems Journal*, vol. 12, no. 4, pp. 3461-3472, Dec. 2018.

the considered system. Our results reveal that the full diversity for secondary system can be achieved as long as the primary interference remains limited, otherwise the performance remarkably deteriorates. We demonstrate that the incremental relaying outperforms fixed relaying in terms of expected spectral efficiency and average transmission time and hence could be a promising candidate for deployment in future wireless systems.

- In Chapter 4[4], we analyze the performance of cognitive multi-relay network (CMRN) with a direct link under the joint impact of transceiver HIs and CEEs. Hereby, we take into account the hardware distortions induced by all the non-ideal secondary nodes and residual interference originating from imperfect channel estimations. We comprehensively investigate the performance of CMRN in presence of hardware and channel imperfections under various operating conditions. Firstly, we consider an AF relaying based CRN and investigate its performance by deriving a new closed-form expression for the outage probability employing selection cooperation over independent and non-identical Rayleigh fading channels. Next, we consider a DF relaying based CRN and analyze its performance by evaluating the outage probability. Based on our studies, we identify various ceiling effects and examine the deleterious impact of these effects on the performance of CMRN. We find that detrimental impact of HIs can potentially cap the fundamental capacity of the system, primarily in the high-rate applications. Based on our examinations, we provide some useful insights into the endurable level of HIs for designing the practical systems with a given rate requirement. We highlight the importance of both direct link and relaying link, and illustrate how one is essential in partially compensating for the incurred performance loss caused due to ceiling effect of the other.

[4]The contributions of this chapter are presented in the following papers:

1. S. Solanki, P. K. Sharma, P. K. Upadhyay, D. B. da Costa, P. S. Bithas, and A. G. Kanatas, "Cognitive multi-relay networks with RF hardware impairments and channel estimation errors," in *Proc. IEEE Global Communications Conference (GLOBECOM)*, Singapore, Dec. 2017.

2. S. Solanki, P. K. Upadhyay, D. B. da Costa, P. S. Bithas, A. G. Kanatas, and U. S. Dias, "Joint impact of RF hardware impairments and channel estimation errors in spectrum sharing multiple-relay networks," *IEEE Transactions on Communications*, vol. 66, no. 9, pp. 3809-3824, Sep. 2018.

- In Chapter 5[5], we analyze the effect of PUs' interference on the performance of CMRN in presence of transceiver HIs and CEEs. Herein, the transmit powers at the SUs are adjusted in such a way that the stipulated QoS requirement of the PUs is satisfied. The power allocation relies upon the average channel gains which are relatively stable in contrast with instantaneous channel gains. For performance assessment, we derive an exact closed-form expression for the outage probability of system by employing selection cooperation between direct and relaying links over Nakagami-m fading channels. Based on the derived outage expressions, we elucidate various ceiling effects, viz., relay cooperation ceiling (RCC), direct link ceiling (DLC), and overall system ceiling (OSC), which are induced in the system due to presence of HIs. Our study shows that the increased PUs' interference and/or CEEs engenders an outage floor. We also perform a comparative study to inspect the robustness of AF and DF relaying schemes against the HIs.

- In Chapter 6[6], we investigate the performance of a non-linear EH-based overlay CRN (EHCRN). Herein, an energy-constrained secondary node acts as a cooperative relay to assist the transmission of PU. In return for the benign cooperation, the secondary node enjoys access to the PU's spectrum for its own information transfer. Specifically, the secondary node first harvests the energy from the received RF signal of primary transmitter during a dedicated EH phase. In the subsequent information transfer phase, secondary node splits the harvested power to forward the primary data as well as its own information intended for another SU. Hereby, we investigate the performance of EHRCN by deriving the expressions for the outage probability of the primary

[5]The contributions of this chapter are presented in the following papers:

1. S. Solanki, P. K. Upadhyay, D. B. da Costa, P. S. Bithas, and A. G. Kanatas, "Performance analysis of cognitive relay networks with RF hardware impairments and CEEs in the presence of primary users' interference," *IEEE Transactions on Cognitive Communications and Networking*, vol. 4, no. 2, pp. 406-421, June 2018.

[6]The contributions of this chapter are presented in the following papers:

1. S. Solanki, P. K. Upadhyay, D. B. da Costa, H. Ding, and J. M. Moualeu, "Non-linear energy harvesting based cooperative spectrum sharing networks," *International Symposium on Wireless Communication Systems (ISWCS)*, Oulu, Finland, Aug. 2019. (Invited paper)
2. S. Solanki, P. K. Upadhyay, D. B. da Costa, H. Ding, and J. M. Moualeu, "Performance analysis of non-linear energy harvesting-based multiuser overlay spectrum sharing networks," *IEEE Transactions on Wireless Communications*, under review.

and secondary networks over Rayleigh fading channels. Further, we employ a distributed user selection policy to select the best user amongst multiple PUs in an effort to extract the benefits of multiuser diversity. We attempt to harness the combined advantages of multiuser diversity and cooperative diversity to improve the performance of primary network. We also compare the performance of considered non-linear model of EH with the widely adopted linear model. We highlight the importance of direct link for the performance of primary network. In addition to the inherent benefit of cooperative diversity, we identify that when the cooperation from the secondary node ceases to exist beyond a certain rate, the primary network can rely on the potential direct links for its information transmission. Furthermore, we propose an improved EH-based relaying scheme which is shown to substantially enhance the overall performance of the EHCRN. For this study, we obtain various numerical and simulation results to extract several useful insights and to validate our theoretical developments. From our performance assessment, we manifest that the value of spectrum sharing factor is crucial and should be judiciously chosen for harnessing the benefits of cooperative diversity. We also conclude that the conventional linear model of EH can provide very misleading results for the deployment of future networks.

Finally, in Chapter 7, we draw the conclusions from the work in this thesis and provide the possible future directions.

CHAPTER 2

RESOURCE SHARING COGNITIVE RELAY NETWORKS WITH TWO-WAY PRIMARY COMMUNICATIONS

Cognitive radio has acquired significant research interest over past few years. This is owing to its capability to efficiently use the available spectrum resources in over-crowded wireless networks. On another front, cooperative relaying has been established as a potential paradigm to enhance the coverage and reliability of the wireless systems [42]. Thus far, several relaying techniques have been studied in the literature considering one-way relaying protocol [3], [43]-[45]. However, compared with one-way relaying, two-way relaying schemes have potential to improve spectral efficiency in bi-directional cognitive radio networks [23]. There are two major protocols for two-way relaying networks, namely two-phase MABC [11] and three-phase TDBC [46]. Recently, such relaying techniques have been incorporated to cognitive radio networks to extract performance gains with efficient spectrum utilization in fading environments. The performance of subsequent CRNs has been extensively analyzed in the literature (e.g., see [15]-[22] and the references therein). However, majority of these works have focused on allocation of the available relay resource to secondary communication system only.

More recently, resource sharing CRN (RSCRN) have been studied in [24]-[26], that permit a secondary relay to assist the primary as well as the secondary transmissions. Such kind of relaying infrastructure can be very useful essentially when the direct link between two end-PUs is weak or absent (due to high shadowing or large separation) and thereby the direct communication between them is inefficacious. As such, performance analysis of RSCRN has been carried out using DF relaying in [24] and with AF relaying in [25] and [26]. Common to these works is that the primary system supports only one-way communication. In [47], a multistage coding scheme for two-way relaying based RSCRN has been studied. However, it is found that the performance of underlay RSCRN supporting bi-directional primary communications has not been yet investigated.

Motivated by the above discussion, in this chapter, we consider a RSCRN where a secondary relay is being shared to facilitate two-way primary communications using AF-based MABC protocol. Specifically, we consider a pair of PUs using two-way relay functionality in conjunction with a secondary relay network having multiple SU destinations. Hereby, with MABC protocol, two end-PUs communicate bi-directionally with each other and a SU source communicates with a best selected SU destination by using a common secondary relay. The direct links between SU source and SU destinations are also present. For this overall set-up, we derive the closed-form expressions of outage probability and average error probability for both primary and secondary systems over Nakagami-m fading channels. Furthermore, with the help of derived outage expressions, we quantify the average system throughput to investigate the spectral efficiency of considered system. We also compare the performance of the two-way primary system for proposed RSCRN with a direct transmission scheme and present useful insights.

The rest of the chapter is organized as follows. In section 2.1, we present the descriptions of RSCRN model and subsequently analyze the performance of primary system by deriving the closed form expressions of outage probability and average error probability in Section 2.2. Likewise, the performance analysis of secondary system is carried out in Section 2.3. In Section 2.4, we quantify the average system throughput offered by RSCRN to delve into the spectral efficiency of system. Numerical and simulation results are provided in Section 2.5, and finally, summary of the chapter is presented in Section 2.6.

2.1 System Descriptions

We consider an underlay RSCRN as shown in Fig. 2.1, where a SU source C_s transmits its signal to multiple SU destinations $\{C_{d_n}\}_{n=1}^{N}$ with the aid of a secondary AF relay C_r and also via direct path. Besides, the relay C_r facilitates bi-directional communication between two PU transceivers T_a and T_b. This primary system may

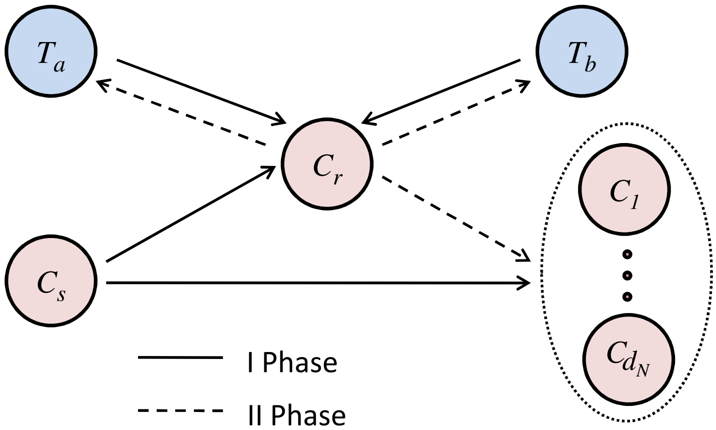

Figure 2.1: System model for RSCRN.

correspond to a cellular scenario wherein a reliable direct link between base station (T_a) and mobile user (T_b) is not feasible. Further, we assume that T_a and T_b are located far from the $\{C_{d_n}\}_{n=1}^{N}$ so that the direct interference from PUs' transmissions at SU destinations is not present. Albeit, the interference constraints from T_a and T_b account for the amplifying gain of C_r. All the channels are assumed to be quasi-static, reciprocal, and subject to independent Nakagami-m fading. We also assume that perfect CSI is available at the nodes. Each transmitting node operates in half-duplex mode. Let the channel between the primary transceiver $T_\imath$ and C_r be denoted as $h_{\imath r}$, where $\imath \in \{a, b\}$. Similarly, the channels for the links $C_s - C_r$, $C_s - C_{d_n}$, and $C_r - C_{d_n}$ are designated as h_{sr}, h_{sd_n}, and h_{rd_n}, respectively. All links are corrupted by additive white Gaussian noise (AWGN) with mean zero and variance unity.

The overall communication in RSCRN takes place in two time phases using MABC protocol. In the first phase, nodes T_a and T_b transmit their respective signals x_a and x_b with equal power P, while C_s transmits its signal x_c with power P_c to the relay node C_r. Thus, the received signal at the node C_r can be given as

$$y_r = \sqrt{P} h_{ar} x_a + \sqrt{P} h_{br} x_b + \sqrt{P_c} h_{sr} x_c + n_r, \tag{2.1}$$

where $\mathbb{E}\{|x_\jmath|^2\} = 1$, for $\jmath \in \{a, b, c\}$, and n_r is the AWGN at C_r. Note that, in (2.1), the interference from secondary transmission is assumed to be large as compared to the noise at C_r and hence n_r can be ignored for the subsequent performance analysis of primary system. In the second phase, the relay first amplifies the combined signal in (2.1) with a gain β and then broadcasts it to the nodes T_a, T_b, and C_{d_n}. As a result, the signals received at T_a and T_b can be expressed, respectively, as

$$y_a = \beta h_{ar}\big(\sqrt{P}h_{ar}x_a + \sqrt{P}h_{br}x_b + \sqrt{P_c}h_{sr}x_c\big) + n_a, \tag{2.2}$$

$$y_b = \beta h_{br}\big(\sqrt{P}h_{ar}x_a + \sqrt{P}h_{br}x_b + \sqrt{P_c}h_{sr}x_c\big) + n_b, \tag{2.3}$$

where n_a and n_b are the AWGNs at the respective nodes. On applying self-interference cancellation, (2.2) and (2.3) can be written as

$$\tilde{y}_a = \beta h_{ar}\sqrt{P}h_{br}x_b + \beta h_{ar}\sqrt{P_c}h_{sr}x_c + n_a, \tag{2.4}$$

$$\tilde{y}_b = \beta h_{br}\sqrt{P}h_{ar}x_a + \beta h_{br}\sqrt{P_c}h_{sr}x_c + n_b. \tag{2.5}$$

Nevertheless, the interference caused by SU transmission to the PUs should not exceed a predefined threshold Q. Hereby, as in [25], we impose the constraints $\mathbb{E}\{(\beta\sqrt{P_c}h_{sr}x_c)^2\} \leq Q/|h_{ar}|^2$ and $\mathbb{E}\{(\beta\sqrt{P_c}h_{sr}x_c)^2\} \leq Q/|h_{br}|^2$. Consequently, the variable gain β can be controlled as

$$\beta^2 = \frac{Q}{P_c|h_{sr}|^2 \max(|h_{ar}|^2, |h_{br}|^2)}. \tag{2.6}$$

On invoking β from (2.6) into (2.4) and (2.5), the resulting instantaneous SINR at T_a and T_b can be expressed, respectively, as

$$\Lambda_{ba} = \frac{QP|h_{ar}|^2|h_{br}|^2}{QP_c|h_{ar}|^2|h_{sr}|^2 + P_c|h_{sr}|^2\max(|h_{ar}|^2, |h_{br}|^2)}, \tag{2.7}$$

$$\Lambda_{ab} = \frac{QP|h_{br}|^2|h_{ar}|^2}{QP_c|h_{br}|^2|h_{sr}|^2 + P_c|h_{sr}|^2\max(|h_{ar}|^2, |h_{br}|^2)}. \tag{2.8}$$

In the secondary system, the SU source C_s communicates with a selected SU destination C_{d_n} via both the direct and the relay links. The received signals at C_{d_n} via the direct and relay links in first and second phases can be given, respectively, as

$$y_{sd_n} = \sqrt{P_c}h_{sd_n}x_c + n_{d_n}^{(\mathrm{I})}, \tag{2.9}$$

$$y_{rd_n} = \beta h_{rd_n}\sqrt{P_c}h_{sr}x_c + \beta h_{rd_n}\sqrt{P}h_{ar}x_a + \beta h_{rd_n}\sqrt{P}h_{br}x_b + \beta h_{rd_n}n_r + n_{d_n}^{(\mathrm{II})}, \tag{2.10}$$

where $n_{d_n}^{(\mathrm{I})}$ and $n_{d_n}^{(\mathrm{II})}$ are the respective AWGNs at C_{d_n}. From (2.10), one can observe that the signal received via relay at C_{d_n} also contains PUs' signal components. As such, the interference caused by these PUs' signals is detrimental for the performance of secondary system. Therefore, relying on multiuser decoding [48], we consider that these signals are successfully decoded at C_{d_n} so that the PUs interference can be cancelled out. Consequently, the SINRs via the direct link and the relay link (after removing PUs interference) at C_{d_n}, can be expressed, respectively, as

$$\Lambda_{sd_n} = P_c|h_{sd_n}|^2, \tag{2.11}$$

$$\Lambda_{rd_n} = \frac{QP_c|h_{rd_n}|^2|h_{sr}|^2}{Q|h_{rd_n}|^2 + P_c|h_{sr}|^2 \max(|h_{ar}|^2, |h_{br}|^2)}. \tag{2.12}$$

For opportunistic scheduling, the best SU destination is considered to be selected based on $n^* = \arg\max_{n\in\{1,\ldots,N\}}\{\Lambda_{sd_n}\}$.

Hereafter, we use $Y_{ar} = |h_{ar}|^2$, $Y_{br} = |h_{br}|^2$, $Y_{sr} = |h_{sr}|^2$, $Y_{sd_n} = |h_{sd_n}|^2$, and $Y_{rd_n} = |h_{rd_n}|^2$ for notational simplicity. Furthermore, we assume that all N destinations are clustered together and thereby experience the same scale fading. Thus, the channel gains Y_{ar}, Y_{br}, Y_{sr}, Y_{sd_n}, and Y_{rd_n} are Gamma random variables (RVs) with fading severity parameter m_{ar}, m_{br}, m_{sr}, m_{sd}, and m_{rd}, and average power levels Ω_{ar}, Ω_{br}, Ω_{sr}, Ω_{sd}, and Ω_{rd}, respectively, for $n = 1, ..., N$. The probability density function (PDF) and cumulative distribution function (CDF) of a Gamma RV X with parameters m and Ω are given, respectively, by $f_X(x) = (\frac{m}{\Omega})^m \frac{x^{m-1}}{\Gamma(m)} \mathrm{e}^{-\frac{mx}{\Omega}}$ and $F_X(x) = \frac{1}{\Gamma(m)}\Upsilon(m, \frac{mx}{\Omega})$.

2.2 Performance Analysis of Primary System

In this section, we conduct performance analysis for the primary system under Nakagami-m fading.

2.2.1 Outage Probability

A two-way relay system is said to be in outage if either of the two end-to-end SINRs falls below a certain threshold. Considering equal rate requirements at PUs, the outage probability (OP) of the primary system for a given threshold γ_{th} can be formulated as

$$\mathcal{P}_{\text{out}}^{\text{Pri}}(\gamma_{\text{th}}) = \Pr[\min(\Lambda_{ab}, \Lambda_{ba}) < \gamma_{\text{th}}], \tag{2.13}$$

which can be re-written as

$$\mathcal{P}_{\text{out}}^{\text{Pri}}(\gamma_{\text{th}}) = \underbrace{\Pr[\Lambda_{ba} < \gamma_{\text{th}}, \Lambda_{ba} < \Lambda_{ab}]}_{\chi_{ab}^{\text{Pri}}(\gamma_{\text{th}})} + \underbrace{\Pr[\Lambda_{ab} < \gamma_{\text{th}}, \Lambda_{ab} < \Lambda_{ba}]}_{\chi_{ba}^{\text{Pri}}(\gamma_{\text{th}})}, \tag{2.14}$$

where Λ_{ba} and Λ_{ab} are SINRs as given in (2.7) and (2.8) respectively. Hereby, to compute the OP in (2.14), we need to obtain $\chi_{ab}^{\text{Pri}}(\gamma_{\text{th}})$ and $\chi_{ba}^{\text{Pri}}(\gamma_{\text{th}})$. Therefore, we first derive $\chi_{ab}^{\text{Pri}}(\gamma_{\text{th}})$ in the following lemma.

Lemma 1. *The $\chi_{ab}^{Pri}(\gamma_{th})$ in (2.14) is given by*

$$\chi_{ab}^{Pri}(\gamma_{th}) = \sum_{p=0}^{m_{ar}-1}\sum_{q=0}^{m_{sr}-1} \frac{\Gamma(m_{br}+p+q)}{p!q!\Gamma(m_{br})}\left(\frac{m_{sr}}{\Omega_{sr}\tilde{\gamma}_{th}}\right)^{q}\left(\frac{m_{br}}{\Omega_{br}}\right)^{m_{br}} \times\left(\frac{m_{ar}}{\Omega_{ar}}\right)^{p}\left(\frac{m_{ar}}{\Omega_{ar}}+\frac{m_{br}}{\Omega_{br}}+\frac{m_{sr}}{\Omega_{sr}\tilde{\gamma}_{th}}\right)^{-(m_{br}+p+q)}, \tag{2.15}$$

where $\tilde{\gamma}_{th} \triangleq \frac{P_c}{P}\gamma_{th}\left(1+\frac{1}{Q}\right)$.

Proof. Based on the SINR in (2.7), one can observe that $\Lambda_{ba} < \Lambda_{ab}$ assimilates with $Y_{br} < Y_{ar}$. Hence, the $\chi_{ab}^{\mathrm{Pri}}(\gamma_{\mathrm{th}})$ can be expressed as

$$\chi_{ab}^{\mathrm{Pri}}(\gamma_{\mathrm{th}}) = \Pr\left[Y_{sr} > \frac{Y_{br}}{\tilde{\gamma}_{th}}, Y_{br} < Y_{ar}\right]. \tag{2.16}$$

which (with involved dependence) can be evaluated as

$$\chi_{ab}^{\mathrm{Pri}}(\gamma_{\mathrm{th}}) = \int_0^\infty \bar{F}_{Y_{sr}}\left(\frac{y}{\tilde{\gamma}_{\mathrm{th}}}\right)\bar{F}_{Y_{ar}}(y)\, f_{Y_{br}}(y)dy, \tag{2.17}$$

wherein $\bar{F}_Y(\cdot) = 1 - F_Y(\cdot)$ represents complementary CDF. Now, on substituting the required CDFs and PDF, and utilizing the series form of gamma function [49, eq. 8.352.1], and performing the resulting integration (with the aid of [49, eq. 3.351.3]), we can arrive at the same expression as in (2.15). ■

Next, as done for $\chi_{ab}^{\mathrm{Pri}}(\gamma_{\mathrm{th}})$ in Lemma 1, the $\chi_{ba}^{\mathrm{Pri}}(\gamma_{\mathrm{th}})$ can be readily evaluated and is equivalent to $\chi_{ab}^{\mathrm{Pri}}(\gamma_{\mathrm{th}})$ in (2.15) with indices $\{a, b\}$ interchanged.

Finally, using $\chi_{ab}^{\mathrm{Pri}}(\gamma_{\mathrm{th}})$ and $\chi_{ba}^{\mathrm{Pri}}(\gamma_{\mathrm{th}})$, the OP for primary system $\mathcal{P}_{\mathrm{out}}^{\mathrm{Pri}}(\gamma_{\mathrm{th}})$ in (2.14) can be computed. As such, based on (2.15), one can observe that the performance of primary system depends on the channel parameters of secondary $C_s - C_r$ link. Thereby, it can be deduced that for lower values of Ω_{sr} i.e., when C_s is located far away from C_r, the performance of primary system improves. This is owing to the decrease in interference power level from the SU source transmission.

2.2.2 Average Error Probability

The average error probability of the primary system for the considered RSCRN can be evaluated using the CDF based method as follows [50]

$$\mathcal{P}_e^{\mathrm{Pri}} = \frac{\alpha}{2}\sqrt{\frac{\eta}{\pi}}\int_0^\infty \frac{\exp(-\eta x)}{\sqrt{x}} F_{\Lambda_{\mathrm{eq}}}^{\mathrm{Pri}}(x)dx, \tag{2.18}$$

where α and η are the arbitrary constants evaluated based on the modulation schemes, e.g., $\alpha = 2$ and $\eta = \sin\left(\frac{\pi}{M}\right)^2$ for M-ary phase shift keying (M-PSK). Here, $F^{\text{Pri}}_{\Lambda_{\text{eq}}}(x)$ is CDF of equivalent SINR $\Lambda_{\text{eq}} \triangleq \min(\Lambda_{ab}, \Lambda_{ba})$, which can be directly obtained from (2.14) by replacing γ_{th} with x, and is given by

$$F^{\text{Pri}}_{\Lambda_{\text{eq}}}(x) = \chi^{\text{Pri}}_{ab}(x) + \chi^{\text{Pri}}_{ba}(x). \tag{2.19}$$

Following this, $\mathcal{P}^{\text{Pri}}_{e}$ in (2.18) can be written as

$$\mathcal{P}^{\text{Pri}}_{e} = \underbrace{\frac{\alpha}{2}\sqrt{\frac{\eta}{\pi}}\int_0^\infty \frac{\exp(-\eta x)}{\sqrt{x}}\chi^{\text{Pri}}_{ab}(x)dx}_{\mathcal{P}^{\text{Pri}}_{e_{ab}}} + \underbrace{\frac{\alpha}{2}\sqrt{\frac{\eta}{\pi}}\int_0^\infty \frac{\exp(-\eta x)}{\sqrt{x}}\chi^{\text{Pri}}_{ba}(x)dx}_{\mathcal{P}^{\text{Pri}}_{e_{ba}}}, \tag{2.20}$$

where $\mathcal{P}^{\text{Pri}}_{e_{ab}}$ is as derived in the following lemma.

Lemma 2. *The $\mathcal{P}^{Pri}_{e_{ab}}$ in (2.20) is given by*

$$\begin{aligned}\mathcal{P}^{Pri}_{e_{ab}} &= \frac{\alpha}{2\sqrt{\pi}}\sum_{p=0}^{m_{ar}-1}\sum_{q=0}^{m_{sr}-1}\frac{1}{\Gamma(m_{br})p!q!}\left(\frac{m_{br}}{\Omega_{br}}\right)^{m_{br}}\left(\frac{m_{ar}}{\Omega_{ar}}\right)^{p} \\ &\times\left(\frac{m_{sr}\eta}{\Omega_{sr}\tilde{P}_c}\right)^{-(m_{br}+p)} G^{1,2}_{2,1}\left[\frac{1}{\eta\tilde{B}}\middle| \begin{matrix}1/2-\tilde{m}_{br}, 1-\tilde{m}_{br}-q\\ 0\end{matrix}\right],\end{aligned} \tag{2.21}$$

where $\tilde{P}_c = \frac{P_c}{P}\left(1+\frac{1}{Q}\right)$, $\tilde{B} = \frac{m_{sr}}{\Omega_{sr}P_c}/\left(\frac{m_{ar}}{\Omega_{ar}}+\frac{m_{br}}{\Omega_{br}}\right)$, and $\tilde{m}_{br} = m_{br}+p$.

Proof. On inserting $\chi^{\text{Pri}}_{ab}(x)$ from (2.15) in (2.19) and obtained result into (2.18), $\mathcal{P}^{\text{Pri}}_{e_{ab}}$ can be written as

$$\begin{aligned}\mathcal{P}^{\text{Pri}}_{e_{ab}} &= \frac{\alpha}{2}\sqrt{\frac{\eta}{\pi}}\sum_{p=0}^{m_{ar}-1}\sum_{q=0}^{m_{sr}-1}\frac{1}{\Gamma(m_{br})p!q!}\left(\frac{m_{br}}{\Omega_{br}}\right)^{m_{br}}\left(\frac{m_{ar}}{\Omega_{ar}}\right)^{p}\left(\frac{m_{sr}}{\Omega_{sr}\tilde{P}_c}\right)^{q} \\ &\times\left(\frac{m_{ar}}{\Omega_{ar}}+\frac{m_{br}}{\Omega_{br}}\right)^{-(m_{br}+p+q)}\int_0^\infty \frac{x^{(m_{br}+p-1/2)}\exp(-\eta x)}{(x+\tilde{B})^{(m_{br}+p+q)}}dx.\end{aligned} \tag{2.22}$$

In order to compute the integral in (2.22), we express the integrand in term of Meijer's G-function. In particular, the term $\frac{1}{(x+\tilde{B})^{(m_{br}+p+q)}}$ can be expressed [51, eq. 30] as follows

$$\frac{1}{(x+\tilde{B})^{\tilde{m}_{br}+q}} = \frac{1}{\tilde{B}^{\tilde{m}_{br}+q}\Gamma(\tilde{m}_{br}+q)}G^{1,1}_{1,1}\left[\frac{x}{\tilde{B}}\middle| \begin{matrix}1-\tilde{m}_{br}-q\\ 0\end{matrix}\right]. \tag{2.23}$$

Then, inserting (2.23) in (2.22) and integrating the result using [49, eq. 7.813.1], we obtain the expression as given in (2.21). ■

Next, by following the same way as in Lemma 2, we can evaluate $\mathcal{P}^{\text{Pri}}_{e_{ba}}$ in (2.18) which would be same as $\mathcal{P}^{\text{Pri}}_{e_{ab}}$ in (2.22) with indices {a,b} interchanged.

Finally, plugging $\mathcal{P}_{e_{ba}}^{\text{Pri}}$ and $\mathcal{P}_{e_{ab}}^{\text{Pri}}$ into (2.20), the average error probability $\mathcal{P}_{e}^{\text{Pri}}$ can be evaluated.

2.3 Performance Analysis of Secondary System

In what follows, we carry out the performance analysis for the secondary system under Nakagami-m fading.

2.3.1 Outage Probability

In the secondary system, the source C_s transmits its message to the best selected SU destination $C_{d_{n^*}}$ through direct and relay links in successive time phases. With selection cooperation at $C_{d_{n^*}}$, the OP for a given threshold γ_{th} is given by

$$\mathcal{P}_{\text{out}}^{\text{Sec}}(\gamma_{\text{th}}) = \Pr\left[\max\left(\Lambda_{sd_{n^*}}, \Lambda_{rd_{n^*}}\right) < \gamma_{\text{th}}\right] = \Pr\left[\Lambda_{sd_{n^*}} < \gamma_{\text{th}}, \Lambda_{rd_{n^*}} < \gamma_{\text{th}}\right], \tag{2.24}$$

which can be determined as

$$\mathcal{P}_{\text{out}}^{\text{Sec}}(\gamma_{\text{th}}) = \left[F_{\Lambda_{sd_n}}(\gamma_{\text{th}})\right]^N F_{\Lambda_{rd_n}}(\gamma_{\text{th}}). \tag{2.25}$$

For evaluation of (2.25), we require the CDFs $F_{\Lambda_{sd_n}}(\gamma_{\text{th}})$ and $F_{\Lambda_{rd_n}}(\gamma_{\text{th}})$. First, by using (2.11), $F_{\Lambda_{sd_n}}(\gamma_{\text{th}})$ can be given as

$$F_{\Lambda_{sd_n}}(\gamma_{\text{th}}) = F_{Y_{sd_n}}\left(\frac{\gamma_{\text{th}}}{P_c}\right) = \frac{1}{\Gamma(m_{sd})}\Upsilon\left(m_{sd}, \frac{m_{sd}\gamma_{\text{th}}}{\Omega_{sd}P_c}\right). \tag{2.26}$$

Then, to derive $F_{\Lambda_{rd_n}}(\gamma_{\text{th}})$ using (2.12), we can represent

$$F_{\Lambda_{rd_n}}(\gamma_{\text{th}}) = \Pr\left[\frac{QP_cY_{sr}Y_{rd_n}}{QY_{rd_n} + P_cY_{sr}\max(Y_{ar}, Y_{br})} < \gamma_{\text{th}}\right], \tag{2.27}$$

which can be re-expressed as

$$\begin{aligned} F_{\Lambda_{rd_n}}(\gamma_{\text{th}}) = {} & \underbrace{\Pr\left[\frac{QP_cY_{sr}Y_{rd_n}}{QY_{rd_n} + P_cY_{sr}Y_{ar}} < \gamma_{\text{th}}, Y_{br} < Y_{ar}\right]}_{\chi_{ab}^{\text{Sec}}(\gamma_{\text{th}})} \\ & + \underbrace{\Pr\left[\frac{QP_cY_{sr}Y_{rd_n}}{QY_{rd_n} + P_cY_{sr}Y_{br}} < \gamma_{\text{th}}, Y_{ar} < Y_{br}\right]}_{\chi_{ba}^{\text{Sec}}(\gamma_{\text{th}})}. \end{aligned} \tag{2.28}$$

Hereby, to evaluate $F_{\Lambda_{rd_n}}(\gamma_{\text{th}})$ in (2.28), we need to obtain $\chi_{ab}^{\text{Sec}}(\gamma_{\text{th}})$ and $\chi_{ba}^{\text{Sec}}(\gamma_{\text{th}})$. Let us proceed to derive $\chi_{ab}^{\text{Sec}}(\gamma_{\text{th}})$ in the following lemma.

Lemma 3. *The function $\chi_{ab}^{Sec}(\gamma_{th})$ in (2.28) is given by*

$$\chi_{ab}^{Sec}(\gamma_{th}) = \chi_{ab}^{1}(\gamma_{th}) + \chi_{ab}^{2}(\gamma_{th}), \tag{2.29}$$

where $\chi_{ab}^{1}(\gamma_{th})$ and $\chi_{ab}^{2}(\gamma_{th})$ are given, respectively, as

$$\begin{aligned}\chi_{ab}^{1}(\gamma_{th}) = &\sum_{\nu=0}^{1}\sum_{p=0}^{\nu(m_{rd}-1)}\sum_{t=0}^{p}\sum_{s=0}^{m_{sr}-1}\sum_{\kappa=0}^{1}\sum_{l=0}^{\kappa(m_{br}-1)}(-1)^{\nu+\kappa}\frac{\omega_p^{\nu}\omega_l^{\kappa}\mathcal{C}_t^{p}\mathcal{C}_s^{m_{sr}-1}}{\Gamma(m_{sr})\Gamma(m_{ar})}e^{-\frac{m_{sr}\gamma_{th}}{\Omega_{sr}P_c}}\\ &\times\left(\frac{m_{sr}}{\Omega_{sr}}\right)^{m_{sr}}\left(\frac{\gamma_{th}}{P_c}\right)^{s+t}\left(\frac{m_{rd}\gamma_{th}}{\Omega_{rd}Q}\right)^{p}\left(\frac{\tilde{\nu}\Omega_{sr}}{m_{sr}}\right)^{\frac{\tilde{m}_{sr}}{2}}\left(\frac{m_{br}}{\Omega_{br}}\right)^{l}\left(\frac{m_{ar}}{\Omega_{ar}}\right)^{m_{ar}}\\ &\times\tilde{\kappa}^{-\frac{\tilde{p}}{2}}e^{\frac{\tilde{\nu}m_{sr}}{2\tilde{\kappa}\Omega_{sr}}}\Gamma(\tilde{m}_{ar})\Gamma(\tilde{m}_{sr}+\tilde{m}_{ar})\left(\frac{\tilde{\nu}m_{sr}}{\Omega_{sr}}\right)^{-\frac{1}{2}}\mathcal{W}_{-\frac{\tilde{p}}{2},\frac{\tilde{m}_{sr}}{2}}\left(\frac{\tilde{\nu}\Omega_{sr}}{\tilde{\kappa}m_{sr}}\right),\end{aligned} \tag{2.30}$$

$$\begin{aligned}\text{and}\quad \chi_{ab}^{2}(\gamma_{th}) = &\sum_{k=0}^{1}\sum_{n=0}^{k(m_{sr}-1)}\sum_{\jmath=0}^{1}\sum_{l=0}^{\jmath(m_{br}-1)}\frac{(-1)^{k+\jmath}\omega_n^{k}\omega_l^{\jmath}}{\Gamma(m_{ar})}\left(\frac{m_{ar}}{\Omega_{ar}}\right)^{m_{ar}}\left(\frac{m_{br}}{\Omega_{br}}\right)^{l}\\ &\times\left(\frac{m_{sr}\gamma_{th}}{\Omega_{sr}P_c}\right)^{n}e^{-\frac{km_{sr}\gamma_{th}}{\Omega_{sr}P_c}}\Gamma(m_{ar}+l)\left(\frac{m_{ar}}{\Omega_{ar}}+\frac{\jmath m_{br}}{\Omega_{br}}\right)^{-(m_{ar}+l)},\end{aligned} \tag{2.31}$$

with $\tilde{\nu}=\frac{\nu\gamma_{th}^2 m_{rd}}{P_c Q\Omega_{rd}}$, $\tilde{m}_{sr}=m_{sr}-s-t$, $\tilde{\kappa}=\frac{m_{ar}}{\Omega_{ar}}+\frac{\kappa m_{br}}{\Omega_{br}}+\frac{\nu m_{rd}\gamma_{th}}{\Omega_{rd}Q}$, $\tilde{p}=m_{ar}+m_{sr}+2p+2l-s-t-1$ and $\tilde{m}_{ar}=m_{ar}+p+l$.

Proof. From (2.28), we can see that the terms in $\chi_{ab}^{\text{Sec}}(\gamma_{\text{th}})$ are dependent due to existence of a common RV Y_{ar}. Therefore, we first obtain conditional expression $\chi_{ab}^{\text{Sec}}(\gamma_{\text{th}}|Y_{ar})$, conditioned on $Y_{ar}=y$, as

$$\chi_{ab}^{\text{Sec}}(\gamma_{\text{th}}|Y_{ar})=\Pr\left[Y_{rd_n}<\frac{P_c\gamma_{\text{th}}yY_{sr}}{QP_cY_{sr}-Q\gamma_{\text{th}}}\right]\Pr\left[Y_{br}<y\right], \tag{2.32}$$

which can be evaluated as

$$\chi_{ab}^{\text{Sec}}(\gamma_{\text{th}}|Y_{ar})=\underbrace{F_{Y_{br}}(y)\int_{\frac{\gamma_{\text{th}}}{P_c}}^{\infty}F_{Y_{rd_n}}\left(\frac{P_c\gamma_{\text{th}}yw}{QP_cw-Q\gamma_{\text{th}}}\right)f_{Y_{sr}}(w)dw}_{\chi_{ab}^{1}(\gamma_{\text{th}}|Y_{ar})}+\underbrace{F_{Y_{sr}}\left(\frac{\gamma_{\text{th}}}{P_c}\right)F_{Y_{br}}(y)}_{\chi_{ab}^{2}(\gamma_{\text{th}}|Y_{ar})}. \tag{2.33}$$

In (2.33), solving $\chi_{ab}^{1}(\gamma_{\text{th}}|Y_{ar})$ with the use of involved CDF and PDF, and integrating (with change of variable after applying binomial expansion [49, eq. 1.111]), we get

$$\begin{aligned}\chi_{ab}^{1}(\gamma_{\text{th}}|Y_{ar}) = &2F_{Y_{br}}(y)\sum_{\nu=0}^{1}\sum_{p=0}^{\nu(m_{rd}-1)}\sum_{t=0}^{p}\sum_{s=0}^{m_{sr}-1}\frac{(-1)^{\nu}\omega_p^{\nu}\mathcal{C}_t^{p}}{\Gamma(m_{sr})}\mathcal{C}_s^{m_{sr}-1}\left(\frac{m_{sr}}{\Omega_{sr}}\right)^{m_{sr}}\left(\frac{\gamma_{\text{th}}}{P_c}\right)^{s+t}\\ &\times e^{-\left[\frac{\nu y m_{rd}\gamma_{\text{th}}}{Q\Omega_{rd}}+\frac{m_{sr}\gamma_{\text{th}}}{\Omega_{sr}P_c}\right]}\left(\frac{m_{rd}\gamma_{\text{th}}y}{\Omega_{rd}Q}\right)^{p}\left(\frac{\tilde{\nu}\Omega_{sr}y}{m_{sr}}\right)^{\frac{\tilde{m}_{sr}}{2}}\mathcal{K}_{\tilde{m}_{sr}}\left(2\sqrt{\frac{\tilde{\nu}m_{sr}y}{\Omega_{sr}}}\right).\end{aligned} \tag{2.34}$$

Further, the term $\chi^2_{ab}(\gamma_{\text{th}}|Y_{ar})$ in (2.33) can be obtained as

$$\chi^2_{ab}(\gamma_{\text{th}}|Y_{ar}) = \sum_{k=0}^{1}\sum_{n=0}^{k(m_{sr}-1)}\sum_{\jmath=0}^{1}\sum_{l=0}^{\jmath(m_{br}-1)}(-1)^{k+\jmath}\omega_n^k\omega_l^\jmath \times \left(\frac{m_{br}y}{\Omega_{br}}\right)^l \left(\frac{m_{sr}\gamma_{\text{th}}}{\Omega_{sr}P_c}\right)^n e^{-\left(\frac{km_{sr}\gamma_{\text{th}}}{\Omega_{sr}P_c}+\frac{\jmath m_{br}y}{\Omega_{br}}\right)}. \quad (2.35)$$

Now, by taking expectation of $\chi^1_{ab}(\gamma_{\text{th}}|Y_{ar})$ and $\chi^2_{ab}(\gamma_{\text{th}}|Y_{ar})$ over Y_{ar} using its PDF, one can obtain $\chi^1_{ab}(\gamma_{\text{th}})$ and $\chi^2_{ab}(\gamma_{\text{th}})$ as given in (2.30) and (2.31), respectively. Finally, with these, the $\chi^{\text{Sec}}_{ab}(\gamma_{\text{th}})$ in (2.29) can be computed. ■

Next, by following Lemma 3, the expression of $\chi^{\text{Sec}}_{ba}(\gamma_{\text{th}})$ can be derived which would be the same as obtained for $\chi^{\text{Sec}}_{ab}(\gamma_{\text{th}})$ in (2.29) with indices $\{a, b\}$ interchanged.

Thus, with the use of $\chi^{\text{Sec}}_{ab}(\gamma_{\text{th}})$ and $\chi^{\text{Sec}}_{ba}(\gamma_{\text{th}})$ in (2.28) and substituting the result alongwith (2.26) into (2.25), the OP of secondary system $\mathcal{P}^{\text{Sec}}_{\text{out}}(\gamma_{\text{th}})$ can be finally evaluated.

2.3.2 Average Error Probability

To derive the average error probability of secondary system, the CDF $F^{\text{Sec}}_{\Lambda_{\text{eq}}}(x)$ corresponding to equivalent SINR $\Lambda_{\text{eq}} \triangleq \max(\Lambda_{sd_{n^*}}, \Lambda_{rd_{n^*}})$ can be readily evaluated by replacing γ_{th} with x in (2.25) and is given by

$$F^{\text{Sec}}_{\Lambda_{\text{eq}}}(x) = \left[F_{\Lambda_{sd_n}}(x)\right]^N F_{\Lambda_{rd_n}}(x). \quad (2.36)$$

Here, $F_{\Lambda_{sd_n}}(x)$ can be obtained from (2.26) and $F_{\Lambda_{rd_n}}(x)$ from (2.28). With this, the average error probability can be written as

$$\mathcal{P}^{\text{Sec}}_{e} = \underbrace{\frac{\alpha}{2}\sqrt{\frac{\eta}{\pi}}\int_0^\infty \frac{\exp(-\eta x)}{\sqrt{x}}\left[F_{\Lambda_{sd_n}}(x)\right]^N \chi^{\text{Sec}}_{ab}(x)dx}_{\mathcal{P}^{\text{Sec}}_{e_{ab}}} + \underbrace{\frac{\alpha}{2}\sqrt{\frac{\eta}{\pi}}\int_0^\infty \frac{\exp(-\eta x)}{\sqrt{x}}\left[F_{\Lambda_{sd_n}}(x)\right]^N \chi^{\text{Sec}}_{ba}(x)dx}_{\mathcal{P}^{\text{Sec}}_{e_{ba}}}, \quad (2.37)$$

where $\mathcal{P}^{\text{Sec}}_{e_{ab}}$ is as derived in the following lemma.

Lemma 4. *Integral $\mathcal{P}_{e_{ab}}^{Sec}$ in (2.37) is given as*

$$\mathcal{P}_{e_{ab}}^{Sec} = \frac{\alpha}{2}\sqrt{\frac{\eta}{\pi}} \sum_{\nu=0}^{1}\sum_{\mu=0}^{1}\sum_{k=0}^{N}\sum_{l=0}^{\nu(m_{rd}-1)}\sum_{n=0}^{\nu(m_{sr}-1)}\sum_{s=0}^{\mu(m_{br}-1)}\sum_{t=0}^{k(m_{sd}-1)} \frac{(-1)^{\nu+\mu+k}\omega_l^{\nu}\omega_n^{\nu}\omega_s^{\mu}\omega_t^{k}}{\Gamma(m_{ar})}$$
$$\times \binom{N}{k}\left(\frac{m_{ar}}{\Omega_{ar}}\right)^{m_{ar}}\left(\frac{m_{br}}{\Omega_{br}}\right)^{s}\left(\frac{m_{rd}}{\Omega_{rd}Q}\right)^{l}\left(\frac{m_{sr}}{\Omega_{sr}P_c}\right)^{n}\frac{\tilde{k}^{-(\tilde{t}+1/2)}}{\left(\frac{\mu m_{br}}{\Omega_{br}}+\frac{m_{ar}}{\Omega_{ar}}\right)^{\tilde{l}}}$$
$$\times G_{2,1}^{1,2}\left[\frac{\frac{\nu m_{rd}}{Q\Omega_{rd}}}{\left(\frac{\mu m_{br}}{\Omega_{br}}+\frac{m_{ar}}{\Omega_{ar}}\right)\tilde{k}}\middle| \begin{matrix} 1-\tilde{t}, 1-\tilde{l} \\ 0 \end{matrix}\right], \tag{2.38}$$

where $\tilde{t} = t + l + n$, $\tilde{l} = l + s + m_{ar}$, and $\tilde{k} = \frac{k m_{sd}}{\Omega_{sd}} + \frac{\nu m_{sr}}{\Omega_{sr}} + \eta$.

Proof. For deriving $\mathcal{P}_{e_{ab}}^{\text{Sec}}$ we first need to obtain $\chi_{ab}^{\text{Sec}}(x)$. From (2.28), the conditional expression $\chi_{ab}^{\text{Sec}}(x|Y_{ar})$ conditioned on $Y_{ar} = y$ can be represented as

$$\chi_{ab}^{\text{Sec}}(x|Y_{ar}) = \Pr\left[\frac{Y_1 Y_2}{Y_1 + Y_2} < x\right]\Pr\left[Y_{br} < y\right], \tag{2.39}$$

where $Y_1 = Q\frac{Y_{rd}}{y}$ and $Y_2 = P_c Y_{sr}$. Using the fact that $\frac{XY}{X+Y} < \min(X, Y)$, we can write

$$\Pr\left[\frac{Y_1 Y_2}{Y_1 + Y_2} < x\right] \approx \Pr\left[\min(Y_1, Y_2) < x\right] \approx 1 - [1 - F_{Y_1}(x)][1 - F_{Y_2}(x)]. \tag{2.40}$$

It is worth mentioning that such an upper bound can be treated as tight approximation over entire range of operating SNR. Further, substituting CDFs $F_{Y_1}(x)$, $F_{Y_2}(x)$ in (2.40) and obtained result in (2.39) alongwith CDF of Y_{br}, and then averaging over Y_{ar} with its PDF, we get

$$\chi_{ab}^{\text{Sec}}(x) \approx \sum_{\nu=0}^{1}\sum_{\mu=0}^{1}\sum_{l=0}^{\nu(m_{rd}-1)}\sum_{n=0}^{\nu(m_{sr}-1)}\sum_{s=0}^{\mu(m_{br}-1)} \frac{(-1)^{\nu+\mu}\omega_l^{\nu}}{\Gamma(m_{ar})}\omega_n^{\nu}\omega_s^{\mu}\Gamma(\tilde{l})\left(\frac{m_{ar}}{\Omega_{ar}}\right)^{m_{ar}}$$
$$\times\left(\frac{m_{br}}{\Omega_{br}}\right)^{s}\left(\frac{m_{rd}}{\Omega_{rd}Q}\right)^{l}\left(\frac{m_{sr}}{\Omega_{sr}P_c}\right)^{n}\frac{x^{l+n}e^{-\frac{\nu m_{sr}x}{\Omega_{sr}P_c}}}{\left(\frac{\nu m_{rd}x}{\Omega_{rd}Q}+\frac{\mu m_{br}}{\Omega_{br}}+\frac{m_{ar}}{\Omega_{ar}}\right)^{\tilde{l}}}. \tag{2.41}$$

On plugging (2.41) in (2.37), while representing the term in denominator with Meijer's G-function as done in (2.23), and then performing the required integration, we get $\mathcal{P}_{e_{ab}}^{\text{Sec}}$ as given in (2.38). Similarly, $\mathcal{P}_{e_{ba}}^{\text{Sec}}$ can be obtained by interchanging indices $\{a, b\}$ in $\mathcal{P}_{e_{ab}}^{\text{Sec}}$. Finally, using $\mathcal{P}_{e_{ab}}^{\text{Sec}}$ and $\mathcal{P}_{e_{ba}}^{\text{Sec}}$, the average error probability can be evaluated from (2.37). ∎

From the preceding analysis, we can infer that although the performance of secondary system depends on the parameters of primary channels, it is greatly influenced by the direct $C_s - C_{d_n}$ channel parameters and number of SU destinations N due to the exploitation of multiuser diversity.

2.4 Average System Throughput

In this section, we evaluate another important performance metric called average system throughput [52], [53] to characterize the mean spectral efficiency of the considered system. Herein, we consider $\mathcal{R}_{\mathcal{P}}$ and $\mathcal{R}_{\mathcal{S}}$ as the target data rates of the primary and secondary systems respectively. As the complete transmission of RSCRN takes place in two time phases, the overall system throughput $\mathcal{R}_{\mathcal{T}}$ can be represented as

$$\mathcal{R}_{\mathcal{T}} = \frac{\mathcal{R}_{\mathcal{P}}}{2}\left[1 - \mathcal{P}_{\text{out}}^{\text{Pri}}(\gamma_P)\right] + \frac{\mathcal{R}_{\mathcal{S}}}{2}\left[1 - \mathcal{P}_{\text{out}}^{\text{Sec}}(\gamma_S)\right], \tag{2.42}$$

with $\gamma_P = 2^{\mathcal{R}_{\mathcal{P}}} - 1$ and $\gamma_S = 2^{2\mathcal{R}_{\mathcal{S}}} - 1$. Here, the overall throughput $\mathcal{R}_{\mathcal{T}}$ for the RSCRN can be readily obtained by substituting $\mathcal{P}_{\text{out}}^{\text{Pri}}(\gamma_P)$ and $\mathcal{P}_{\text{out}}^{\text{Sec}}(\gamma_S)$ from (2.14) and (2.25), respectively, into (2.42).

2.5 Numerical and Simulation Results

In this section, we present the numerical and simulation results to validate our theoretical analysis for considered RSCRN. For this, we consider a two-dimensional (x, y) topology, whereby the primary network nodes T_a and T_b are located at $(0, 0.5)$ and $(1, 0.5)$ respectively. Whereas, the secondary nodes C_s, C_{d_n}, and C_r are placed at $(0, 0)$, $(1, 0)$, and $(0.5, d)$, respectively. We set $\gamma_{\text{th}} = 0$ dB, $P_c = 5$ dB, and assume d_{ij} as the distance between corresponding links so that $\Omega_{ij} = d_{ij}^{-4}$.

In Fig. 2.2, we plot the OP curves for primary system versus power P under different fading parameters (m_{ar}, m_{br}), and relay locations. We also set $Q = 5$ dB and $m_{sr} = 2$. First, we found that the analytical curves are in perfect match with the simulation results. From various curves, it is apparent that the outage performance of two-way primary system improves as fading parameters (m_{ar}, m_{br}) increase from $(2, 2)$ to $(3, 3)$. Further, we examine the impact of relay position d on the performance of primary system. Clearly, the performance of primary system degrades as d changes from 0.5 to 0.4. This is due to the increase in interference power level at the PU terminals since the relay moves closer to the SU transmitter

C_s. On the contrary, performance of primary system improves when relay moves away from C_s i.e., when d increases.

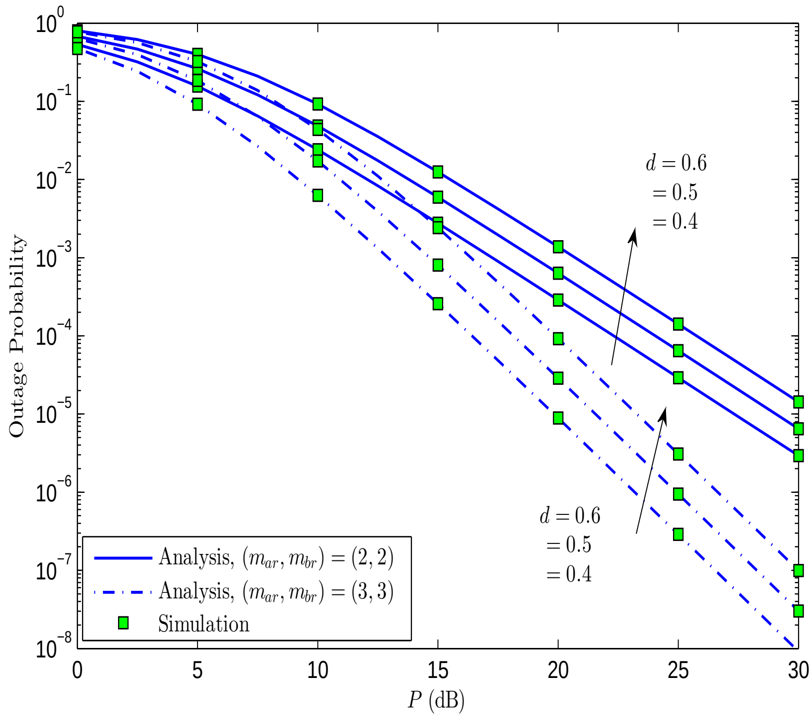

Figure 2.2: Outage probability of primary system with varying d and fading parameters.

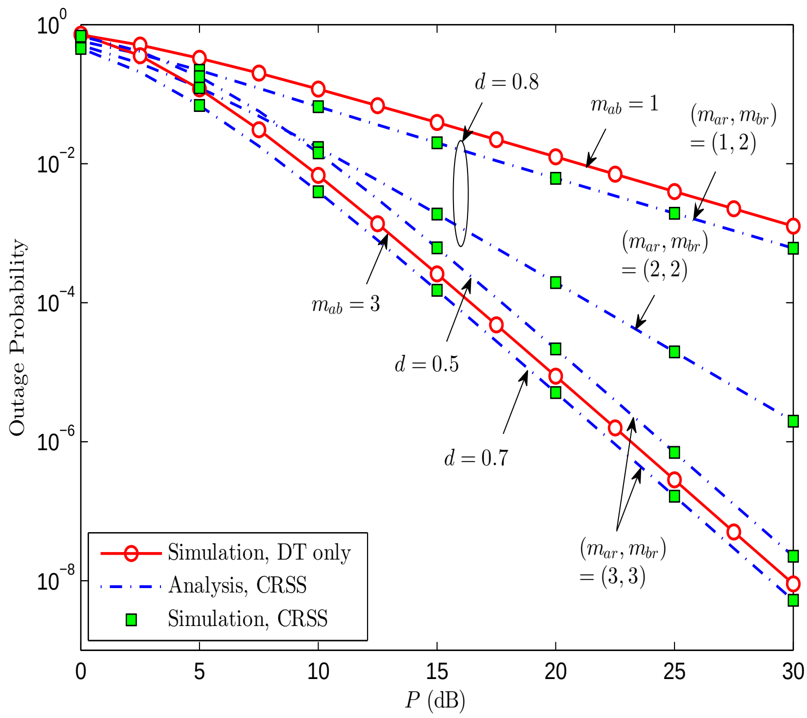

Figure 2.3: Outage probability of primary system with or without relay sharing.

To investigate the effectiveness of the proposed RSCRN, we also compare the performance of primary system with bi-directional direct transmissions (DT) only (i.e., without relay sharing) in Fig. 2.3. Herein, we obtain the outage performance of DT only through simulations by assuming (m_{ab}, Ω_{ab}) as the parameters for direct channel between T_a and T_b. By setting $\Omega_{ab} = 1$, we plot OP curves of DT only for the cases $m_{ab} = 1$ and $m_{ab} = 3$. Comparing the curve for $m_{ab} = 1$ with $(m_{ar}, m_{br}) = (1, 2)$ and $Q = 5$ dB at fixed relay location $d = 0.8$, we can see that the considered RSCRN outperforms DT only in terms of primary system performance. However, the performance of former improves significantly when relay links become better i.e., $(m_{ar}, m_{br}) = (2, 2)$. Note that, depending upon the relay location d, there may be instances where the performance of RSCRN is poorer than the DT only (e.g., refer the case for $d = 0.5$ when $m_{ab} = 3$, $(m_{ar}, m_{br}) = (3, 3)$). Importantly, even for such cases, the performance of RSCRN can be made better if the relay location is chosen appropriately i.e., $d = 0.7$.

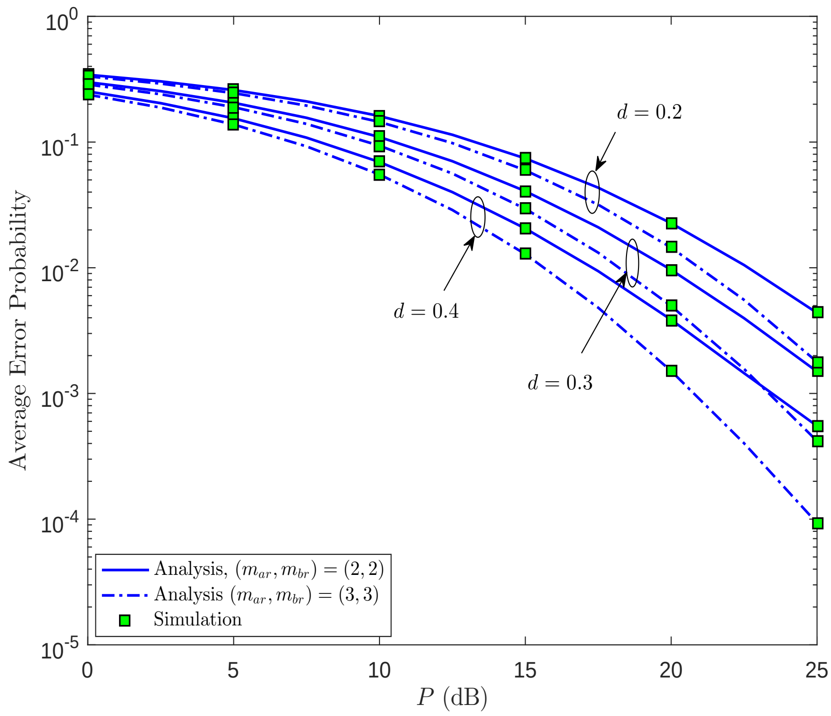

Figure 2.4: Average error probability of primary system for BPSK with varying d and fading parameters.

Fig. 2.4 shows the average error probability curves versus P for primary system considering BPSK modulation. Setting $P_c = Q = 10$ dB, it is apparent that the error performance improves as the fading severity reduces. Also, as expected, the

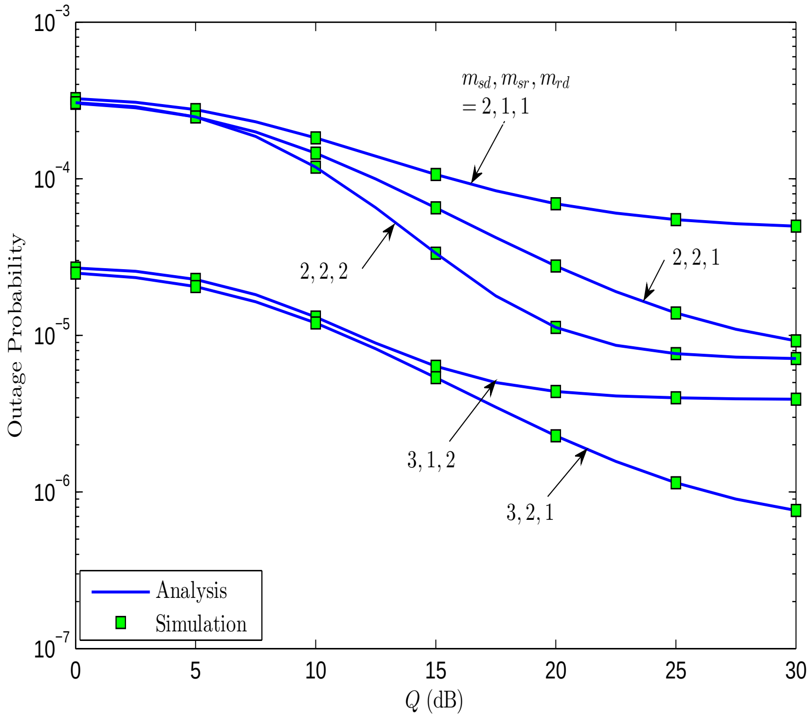

Figure 2.5: Outage probability of secondary system with various fading parameters.

variation in d affects the performance significantly. As the relay moves away from the SU source (i.e., as the value of d increases), the interference from SU signal weakens and thereby the error performance improves.

In Fig. 2.5, we investigate the outage performance of secondary system for the proposed RSCRN model. Setting $(m_{ar}, m_{br}) = (2, 1)$ and $N = 4$, we plot OP curves against Q for various fading parameters (m_{sd}, m_{sr}, m_{rd}). We can see that the simulation results are perfectly matching with the analytical curves. From these curves, one can observe that the outage performance of secondary system improves with the increase of parameters (m_{sd}, m_{sr}, m_{rd}). This is expected because of the improved fading conditions of the direct and/or relaying paths. More importantly, referring the cases $(m_{sd}, m_{sr}, m_{rd}) = (3, 1, 2)$ and $(3, 2, 1)$, we infer that the performance of secondary system is dominated by the fading condition of the first hop ($C_s \to C_r$ link) as compared to the second hop ($C_r \to C_{d_n}$ link). Furthermore, at high Q, secondary system performance appears to be saturated, as SU transmit power P_c is kept fixed.

Fig. 2.6 illustrates the impact of relay location d and number of SU destinations N on the performance of secondary system. Here, it can be observed that the performance of secondary system improves as d changes from 0.7 to 0.5 (or 0.3).

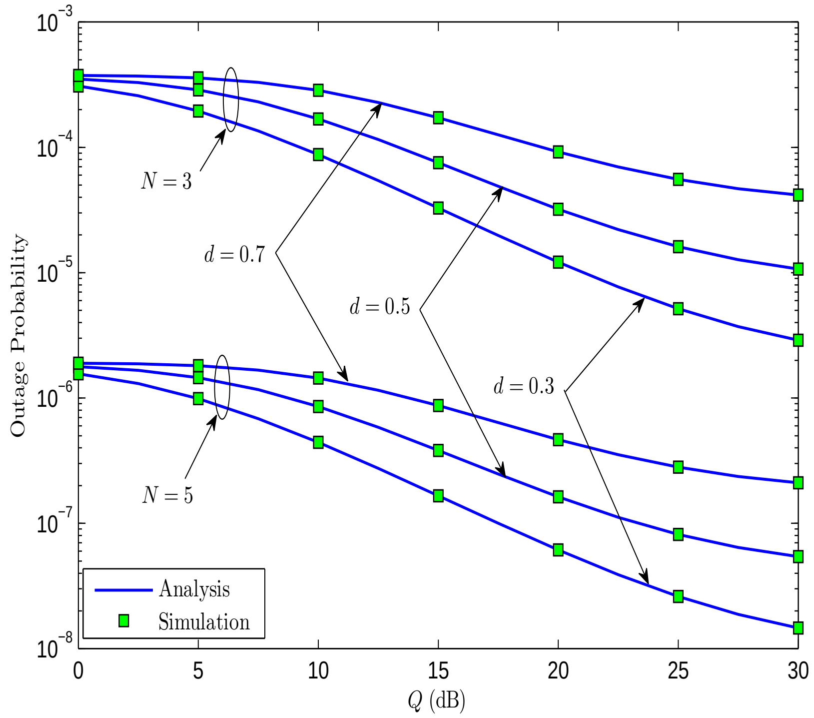

Figure 2.6: Outage probability of secondary system with varying d and N.

This is attributed to the fact that as the relay shifts near to the SU terminals (i.e., C_s and C_{d_n}), the attenuation due to path loss lessens. Moreover, the secondary system performance improves notably with the increase of N. This could be due to the exploitation of multiuser diversity in the secondary system.

In Fig. 2.7, we plot the average error probability curves versus Q for the secondary system. With $(m_{ar}, m_{br}) = (1, 1)$, we investigate the error performance with various fading parameters for BPSK modulation. From the curves, it is apparent that for lower values of Q, the error performance remains unchanged for the same m_{sd}. While the performance improves at high Q with better channel conditions. Furthermore, increase in N also aids in the performance because of multiuser scheduling.

Fig. 2.8 demonstrates the average throughput offered by RSCRN against Q. Here, we set $P_s = 10$ dB, $P = 15$ dB, and $m_{ij} = 3$, where $i \in \{a, b, s, r\}$, $j \in \{r, d\}$ and $i \neq j$. By assuming $\mathcal{R}_{\mathcal{P}} = \mathcal{R}_{\mathcal{S}} = \mathcal{R}_{\mathcal{T}}/2$, it can be seen from the respective curves that when the target rate is kept low as $\mathcal{R}_{\mathcal{T}} = 1$ bps/Hz, the achievable rate of RSCRN rapidly approaches the target rate. While for the higher target rate such as $\mathcal{R}_{\mathcal{T}} = 3$ bps/Hz, the average throughput is limited for lower values of Q. However, as the value of Q increases, the average throughput offered by RSCRN tends to approach the target rate.

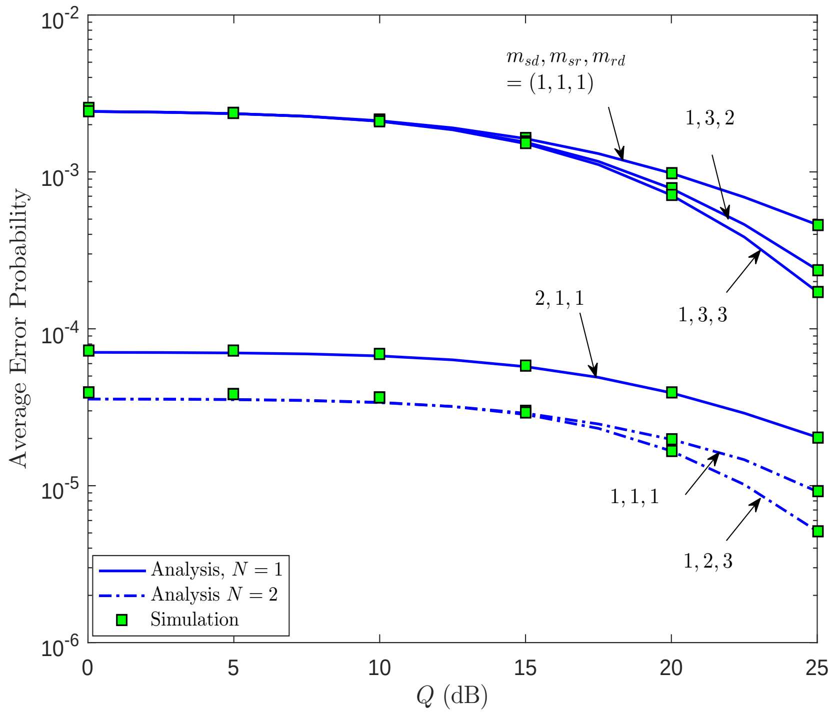

Figure 2.7: Average error probability of secondary system for BPSK with various fading parameters.

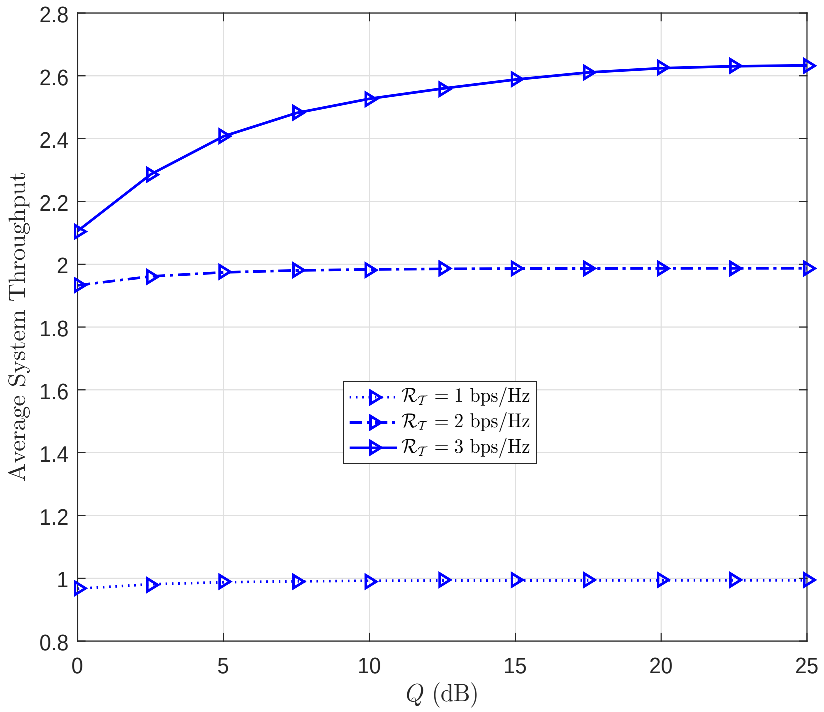

Figure 2.8: The average throughput of overall system.

2.6 Summary

In this chapter, we analyzed the performance of a RSCRN with bi-directional primary communications employing AF-based MABC protocol. We derived the closed-form expressions of outage probability and average error probability for both primary and secondary systems under Nakagami-m fading channels. We have also investigated the average system throughput offered by the RSCRN. Our results illustrated that, leveraging with two-way primary communications, the proposed RSCRN offers higher spectral efficiency. Moreover, by exploiting the advantages of multiuser cooperation, reliability of SU communication is also improved significantly. Finally, we validated our theoretical developments using Monte Carlo simulations.

CHAPTER 3

ADAPTIVE LINK UTILIZATION FOR COGNITIVE TWO-WAY RELAY NETWORKS

The wireless mobile data traffic is assumed to increase 1000-fold by the year 2020, which inevitably necessitates the efficient utilization of available scarce spectrum resources for 5G and beyond wireless networks [54]. To this end, the concept of spectrum sharing with cognitive radio has been envisioned as a promising technology to alleviate the problem of spectrum scarcity [2]. This hierarchical dynamic spectrum access technique enables the SUs to share the spectrum concurrently with the PUs without deteriorating the QoS of PUs. In a cognitive radio network, access to the licensed spectrum can be facilitated by using underlay, overlay, and interweave approaches [5]. To realize this in underlay spectrum sharing approach, the transmission power of SU is strictly constrained to avoid any harmful interference to the PU [55]. Moreover, the interference from primary transmissions to the SU can cause significant degradation in its performance. It would thus be implausible for the SUs to maintain their own QoS under spectrum sharing conditions. For this reason, cooperative relaying techniques [3] have been applied to such systems and shown to provide notable performance improvement over fading channels [56]. While various works investigated the performance of underlay CRNs using traditional AF [57], [22] and DF [58], [59] relaying protocols, they have neglected the primary transmitter's interference on the secondary communications. The impact of PU's interference on the performance of SUs has been considered in [60], [61]. As such, few works have considered incremental relaying [62]-[65] over conventional AF and DF relaying in the context of cognitive radio networks. Albeit, most of these works have focused on obtaining instantaneous CSI pertaining to the links between secondary transmitters and primary receivers to constrain the SUs' transmit power.

However, acquiring this instantaneous CSI is typically difficult and may invoke additional complexity. In contrast, the average CSI seems more viable as it can be determined using transmission distance, frequency of radio waves, etc. With regards to this, the authors in [56], [66], [67] have considered fading-averaged interference constraints at the primary receiver.

On another front, two-way CRNs (TWCRNs) have been studied extensively in the literature that exploits network coding techniques to further improve the spectral efficiency [43], [68]. Mainly two protocols have been considered for such TWCRNs, namely two-phase MABC [11] and three-phase TDBC [69], [12], that offer higher spectral efficiency than the conventional one-way relaying counterparts. These protocols are integrated with traditional AF and DF-based relay processing for bi-directional communications in TWCRNs. Nevertheless, MABC protocol needs to satisfy more pronounced interference constraints in anticipation with the simultaneous transmissions from two sources, and thereby poses an impediment to its application in underlay TWCRNs. On the contrary, the TDBC protocol seems to be more viable for such networks since it avoids simultaneous transmissions at the two sources. More importantly, TDBC can make use of the direct link which could help attaining the required QoS for SUs. Although some recent works have studied the performance of underlay TWCRNs using DF-based TDBC [70], [71] and MABC [72] in Rayleigh fading, they have ignored the utilization of direct link that can potentially improve the performance of SUs without incurring any additional costs. Despite a quantum of works on overlay models [73]-[75], the literature considering underlay TWCRNs with exploitation of a direct link remain scarce. For instance, more recent works have considered underlay models with focus on utilizing either an idle PU [76] or full-duplex radios [77] for two-way relaying in the absence of direct link.

Aiming to ensure QoS of the SUs, in this chapter, we investigate the performance of a TDBC protocol in underlay TWCRNs by considering the joint effects of direct and relay links in the presence of both PU's interference and constraints. Specifically, we consider two DF-based relaying strategies viz., fixed relaying and incremental relaying, and compare their performances in terms of important metrics to provide useful insights for the design of 5G and beyond wireless networks. We propose an adaptive link utilization scheme (ALUS) that can exploit either a direct link or relay link or both by making use of appropriate diversity combining techniques to improve the performance of underlay TWCRNs employing TDBC protocol. Based on ALUS, we derive closed-form expressions for the outage probability of both DF-based fixed and incremental relaying strategies over generalized Nakagami-m fading channels. We then simplify the obtained expressions in the high-SINR regime to investigate into the achievable diversity orders of the considered system. To further investigate the SUs performance, we conduct a comparative study between the two relaying strategies in terms of expected spectral efficiency and average transmission time. As the incremental relaying makes an efficient use of the degrees of freedom of the channel by exploiting the limited feedback from the destination, it shows superior performance over fixed one towards the deployment in 5G and beyond wireless networks.

The rest of the chapter is organized as follows. In Section 3.1, we present the descriptions of TWCRN. In Section 3.2, we analyze the performance of secondary system for DF-based fixed relaying by deriving the closed-form expression of outage probability, its approximation at high SINR, and expected spectral efficiency. Likewise, the performance analysis is carried out in Section 3.3 for the case of incremental relaying. In Section 3.4, we quantify the average end-to-end transmission time for both fixed and incremental relaying. Numerical and simulation results are provided in Section 3.5, and finally, summary of the chapter is presented in Section 3.6.

3.1 System Descriptions

As shown in Fig. 3.1, we consider an underlay TWCRN[1], wherein secondary sources S_a and S_b exchange their messages with the help of a secondary relay[2] S_r employing a TDBC protocol. The nodes T_c and T_p represent primary transmitter and primary receiver, respectively[3]. Herein, we consider that the secondary nodes S_a, S_r, and S_b are inflicted by the interference from primary transmitter T_c. Albeit, the primary

[1]The considered TWCRN may find potential applications in 5G cellular systems wherein the QoS for SUs is also anticipated. For instance, the SUs may correspond to the femtocell users underlaying in a macrocell [76].

[2]Since the femotocell SUs generally have low power and shorter transmission distance, their coverage can be extended by employing a relay S_r.

[3]Specifically, PUs T_c and T_p may represent a base station and a mobile user, respectively, in a macrocell having the licensed spectrum. Whereas, SUs S_a and S_b can represent a general device-to-device communication system. Moreover, large number of sensors and/or devices in the IoT and in the future massive machine-type communication networks [9], [54] can exchange information using the spectrum sharing technique.

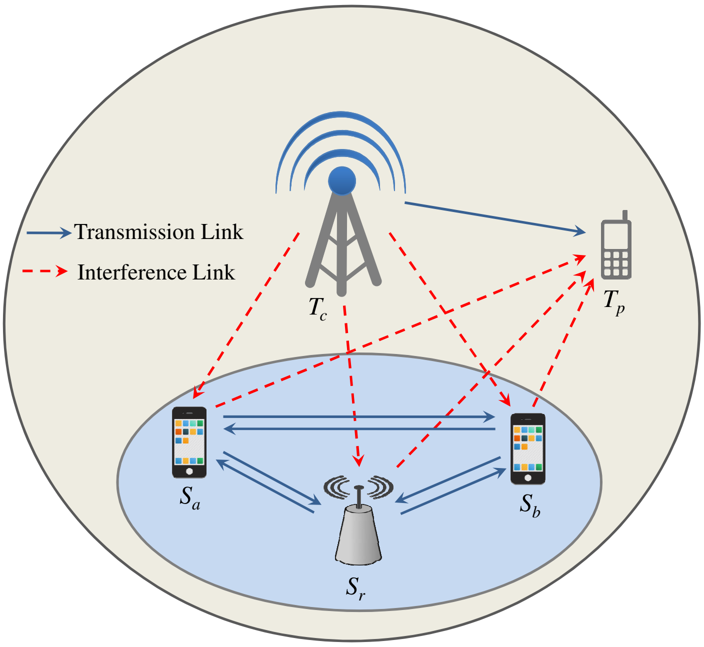

Figure 3.1: System model for TWCRN with direct link.

receiver T_p imposes interference constraints on the transmission powers at the nodes S_a, S_r, and S_b. Each transmitting node operates in half-duplex mode. All the channels are assumed to follow block fading so as they remain constant during a packet transmission but changes independently during the next packet transmission [70], [71]. Let the channels between the transceivers $S_\imath$ and $S_\jmath$ are denoted by $h_{\imath\jmath}$, where $\imath, \jmath \in \{a, r, b\}$ and $\imath \neq \jmath$. Similarly, the channels from $S_\imath$ to PU receiver T_p are denoted as $h_{\imath p}$. And, the channels from T_c to $S_\imath$ are represented as $h_{c\imath}$. All links are assumed to undergo independent Nakagami-m fading and the thermal noise at each receiver is modeled as AWGN variables with mean zero and variance N_o.

With TDBC protocol, the bi-directional message exchange between S_a and S_b takes place in three time phases. In the first phase, S_a transmits its signal x_a with power P_a, and the signals received at S_b and S_r are given, respectively, by

$$y_b^{(\mathrm{I})} = \sqrt{P_a} h_{ab} x_a + \sqrt{P_c} h_{cb} x_c + n_b^{(\mathrm{I})} \tag{3.1a}$$

$$\text{and } y_r^{(\mathrm{I})} = \sqrt{P_a} h_{ar} x_a + \sqrt{P_c} h_{cr} x_c + n_r^{(\mathrm{I})}, \tag{3.1b}$$

where x_c and P_c represent respectively the primary transmit signal and power at T_c, and $n_b^{(\mathrm{I})}$ and $n_r^{(\mathrm{I})}$ represent the respective AWGNs at S_b and S_r. In the second phase, S_b transmits its signal x_b with power P_b, and hence the signals received at S_a and S_r are given, respectively, by

$$y_a^{(\mathrm{II})} = \sqrt{P_b} h_{ba} x_b + \sqrt{P_c} h_{ca} x_c + n_a^{(\mathrm{II})} \tag{3.2a}$$

$$\text{and } y_r^{(\mathrm{II})} = \sqrt{P_b} h_{br} x_b + \sqrt{P_c} h_{cr} x_c + n_r^{(\mathrm{II})}, \tag{3.2b}$$

where $n_a^{(\mathrm{II})}$ and $n_r^{(\mathrm{II})}$ are AWGNs at the respective nodes. As stated before, to limit the interference at primary receiver T_p, the transmit power at S_a and S_b are constrained as $P_a = \frac{Q}{\mathbb{E}(|h_{ap}|^2)}$ and $P_b = \frac{Q}{\mathbb{E}(|h_{bp}|^2)}$, respectively, where Q denotes the maximum tolerable interference at T_p. Consequently, the resultant SINR via direct link at S_b and S_a (in first and second phases) can be given, respectively, by

$$\gamma_{ab} = \frac{\lambda_Q |h_{ab}|^2}{\mathbb{E}(|h_{ap}|^2)\big(\lambda_c |h_{cb}|^2 + 1\big)} \tag{3.3a}$$

$$\text{and } \gamma_{ba} = \frac{\lambda_Q |h_{ba}|^2}{\mathbb{E}(|h_{bp}|^2)\big(\lambda_c |h_{ca}|^2 + 1\big)}, \tag{3.3b}$$

where $\lambda_Q = \frac{Q}{N_o}$ and $\lambda_c = \frac{P_c}{N_o}$. Further, the SINR at S_r in the first and second phases can be given, respectively, as

$$\gamma_{ar} = \frac{\lambda_Q |h_{ar}|^2}{\mathbb{E}(|h_{ap}|^2)\big(\lambda_c |h_{cr}|^2 + 1\big)} \tag{3.4a}$$

$$\text{and } \gamma_{br} = \frac{\lambda_Q |h_{br}|^2}{\mathbb{E}(|h_{bp}|^2)\big(\lambda_c |h_{cr}|^2 + 1\big)}. \tag{3.4b}$$

In what follows, we discuss the relaying strategies with ALUS for the bi-directional communication in underlay TWCRN.

3.1.1 DF-based Fixed Relaying

In fixed relaying transmission, the relay first attempts to decode the received signals broadcasted from transceiver nodes S_a and S_b in first and second phases. After decoding, it forwards the signal to the respective destinations in an attempt to achieve diversity. Let $\mathcal{R}_T$ be the target rate for successful decoding and $\mathcal{D}(r)$ be the associated successful decoding set for any or both of the signals x_a and x_b at S_r. The successful decoding set $\mathcal{D}(r)$ can be represented as

$$\mathcal{D}(r) = \{i \in \{a, b\} : \mathcal{I}_{ir} \geq \mathcal{R}_T\}, \tag{3.5}$$

with $\mathcal{I}_{ir}$ as the mutual information given by

$$\mathcal{I}_{ir} = \frac{1}{3} \log_2 (1 + \gamma_{ir}), \tag{3.6}$$

where the pre-log factor $1/3$ accounts for the three-phase transmission process. Then, for the case $\mathcal{D}(r) \neq \{\varnothing\}$, the relay broadcasts a processed signal x_r with power $P_r = \frac{Q}{\mathbb{E}(|h_{rp}|^2)}$ in the third phase. Hereby, $x_r \in \{x_a, x_b\}$ when either x_a or x_b is decoded successfully and $x_r \in \{x_a \oplus x_b\}$ when both the signals are decoded successfully at S_r. Hence, the signals received at S_a and S_b in the third phase are given, respectively, by

$$y_a^{(\mathrm{III})} = \sqrt{P_r} h_{ra} x_r + \sqrt{P_c} h_{ca} x_c + n_a^{(\mathrm{III})} \tag{3.7a}$$

$$\text{and} \quad y_b^{(\mathrm{III})} = \sqrt{P_r} h_{rb} x_r + \sqrt{P_c} h_{cb} x_c + n_b^{(\mathrm{III})}, \tag{3.7b}$$

where $n_a^{(\mathrm{III})}$ and $n_b^{(\mathrm{III})}$ represent the AWGNs at the respective nodes in the third phase. Thus, the resulting SINRs at S_a and S_b in the third phase are given, respectively, by

$$\gamma_{ra} = \frac{\lambda_Q |h_{ra}|^2}{\mathbb{E}(|h_{rp}|^2)\big(\lambda_c |h_{ca}|^2 + 1\big)} \tag{3.8a}$$

$$\text{and} \quad \gamma_{rb} = \frac{\lambda_Q |h_{rb}|^2}{\mathbb{E}(|h_{rp}|^2)\big(\lambda_c |h_{cb}|^2 + 1\big)}. \tag{3.8b}$$

The corresponding mutual information can be given as $\mathcal{I}_{ra} = \frac{1}{3} \log_2 (1 + \gamma_{ra})$ and $\mathcal{I}_{rb} = \frac{1}{3} \log_2 (1 + \gamma_{rb})$. While the mutual information at the nodes via direct link are given as

$$\mathcal{I}_{ab} = \frac{1}{3} \log_2 (1 + \gamma_{ab}) \tag{3.9a}$$

$$\text{and} \quad \mathcal{I}_{ba} = \frac{1}{3} \log_2 (1 + \gamma_{ba}). \tag{3.9b}$$

Note that, for $\mathcal{D}(r) = \{\varnothing\}$, the relay S_r cannot decode any of the signals and no data is further broadcasted. Next, we describe the DF-based incremental relaying strategy.

3.1.2 DF-based Incremental Relaying

Incremental relaying is an efficient way to substantially aid to the performance of TWCRN. It exploits the limited feedback from the destination terminal to dramatically improve the spectral efficiency [3]. In this, the cooperation from the relay is invoked only when the direct transmission fails. And, once the cooperation is triggered, its operation becomes similar to the fixed relaying. Hereby, firstly, nodes S_a and S_b transmit signals to their respective destinations as well as to the relay node S_r in first two consecutive time slots. Then, depending on the quality of the received direct link signals, corresponding receiver nodes S_b and S_a decide whether relaying transmission is required or not by sending a feedback to the relay. For deciding the success/failure of the direct communications, their mutual information can be defined as

$$\mathcal{I}_{ab}^{d} = \log_2\left(1+\gamma_{ab}\right) \tag{3.10a}$$

$$\text{and} \quad \mathcal{I}_{ba}^{d} = \log_2\left(1+\gamma_{ba}\right). \tag{3.10b}$$

For instance, considering the signal reception at node S_b, if the mutual information exceeds the one-sided target transmission rate $\mathcal{R}_{\mathcal{T}}$ i.e., $\mathcal{I}_{ab}^{d} > \mathcal{R}_{\mathcal{T}}$, S_b provides a positive acknowledgment to S_r by sending a single bit indicating the success of the direct transmission. In such a case, relaying transmission is not needed. Otherwise, a negative acknowledgment is given and the relay S_r forwards the processed signal x_r in the subsequent time slot. In the next subsection, we present the detailed discussion on the processing at the nodes S_a and S_b to retrieve their respective intended signals.

3.1.3 Proposed Adaptive Link Utilization Scheme (ALUS)

Herein, we discuss the ALUS[4] for bi-directional exchange of messages between the secondary nodes in TWCRNs. As noted earlier, based on the decoding of signals received in the first two phases, the relay S_r transmits different signals in the third phase. There are four possible scenarios at S_r: (i) only x_a is decoded, (ii) only x_b is decoded, (iii) both x_a and x_b are decoded, and (iv) neither x_a nor x_b is decoded. Consequently, the signals received at S_a and S_b would also depend on these decoding scenarios. To retrieve their desired messages, S_a and S_b can perform an appropriate combining over the received direct link and relay link signals[5]. As such, for the case when relay successfully decodes the signal either from S_a or S_b, the corresponding receiver employs maximal ratio combining (MRC) on the two received copies viz., direct and relaying link signals. When the relay successfully decodes the signal from both S_a and S_b, relay combines the decoded symbols using bitwise xor operation. In such case, the relay link signal and direct link signal are different due to use of network coding hence MRC can not be applied at the nodes S_a and S_b. In fact, they can adopt selection combining (SC) to select best available signal among the direct

[4]The scheme is named adaptive as it exploits both direct and relay links in an adaptive manner depending on the decoding at the relay, and is, thereby, helpful essentially in deploying the appropriate diversity combining receiver at the destination nodes.

[5]The occurrence of a particular scenario is assumed to be conveyed to the nodes S_a and S_b via a simple medium-access control messages [73] in order to facilitate the appropriate combining of signals.

and relay links. For the case when relay is unable to decode any of the signals from S_a or S_b, the corresponding receivers still have availability of the direct link signals. We summarize the ALUS in Algorithm 1.

Algorithm 1 : ALUS

Relay S_r receives the signals from S_a and S_b in first two time phases
for $\mathcal{D}(r) \neq \{\varnothing\}$ **do**
  if $x_r = x_a$ **then**
S_b performs MRC on the two received signals viz., direct link and relay link signals. Whereas, S_a retrieves the message from direct link signal only
  else if $x_r = x_b$ **then**
S_b selects the available direct link signal. Whereas, S_a performs MRC on the direct link and the relay link signal components
  else if $x_r = x_a \oplus x_b$ **then**
S_a and S_b adopt SC on the direct and relay links signal
  end if
end for
for $\mathcal{D}(r) = \{\varnothing\}$ **do**
Both S_a and S_b extract their messages from available direct link signals
end for

Although the ALUS utilizes three time phases, it would improve the system performance with the exploitation of direct link, as illustrated in subsequent sections.

It is worth remarking that the ALUS can offer a low complexity implementation than the two-phase MABC owing to use of time division multiplexing. In fact, the proposed scheme allows the relay S_r to receive signals from S_a and S_b in successive phases and thereby easing out the decoding process, especially in the presence of interference [75]. This is in contrast to the two-phase MABC scheme [11], wherein the signals are received simultaneously under a multi-access scenario. Furthermore, the implementation of ALUS remains same for both the DF-based relaying strategies.

3.2 Performance Analysis of Fixed Relaying

In this section, we conduct performance analysis for fixed relaying with ALUS under Nakagami-m fading. For subsequent analysis, we use $g_{uv} = |h_{uv}|^2$, with $u, v \in \{a, r, b, p, c\}$ and $u \neq v$ for notational simplicity. As such, g_{uv} follows Gamma distribution with severity parameter m_{uv} and fading power Ω_{uv}. Its PDF and CDF are given, respectively, by

$$f_{g_{uv}}(z) = \frac{1}{\Gamma(m_{uv})} \left(\frac{m_{uv}}{\Omega_{uv}}\right)^{m_{uv}} z^{m_{uv}-1} e^{-\frac{m_{uv} z}{\Omega_{uv}}} \tag{3.11}$$

$$\text{and} \quad F_{g_{uv}}(z) = \frac{1}{\Gamma(m_{uv})} \Upsilon\left(m_{uv}, \frac{m_{uv} z}{\Omega_{uv}}\right). \tag{3.12}$$

3.2.1 Outage Probability Evaluation

An outage event is said to occur in the system when the instantaneous SINR at any SU receiver falls below a specified threshold γ_{th}, where $\gamma_{\text{th}} = 2^{3\mathcal{R}_{\mathcal{T}}} - 1$. Therefore, based on the ALUS, the outage probability at S_b can be formulated as

$$\mathcal{P}_{\text{out}}^{\text{FR}}(\gamma_{\text{th}}) = \underbrace{\Pr\left[\gamma_{ab} < \gamma_{\text{th}}, \gamma_{ar} < \gamma_{\text{th}}\right]}_{\mathcal{P}_{\text{DL}}^{\text{FR}}(\gamma_{\text{th}})} + \underbrace{\Pr\left[\gamma_{ab} + \gamma_{rb} < \gamma_{\text{th}}, \gamma_{ar} \geq \gamma_{\text{th}}, \gamma_{br} < \gamma_{\text{th}}\right]}_{\mathcal{P}_{\text{MRC}}^{\text{FR}}(\gamma_{\text{th}})}$$
$$+ \underbrace{\Pr\left[\max(\gamma_{ab}, \gamma_{rb}) < \gamma_{\text{th}}, \gamma_{ar} \geq \gamma_{\text{th}}, \gamma_{br} \geq \gamma_{\text{th}}\right]}_{\mathcal{P}_{\text{SC}}^{\text{FR}}(\gamma_{\text{th}})}, \tag{3.13}$$

wherein the three terms are followed from Algorithm 1. Clearly, to derive the $\mathcal{P}_{\text{out}}^{\text{FR}}(\gamma_{\text{th}})$ in (3.13), we need to evaluate the three probabilities $\mathcal{P}_{\text{DL}}^{\text{FR}}(\gamma_{\text{th}})$, $\mathcal{P}_{\text{MRC}}^{\text{FR}}(\gamma_{\text{th}})$ and $\mathcal{P}_{\text{SC}}^{\text{FR}}(\gamma_{\text{th}})$. On invoking the SINR expressions from (3.3) and (3.4), one can represent $\mathcal{P}_{\text{DL}}^{\text{FR}}(\gamma_{\text{th}})$ as

$$\mathcal{P}_{\text{DL}}^{\text{FR}}(\gamma_{\text{th}}) = \Pr\left[\lambda_Q^{ap}\frac{g_{ab}}{X} < \gamma_{\text{th}}, \lambda_Q^{ap}\frac{g_{ar}}{Y} < \gamma_{\text{th}}\right], \tag{3.14}$$

where $\lambda_Q^{ap} = \frac{\lambda_Q}{\mathbb{E}(g_{ap})}$, $X = \lambda_c g_{cb} + 1$ and $Y = \lambda_c g_{cr} + 1$. As the two events in (3.14) are independent, we can express

$$\mathcal{P}_{\text{DL}}^{\text{FR}}(\gamma_{\text{th}}) = \int_0^\infty \int_0^\infty F_{g_{ab}|X}\Big(\frac{\gamma_{\text{th}}x}{\lambda_Q^{ap}}\Big) F_{g_{ar}|Y}\Big(\frac{\gamma_{\text{th}}y}{\lambda_Q^{ap}}\Big) f_X(x) f_Y(y) dx dy. \tag{3.15}$$

Since X is a linear transformation of g_{cb}, its PDF $f_X(x)$ can be determined under Nakagami-m fading as

$$f_X(x) = \frac{\left(\frac{m_{cb}}{\Omega_{cb}}\right)^{m_{cb}}}{\lambda_c \Gamma(m_{cb})}\Big(\frac{x-1}{\lambda_c}\Big)^{m_{cb}-1} e^{-\frac{m_{cb}(x-1)}{\lambda_c \Omega_{cb}}}. \tag{3.16}$$

Similarly, the PDF $f_Y(y)$ can be obtained and given by replacing X, x, m_{cb}, and Ω_{cb} with Y, y, m_{cr}, and Ω_{cr} respectively in (3.16). On simplifying $f_X(\cdot)$ and $f_Y(\cdot)$ using binomial expansion [49, eq. 1.111] and using the results along with the required CDFs into (3.15), and after manipulating, we obtain

$$\mathcal{P}_{\text{DL}}^{\text{FR}}(\gamma_{\text{th}}) = \int_1^\infty \int_1^\infty \sum_{n=0}^{m_{cb}-1} \mathcal{C}_n^{m_{cb}-1} \frac{(-1)^{m_{cb}-n-1} e^{\frac{m_{cb}}{\Omega_{cb}\lambda_c}}}{\Gamma(m_{cb})\Gamma(m_{ab})} \Big(\frac{m_{cb}}{\Omega_{cb}\lambda_c}\Big)^{m_{cb}} \Upsilon\Big(m_{ab}, \frac{m_{ab}\gamma_{\text{th}}}{\Omega_{ab}\lambda_Q^{ap}}x\Big) x^n$$
$$\times e^{-\frac{m_{cb}}{\Omega_{cb}\lambda_c}x} \sum_{s=0}^{m_{cr}-1} \mathcal{C}_s^{m_{cr}-1} \frac{(-1)^{m_{cr}-s-1} e^{\frac{m_{cr}}{\Omega_{cr}\lambda_c}}}{\Gamma(m_{cr})\Gamma(m_{ar})} \Big(\frac{m_{cr}}{\Omega_{cr}\lambda_c}\Big)^{m_{cr}} \Upsilon\Big(m_{ar}, \frac{m_{ar}\gamma_{\text{th}}}{\Omega_{ar}\lambda_Q^{ap}}y\Big) y^s e^{-\frac{m_{cr}}{\Omega_{cr}\lambda_c}y} dx dy. \tag{3.17}$$

Finally, on applying the series form of $\Upsilon(\alpha, x)$ [49, eq. 8.352.1] into (3.17), and subsequently simplifying the result with the aid of [49, eqs. 0.314, 3.351.2], we get the expression of $\mathcal{P}_{\text{DL}}^{\text{FR}}(\gamma_{\text{th}})$ as

$$\begin{aligned}\mathcal{P}_{\text{DL}}^{\text{FR}}(\gamma_{\text{th}}) = &\sum_{n=0}^{m_{cb}-1}\sum_{s=0}^{m_{cr}-1}\sum_{t=0}^{1}\sum_{v=0}^{t(m_{ab}-1)}\sum_{\imath=0}^{1}\sum_{q=0}^{\imath(m_{ar}-1)} \frac{(-1)^{\tilde{\kappa}}\omega_v^t\omega_q^\imath \mathcal{C}_n^{m_{cb}-1}\mathcal{C}_s^{m_{cr}-1}}{\Gamma(m_{cb})\Gamma(m_{cr})} e^{\left(\frac{m_{cb}}{\Omega_{cb}\lambda_c}+\frac{m_{cr}}{\Omega_{cr}\lambda_c}\right)} \\ &\times \left(\frac{m_{cb}}{\Omega_{cb}\lambda_c}\right)^{m_{cb}}\left(\frac{m_{cr}}{\Omega_{cr}\lambda_c}\right)^{m_{cr}}\left(\frac{m_{ab}\gamma_{\text{th}}}{\Omega_{ab}\lambda_Q^{ap}}\right)^{v}\left(\frac{m_{ar}\gamma_{\text{th}}}{\Omega_{ar}\lambda_Q^{ap}}\right)^{q}\left(\frac{t m_{ab}\gamma_{\text{th}}}{\Omega_{ab}\lambda_Q^{ap}}+\frac{m_{cb}}{\Omega_{cb}\lambda_c}\right)^{-\tilde{v}} \\ &\times \left(\frac{\imath m_{ar}\gamma_{\text{th}}}{\Omega_{ar}\lambda_Q^{ap}}+\frac{m_{cr}}{\Omega_{cr}\lambda_c}\right)^{-\tilde{s}}\Gamma\left(\tilde{v}, \frac{t m_{ab}\gamma_{\text{th}}}{\Omega_{ab}\lambda_Q^{ap}}+\frac{m_{cb}}{\Omega_{cb}\lambda_c}\right)\Gamma\left(\tilde{s}, \frac{\imath m_{ar}\gamma_{\text{th}}}{\Omega_{ar}\lambda_Q^{ap}}+\frac{m_{cr}}{\Omega_{cr}\lambda_c}\right), \end{aligned} \tag{3.18}$$

where $\tilde{\kappa} = m_{cb} + m_{cr} + t + \imath - n - s - 2$, $\tilde{v} = n + v + 1$, $\tilde{s} = s + q + 1$, and the coefficients $\omega_l^\jmath$, for $0 \le l \le \jmath(m_o - 1)$, can be calculated recursively (with $\varepsilon_l = \frac{1}{l!}$) as $\omega_0^\jmath = (\varepsilon_0)^\jmath$, $\omega_1^\jmath = \jmath(\varepsilon_1)$, $\omega_{\jmath(m_o-1)}^\jmath = (\varepsilon_{m_o-1})^\jmath$, $\omega_l^\jmath = \frac{1}{l\varepsilon_0}\sum_{q=1}^{l}[q\jmath - l + q]\varepsilon_q\omega_{l-q}^\jmath$ for $2 \le l \le m_o - 1$, and $\omega_l^\jmath = \frac{1}{l\varepsilon_0}\sum_{q=1}^{m_o-1}[q\jmath - l + q]\varepsilon_q\omega_{l-q}^\jmath$ for $m_o \le l < \jmath(m_o - 1)$, with $m_o \in \{m_{ab}, m_{ar}\}$. Next, the $\mathcal{P}_{\text{MRC}}^{\text{FR}}(\gamma_{\text{th}})$ in (3.13) is derived in following lemma.

Lemma 5. *The probability $\mathcal{P}_{MRC}^{FR}(\gamma_{th})$ is given by*

$$\mathcal{P}_{MRC}^{FR}(\gamma_{th}) \approx \Xi\left(1, \frac{1}{2}; \gamma_{th}\right) + \Xi\left(\frac{1}{2}, 1; \gamma_{th}\right) - \Xi\left(\frac{1}{2}, \frac{1}{2}; \gamma_{th}\right), \tag{3.19}$$

where $\Xi(\alpha, \beta; \gamma_{th})$ is given by

$$\begin{aligned}\Xi(\alpha, \beta; \gamma_{th}) = \Theta(\alpha, \beta; \gamma_{th}) &\sum_{s=0}^{m_{cr}-1}\sum_{q=0}^{m_{ar}-1}\sum_{\mu=0}^{1}\sum_{r=0}^{\mu(m_{br}-1)} e^{\frac{m_{cr}}{\Omega_{cr}\lambda_c}}(-1)^{\tilde{s}+\mu}\frac{\omega_r^\mu \mathcal{C}_s^{m_{cr}-1}}{q!\Gamma(m_{cr})}\left(\frac{m_{cr}}{\Omega_{cr}\lambda_c}\right)^{m_{cr}} \\ &\times \left(\frac{m_{ar}\gamma_{th}}{\Omega_{ar}\lambda_Q^{ap}}\right)^{q}\left(\frac{m_{br}\gamma_{th}}{\Omega_{br}\lambda_Q^{bp}}\right)^{r}\left(\frac{m_{ar}\gamma_{th}}{\Omega_{ar}\lambda_Q^{ap}}+\frac{\mu m_{br}\gamma_{th}}{\Omega_{br}\lambda_Q^{bp}}+\frac{m_{cr}}{\Omega_{cr}\lambda_c}\right)^{-\tilde{q}} \\ &\times \Gamma\left(\tilde{q}, \frac{m_{ar}\gamma_{th}}{\Omega_{ar}\lambda_Q^{ap}}+\frac{\mu m_{br}\gamma_{th}}{\Omega_{br}\lambda_Q^{bp}}+\frac{m_{cr}}{\Omega_{cr}\lambda_c}\right). \end{aligned} \tag{3.20}$$

with $\tilde{s} = m_{cr} - s - 1$, $\tilde{q} = q + r + s + 1$, $\lambda_Q^{rp} = \frac{\lambda_Q}{\mathbb{E}(g_{rp})}$, $\lambda_Q^{bp} = \frac{\lambda_Q}{\mathbb{E}(g_{bp})}$, and $\Theta(\alpha, \beta; \gamma_{th})$ is given by

$$\begin{aligned}\Theta(\alpha, \beta; \gamma_{th}) = &\sum_{n=0}^{m_{cb}-1}\sum_{t=0}^{1}\sum_{v=0}^{t(m_{ab}-1)}\sum_{k=0}^{1}\sum_{p=0}^{k(m_{rb}-1)} \frac{1}{\Gamma(m_{cb})}(-1)^{m_{cb}+t+k-n-1}\omega_v^t\omega_p^k\mathcal{C}_n^{m_{cb}-1}e^{\frac{m_{cb}}{\Omega_{cb}\lambda_c}} \\ \times &\left(\frac{m_{cb}}{\Omega_{cb}\lambda_c}\right)^{m_{cb}}\left(\frac{m_{ab}\alpha\gamma_{th}}{\Omega_{ab}\lambda_Q^{ap}}\right)^{v}\left(\frac{m_{rb}\beta\gamma_{th}}{\Omega_{rb}\lambda_Q^{rp}}\right)^{p}\left(\frac{t m_{ab}\alpha\gamma_{th}}{\Omega_{ab}\lambda_Q^{ap}}+\frac{k m_{rb}\beta\gamma_{th}}{\Omega_{rb}\lambda_Q^{rp}}+\frac{m_{cb}}{\Omega_{cb}\lambda_c}\right)^{-(n+v+p+1)} \\ \times &\Gamma\left(n+v+p+1, \frac{t m_{ab}\alpha\gamma_{th}}{\Omega_{ab}\lambda_Q^{ap}}+\frac{k m_{rb}\beta\gamma_{th}}{\Omega_{rb}\lambda_Q^{rp}}+\frac{m_{cb}}{\Omega_{cb}\lambda_c}\right). \end{aligned} \tag{3.21}$$

Proof. Proof is relegated to Appendix A. ■

Likewise, we can express the term $\mathcal{P}_{\rm SC}^{\rm FR}(\gamma_{\rm th})$ in (3.13) as

$$\mathcal{P}_{\rm SC}^{\rm FR}(\gamma_{\rm th}) = \Pr\Big[\lambda_Q^{ap}\frac{g_{ab}}{X} < \gamma_{\rm th}, \lambda_Q^{rp}\frac{g_{rb}}{X} < \gamma_{\rm th}, \lambda_Q^{ap}\frac{g_{ar}}{Y} \geq \gamma_{\rm th}, \lambda_Q^{bp}\frac{g_{br}}{Y} \geq \gamma_{\rm th}\Big]. \tag{3.22}$$

Applying the conditioning approach similar to the previous ones, (3.22) can be further represented as

$$\mathcal{P}_{\rm SC}^{\rm FR}(\gamma_{\rm th}) = \int_0^\infty \int_0^\infty F_{g_{ab}|X}\left(\frac{\gamma_{\rm th}x}{\lambda_Q^{ap}}\right) F_{g_{rb}|X}\left(\frac{\gamma_{\rm th}x}{\lambda_Q^{rp}}\right) \times \overline{F}_{g_{ar}|Y}\left(\frac{\gamma_{\rm th}y}{\lambda_Q^{ap}}\right) \overline{F}_{g_{br}|Y}\left(\frac{\gamma_{\rm th}y}{\lambda_Q^{bp}}\right) f_X(x) f_Y(y) dx dy. \tag{3.23}$$

On inserting the expressions of involved CDFs and PDFs in (3.23), and simplifying the result, $\mathcal{P}_{\rm SC}^{\rm FR}(\gamma_{\rm th})$ can be obtained as

$$\mathcal{P}_{\rm SC}^{\rm FR}(\gamma_{\rm th}) = \Theta(1,1;\gamma_{\rm th}) \sum_{s=0}^{m_{cr}-1} \sum_{q=0}^{m_{ar}-1} \sum_{r=0}^{m_{br}-1} \frac{(-1)^{\tilde{s}}}{q! r! \Gamma(m_{cr})} \mathcal{C}_s^{m_{cr}-1} e^{\frac{m_{cr}}{\Omega_{cr}\lambda_c}} \left(\frac{m_{cr}}{\Omega_{cr}\lambda_c}\right)^{m_{cr}} \left(\frac{m_{ar}\gamma_{\rm th}}{\Omega_{ar}\lambda_Q^{ap}}\right)^q \times \left(\frac{m_{br}\gamma_{\rm th}}{\Omega_{br}\lambda_Q^{bp}}\right)^r \left(\frac{m_{ar}\gamma_{\rm th}}{\Omega_{ar}\lambda_Q^{ap}} + \frac{m_{br}\gamma_{\rm th}}{\Omega_{br}\lambda_Q^{bp}} + \frac{m_{cr}}{\Omega_{cr}\lambda_c}\right)^{-\tilde{q}} \Gamma\left(\tilde{q}, \frac{m_{ar}\gamma_{\rm th}}{\Omega_{ar}\lambda_Q^{ap}} + \frac{m_{br}\gamma_{\rm th}}{\Omega_{br}\lambda_Q^{bp}} + \frac{m_{cr}}{\Omega_{cr}\lambda_c}\right), \tag{3.24}$$

with $\tilde{s} = m_{cr} - s - 1$, $\tilde{q} = q + r + s + 1$, and the function $\Theta(\alpha, \beta; \gamma_{\rm th})$ is the same as given in (3.21). Thus, by invoking (3.18), (3.19), and (3.24) into (3.13), a closed-form expression for the outage probability of fixed relaying strategy is obtained.

3.2.2 High-SINR Analysis of the Outage Probability

To gain better insight, we simplify the previously derived outage probability expression for asymptotic high-SINR regime ($\lambda_Q \to \infty$). For this, we first make use of the series expansion of $\Upsilon(\alpha, x)$ [49, eq. 8.354.1] as

$$\Upsilon(\alpha, x) = x^\alpha \sum_{\varepsilon=0}^{\infty} \frac{(-1)^\varepsilon x^\varepsilon}{\varepsilon!(\alpha+\varepsilon)} \underset{x\to 0}{\simeq} \frac{x^\alpha}{\alpha}, \tag{3.25}$$

into (3.17), and then evaluate the resulting integral to obtain the probability $\mathcal{P}_{\rm DL}^{\rm FR}(\gamma_{\rm th})$ at high SINR as

$$\mathcal{P}_{\rm DL}^{\rm FR}(\gamma_{\rm th}) \simeq \sum_{n=0}^{m_{cb}-1} \sum_{s=0}^{m_{cr}-1} \mathcal{C}_n^{m_{cb}-1} \mathcal{C}_s^{m_{cr}-1} \frac{(-1)^{m_{cb}+m_{cr}-s-n-2} e^{\left(\frac{m_{cb}}{\Omega_{cb}\lambda_c} + \frac{m_{cr}}{\Omega_{cr}\lambda_c}\right)}}{\Gamma(m_{cr})\Gamma(m_{cb})\Gamma(m_{ab}+1)\Gamma(m_{ar}+1)} \times \left(\frac{m_{ab}\Omega_{ap}\gamma_{\rm th}}{\Omega_{ab}}\right)^{m_{ab}} \left(\frac{m_{ar}\Omega_{ap}\gamma_{\rm th}}{\Omega_{ar}}\right)^{m_{ar}} \left(\frac{m_{cb}}{\Omega_{cb}\lambda_c}\right)^{m_{cb}-\tilde{m}_{ab}} \left(\frac{m_{cr}}{\Omega_{cr}\lambda_c}\right)^{m_{cr}-\tilde{m}_{ar}} \times \Gamma\left(\tilde{m}_{ab}, \frac{m_{cb}}{\Omega_{cb}\lambda_c}\right) \Gamma\left(\tilde{m}_{ar}, \frac{m_{cr}}{\Omega_{cr}\lambda_c}\right) \frac{1}{\lambda_Q^{m_{ab}+m_{ar}}}, \tag{3.26}$$

where $\tilde{m}_{ab} = m_{ab} + n + 1$, $\tilde{m}_{ar} = m_{ar} + s + 1$.

Next, to express the probability $\mathcal{P}_{\mathrm{MRC}}^{\mathrm{FR}}(\gamma_{\mathrm{th}})$ at high-SINR, we can asymptotically represent (3.19) as

$$\mathcal{P}_{\mathrm{MRC}}^{\mathrm{FR}}(\gamma_{\mathrm{th}}) \simeq \Psi\Big(1, \frac{1}{2}; \gamma_{\mathrm{th}}\Big) + \Psi\Big(\frac{1}{2}, 1; \gamma_{\mathrm{th}}\Big) - \Psi\Big(\frac{1}{2}, \frac{1}{2}; \gamma_{\mathrm{th}}\Big), \tag{3.27}$$

where $\Psi(\alpha, \beta; \gamma_{\mathrm{th}})$ can be obtained, by applying (3.25) into (3.19) and simplifying subsequently, as

$$\begin{aligned}\Psi(\alpha, \beta; \gamma_{\mathrm{th}}) = &\sum_{s=0}^{m_{cr-1}} \sum_{n=0}^{m_{cb}-1} \frac{\mathcal{C}_n^{m_{cb}-1} \mathcal{C}_s^{m_{cr}-1} (-1)^{m_{cb}+m_{cr}-n-s-2} e^{\left(\frac{m_{cb}}{\Omega_{cb}\lambda_c} + \frac{m_{cr}}{\Omega_{cr}\lambda_c}\right)}}{\Gamma(m_{cb})\Gamma(m_{ab}+1)\Gamma(m_{rb}+1)\Gamma(m_{cr})\Gamma(m_{br}+1)} \\ &\times \left(\frac{m_{ab}\Omega_{ap}\alpha\gamma_{\mathrm{th}}}{\Omega_{ab}}\right)^{m_{ab}} \left(\frac{m_{rb}\Omega_{rp}\beta\gamma_{\mathrm{th}}}{\Omega_{rb}}\right)^{m_{rb}} \left(\frac{m_{cb}}{\Omega_{cb}\lambda_c}\right)^{m_{cb}-\tilde{m}_{ab}} \left(\frac{m_{br}\Omega_{bp}\gamma_{\mathrm{th}}}{\Omega_{br}}\right)^{m_{br}} \\ &\times \left(\frac{m_{cr}}{\Omega_{cr}\lambda_c}\right)^{m_{cr}-\tilde{m}_{br}} \Gamma\left(\tilde{m}_{ab}, \frac{m_{cb}}{\Omega_{cb}\lambda_c}\right) \Gamma\left(\tilde{m}_{br}, \frac{m_{cr}}{\Omega_{cr}\lambda_c}\right) \frac{1}{{\lambda_Q}^{m_{ab}+m_{rb}+m_{br}}}.\end{aligned} \tag{3.28}$$

where $\tilde{m}_{ab} = m_{ab} + m_{rb} + n + 1$ and $\tilde{m}_{br} = m_{br} + s + 1$.

As done for $\mathcal{P}_{\mathrm{MRC}}^{\mathrm{FR}}(\gamma_{\mathrm{th}})$, applying the similar procedure to (3.23), the term $\mathcal{P}_{\mathrm{SC}}^{\mathrm{FR}}(\gamma_{\mathrm{th}})$ at high-SINR can be obtained as

$$\begin{aligned}\mathcal{P}_{\mathrm{SC}}^{\mathrm{FR}}(\gamma_{\mathrm{th}}) \simeq &\sum_{n=0}^{m_{cb}-1} \frac{\mathcal{C}_n^{m_{cb}-1} (-1)^{m_{cb}-n-1}}{\Gamma(m_{cb})\Gamma(m_{ab}+1)\Gamma(m_{rb}+1)} e^{\frac{m_{cb}}{\Omega_{cb}\lambda_c}} \left(\frac{m_{ab}\Omega_{ap}\gamma_{\mathrm{th}}}{\Omega_{ab}}\right)^{m_{ab}} \\ &\times \left(\frac{m_{rb}\Omega_{rp}\gamma_{\mathrm{th}}}{\Omega_{rb}}\right)^{m_{rb}} \left(\frac{m_{cb}}{\Omega_{cb}\lambda_c}\right)^{m_{cb}-\tilde{m}_{ab}} \Gamma\left(\tilde{m}_{ab}, \frac{m_{cb}}{\Omega_{cb}\lambda_c}\right) \frac{1}{{\lambda_Q}^{m_{ab}+m_{rb}}},\end{aligned} \tag{3.29}$$

where $\tilde{m}_{ab} = m_{ab} + m_{rb} + n + 1$.

Thus, by using (3.26), (3.27) and (3.29) into (3.13), the asymptotic outage probability expression is reached. With this, one can infer that the achievable diversity order is $m_{ab} + \min(m_{ar}, m_{rb})$. Note that, at high-SINR, $\mathcal{P}_{\mathrm{MRC}}^{\mathrm{FR}}(\gamma_{\mathrm{th}})$ does not contribute towards quantifying the coding and diversity gains of the system.

3.2.3 Expected Spectral Efficiency

In this subsection, we evaluate another performance metric called expected spectral efficiency [3] for the considered scheme. With fixed relaying, the overall transmission takes place in three time phases and hence the expected spectral efficiency for one-sided transmission can be expressed as

$$\mathcal{R}_s^{\mathrm{FR}} = \frac{\mathcal{R}_{\mathcal{T}}}{3} \left[1 - \mathcal{P}_{\mathrm{out}}^{\mathrm{FR}}(\gamma_{\mathrm{th}})\right]. \tag{3.30}$$

One can readily compute the $\mathcal{R}_s^{\mathrm{FR}}$ in (3.30) by substituting $\mathcal{P}_{\mathrm{out}}^{\mathrm{FR}}(\gamma_{\mathrm{th}})$ from (13). However, at a high-SINR, $\lambda_Q \to \infty$, the expected spectral efficiency approaches to $\mathcal{R}_s^{\mathrm{FR}} \simeq \frac{\mathcal{R}_{\mathcal{T}}}{3}$.

3.3 Performance Analysis of Incremental Relaying

In this section, we derive the outage probability, its high-SINR approximation, and expected spectral efficiency for incremental relaying strategy under Nakagami-m fading.

3.3.1 Outage Probability Evaluation

Based on our proposed ALUS, the outage probability for incremental relaying at S_b can be formulated as

$$\mathcal{P}_{\text{out}}^{\text{IR}} = \underbrace{\Pr[\gamma_{ab} < \gamma_{\text{th}}^{\text{d}}, \gamma_{ar} < \gamma_{\text{th}}]}_{\mathcal{P}_{\text{DL}}^{\text{IR}}} + \underbrace{\Pr[\gamma_{ab} + \gamma_{rb} < \gamma_{\text{th}}, \gamma_{ab} < \gamma_{\text{th}}^{\text{d}}, \gamma_{ar} \geq \gamma_{\text{th}}, \gamma_{br} < \gamma_{\text{th}}]}_{\mathcal{P}_{\text{MRC}}^{\text{IR}}}$$
$$+ \underbrace{\Pr[\max(\gamma_{ab}, \gamma_{rb}) < \gamma_{\text{th}}, \gamma_{ab} < \gamma_{\text{th}}^{\text{d}}, \gamma_{ar} \geq \gamma_{\text{th}}, \gamma_{br} \geq \gamma_{\text{th}}]}_{\mathcal{P}_{\text{SC}}^{\text{IR}}}, \tag{3.31}$$

where $\gamma_{\text{th}}^{\text{d}} = 2^{\mathcal{R}_{\mathcal{T}}} - 1$ and all three terms are followed from the Algorithm 1. Apparently, the probability $\mathcal{P}_{\text{DL}}^{\text{IR}}$ in (3.31) is similar to $\mathcal{P}_{\text{DL}}^{\text{FR}}$ in (3.13) and hence can directly be obtained from (3.18) by replacing the term $m_{ab}\gamma_{\text{th}}$ with $m_{ab}\gamma_{\text{th}}^{\text{d}}$.

Next, the probability $\mathcal{P}_{\text{MRC}}^{\text{IR}}$ is derived in following lemma.

Lemma 6. *The probability $\mathcal{P}_{MRC}^{IR}$ in (3.31) is given as follows*

$$\mathcal{P}_{MRC}^{IR} = \Bigg[\sum_{n=0}^{m_{cb}-1}\sum_{t=0}^{1}\sum_{v=0}^{t(m_{ab}-1)}\sum_{k=0}^{1}\sum_{p=0}^{k(m_{rb}-1)} \frac{1}{\Gamma(m_{cb})}(-1)^{m_{cb}+t+k-n-1}\omega_v^t\omega_p^k\mathcal{C}_n^{m_{cb}-1}e^{\frac{m_{cb}}{\Omega_{cb}\lambda_c}}$$
$$\times\left(\frac{m_{cb}}{\Omega_{cb}\lambda_c}\right)^{m_{cb}}\left(\frac{m_{ab}\gamma_{th}^{d}}{\Omega_{ab}\lambda_Q^{ap}}\right)^{v}\left(\frac{m_{rb}\tilde{\gamma}_{th}}{\Omega_{rb}\lambda_Q^{rp}}\right)^{p}\left(\frac{tm_{ab}\gamma_{th}^{d}}{\Omega_{ab}\lambda_Q^{ap}}+\frac{km_{rb}\tilde{\gamma}_{th}}{\Omega_{rb}\lambda_Q^{rp}}+\frac{m_{cb}}{\Omega_{cb}\lambda_c}\right)^{-(n+v+p+1)}$$
$$\times\Gamma\left(n+v+p+1,\frac{tm_{ab}\gamma_{th}^{d}}{\Omega_{ab}\lambda_Q^{ap}}+\frac{km_{rb}\tilde{\gamma}_{th}}{\Omega_{rb}\lambda_Q^{rp}}+\frac{m_{cb}}{\Omega_{cb}\lambda_c}\right)+\sum_{n=0}^{m_{cb}-1}\sum_{t=0}^{1}\sum_{v=0}^{t(m_{ab}-1)}\sum_{v'=0}^{v}\sum_{l=0}^{m_{rb}+v'-1}$$
$$\times\frac{l!\omega_v^t\mathcal{C}_n^{m_{cb}-1}\mathcal{C}_{v'}^{v}\mathcal{C}_l^{m_{rb}+v'-1}}{\Gamma(m_{rb})\Gamma(m_{cb})}\frac{(-1)^{t+v'+l+m_{cb}-n-1}e^{\frac{m_{cb}}{\Omega_{cb}\lambda_c}}}{\left(\frac{tm_{ab}\lambda_Q^{rp}}{\Omega_{ab}\lambda_Q^{ap}}-\frac{m_{rb}}{\Omega_{rb}}\right)^{l+1}}\left(\frac{\gamma_{th}}{\lambda_Q^{rp}}\right)^{v-v'}\left(\frac{m_{cb}}{\Omega_{cb}\lambda_c}\right)^{m_{cb}}\left(\frac{\lambda_Q^{rp}}{\lambda_Q^{ap}}\right)^{v'}$$
$$\times\left(\frac{m_{ab}}{\Omega_{ab}}\right)^{v}\left(\frac{m_{rb}}{\Omega_{rb}}\right)^{m_{rb}}\Bigg[\left(\frac{m_{cb}}{\Omega_{cb}\lambda_c}+\frac{m_{rb}\gamma_{th}}{\Omega_{rb}\lambda_Q^{rp}}\right)^{-\tilde{m}_{rb}}\Gamma\left(\tilde{m}_{rb},\frac{m_{cb}}{\Omega_{cb}\lambda_c}+\frac{m_{rb}\gamma_{th}}{\Omega_{rb}\lambda_Q^{rp}}\right)$$
$$\times\left(\frac{\gamma_{th}}{\lambda_Q^{rp}}\right)^{m_{rb}+v'-l-1}-\left(\frac{\tilde{\gamma}_{th}}{\lambda_Q^{rp}}\right)^{m_{rb}+v'-l-1}\left(\frac{m_{cb}}{\Omega_{cb}\lambda_c}+\frac{m_{rb}\tilde{\gamma}_{th}}{\Omega_{rb}\lambda_Q^{rp}}+\frac{tm_{ab}\gamma_{th}^{d}}{\Omega_{ab}\lambda_Q^{ap}}\right)^{-\tilde{m}_{rb}}$$
$$\times\Gamma\left(\tilde{m}_{rb},\frac{m_{cb}}{\Omega_{cb}\lambda_c}+\frac{m_{rb}\tilde{\gamma}_{th}}{\Omega_{rb}\lambda_Q^{rp}}+\frac{tm_{ab}\gamma_{th}^{d}}{\Omega_{ab}\lambda_Q^{ap}}\right)\Bigg]\Bigg]\frac{\Xi(1,1,;\gamma_{th})}{\Theta(1,1,;\gamma_{th})}, \tag{3.32}$$

where $\tilde{\gamma}_{th} = (\gamma_{th} - \gamma_{th}^{d})$ and $\tilde{m}_{rb} = m_{rb} + v + n - l$.

Proof. Proof is relegated to the Appendix B. ∎

From (3.31), the probability $\mathcal{P}_{\mathrm{SC}}^{\mathrm{IR}}$ is given as

$$\mathcal{P}_{\mathrm{SC}}^{\mathrm{IR}} = \Pr\Big[\lambda_Q^{ap}\frac{g_{ab}}{X}<\gamma_{\mathrm{th}}, \lambda_Q^{rp}\frac{g_{rb}}{X}<\gamma_{\mathrm{th}}, \lambda_Q^{ap}\frac{g_{ab}}{X}<\gamma_{\mathrm{th}}^{\mathrm{d}}, \lambda_Q^{ap}\frac{g_{ar}}{Y}\geq\gamma_{\mathrm{th}}, \lambda_Q^{bp}\frac{g_{br}}{Y}\geq\gamma_{\mathrm{th}}\Big]. \quad (3.33)$$

As $\gamma_{\mathrm{th}}^{\mathrm{d}} < \gamma_{\mathrm{th}}$, the integral form of (3.33) can be expressed as

$$\mathcal{P}_{\mathrm{SC}}^{\mathrm{IR}} = \int_0^\infty \int_0^\infty \int_{w=0}^{\frac{\gamma_{\mathrm{th}}^{\mathrm{d}} x}{\lambda_Q^{ap}}} f_{g_{ab}}(w)\, F_{g_{rb}|X}\left(\frac{\gamma_{\mathrm{th}} x}{\lambda_Q^{rp}}\right) \quad (3.34)$$
$$\times\, \overline{F}_{g_{ar}|Y}\left(\frac{\gamma_{\mathrm{th}} y}{\lambda_Q^{ap}}\right)\overline{F}_{g_{br}|Y}\left(\frac{\gamma_{\mathrm{th}} y}{\lambda_Q^{bp}}\right) f_X(x) f_Y(y)\, dx dy.$$

Evaluating the required integration, after some involved manipulations, yields the result in (3.35)

$$\mathcal{P}_{\mathrm{SC}}^{\mathrm{IR}} = \sum_{s=0}^{m_{cr}-1}\sum_{q=0}^{m_{ar}-1}\sum_{r=0}^{m_{br}-1}\sum_{n=0}^{m_{cb}-1}\sum_{t=0}^{1}\sum_{v=0}^{t(m_{ab}-1)}\sum_{k=0}^{1}\sum_{p=0}^{k(m_{rb}-1)} \frac{(-1)^{\tilde{s}+m_{cb}+t+k-n-1}}{q!r!\Gamma(m_{cb})\Gamma(m_{cr})}\omega_v^t\omega_p^k \mathcal{C}_n^{m_{cb}-1}$$
$$\times\, \mathcal{C}_s^{m_{cr}-1} e^{\frac{m_{cb}}{\Omega_{cb}\lambda_c}+\frac{m_{cr}}{\Omega_{cr}\lambda_c}} \left(\frac{m_{cb}}{\Omega_{cb}\lambda_c}\right)^{m_{cb}} \left(\frac{m_{cr}}{\Omega_{cr}\lambda_c}\right)^{m_{cr}} \left(\frac{m_{ar}\gamma_{\mathrm{th}}}{\Omega_{ar}\lambda_Q^{ap}}\right)^{q} \left(\frac{m_{br}\gamma_{\mathrm{th}}}{\Omega_{br}\lambda_Q^{bp}}\right)^{r} \left(\frac{m_{ab}\gamma_{\mathrm{th}}^{\mathrm{d}}}{\Omega_{ab}\lambda_Q^{ap}}\right)^{v}$$
$$\times \left(\frac{m_{rb}\gamma_{\mathrm{th}}}{\Omega_{rb}\lambda_Q^{rp}}\right)^{p} \left(\frac{m_{ar}\gamma_{\mathrm{th}}}{\Omega_{ar}\lambda_Q^{ap}}+\frac{m_{br}\gamma_{\mathrm{th}}}{\Omega_{br}\lambda_Q^{bp}}+\frac{m_{cr}}{\Omega_{cr}\lambda_c}\right)^{-\tilde{q}} \left(\frac{t m_{ab}\gamma_{\mathrm{th}}^{\mathrm{d}}}{\Omega_{ab}\lambda_Q^{ap}}+\frac{k m_{rb}\gamma_{\mathrm{th}}}{\Omega_{rb}\lambda_Q^{rp}}+\frac{m_{cb}}{\Omega_{cb}\lambda_c}\right)^{-\tilde{n}}$$
$$\times\, \Gamma\left(\tilde{q}, \frac{m_{ar}\gamma_{\mathrm{th}}}{\Omega_{ar}\lambda_Q^{ap}}+\frac{m_{br}\gamma_{\mathrm{th}}}{\Omega_{br}\lambda_Q^{bp}}+\frac{m_{cr}}{\Omega_{cr}\lambda_c}\right)\Gamma\left(\tilde{n}, \frac{t m_{ab}\gamma_{\mathrm{th}}^{\mathrm{d}}}{\Omega_{ab}\lambda_Q^{ap}}+\frac{k m_{rb}\gamma_{\mathrm{th}}}{\Omega_{rb}\lambda_Q^{rp}}+\frac{m_{cb}}{\Omega_{cb}\lambda_c}\right), \quad (3.35)$$

where $\tilde{n} = n + v + p + 1$.

Finally, adding together all the probabilities $\mathcal{P}_{\mathrm{DL}}^{\mathrm{IR}}$, $\mathcal{P}_{\mathrm{MRC}}^{\mathrm{IR}}$, and $\mathcal{P}_{\mathrm{SC}}^{\mathrm{IR}}$, closed-form expression of outage probability $\mathcal{P}_{\mathrm{out}}^{\mathrm{IR}}$ in (3.31) for incremental relaying can be evaluated.

3.3.2 High-SINR Analysis of Outage Probability

For simplifying the derived outage expressions, we make use of result given in (3.25). Consequently, $\mathcal{P}_{\mathrm{DL}}^{\mathrm{IR}}$ at high-SINR, $\lambda_Q \to \infty$, regime is obtained and can directly be expressed by replacing $m_{ab}\gamma_{\mathrm{th}}$ with $m_{ab}\gamma_{\mathrm{th}}^{\mathrm{d}}$ in (3.26). As such, the probability $\mathcal{P}_{\mathrm{MRC}}^{\mathrm{IR}}$ at high-SINR can be, asymptotically, represented as

$$\mathcal{P}_{\mathrm{MRC}}^{\mathrm{IR}} \simeq \sum_{s=0}^{m_{cr-1}}\sum_{n=0}^{m_{cb}-1} e^{\left(\frac{m_{cb}}{\Omega_{cb}\lambda_c}+\frac{m_{cr}}{\Omega_{cr}\lambda_c}\right)} \frac{\mathcal{C}_n^{m_{cb}-1}\mathcal{C}_s^{m_{cr}-1}(-1)^{m_{cb}+m_{cr}-n-s-2}}{\Gamma(m_{cb})\Gamma(m_{ab}+1)\Gamma(m_{rb}+1)} \left(\frac{m_{ab}\Omega_{ap}\gamma_{\mathrm{th}}^{\mathrm{d}}}{\Omega_{ab}}\right)^{m_{ab}}$$
$$\times \left(\frac{m_{rb}\Omega_{rp}(\gamma_{\mathrm{th}}-\gamma_{\mathrm{th}}^{\mathrm{d}})}{\Omega_{rb}}\right)^{m_{rb}} \frac{1}{\Gamma(m_{cr})\Gamma(m_{br}+1)} \left(\frac{m_{cb}}{\Omega_{cb}\lambda_c}\right)^{m_{cb}-\tilde{m}_{ab}} \left(\frac{m_{br}\Omega_{bp}\gamma_{\mathrm{th}}}{\Omega_{br}}\right)^{m_{br}}$$
$$\times \left(\frac{m_{cr}}{\Omega_{cr}\lambda_c}\right)^{m_{cr}-\tilde{m}_{br}} \Gamma\left(\tilde{m}_{ab}, \frac{m_{cb}}{\Omega_{cb}\lambda_c}\right)\Gamma\left(\tilde{m}_{br}, \frac{m_{cr}}{\Omega_{cr}\lambda_c}\right) \frac{1}{\lambda_Q{}^{m_{ab}+m_{rb}+m_{br}}}. \quad (3.36)$$

Likewise, asymptotic approximation of $\mathcal{P}_{\text{SC}}^{\text{IR}}$ is evaluated, expression for which can be directly obtained by replacing $m_{ab}\gamma_{\text{th}}$ with $m_{ab}\gamma_{\text{th}}^{\text{d}}$ in (3.29). Thus, by adding $\mathcal{P}_{\text{DL}}^{\text{IR}}$, $\mathcal{P}_{\text{MRC}}^{\text{IR}}$, and $\mathcal{P}_{\text{SC}}^{\text{IR}}$, the probability $\mathcal{P}_{\text{out}}^{\text{IR}}$ in (3.31) at high-SINR regime for DF-based incremental relaying can be evaluated. Note that, the diversity order of the incremental relaying remains same as that of fixed relaying.

3.3.3 Expected Spectral Efficiency

For incremental relaying, depending upon the success of direct transmission, the overall communication takes place in either two or three time phases. Hence, the expected spectral efficiency [52], [78] for one-sided transmission can be quantified as

$$\mathcal{R}_s^{\text{IR}} = \mathcal{R}_{\mathcal{T}}\text{Pr}[\gamma_{ab} \geq \gamma_{\text{th}}^{\text{d}}] + \frac{\mathcal{R}_{\mathcal{T}}}{3}\text{Pr}[\gamma_{ab} < \gamma_{\text{th}}^{\text{d}}]. \tag{3.37}$$

Here, we can evaluate $\text{Pr}[\gamma_{ab} \geq \gamma_{\text{th}}^{\text{d}}]$ using (3.3) as

$$\begin{aligned}\text{Pr}[\gamma_{ab} \geq \gamma_{\text{th}}^{\text{d}}] = &\sum_{v=0}^{m_{ab}-1}\sum_{n=0}^{m_{cb}-1} \mathcal{C}_n^{m_{cb}-1} e^{\frac{m_{cb}}{\Omega_{cb}\lambda_c}} \left(\frac{m_{ab}\gamma_{\text{th}}^{\text{d}}}{\Omega_{ab}\lambda_Q^{ap}}\right)^v \frac{(-1)^{m_{cb}-n-1}}{v!\Gamma(m_{cb})} \left(\frac{m_{cb}}{\Omega_{cb}\lambda_c}\right)^{m_{cb}} \\ &\times \left(\frac{m_{ab}\gamma_{\text{th}}^{\text{d}}}{\Omega_{ab}\lambda_Q^{ap}} + \frac{m_{cb}}{\Omega_{cb}\lambda_c}\right)^{-(n+v+1)} \Gamma\left(n+v+1, \frac{m_{ab}\gamma_{\text{th}}^{\text{d}}}{\Omega_{ab}\lambda_Q^{ap}} + \frac{m_{cb}}{\Omega_{cb}\lambda_c}\right),\end{aligned} \tag{3.38}$$

whereas $\text{Pr}[\gamma_{ab} < \gamma_{\text{th}}^{\text{d}}] = 1 - \text{Pr}[\gamma_{ab} \geq \gamma_{\text{th}}^{\text{d}}]$. In (3.37), the first term arises when the direct transmission is successful and hence the overall bi-directional communication occurs in two time phases only. Whereas, the second term corresponds to the unsuccessful direct transmission and three-phase bi-directional communication. It is important to note that, at a high-SINR, $\lambda_Q \to \infty$, the expected spectral efficiency of incremental relaying approaches to $\mathcal{R}_s^{\text{IR}} \simeq \mathcal{R}_{\mathcal{T}}$, which is three-fold as compared to that of fixed relaying.

3.4 Average End-to-End Transmission Time

For practical deployment of future generation wireless networks, one of the main design objectives is to reduce the network latency. For this, herein, we attempt to estimate the end-to-end (e2e) transmission time for a packet to reach the intended destination, which may be useful for designing the wireless network with the anticipated latency requirements. As per the third Shannon theorem, the transmission time is inversely proportional to the transmission rate of the channel [79], [80].

Hence, the time taken by a packet to reach the destination node S_j after leaving the source S_i is given by

$$\mathcal{T}_{ij} = \frac{L}{B\log_2(1+\gamma_{ij})} = \frac{\tilde{B}}{\log_e(1+\gamma_{ij})}, \tag{3.39}$$

where L is the length of the packet, B is the channel bandwidth, and $\tilde{B}$=$(L\log_e(2))/B$. Further, we assume that the transmitted packet reaches the destination successfully before time-out. Moreover, the transmission time and processing delay of feedback/acknowledgment message are assumed negligible as compared to the packet transmission time [81], [82]. Based on these, the average e2e transmission time for the two relaying strategies can be obtained as follows.

3.4.1 Fixed Relaying

For fixed relaying strategy, the average e2e transmission time for a packet to reach S_b from S_a can be computed as

$$\mathcal{T}^{\mathrm{FR}}_{a\to b} = \mathbb{E}(\mathcal{T}_{ar}) + \mathbb{E}(\mathcal{T}_{br}) + \mathbb{E}(\mathcal{T}_{rb}), \tag{3.40}$$

where $\mathcal{T}_{ar}$, $\mathcal{T}_{br}$, and $\mathcal{T}_{rb}$ can be obtained using (3.39). Here, since the transmission takes place in three time phases, the average e2e transmission time is predominantly depends on the relaying path.

3.4.2 Incremental Relaying

For incremental relaying, the average e2e transmission time for a packet to reach S_b from S_a can be formulated as

$$\mathcal{T}^{\mathrm{IR}}_{a\to b} = \mathbb{E}(\mathcal{T}_{ab})\Pr[\gamma_{ab} \geq \gamma^{\mathrm{d}}_{\mathrm{th}}] + [\mathbb{E}(\mathcal{T}_{ar}) + \mathbb{E}(\mathcal{T}_{br}) + \mathbb{E}(\mathcal{T}_{rb})]\Pr[\gamma_{ab} < \gamma^{\mathrm{d}}_{\mathrm{th}}], \tag{3.41}$$

where $\Pr[\gamma_{ab} \geq \gamma^{\mathrm{d}}_{\mathrm{th}}]$ is given by (3.38), $\Pr[\gamma_{ab} < \gamma^{\mathrm{d}}_{\mathrm{th}}] = 1 - \Pr[\gamma_{ab} \geq \gamma^{\mathrm{d}}_{\mathrm{th}}]$, and the $\mathbb{E}(\mathcal{T}_{ij})$ can be expressed as

$$\mathbb{E}(\mathcal{T}_{ij}) = \int_0^\infty x f_{\mathcal{T}_{ij}}(x)dx, \tag{3.42}$$

where $f_{\mathcal{T}_{ij}}(x)$ is PDF of $\mathcal{T}_{ij}$. Note that, using (3.42), it is cumbersome to derive the closed-form expressions for (3.40) and (3.41). Hence, we compute them with simulation and based on that we compare the average e2e transmission times of the two relaying strategies in the next section.

3.5 Numerical and Simulation Results

In this section, we perform numerical investigations of the considered TWCRNs using both the fixed and incremental relaying strategies with ALUS. We adopt a two-dimensional (x, y) network topology, where the nodes T_c, T_p, S_a, S_r and S_b are located at $(0, 0.5)$, $(1, 0.5)$, $(0, 0)$, $(0.5, d)$, and $(1, 0)$, respectively. Following path-loss model, we set $\Omega_{\imath\jmath} = D_{\imath\jmath}^{-\alpha}$, where $D_{\imath\jmath}$ is the distance between two arbitrary nodes with path loss exponent α equals to 4. Further, we set $\mathcal{R}_{\mathcal{T}} = 1/2$ bps/Hz, $N_o = 1$, $d = 0$, and $(m_{cb}, m_{cr}, m_{br}) = (1, 1, 1)$ unless otherwise specified.

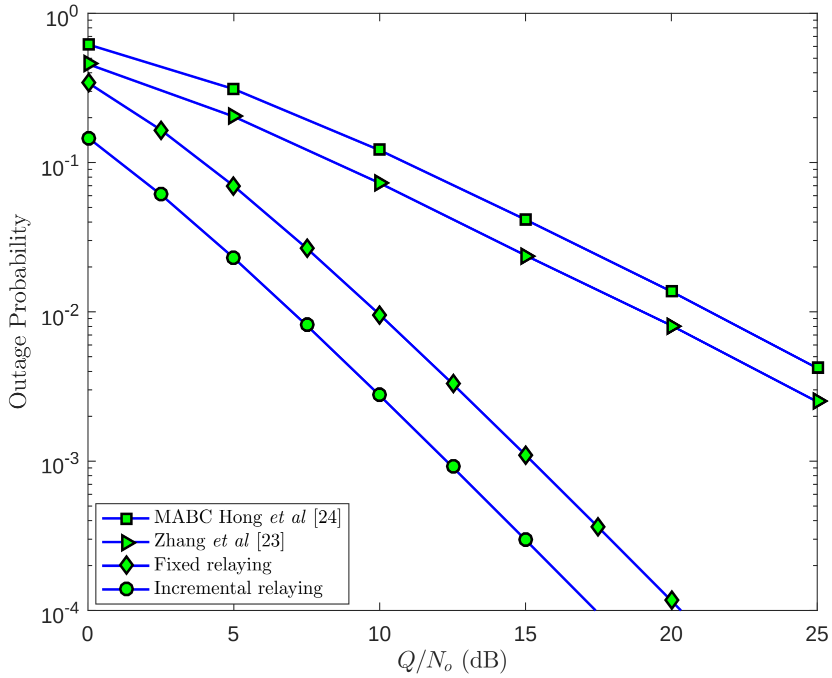

Figure 3.2: Outage performance comparison for different schemes.

Comparison of Proposed Scheme with Existing Schemes

In this subsection, we compare the performance of the proposed scheme with the existing schemes in the literature. Firstly, we consider the work of Zhang *et al.* [71] as benchmark for the comparison. As their study is based on Rayleigh fading channels, we set all the Nakagami-m fading parameters for our system as $m_{u,v} = 1$, where $u, v \in \{c, p, a, r, b\}$. For comparison purpose, all the other parameters are kept same and given as $\lambda_c = P_p = 2$ dB, $N_o = 1$, $\gamma_{\text{th}} = 1$, $\mathcal{R}_{\mathcal{T}} = 1/3$, and $M = 1$. With this, Fig. 3.2 establishes the SUs' outage performance comparison between the proposed scheme and the benchmark scheme. It is evident from the respective curves that the proposed scheme significantly outperforms the benchmark scheme.

Moreover, the performance gap between the two schemes expands even further for the incremental relaying strategy. Next, we compare the proposed scheme with another benchmark scheme studied in [72]. We illustrate the user outage performance comparison between the proposed scheme and two-phase MABC protocol in [72]. For this, we fix $\mathcal{R}_{AR} = \mathcal{R}_{BR} = \mathcal{R}_{RB} = \mathcal{R}_{\mathcal{T}} = 1/3$, $\sigma^2 = 1$, $\alpha = 0.5$, and $I_{th} = Q$. It can be manifestly observed from Fig. 3.2 that proposed scheme performs better than its two-phase counterpart, even though the interference from PU is absent in the study of [72].

In essence, it is inferred that the proposed ALUS scheme outperforms both the existing benchmark schemes viz., three-phase TDBC [71] and two-phase MABC [72] due to the appropriate usage of available direct link. As such, the proposed scheme harvests the benefits of cooperative diversity for TWCRNs which was overlooked in the existing literature.

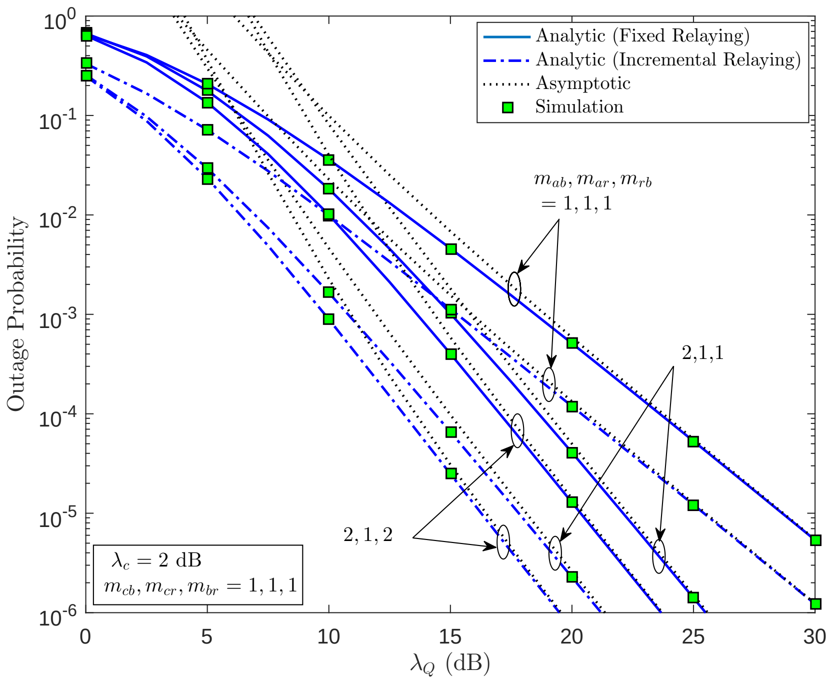

Figure 3.3: Outage performance for various fading parameters.

Outage Performance Evaluation

In Fig. 3.3, we plot the outage probability curves of both the DF-based relaying strategies versus λ_Q for various fading severity parameters keeping primary transmit power fixed ($\lambda_c = 2$ dB). Apparently, the analytical curves are in well agreement with the exact simulation results. The asymptotic curves are also found corroboratory with the exact results in the high-SINR regime. From these curves, it can be observed that, for the same set of parameters, incremental relaying performs better than the fixed relaying. However, the performance gap between the two relaying strategies tends to grow as the direct link parameter m_{ab} increases. Moreover, one can clearly visualize the achievable diversity order of the considered system as $m_{ab} + \min(m_{ar}, m_{rb})$. Further, the relative performance gain with a better quality of direct link channel (i.e., with a higher value of m_{ab}) justifies its importance for the considered cognitive two-way relay system.

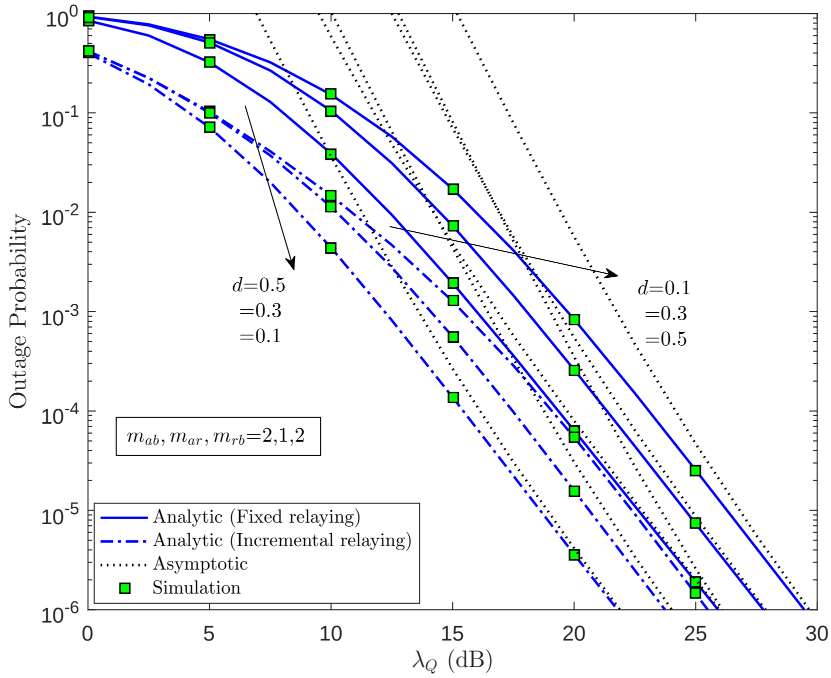

Figure 3.4: Outage performance for various relay locations with $\lambda_c = 5$ dB.

In Fig. 3.4, we depict the impact of relay location on the outage performance of the two relaying strategies. With relay positioned at $(0.5, d)$, if d changes from 0.5 to 0.3 or 0.1 i.e., the relay S_r is moved away from the primary transmitter and receiver, the outage probability of both fixed and incremental relaying decrease. This is due to the relaxed interference constraints from primary receiver and lessen interference from primary transmitter.

Fig. 3.5 and Fig. 3.6 illustrate the impact of the primary transmit power λ_c on the outage performance of the considered system for fixed relaying and incremental relaying respectively. Here, curves are drawn for various values of λ_c and channel parameters (m_{ab}, m_{ar}, m_{br}). It can be seen that the outage performance degrades as λ_c increases. However, the performance is shown to improve clearly when λ_c decreases from 4 dB to 2 dB (see the curves for $m_{ab}, m_{ar}, m_{br} = 3, 2, 3$). It follows from these figures that the system diversity gain could be extracted for a small primary interference power.

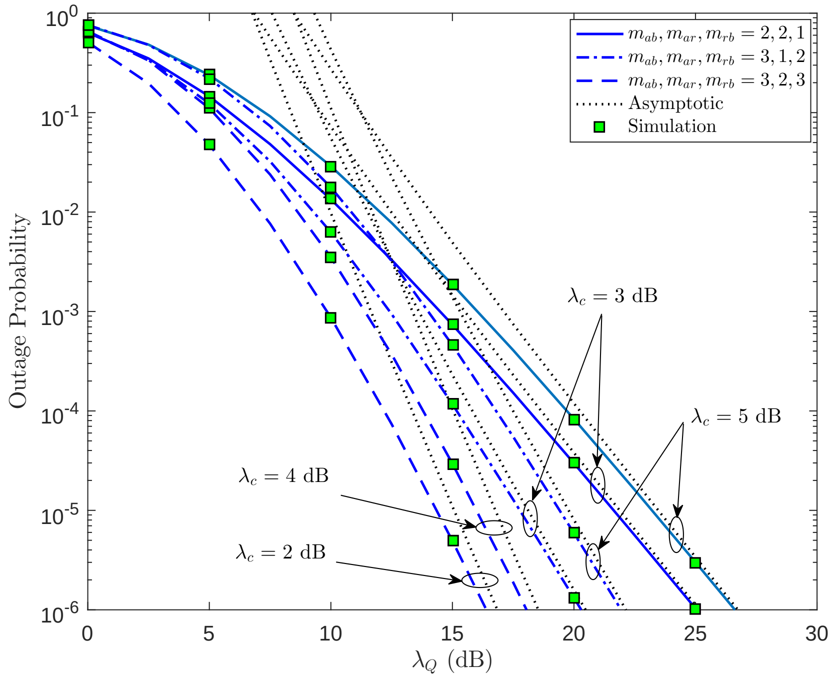

Figure 3.5: Outage performance of fixed relaying for various values of λ_c.

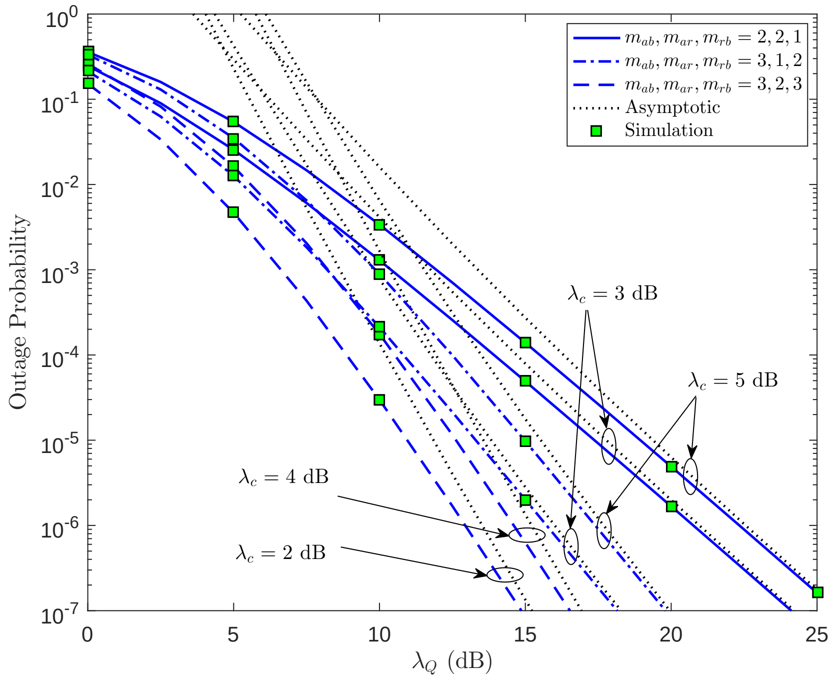

Figure 3.6: Outage performance of incremental relaying for various values of λ_c.

In Fig. 3.7 and Fig. 3.8, we plot the outage probability curves for different levels of λ_Q/λ_c. It can be observed that when primary interference power level λ_c is low i.e., λ_Q/λ_c is 25 dB, the system can exploit diversity gain effectively

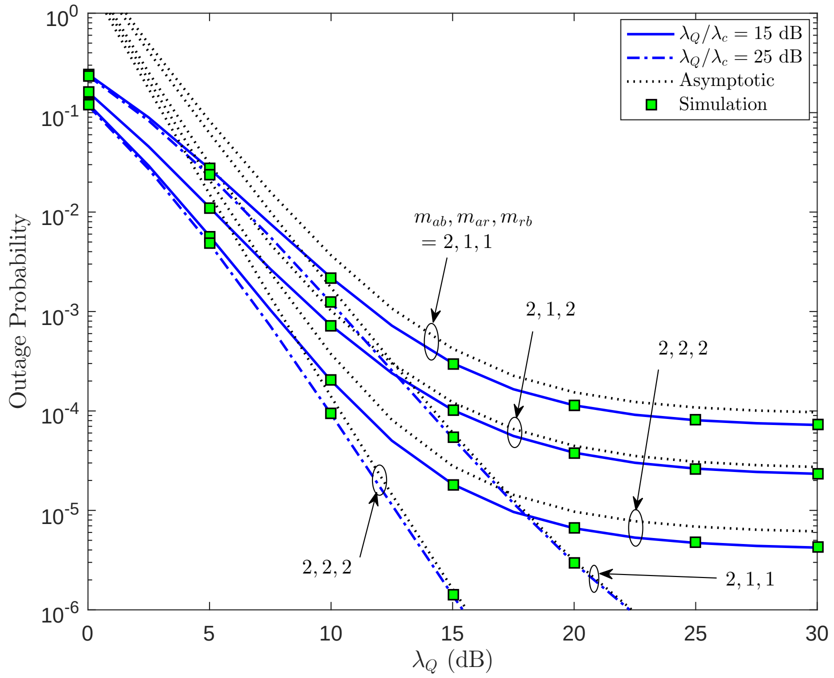

Figure 3.7: Outage performance of fixed relaying for different levels of λ_Q/λ_c.

(see m_{ab}, m_{ar}, m_{br}=2, 1, 1 or 2, 2, 2). However, for high interference power level (λ_Q/λ_c=15 dB), an outage floor phenomenon occurs at high-SINR. Importantly, the system coding gain is still affected by the channel/system parameters (as implied by the shift of the curves), but the relative improvement in performance remains marginal. Hence, PU's interference is critical for the SUs to maintain their QoS requirements.

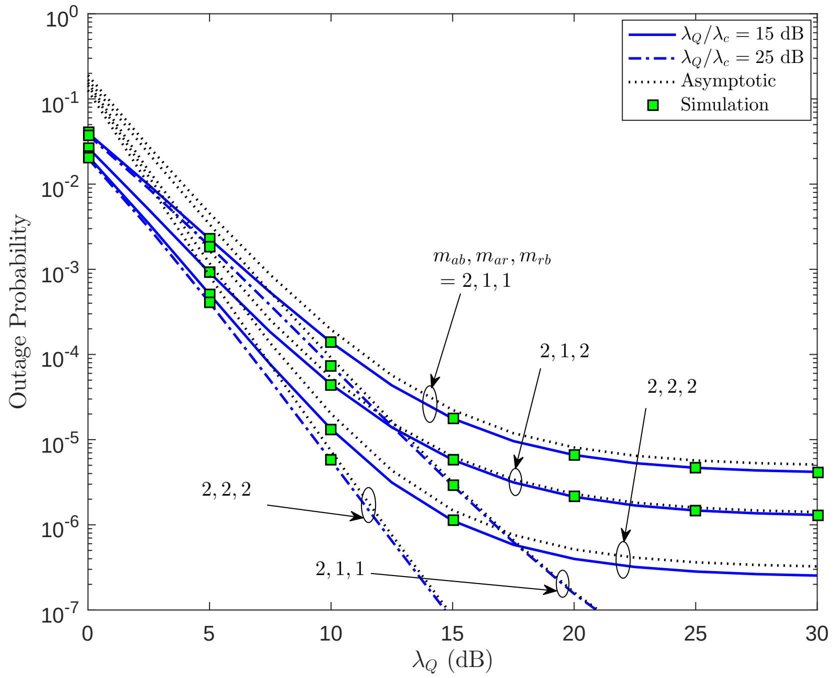

Figure 3.8: Outage performance of incremental relaying for different λ_Q/λ_c levels.

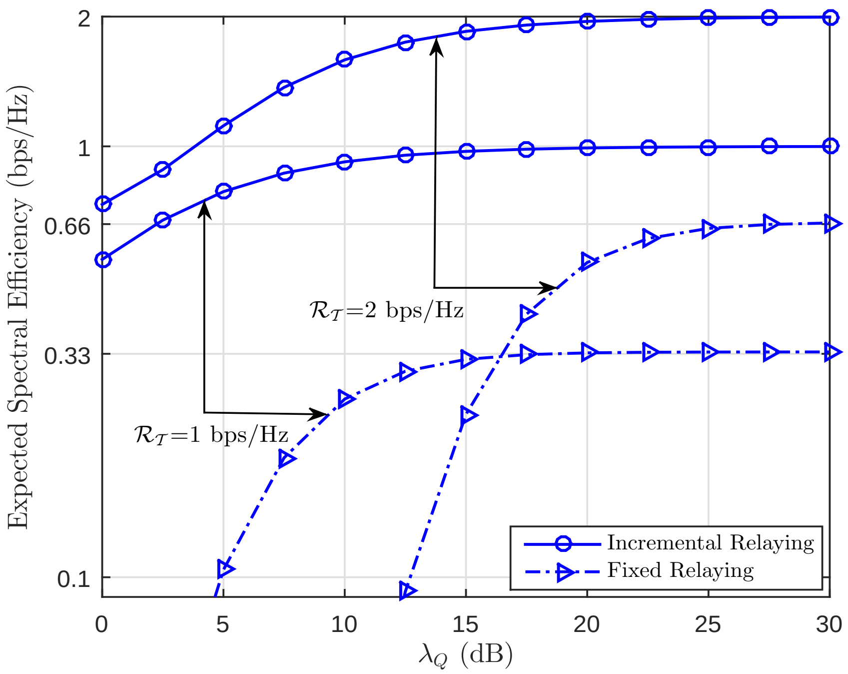

Figure 3.9: Expected spectral efficiency against λ_Q.

Expected Spectral Efficiency

In Fig. 3.9, we demonstrate the expected spectral efficiency achievable by the two considered relaying strategies. It is apparent that the incremental relaying dramatically improves the spectral efficiency. For instance, when the target rate is $\mathcal{R}_{\mathcal{T}} = 1$ bps/Hz, the maximum expected spectral efficiency offered by fixed relaying approaches to $\frac{\mathcal{R}_{\mathcal{T}}}{3} \simeq 0.33$. In contrast, the maximum expected spectral efficiency offered by incremental relaying approaches the target rate $\mathcal{R}_{\mathcal{T}}$. Thus, it can be concluded that incremental relaying is more spectrally efficient than traditional fixed relaying for TWCRNs, and hence may be preferred for deployment in future 5G and beyond wireless networks.

Average End-to-End Transmission Time

In Fig. 3.10, we depict and compare the average e2e transmission times for the two considered relaying strategies. We assume that the system bandwidth is $B = 1$ MHz and packet length is $L = 4096$ bits. It can be manifestly observed from the curves that transmission time for incremental relaying is less as compared with fixed relaying. This is due to the fact that when direct transmission is successful, incremental relaying utilizes only two time slots and thereby reducing the transmission time significantly. Moreover, increasing the primary transmit power λ_c eventually increases the transmission time due to degradation in the SINR as can be witnessed from (3.39).

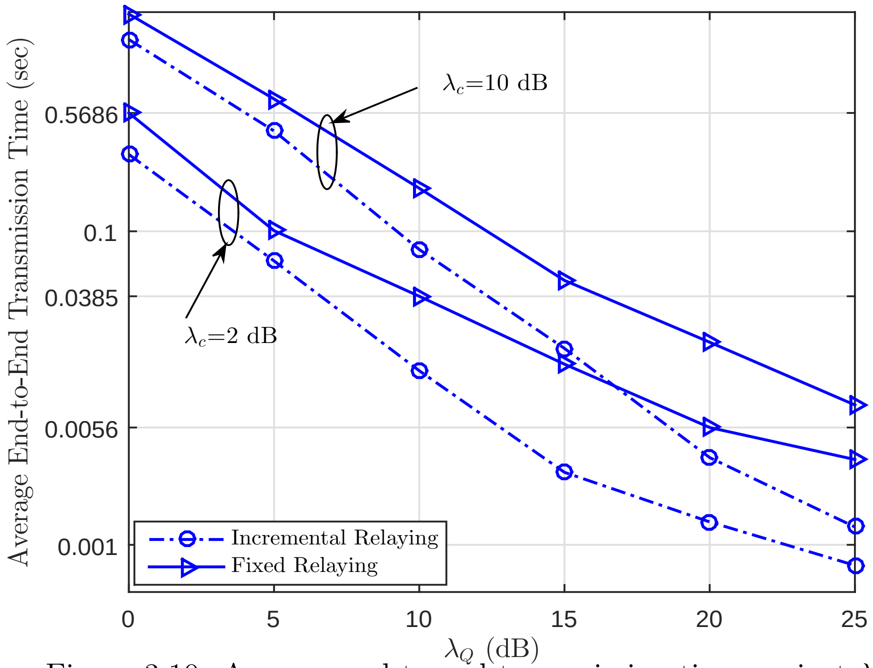

Figure 3.10: Average end-to-end transmission time against λ_Q.

3.6 Summary

In this chapter, we conducted performance analysis for an underlay TWCRN with a direct link by employing a TDBC protocol in the presence of primary interference. An adaptive link utilization scheme is proposed to exploit both the direct and the relay links. Based on the proposed link utilization scheme, we derived the tight closed-form expressions of outage probability for two different DF-based relaying strategies, viz., fixed relaying and incremental relaying under Nakagami-m fading. It is shown that the incremental relaying performs better than the fixed relaying for the same set of system parameters. Moreover, the performance gap between the two relaying strategies increases as the quality of direct link improves. Furthermore, with the help of simulation results, we disclosed that the proposed scheme outperforms the existing two-phase and three-phase benchmark transmission schemes in terms of the outage probability. To attain further insight, we carried out the analysis to high-SINR regime, and examined the impact of system parameters on the performance gain. Our results revealed that the full diversity for secondary system can be achieved as long as the primary interference remains limited, otherwise the performance remarkably deteriorates. Above all, we demonstrated that the incremental relaying outperforms fixed relaying in terms of expected spectral efficiency and average transmission time and hence could be a promising candidate for deployment in future wireless systems.

CHAPTER 4

IMPACT OF HARDWARE AND CHANNEL IMPERFECTIONS IN COGNITIVE RELAY NETWORKS

In the recent past, CRNs have been extensively studied by employing AF- or DF-based relay cooperation in order to enhance the system's performance (e.g., see [83]-[87] and references cited therein). However, most of the existing studies on CRNs have presented performance analysis by assuming ideal hardware for the network nodes.

In practice, RF transceivers are afflicted with several hardware imperfections such as IQ imbalances, amplifier non-linearities, and phase noise [27], [88]-[91]. As a result, a non-ideal transceiver induces undesirable distortions in the transmitted and received signals which limit the system capacity primarily in the high-rate applications. To this end, various works have analyzed the impact of hardware imperfections on the performance of cognitive radio networks [92]-[98]. Specifically, authors in [92] studied the effects of non-ideal RF chain on the cyclo-stationary spectrum sensing. In [93], the impact of RF imperfections on the sensing performance of an energy detector and a cyclo-stationarity detector has been examined. The effect of IQ imbalance on the blind spectrum sensing for overlay cognitive radio networks was investigated in [94]. Authors in [95] considered the spectrum sensing problem in orthogonal frequency-division multiplexing-based cognitive radio networks under IQ imbalance. In [96], an energy detection based spectrum sensing has been studied for both single-channel and multi-channel direct-conversion receiver scenarios impaired by IQ imbalance. Authors in [97] and [98] examined the impact of hardware imperfections on the spectrum sensing in half-duplex and full duplex networks, respectively. Some other works have analyzed the performance of CRNs considering hardware impairments (HIs) [99]-[104]. For instance, the performance analysis of full-duplex cooperative cognitive radio in presence of transmit imperfections was reported in [99]. Authors in [100] have studied CRNs with HIs, but with a single relay and without a direct link. In [101], the performance of underlay cognitive relaying system has been investigated using multiple antennas with HIs under the assumption of no direct link. Authors in [102] examined partial relay selection protocols in underlay cognitive radio under impact of HIs. In [103], the performance of underlay spectrum sharing network has been analyzed in presence of HIs, whereas the study in [104] considered the HIs only at the relay node and not on the source and destination nodes. Nonetheless, all these works considered perfect CSI for all the links. Besides HIs, the performance of cooperative relay systems may also get impaired by imperfect CSI due to channel estimation errors (CEEs) [28]. CRNs with imperfect CSI for ideal hardware were analyzed in [105] and [106]. Recently, the authors in [107] and [108] have studied the joint impact of HIs and CEEs, but not in the context of spectrum sharing networks.

Motivated by the aforementioned facts, in this chapter, we investigate the performance of CRNs considering both AF and DF relaying schemes with direct link under the joint impact of two practical and detrimental imperfections, called transceiver HIs and CEEs. Herein, we consider the hardware distortions induced by all the non-ideal secondary nodes and residual interference originating from imperfect channel estimations.

In the sequel, we first present the signal model in Section 4.1 that incorporates HIs and CEEs and will be utilized for the subsequent analysis in the chapter. Next, we analyze the joint impact of HIs and CEEs on the performance of AF relaying based CRNs in Section 4.2 and on the DF relaying based CRNs in Section 4.3.

4.1 Signal Model with HIs and CEEs

In this section, we describe the signal model that takes into account both HIs and CEEs. For this, let $h_{\imath\jmath}$ be the channel coefficient between two arbitrary nodes $\imath$ and $\jmath$, which is assumed to follow $\mathcal{CN}(0, \Omega_{\imath\jmath})$. Then, considering minimum mean-square error (MMSE) channel estimation model, we have $h_{\imath\jmath} = \hat{h}_{\imath\jmath} + e_{h_{\imath\jmath}}$, where $\hat{h}_{\imath\jmath}$ is the estimate for the channel $h_{\imath\jmath}$ and $e_{h_{\imath\jmath}}$ is the estimation error which follows $\mathcal{CN}(0, \sigma^2_{e,\imath\jmath})$, where $\sigma^2_{e,\imath\jmath} = \mathbb{E}\{|h_{\imath\jmath}|^2\} - \mathbb{E}\{|\hat{h}_{\imath\jmath}|^2\}$ implies the quality of estimation and is chosen appropriately based on the estimation schemes [28]. Further, we assume that $\hat{h}_{\imath\jmath}$ and $e_{h_{\imath\jmath}}$ are mutually independent. This assumption is valid for MMSE estimator wherein the estimate and error are orthogonal. Hence, we have $\hat{h}_{\imath\jmath} \sim \mathcal{CN}(0, \hat{\Omega}_{\imath\jmath})$, where $\hat{\Omega}_{\imath\jmath} = \Omega_{\imath\jmath} - \sigma^2_{e,\imath\jmath}$. Further, referring to HIs model in [88], let x_s be the transmitted signal over the channel $h_{\imath\jmath}$, then the signal at the receiving node $\jmath$ can be expressed as

$$\begin{aligned} y_\jmath &= (\hat{h}_{\imath\jmath} + e_{h_{\imath\jmath}})(x_s + \eta_{t\imath}) + \eta_{r\jmath} + \nu_\jmath \\ &= (\hat{h}_{\imath\jmath} + e_{h_{\imath\jmath}})x_s + \underbrace{\underbrace{\hat{h}_{\imath\jmath}\eta_{t\imath} + e_{h_{\imath\jmath}}\eta_{t\imath} + \eta_{r\jmath}}_{\text{effective distortion noise}} + \nu_\jmath}_{\text{overall effective noise}}, \end{aligned} \tag{4.1}$$

where $\nu_\jmath \sim \mathcal{CN}(0, N_0)$ denotes AWGN, $\eta_{t\imath} \sim \mathcal{CN}(0, \kappa^2_{t\imath} P_s)$ and $\eta_{r\jmath} \sim \mathcal{CN}(0, \kappa^2_{r\jmath} P_s(|\hat{h}_{\imath\jmath}|^2 + \sigma^2_{e,\imath\jmath}))$ represent distortion noises[1] at the transmitter and receiver, respectively, with $P_s = \mathbb{E}\{|x_s|^2\}$. All these noises are assumed to be independent from each other. Hereby, the parameters $\kappa_{t\imath}$, $\kappa_{r\jmath} \geq 0$ quantify the level of impairments and are measured experimentally as error vector magnitudes (EVMs)[2]. From (4.1), it can be observed that the true distribution of overall effective noise is not Gaussian since it involves the terms having product of two complex Gaussian random variables. However, for a given channel realization, the term $\hat{h}_{\imath\jmath}\eta_{t\imath}$ can be assumed to be complex Gaussian distributed [88]. Further, by considering the small levels of estimation error and hardware impairments in practical scenarios, the distribution of $e_{h_{\imath\jmath}}\eta_{t\imath}$ can also be tightly approximated as $\mathcal{CN}(0, P_s\kappa^2_{t\imath}\sigma^2_{e,\imath\jmath})$ [109]. Consequently, the overall effective noise can be treated as complex Gaussian. As such, from (4.1), we can write the aggregate power of the effective distortion noise at the receiver, for a given channel realization, as

$$\mathbb{E}\{|(\hat{h}_{\imath\jmath} + e_{h_{\imath\jmath}})\eta_{t\imath} + \eta_{r\jmath}|^2\} = P_s(|\hat{h}_{\imath\jmath}|^2 + \sigma^2_{e,\imath\jmath})(\kappa^2_{t\imath} + \kappa^2_{r\jmath}). \tag{4.2}$$

Using (4.2), we can write the equivalent expression of (4.1) as

$$\begin{aligned} y_\jmath &= (\hat{h}_{\imath\jmath} + e_{h_{\imath\jmath}})(x_s + \eta_{\imath,\jmath}) + \nu_\jmath \\ &= (\hat{h}_{\imath\jmath} + e_{h_{\imath\jmath}})x_s + \underbrace{\hat{h}_{\imath\jmath}\eta_{\imath,\jmath} + e_{h_{\imath\jmath}}\eta_{\imath,\jmath} + \nu_\jmath}_{\text{overall effective noise}}, \end{aligned} \tag{4.3}$$

where $\eta_{\imath,\jmath} \sim \mathcal{CN}(0, \kappa^2_{\imath,\jmath} P_s)$ represents the equivalent distortion noise which accounts for the HIs at both the transmitter and the receiver nodes, such that $\kappa_{\imath,\jmath} = \sqrt{\kappa^2_{t\imath} + \kappa^2_{r\jmath}}$.

[1] The fundamental difference between distortion noise (due to HIs) and thermal noise lies in a fact that unlike thermal noise, distortion noise power is proportional to the signal power and the instantaneous channel gain.

[2] These EVMs can be defined as the ratio of distortion-to-signal magnitude, and can be obtained as given in [110].

As discussed above, the overall effective noise in (4.3) can be assumed to be complex Gaussian distributed where the distribution of $e_{h_{\imath\jmath}}\eta_{\imath,\jmath}$ is approximated as $\mathcal{CN}(0, P_s\kappa_{\imath,\jmath}^2\sigma_{e,\imath\jmath}^2)$. Hereafter, without loss of generality, we use the characterization in (4.3) for the subsequent analysis.

4.2 Cognitive AF Multi-Relay Networks with RF HIs and CEEs

In this section, we analyze the performance of an AF relaying based cognitive multi-relay network (CMRN) under the joint impact of HIs and CEEs. Based on the model presented in Section 4.1, we derive a new closed-form outage probability expression of the considered system by considering imperfect CSI for all links and HIs at all secondary nodes over independent and non-identically distributed (i.ni.d.) Rayleigh fading channels. We also derive an asymptotic outage expression to examine the system diversity order. Moreover, we identify the key parameters influencing the system performance and present important insights.

4.2.1 System Descriptions

As shown in Fig. 4.1, we consider a CMRN where one secondary source S communicates with one secondary destination D using the cooperation of K secondary AF relays $\{R_m\}_{m=1}^{K}$ in the presence of a primary receiver T_p. It is assumed that a direct link between S and D also exists. The intuitive reason for this assumption is as follows. In underlay spectrum sharing networks, the power at the SU transmitter is a random quantity due to which sustaining the QoS of SUs becomes challenging. To circumvent this, the relays are employed even for the shorter communication distance between source and destination nodes. Hence, the presence of a direct link can not be overlooked in such networks.

In 5G cellular systems, the SUs may correspond to the femtocell users underlaying in a macrocell [76], [111]. Further, as in many earlier works [87], [112], [113], we assume that the primary transmitter is located far away from the secondary nodes such that its interference on secondary receivers can be ignored. This is a widely adopted assumption in underlay paradigm and could be applicable in the scenarios where the femtocell SU receivers are situated beyond the coverage of macrocell PU transmitter. Another practical example for such scenarios is when primary and secondary networks are owned and controlled by the same operator so that the interference at the SUs can be limited.

Herein, all the secondary nodes (i.e., S, D, and R_m) are afflicted with HIs. Like most of the previous works [100]-[104], we assume the hardware at the PU to be ideal[3]. Further, all the channels are assumed to follow block fading so that they remain constant during a packet transmission but changes independently during the next packet transmission [70], [71]. The channels $h_{\imath\jmath}$ between any two arbitrary nodes $\imath$ and $\jmath$ are subject to independent and non-identically distributed Rayleigh fading. In this analytical framework, the overall secondary communication takes place in

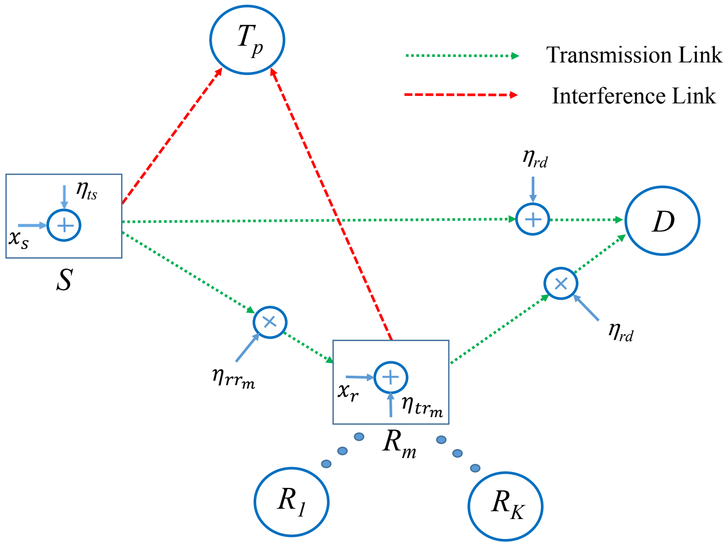

Figure 4.1: System model for CMRN.

two phases. In first phase, S transmits its signal x_s (satisfying $\mathbb{E}\{|x_s|^2\} = P_s$) to D and all the relays. Consequently, the received signal at D and at the relay R_m can be given, respectively, by

$$y_{d,1} = (\hat{h}_{sd} + e_{h_{sd}})(x_s + \eta_{s,d}) + \nu_{d,1} \tag{4.4}$$

$$\text{and } y_{r_m} = (\hat{h}_{sr_m} + e_{h_{sr_m}})(x_s + \eta_{s,r_m}) + \nu_{r_m}, \tag{4.5}$$

where $\eta_{s,d} \sim \mathcal{CN}(0, \kappa_{s,d}^2 P_s)$ and $\eta_{s,r_m} \sim \mathcal{CN}(0, \kappa_{s,r_m}^2 P_s)$ are distortion noises. And, $\nu_{d,1}$ and ν_{r_m} represent AWGN variables at the respective nodes. During second phase, R_m first amplifies the received signal y_{r_m} with a variable gain $\mathcal{G}$ given by

$$\mathcal{G} = \sqrt{\frac{P_{r_m}}{P_s|\hat{h}_{sr_m}|^2(1+\kappa_{s,r_m}^2) + P_s\sigma_{e,sr_m}^2(1+\kappa_{s,r_m}^2) + N_o}}, \tag{4.6}$$

[3]Since our present study primarily focuses on the performance evaluation of SUs, the analysis of PUs with HIs can be treated as problems for future research works.

where P_{r_m} is transmit power at R_m, and then forwards it to D. Consequently, the signal received (after amplification) at D is given as

$$y_{d,2} = (\hat{h}_{r_m d} + e_{h_{r_m d}})(\mathcal{G} y_{r_m} + \eta_{r_m,d}) + \nu_{d,2}, \tag{4.7}$$

where $\eta_{r_m,d} \sim \mathcal{CN}(0, \kappa^2_{r_m,d} P_{r_m})$ represents distortion noise with $P_{r_m} = \mathbb{E}\{|\mathcal{G} y_{r_m}|^2\}$, and $\nu_{d,2}$ is AWGN at D in second phase. Further, in an underlay scenario with HIs and CEEs, to limit the interference power at primary receiver T_p below a pre-determined threshold Q, the instantaneous powers at S and R_m are constrained as $\mathbb{E}\{|(\hat{h}_{sp} + e_{h_{sp}})(x_s + \eta_{ts})|^2\} \leq Q$ and $\mathbb{E}\{|(\hat{h}_{r_m p} + e_{h_{r_m p}})(\mathcal{G} y_{r_m} + \eta_{tr_m})|^2\} \leq Q$ respectively, where $\eta_{ts} \sim \mathcal{CN}(0, \kappa^2_{ts} P_s)$ and $\eta_{tr_m} \sim \mathcal{CN}(0, \kappa^2_{tr_m} P_{r_m})$ are the distortion noises induced in transmit processing at S and R_m respectively. As a result, we have $P_s = \frac{Q}{(|\hat{h}_{sp}|^2 + \sigma^2_{e,sp})(1+\kappa^2_{ts})}$ and $P_{r_m} = \frac{Q}{(|\hat{h}_{r_m p}|^2 + \sigma^2_{e,r_m p})(1+\kappa^2_{tr_m})}$. Hereby, it has been assumed that the maximum transmit power at S and R_m is large enough and hence can be neglected to meet the interference constraint at T_p [114]. Thus, from (4.4), the resulting signal-to-noise-and-distortion ratio (SNDR) at D via direct link transmission of first phase can be given by

$$\Lambda_{sd} = \frac{\frac{\varrho |\hat{h}_{sd}|^2}{|\hat{h}_{sp}|^2}}{\frac{|\hat{h}_{sd}|^2 \kappa^2_{s,d} \varrho}{|\hat{h}_{sp}|^2} + \frac{\sigma^2_{e,sd}\varrho(1+\kappa^2_{s,d}) + \sigma^2_{e,sp}(1+\kappa^2_{ts})}{|\hat{h}_{sp}|^2} + (1+\kappa^2_{ts})}, \tag{4.8}$$

where $\varrho = Q/N_0$ SNR. Further, using (4.8) with an estimation error variance as decreasing function of SNR, i.e., $\sigma^2_{e,ıȷ} = 1/\varrho$ [28], [106], we can write

$$\Lambda_{sd} = \frac{\frac{\varrho |\hat{h}_{sd}|^2}{|\hat{h}_{sp}|^2}}{\frac{\varrho \kappa^2_{s,d} |\hat{h}_{sd}|^2}{|\hat{h}_{sp}|^2} + \frac{\alpha_{s,d}}{|\hat{h}_{sp}|^2} + \delta_s}, \tag{4.9}$$

where $\alpha_{s,d} = (1+\kappa^2_{s,d}) + (1+\kappa^2_{ts})/\varrho$ and $\delta_s = 1 + \kappa^2_{ts}$. Now, using (4.5), (4.6), and (4.7), SNDR at D via relay link transmission of second phase can be obtained as

$$\Lambda_m = \frac{\varrho^2 |\hat{h}_{sr_m}|^2 |\hat{h}_{r_m d}|^2}{\alpha_{1,m}|\hat{h}_{r_m d}|^2 + \alpha_{2,m}|\hat{h}_{sr_m}|^2|\hat{h}_{r_m d}|^2 + \alpha_{3,m}|\hat{h}_{r_m d}|^2|\hat{h}_{sp}|^2 + \alpha_{4,m}|\hat{h}_{sr_m}|^2 + \alpha_{5,m}|\hat{h}_{sr_m}|^2|\hat{h}_{r_m p}|^2 + \alpha_{6,m}}, \tag{4.10}$$

where $\alpha_{1,m} = \varrho\kappa^2_{s,r_m} + \kappa^2_{ts} + \varrho\kappa^2_{r_m,d}(1+\kappa^2_{s,r_m}) + \kappa^2_{r_m,d}(1+\kappa^2_{ts})$,
$\alpha_{2,m} = \varrho^2\kappa^2_{s,r_m} + \varrho^2\kappa^2_{r_m,d}(1+\kappa^2_{s,r_m})$,
$\alpha_{3,m} = \varrho\kappa^2_{ts} + \varrho\kappa^2_{r_m,d}(1+\kappa^2_{ts})$,

$$
\begin{aligned}
\alpha_{4,m} &= \varrho(1+\kappa_{s,r_m}^2)+\varrho\kappa_{r_m,d}^2(1+\kappa_{s,r_m}^2)+(1+\kappa_{s,r_m}^2)(1+\kappa_{tr_m}^2),\\
\alpha_{5,m} &= \varrho(1+\kappa_{s,r_m}^2)(1+\kappa_{tr_m}^2),\\
\alpha_{6,m} &= \alpha_{7,m}|\hat{h}_{sp}|^2+\alpha_{8,m}|\hat{h}_{r_mp}|^2+\alpha_{9,m}|\hat{h}_{r_mp}|^2|\hat{h}_{sp}|^2+\alpha_{10,m},\\
\alpha_{7,m} &= (1+\kappa_{ts}^2)+\kappa_{r_m,d}^2(1+\kappa_{ts}^2)+(1+\kappa_{ts}^2)(1+\kappa_{tr_m}^2)/\varrho,\\
\alpha_{8,m} &= (1+\kappa_{s,r_m}^2)(1+\kappa_{tr_m}^2)+(1+\kappa_{ts}^2)(1+\kappa_{tr_m}^2)/\varrho,\\
\alpha_{9,m} &= (1+\kappa_{ts}^2)(1+\kappa_{tr_m}^2),\\
\alpha_{10,m} &= (1+\kappa_{s,r_m}^2)+(1+\kappa_{ts}^2)/\varrho+\kappa_{r_m,d}^2(1+\kappa_{s,r_m}^2)+\kappa_{r_m,d}^2(1+\kappa_{ts}^2)/\varrho\\
&\quad +(1+\kappa_{s,r_m}^2)(1+\kappa_{tr_m}^2)/\varrho+(1+\kappa_{ts}^2)(1+\kappa_{tr_m}^2)/\varrho^2.
\end{aligned}
$$

Among all the available relays, the best relay can be selected opportunistically as

$$
m^* = \arg\max_{m=1,\ldots,K}\{\Lambda_m\}. \tag{4.11}
$$

Herein, we assume that the selection process is executed in a controller unit where all information about channel estimates are gathered and conveyed to the relays through feedback.

The channel gains $|h_{\imath\jmath}|^2$ and $|\hat{h}_{\imath\jmath}|^2$ follow exponential distribution with mean $\Omega_{\imath\jmath}$ and $\hat{\Omega}_{\imath\jmath} = \Omega_{\imath\jmath} - \sigma_{e,\imath\jmath}^2$, respectively, where $\imath \in \{s, r_m\}, \jmath \in \{d, r_m, p\}$, and $\imath \neq \jmath$. In general, the PDF and CDF for exponential random variable V with mean Ω are given by $f_V(v) = \frac{1}{\Omega}\mathrm{e}^{-\frac{v}{\Omega}}$ and $F_V(v) = 1 - \mathrm{e}^{-\frac{v}{\Omega}}$, respectively.

4.2.2 Outage Performance

In this section, we conduct outage performance analysis of the considered CMRN. With the application of selection combining on the destination D, the outage probability for a given threshold γ_{th} can be defined as

$$
\mathcal{P}_{\text{out}}(\gamma_{\text{th}}) = \Pr\left[\max\{\Lambda_{sd}, \Lambda_{m^*}\} < \gamma_{\text{th}}\right]. \tag{4.12}
$$

As apparent from (4.8) and (4.10), Λ_{sd} and Λ_{m^*} are dependent owing to the existence of a common random variable $|\hat{h}_{sp}|^2$. Hence, we first evaluate the conditional outage probability, conditioned on $W = |\hat{h}_{sp}|^2$, as

$$
\mathcal{P}_{\text{out}}(\gamma_{\text{th}}|W) = \int_0^{\gamma_{\text{th}}}\int_0^{\gamma_{\text{th}}} f_{\Lambda_{sd}}(u|W) f_{\Lambda_{m^*}}(v|W)\,du\,dv = F_{\Lambda_{sd}}(\gamma_{\text{th}}|W) F_{\Lambda_{m^*}}(\gamma_{\text{th}}|W). \tag{4.13}
$$

Then, the unconditional $\mathcal{P}_{\text{out}}(\gamma_{\text{th}})$ is obtained, by averaging over W, as

$$
\mathcal{P}_{\text{out}}(\gamma_{\text{th}}) = \int_0^{\infty} \mathcal{P}_{\text{out}}(\gamma_{\text{th}}|W) f_W(w)\,dw. \tag{4.14}
$$

Evaluation of (4.14) requires CDFs $F_{\Lambda_{sd}}(\gamma_{\text{th}}|W)$ and $F_{\Lambda_{m^*}}(\gamma_{\text{th}}|W)$ which are obtained as follows. Using (4.9), we can write

$$F_{\Lambda_{sd}}(\gamma_{\text{th}}|W) = \Pr\left[\Lambda_{sd} < \gamma_{\text{th}}|W\right] = \Pr\left[|\hat{h}_{sd}|^2 < \frac{\gamma_{\text{th}}(\alpha_{s,d}+\delta_s w)}{\varrho(1-\kappa_{s,d}^2\gamma_{\text{th}})}\right]$$
$$= \begin{cases} 1-\mathrm{e}^{-\frac{\gamma_{\text{th}}(\alpha_{s,d}+\delta_s w)}{\hat{\Omega}_{sd}\varrho(1-\kappa_{s,d}^2\gamma_{\text{th}})}}, \text{ for } \gamma_{\text{th}} < 1/\kappa_{s,d}^2, \\ 1, \text{ otherwise.} \end{cases} \tag{4.15}$$

For evaluating $F_{\Lambda_{m^*}}(\gamma_{\text{th}}|W)$, we apply order statistics based on (4.11) to write

$$F_{\Lambda_{m^*}}(\gamma_{\text{th}}|W) = \prod_{m=1}^{K} F_{\Lambda_m}(\gamma_{\text{th}}|W), \tag{4.16}$$

where $F_{\Lambda_m}(\gamma_{\text{th}}|W)$ can be obtained as

$$F_{\Lambda_m}(\gamma_{\text{th}}|W) = \Pr[\Lambda_m < \gamma_{\text{th}}|W]. \tag{4.17}$$

For notational simplicity in subsequent analysis, we assume $|\hat{h}_{sr_m}|^2 = X$, $|\hat{h}_{r_m d}|^2 = Y$, and $|\hat{h}_{r_m p}|^2 = Z$. Also, as followed in [70], for similar hardware of relays, we denote $\kappa_{s,r_m}^2 = \kappa_{s,r}^2$, $\kappa_{r_m,d}^2 = \kappa_{r,d}^2$, $\kappa_{tr_m}^2 = \kappa_{tr}^2$, and $\alpha_{i,m} = \alpha_i$ (where $i \in \{1, ..., 10\}$). With this, we can represent (4.17), using (4.10), as

$$F_{\Lambda_m}(\gamma_{\text{th}}|W) = \Pr\left[X < \frac{\gamma_{\text{th}}(\alpha_1 Y + \alpha_3 w Y + \alpha_6)}{Y(\varrho^2 - \gamma_{\text{th}}\alpha_2) - \gamma_{\text{th}}(\alpha_4 + \alpha_5 Z)}\middle| W\right]$$
$$= \begin{cases} \Psi(\gamma_{\text{th}}, w), \text{ for } \gamma_{\text{th}} < \frac{1}{\kappa_{s,r}^2+\kappa_{r,d}^2+\kappa_{s,r}^2\kappa_{r,d}^2}, \\ 1, \text{ otherwise,} \end{cases} \tag{4.18}$$

where $\Psi(\gamma_{\text{th}}, w)$ is given by

$$\Psi(\gamma_{\text{th}}, w) = \int_{z=0}^{\infty}\int_{y=\xi(z)}^{\infty} F_X\left(\frac{\gamma_{\text{th}}(\alpha_1 y + \alpha_3 w y + \alpha_6)}{y(\varrho^2 - \gamma_{\text{th}}\alpha_2) - \gamma_{\text{th}}(\alpha_4 + \alpha_5 z)}\right) f_Y(y) f_Z(z)\, dy\, dz, \tag{4.19}$$

with $\xi(z) = \frac{\gamma_{\text{th}}(\alpha_4+\alpha_5 z)}{(\varrho^2-\gamma_{\text{th}}\alpha_2)}$. Substituting the required CDF and PDFs into (4.19) and performing the required integration with the aid of [49, eq. 3.324], we obtain (after some involved manipulations)

$$\Psi(\gamma_{\text{th}}, w) = 1 - \int_{z=0}^{\infty} \mathrm{e}^{-\left(\frac{\gamma_{\text{th}}(\alpha_1+\alpha_3 w)}{\hat{\Omega}_{sr_m}(\varrho^2-\gamma_{\text{th}}\alpha_2)} + \frac{\gamma_{\text{th}}(\alpha_4+\alpha_5 z)}{\hat{\Omega}_{r_m d}(\varrho^2-\gamma_{\text{th}}\alpha_2)}\right)}$$
$$\times \frac{\sqrt{\zeta(z)(\varrho^2-\gamma_{\text{th}}\alpha_2)}}{\varrho^2-\gamma_{\text{th}}\alpha_2}\mathcal{K}_1\left(\sqrt{\frac{\zeta(z)}{\varrho^2-\gamma_{\text{th}}\alpha_2}}\right) f_Z(z)\, dz, \tag{4.20}$$

where $\zeta(z) = \frac{4\gamma_{\rm th}}{\hat{\Omega}_{srm}}\left(\frac{\gamma_{\rm th}(\alpha_4+\alpha_5 z)}{\varrho^2-\gamma_{\rm th}\alpha_2}+\alpha_6\right)$ and $\mathcal{K}_1(\cdot)$ denotes the first-order modified bessel function of the second kind [49, eq. 8.432.6]. However, it would be very difficult to solve (4.20) in a closed-form, we make use of the fact $\mathcal{K}_1(x) \approx 1/x$ as in [115], and evaluate the resultant expression to obtain $\Psi(\gamma_{\rm th}, w)$ as

$$\Psi(\gamma_{\rm th}, w) \approx 1 - e^{-\left(\frac{\gamma_{\rm th}(\alpha_1+\alpha_3 w)}{\hat{\Omega}_{srm}(\varrho^2-\gamma_{\rm th}\alpha_2)}+\frac{\gamma_{\rm th}\alpha_4}{\hat{\Omega}_{rmd}(\varrho^2-\gamma_{\rm th}\alpha_2)}\right)}\left(1+\frac{\alpha_5\gamma_{\rm th}\hat{\Omega}_{rmp}}{\varrho^2-\gamma_{\rm th}\alpha_2}\right)^{-1}. \tag{4.21}$$

Note that such approximation leads to very tight results in broad SNR region, as illustrated in Section 4.2.4. Consequently, on using (4.17), (4.18), (4.21) in (4.16) and the result along with (4.15) in (4.13), we get $\mathcal{P}_{\rm out}(\gamma_{\rm th}|W)$. Finally, substituting the so obtained $\mathcal{P}_{\rm out}(\gamma_{\rm th}|W)$ and PDF $f_W(w)$ in (4.14) and then evaluating the resultant integral, the outage probability of CMRN is obtained as

$$\mathcal{P}_{\rm out}(\gamma_{\rm th}) \approx \begin{cases} \mathcal{P}_1, \text{ for } \gamma_{\rm th} < \frac{1}{\kappa_{s,r}^2+\kappa_{r,d}^2+\kappa_{s,r}^2\kappa_{r,d}^2}, \\ \mathcal{P}_2, \text{ for } \frac{1}{\kappa_{s,r}^2+\kappa_{r,d}^2+\kappa_{s,r}^2\kappa_{r,d}^2} \le \gamma_{\rm th} < 1/\kappa_{s,d}^2, \\ 1, \text{ otherwise}, \end{cases} \tag{4.22}$$

in which the component $\mathcal{P}_1$ is given by

$$\begin{aligned}\mathcal{P}_1 = &\sum_{n=0}^{1}\sum_{n_1=0}^{1}\sum_{n_2=0}^{1}\cdots\sum_{n_K=0}^{1}(-1)^{n+\sum_{i=1}^K n_i} e^{-\sum_{i=1}^K\left[\frac{n_i\gamma_{\rm th}\alpha_1}{\hat{\Omega}_{sr_i}(\varrho^2-\alpha_2\gamma_{\rm th})}+\frac{n_i\gamma_{\rm th}\alpha_4}{\hat{\Omega}_{r_id}(\varrho^2-\alpha_2\gamma_{\rm th})}\right]} \\ &\times\left[\prod_{i=1}^{K}\left(1+\frac{\alpha_5\gamma_{\rm th}\hat{\Omega}_{r_ip}}{\hat{\Omega}_{r_id}(\varrho^2-\alpha_2\gamma_{\rm th})}\right)^{-n_i}\right] e^{-\frac{n\gamma_{\rm th}\alpha_{s,d}}{\hat{\Omega}_{sd}\varrho(1-\kappa_{s,d}^2\gamma_{\rm th})}} \\ &\times\left[1+\hat{\Omega}_{sp}\left\{\frac{n\delta_s\gamma_{\rm th}}{\hat{\Omega}_{sd}\varrho(1-\kappa_{s,d}^2\gamma_{\rm th})}+\sum_{i=1}^{K}\frac{n_i\gamma_{\rm th}\alpha_3}{\hat{\Omega}_{sr_i}(\varrho^2-\alpha_2\gamma_{\rm th})}\right\}\right]^{-1},\end{aligned} \tag{4.23}$$

and the component $\mathcal{P}_2$ is given as

$$\mathcal{P}_2 = \sum_{n=0}^{1}(-1)^n e^{-\frac{n\gamma_{\rm th}\alpha_{s,d}}{\hat{\Omega}_{sd}\varrho(1-\kappa_{s,d}^2\gamma_{\rm th})}}\left[1+\frac{n\delta_s\hat{\Omega}_{sp}\gamma_{\rm th}}{\hat{\Omega}_{sd}\varrho(1-\kappa_{s,d}^2\gamma_{\rm th})}\right]^{-1}. \tag{4.24}$$

Herein, the component $\mathcal{P}_1$ accounts for the selection cooperation between both direct and relay links. While $\mathcal{P}_2$ arises from the transmission via direct link only, that is, without cooperation from the relay. From (4.22), it is important to observe that HIs impose undesirable constraints on $\gamma_{\rm th}$ which in turn cause ceiling effects in the system. When $\gamma_{\rm th} \ge \frac{1}{\kappa_{s,r}^2+\kappa_{r,d}^2+\kappa_{s,r}^2\kappa_{r,d}^2}$, the relay ceases to cooperate the transmission and hence the system relies only on the transmission from direct link. This effect is called relay cooperation ceiling (RCC) [104]. Whereas, for $\gamma_{\text{th}} \geq 1/\kappa_{s,d}^2$, the direct transmission also fails, and as a result, overall system goes into outage, which is referred hereby as overall system ceiling (OSC). This is clearly reflected by the fact that probability term in (4.22) evaluates to unity for $\gamma_{\text{th}} \geq 1/\kappa_{s,d}^2$. Note that, as $\kappa_{s,r}^2 + \kappa_{r,d}^2 + \kappa_{s,r}^2\kappa_{r,d}^2 > \kappa_{s,d}^2$, RCC always appears before OSC. Altogether, it is worth remarking that HIs are deleterious for system performance and hence it is important to take them into consideration while designing the practical systems for high-rate applications.

4.2.3 Asymptotic Outage Performance

In this section, we derive asymptotic outage expression in the high-SNR regime ($\varrho \to \infty$). Herein, without losing generality, we assume independent and identically distributed channels, i.e., $\Omega_{sr_m} = \Omega_{sr}$, $\Omega_{r_md} = \Omega_{rd}$, $\Omega_{r_mp} = \Omega_{rp}$ $\forall$ $m \in \{1, ..., K\}$. Also, for attaining better insights, we assume that $\kappa_{s,r}^2 = \kappa_{r,d}^2 = \kappa_{s,d}^2 = \kappa^2$. For deriving outage probability at high-SNR regime, we need to simplify the CDFs $F_{\Lambda_{sd}}(\gamma_{\text{th}}|W)$ and $F_{\Lambda_{m^*}}(\gamma_{\text{th}}|W)$. For this, we first obtain $F_{\Lambda_{sd}}(\gamma_{\text{th}}|W)$, by using (4.15) along with the fact that $\mathrm{e}^{-x} \simeq 1 - x$ for small x, as

$$F_{\Lambda_{sd}}(\gamma_{\text{th}}|W) = \begin{cases} \frac{\gamma_{\text{th}}(1+\kappa^2)}{\hat{\Omega}_{sd}\varrho(1-\kappa^2\gamma_{\text{th}})} + \frac{\gamma_{\text{th}}\delta_s w}{\hat{\Omega}_{sd}\varrho(1-\kappa^2\gamma_{\text{th}})}, & \text{for } \gamma_{\text{th}} < 1/\kappa^2, \\ 1, & \text{otherwise.} \end{cases} \tag{4.25}$$

Next, at high-SNR, (4.21) can be approximated by

$$\psi(\gamma_{\text{th}}, w) \simeq 1 - \mathrm{e}^{-\left(\frac{\gamma_{\text{th}}(\bar{a}_1+\bar{a}_2 w)}{\hat{\Omega}_{sr}\varrho(1-\gamma_{\text{th}}\bar{a}_1)} + \frac{\gamma_{\text{th}}\bar{a}_3}{\hat{\Omega}_{rd}\varrho(1-\gamma_{\text{th}}\bar{a}_1)}\right)} \left(1 + \frac{\bar{a}_4\gamma_{\text{th}}\hat{\Omega}_{rp}}{\varrho\hat{\Omega}_{rd}(1-\gamma_{\text{th}}\bar{a}_1)}\right)^{-1}, \tag{4.26}$$

where $\bar{a}_1 = 2\kappa^2 + \kappa^4$, $\bar{a}_2 = \kappa_{ts}^2 + \kappa^2(1 + \kappa_{ts}^2)$, $\bar{a}_3 = 1 + \bar{a}_1$, $\bar{a}_4 = (1 + \kappa^2)(1 + \kappa_{tr}^2)$. Now, using $(1 + x)^{-1} \simeq 1 - x$ and $\mathrm{e}^{-x} \simeq 1 - x$ for small x, (4.26) can be written as

$$\psi(\gamma_{\text{th}}, w) \simeq 1 - \left(1 - \frac{\gamma_{\text{th}}(\bar{a}_1 + \bar{a}_2 w)}{\hat{\Omega}_{sr}\varrho(1-\gamma_{\text{th}}\bar{a}_1)} - \frac{\gamma_{\text{th}}\bar{a}_3}{\hat{\Omega}_{rd}\varrho(1-\gamma_{\text{th}}\bar{a}_1)}\right)\left(1 - \frac{\bar{a}_4\gamma_{\text{th}}\hat{\Omega}_{rp}}{\varrho\hat{\Omega}_{rd}(1-\gamma_{\text{th}}\bar{a}_1)}\right). \tag{4.27}$$

Further, inserting (4.27) in (4.18) and the so obtained result in (4.16), we get

$$F_{\Lambda_{m^*}}(\gamma_{\text{th}}|W) \simeq \begin{cases} [\psi(\gamma_{\text{th}}, w)]^K, & \text{for } \gamma_{\text{th}} < \frac{1}{2\kappa^2+\kappa^4}, \\ 1, & \text{otherwise .} \end{cases} \tag{4.28}$$

Finally, using (4.25) and (4.28) in (4.13) and obtained result in (4.14), and then after integrating the resultant expression, we get the outage probability at asymptotic limit as

$$\mathcal{P}_{\rm out}(\gamma_{\rm th}) \simeq \begin{cases} \mathcal{P}_{\rm asy1}\left(\frac{1}{\varrho}\right)^{K+1}, \text{ for } \gamma_{\rm th} < \frac{1}{2\kappa^2+\kappa^4}, \\ \mathcal{P}_{\rm asy2}\left(\frac{1}{\varrho}\right), \text{ for } \frac{1}{2\kappa^2+\kappa^4} \leq \gamma_{\rm th} < 1/\kappa^2, \\ 1, \text{ otherwise }, \end{cases} \tag{4.29}$$

where $\mathcal{P}_{\rm asy1}$ and $\mathcal{P}_{\rm asy2}$ are given, respectively, by

$$\begin{aligned} \mathcal{P}_{\rm asy1} = & \sum_{r=0}^{K}\binom{K}{r}\left(\frac{\gamma_{\rm th}\bar{a}_1}{\hat{\Omega}_{sr}(1-\gamma_{\rm th}\bar{a}_1)} + \frac{\gamma_{\rm th}(\bar{a}_3+\bar{a}_4\hat{\Omega}_{rp})}{\hat{\Omega}_{rd}(1-\gamma_{\rm th}\bar{a}_1)}\right)^{K-r} \\ & \times\left(\frac{\gamma_{\rm th}(1+\kappa^2)r!\hat{\Omega}_{sp}^{r}}{\hat{\Omega}_{sd}(1-\kappa^2\gamma_{\rm th})} + \frac{\gamma_{\rm th}\delta_s(r+1)!\hat{\Omega}_{sp}^{r+1}}{\hat{\Omega}_{sd}(1-\kappa^2\gamma_{\rm th})}\right)\left(\frac{\gamma_{\rm th}\bar{a}_2}{\hat{\Omega}_{sr}(1-\gamma_{\rm th}\bar{a}_1)}\right)^{r} \end{aligned} \tag{4.30}$$

$$\text{and} \quad \mathcal{P}_{\rm asy2} = \left(\frac{\gamma_{\rm th}(1+\kappa^2)}{\hat{\Omega}_{sd}(1-\kappa^2\gamma_{\rm th})} + \frac{\gamma_{\rm th}\delta_s\hat{\Omega}_{sp}}{\hat{\Omega}_{sd}(1-\kappa^2\gamma_{\rm th})}\right). \tag{4.31}$$

Re-expressing $\mathcal{P}_{\rm out}(\gamma_{\rm th})$ in (4.29) as $(\mathcal{G}_c\varrho)^{-\mathcal{G}_d}$, it can be inferred that system achieves full diversity gain of $\mathcal{G}_d = K+1$ as long as $\gamma_{\rm th} < \frac{1}{2\kappa^2+\kappa^4}$. After the RCC and before the occurrence of OSC $\left(\frac{1}{2\kappa^2+\kappa^4} \leq \gamma_{\rm th} < 1/\kappa^2\right)$, as the system relies on direct link only, the diversity gain becomes $\mathcal{G}_d = 1$. And, once the OSC phenomenon occurs, the system goes in outage and thereby the diversity gain reduces to zero. Additionally, it can be deduced that the HIs also affect the coding gain $\mathcal{G}_c$ of system. It is worth noting that since CEEs are decreasing function of SNR, they do not affect the diversity gain of the system. However, CEEs pose critical impact on the coding gain, as illustrated in Section 4.2.4.

4.2.4 Numerical and Simulation Results

For numerical analysis, we place the network nodes S, $\{R_m\}_{m=1}^{K}$, D, and T_p at two-dimensional (2-D) space coordinates $(0,0)$, $(0.5,0)$, $(1,0)$, and $(0.5,0.5)$, respectively. Considering path-loss model with exponent $\alpha = 4$ and d_{ij} as the distance between the nodes i and j, we set $\Omega_{ij} = d_{ij}^{-\alpha}$. We also set $\kappa_{ts} = \kappa_{rd} = \kappa_{tr_m} = \kappa_{rr_m} = \kappa_i$ such that $\kappa_{s,d} = \kappa_{r,d} = \kappa_{s,r} = \kappa = \sqrt{2}\kappa_i$. Note that, for a fair comparison, we readily obtain the outage expression for an ideal system (without HIs and CEEs) by considering a single PU in [22].

Fig. 4.2 plots the outage probability curves versus ϱ for the considered CMRN.

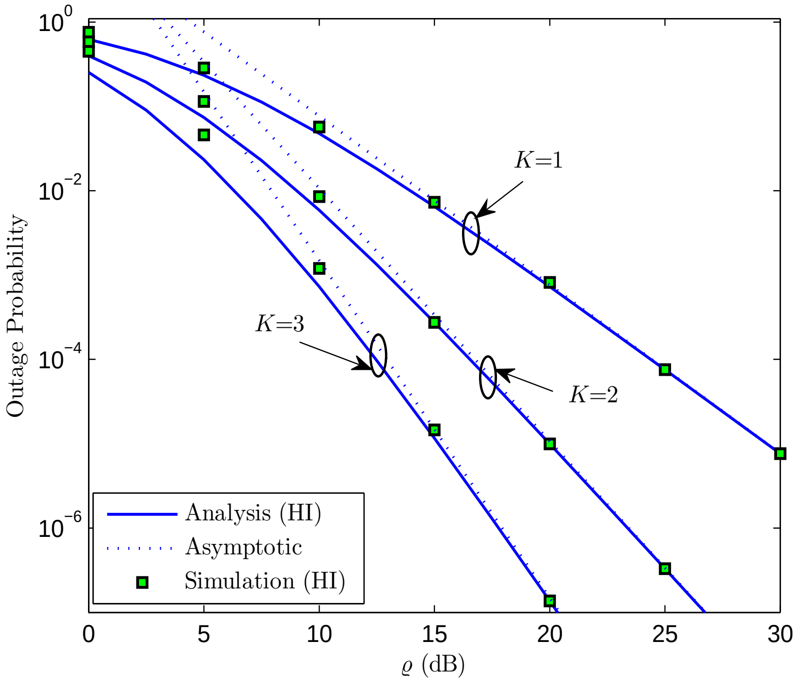

Figure 4.2: Outage performance of the system against ϱ.

Herein, we set $\gamma_{\text{th}} = 1$, $\kappa_i = 0.175$, and vary the number of relays K. We can clearly see that the analytical curves are in well agreement to the simulation results. Also, the asymptotic curves closely follow analytical curves at high ϱ. As such, for the given HIs levels, the threshold γ_{th} is maintained below RCC point (≈ 7.921) and thereby the system can exploit full diversity in such instances of lower target rates. This is also evident from the respective curves for different values of K.

In Fig. 4.3, we illustrate the impact of γ_{th} and HIs level on the system performance. From the respective curves, it is apparent that as γ_{th} increases, the performance of system deteriorates due to high-rate requirements. Evidently, the performance gap between the ideal system and impaired system also expands with increase in γ_{th} (see curves for $\gamma_{\text{th}} = 1, 2, 3$). Moreover, when HIs level κ_i increases from 0.2 to 0.3, the system performance degrades significantly. It can be further seen that for a fixed γ_{th}, there exists a performance gap between ideal and impaired system which arises primarily due to the joint impact of HIs and CEEs on coding gain, and this gap is preserved for the entire range of SNR. This is associated with the fact that a fixed γ_{th} implies a fixed diversity gain ($\mathcal{G}_d = K + 1$ in this case). And, since CEEs are decreasing with the SNR ($\sigma^2_{e,\imath\jmath} = 1/\varrho$), the performance loss due to CEEs also decreases with increase in SNR. Therefore, the performance gap between ideal and impaired system is preserved irrespective of the SNR.

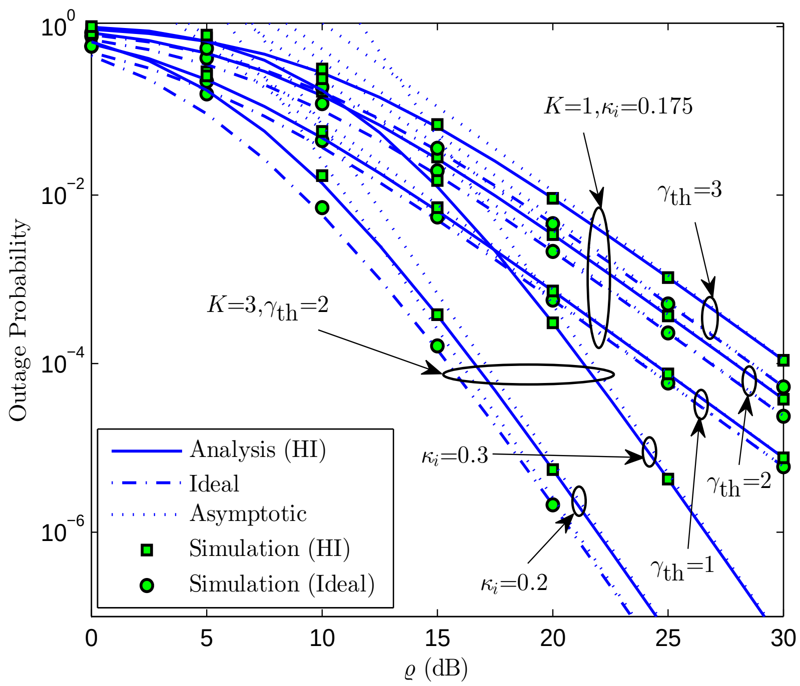

Figure 4.3: Outage performance of the system against ϱ.

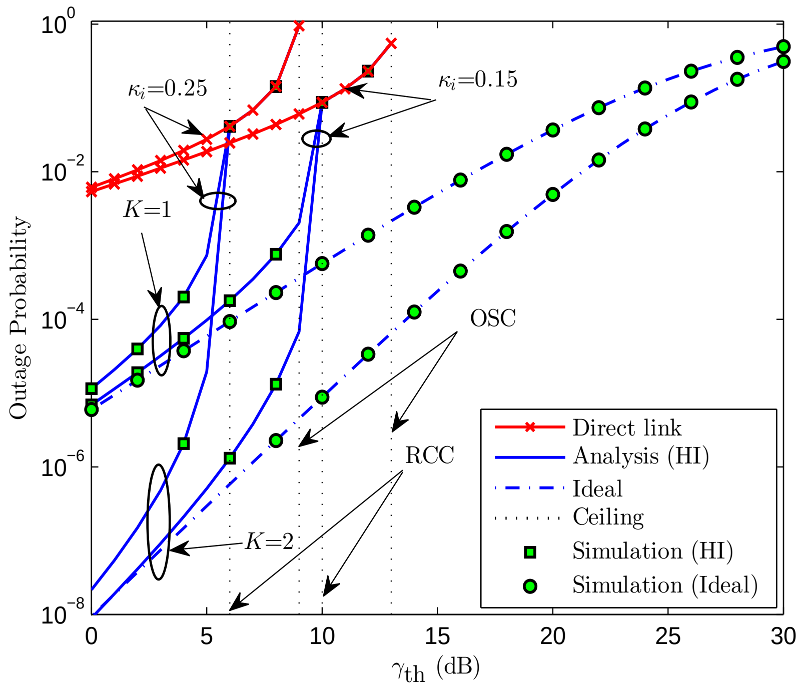

Figure 4.4: Outage performance of the system against $\gamma_{\rm th}$.

In Fig. 4.4, we plot the outage probability curves against the $\gamma_{\rm th}$. Herein, we set $\varrho = 30$ dB to analyze the effect of RCC on the performance of considered CMRN with CEEs. For instance, if $\kappa_i = 0.15(0.25)$, the RCC and OSC effect occurs at the threshold of ≈ 6 dB(10 dB) and ≈ 9 dB(13 dB) respectively. It can be manifestly observed from the curves that as $\gamma_{\rm th}$ crosses the RCC, the system performance converges to that of a pure direct link. Apparently, the direct link partially compensates for RCC, by providing diversity gain of unity, until the occurrence of OSC. Afterwards, when γ_{th} further increases to OSC point, the system outage probability approaches to unity. Thus, we conclude that HIs are detrimental for system to keep with its performance standards in high-rate applications.

4.3 Cognitive DF Multi-Relay Networks with RF HIs and CEEs

In the previous section, we investigated the performance of AF-based CMRN. However, for the conventional cooperative systems with HIs, DF relaying is shown to be more advantageous and preferable over AF relaying for designing the high-rate systems [88]. This is because, unlike AF relaying, the additional distortion noises in the first hop of DF relaying do not carry on to the second hop which makes it more resilient and robust to HIs. Therefore, in this section, we analyze the performance of a DF relaying based CMRN with a direct link in presence of HIs and CEEs. We manifest that the distortion noises induced in the direct link and relaying link chains cause three ceiling effects viz., relay cooperation ceiling (RCC), direct link ceiling (DLC), and overall system ceiling (OSC), and thereby, cap the fundamental capacity of the considered system. Herein, we also consider both the power constraints, i.e., maximum available transmit power and maximum tolerable interference at the PU. Such consideration is more practical for the SU transmitters to ensure the QoS requirements at the PU receiver in an underlay spectrum sharing model.

4.3.1 System Descriptions

As shown in Fig. 4.1, we consider a CMRN where one secondary source S communicates with one secondary destination D using the cooperation of K secondary DF relays $\{R_m\}_{m=1}^{K}$ in the presence of a primary receiver T_p. In the considered DF-based CMRN, the overall secondary communication takes place in two time phases. In first phase, S transmits its signal x_s (satisfying $\mathbb{E}\{|x_s|^2\} = P_s$) to D and all the relays. Consequently, the received signals at D and R_m can be given, respectively, by

$$y_{d,1} = (\hat{h}_{sd} + e_{h_{sd}})(x_s + \eta_{s,d}) + \nu_{d,1} \tag{4.32}$$

$$\text{and} \quad y_{r_m} = (\hat{h}_{sr_m} + e_{h_{sr_m}})(x_s + \eta_{s,r_m}) + \nu_{r_m}, \tag{4.33}$$

where $\nu_{d,1}$ and ν_{r_m} represent AWGN variables at the respective nodes, while $\eta_{s,d} \sim \mathcal{CN}(0, \kappa_{s,d}^2 P_s)$ and $\eta_{s,r_m} \sim \mathcal{CN}(0, \kappa_{s,r_m}^2 P_s)$ denote equivalent distortion noises at D and R_m, respectively, with $\kappa_{\imath,\jmath} = \sqrt{\kappa_{t\imath}^2 + \kappa_{r\jmath}^2}$, where $\imath \in \{s, r_m\}$, $\jmath \in \{d, r_m\}$, and $\imath \neq \jmath$. In an underlay scenario with HIs and CEEs, to limit the interference power at primary receiver T_p below a pre-determined threshold Q, the transmit power at S should be constrained as $\mathbb{E}\{|(\hat{h}_{sp} + e_{h_{sp}})(x_s + \eta_{ts})|^2\} \leq Q$. In addition, since the source S has maximum transmit power limit of P, the transmit power P_s at S can be expressed as

$$P_s = \min\left(P, \frac{Q}{(|\hat{h}_{sp}|^2 + \sigma_{e,sp}^2)(1 + \kappa_{ts}^2)}\right). \tag{4.34}$$

Thereby, from (4.32) and (4.33), the resulting SNDRs at D and R_m in the first phase can be given, respectively, as

$$\Lambda_{sd} = \frac{P_s|\hat{h}_{sd}|^2}{P_s\kappa_{s,d}^2|\hat{h}_{sd}|^2 + P_s\sigma_{e,sd}^2(1 + \kappa_{s,d}^2) + N_0} \tag{4.35}$$

$$\text{and} \quad \Lambda_{sr_m} = \frac{P_s|\hat{h}_{sr_m}|^2}{P_s\kappa_{s,r_m}^2|\hat{h}_{sr_m}|^2 + P_s\sigma_{e,sr_m}^2(1 + \kappa_{s,r_m}^2) + N_0}. \tag{4.36}$$

In second phase, the relays $\{R_m\}$ first attempt to decode the signal received from S. Let $\mathcal{D}_0$ denote the set of relays that can successfully decode the signal received in first phase. With target rate $\mathcal{R}$ for successful decoding, we have

$$\mathcal{D}_0 = \{R_m | \Lambda_{sr_m} \geq \gamma_{\text{th}}, m \in \{1, ..., K\}\}, \tag{4.37}$$

where $\gamma_{\text{th}} = 2^{2\mathcal{R}} - 1$. Amongst all the relays in $\mathcal{D}_0$, the best relay (say mth relay) is selected in a reactive manner to forward the re-encoded signal x_r (satisfying $\mathbb{E}\{|x_r|^2\} = P_{r_m}$) to D. Another possible way of selecting the relay is proactive relay selection in which the best relay is selected based on max-min criterion. However, such proactive selection requires much larger feedback overhead to obtain CSI of all links [116]. Therefore, we resort to the reactive relay selection as disclosed in next section. As such, the received signal at D via relay R_m can be expressed as

$$y_{d,2} = (\hat{h}_{r_m d} + e_{h_{r_m d}})(x_r + \eta_{r_m,d}) + \nu_{d,2}, \tag{4.38}$$

where $\nu_{d,2}$ represents AWGN at D and $\eta_{r_m,d} \sim \mathcal{CN}(0, \kappa_{r_m,d}^2 P_{r_m})$. Further, due to maximum tolerable interference constraint of Q from T_p, the transmit power at the relay must be constrained to $\mathbb{E}\{|(\hat{h}_{r_m p} + e_{h_{r_m p}})(x_r + \eta_{tr_m})|^2\} \leq Q$. Also, since the relay has its maximum transmit power limit P, the transmit power P_{r_m} at the mth relay can be written as

$$P_{r_m} = \min\left(P, \frac{Q}{(|\hat{h}_{r_m p}|^2 + \sigma^2_{e,r_m p})(1+\kappa^2_{tr_m})}\right). \tag{4.39}$$

Using (4.38), the SNDR at D via relaying link transmission in second phase can be written as

$$\Lambda_{r_m d} = \frac{P_{r_m}|\hat{h}_{r_m d}|^2}{P_{r_m}\kappa^2_{r_m,d}|\hat{h}_{r_m d}|^2 + P_{r_m}\sigma^2_{e,r_m d}(1+\kappa^2_{r_m,d}) + N_0}. \tag{4.40}$$

Herein, all the channel gains $|h_{\imath\jmath}|^2$ and $|\hat{h}_{\imath\jmath}|^2$ follow exponential distribution with mean $\Omega_{\imath\jmath}$ and $\hat{\Omega}_{\imath\jmath} = \Omega_{\imath\jmath} - \sigma^2_{e,\imath\jmath}$, respectively, where $\imath \in \{s, r_m\}$, $\jmath \in \{d, r_m, p\}$, and $\imath \neq \jmath$. In general, PDF and CDF for exponential random variable V with mean Ω are given by $f_V(v) = \frac{1}{\Omega}\exp\left(-\frac{v}{\Omega}\right)$ and $F_V(v) = 1 - \exp\left(-\frac{v}{\Omega}\right)$, respectively, where $v \geq 0$. Further, as in various previous works [103], [104], [117], we consider $\kappa^2_{s,r_m} = \kappa^2_{s,r}$, $\kappa^2_{r_m,d} = \kappa^2_{r,d}$, $\kappa^2_{tr_m} = \kappa^2_{tr}$ for similar hardware of relays.

4.3.2 Outage Performance

In this section, we conduct outage performance analysis of the considered CMRN. Let $\mathcal{D}_m$ be a decoding subset having m active relays (i.e., cardinality $|\mathcal{D}_m| = m$). Then, for a given threshold γ_{th}, the outage probability of the CMRN can be formulated using total probability theorem [118] as

$$\mathcal{P}_{\text{out}}(\gamma_{\text{th}}) = \overbrace{\Pr\left[\Lambda_{sd} < \gamma_{\text{th}}, \mathcal{D}_0 = \emptyset\right]}^{\mathcal{P}_{\emptyset}} + \overbrace{\sum_{m=1}^{K}\sum_{\mathcal{D}_m}\Pr\left[\Lambda_{sd} < \gamma_{\text{th}}, \Lambda_{r_m d} < \gamma_{\text{th}}, \mathcal{D}_m\right]}^{\mathcal{P}_{\bar{\emptyset}}}. \tag{4.41}$$

In (4.41), the first component $\mathcal{P}_{\emptyset}$ accounts for the case when no relay can successfully decode the signal received in the first phase, i.e., $\mathcal{D}_0$ is empty, and as a result, system relies on the direct link transmission only. Whereas, the other component $\mathcal{P}_{\bar{\emptyset}}$ corresponds to the case when $\mathcal{D}_0$ is nonempty, and consequently, the destination D applies the selection cooperation to combine the signals received from direct link and best relaying link. The internal sum in $\mathcal{P}_{\bar{\emptyset}}$ spans over all $\binom{K}{m}$ possible decoding subsets $\mathcal{D}_m$ of size m from the set of K candidate relays. On observing (4.35) and (4.37), with the help of (4.34) and (4.36), we notice that each of the components $\mathcal{P}_{\bar{\emptyset}}$ and $\mathcal{P}_{\emptyset}$ in (4.41) contains joint events with dependence due to presence of a common random variable $W = |\hat{h}_{sp}|^2$. Hence, these components can not be evaluated using conventional analysis any more. Hereby, we apply the conditioning approach to carry out the computation of $\mathcal{P}_{\bar{\emptyset}}$ and $\mathcal{P}_{\emptyset}$ in the following subsections.

Computation of $\mathcal{P}_{\bar{\emptyset}}$

We obtain $\mathcal{P}_{\bar{\emptyset}}$ by first conditioning on W and then taking the expectation over W as

$$\mathcal{P}_{\bar{\emptyset}} = \int_0^{\infty} \sum_{m=1}^{K} \sum_{\mathcal{D}_m} \Pr\left[\Lambda_{sd} < \gamma_{\mathrm{th}} | W\right] \Pr\left[\mathcal{D}_m | W\right] \Pr\left[\Lambda_{r_m d} < \gamma_{\mathrm{th}} | \mathcal{D}_m, W\right] f_W(w) dw. \quad (4.42)$$

To evaluate (4.42), we require the probabilities $\Pr\left[\Lambda_{sd} < \gamma_{\mathrm{th}} | W\right]$, $\Pr\left[\mathcal{D}_m | W\right]$, and $\Pr\left[\Lambda_{r_m d} < \gamma_{\mathrm{th}} | \mathcal{D}_m, W\right]$. Firstly, let us derive $\Pr\left[\mathcal{D}_m | W\right]$ in the following lemma.

Lemma 7. *The decoding probability $Pr[\mathcal{D}_m|W]$, conditioned on W, can be derived as*

$$Pr\left[\mathcal{D}_m | W\right] = \begin{cases} \Xi_m(\gamma_{th}, w), \ \text{for } \gamma_{th} < 1/\kappa_{s,r}^2, \\ 0, \ \text{for } \gamma_{th} \geq 1/\kappa_{s,r}^2, \end{cases} \quad (4.43)$$

where $\Xi_m(\gamma_{th}, w)$ is given by

$$\Xi_m(\gamma_{th}, w) = \left[\prod_{\ell=1}^{m} exp\left(-\frac{\gamma_{th}(\alpha_{s,r_\ell}\lambda_P + 1)}{\hat{\Omega}_{sr_\ell}\lambda_P(1-\kappa_{s,r}^2\gamma_{th})}\right)\right] \sum_{n_{m+1}=0}^{1} \cdots \sum_{n_K=0}^{1} (-1)^{\sum_{i=m+1}^{K} n_i} \times exp\left(-\sum_{i=m+1}^{K} \frac{n_i\gamma_{th}(\alpha_{s,r_i}\lambda_P + 1)}{\hat{\Omega}_{sr_i}\lambda_P(1-\kappa_{s,r}^2\gamma_{th})}\right), \ \text{for } W \leq Q_{sp} \quad (4.44)$$

and

$$\Xi_m(\gamma_{th}, w) = \left[\prod_{\ell=1}^{m} exp\left(-\frac{\gamma_{th}(\bar{\alpha}_{s,r_\ell} + \delta_s w)}{\hat{\Omega}_{sr_\ell}\lambda_Q(1-\kappa_{s,r}^2\gamma_{th})}\right)\right] \sum_{n_{m+1}=0}^{1} \cdots \sum_{n_K=0}^{1} (-1)^{\sum_{i=m+1}^{K} n_i} \times exp\left(-\sum_{i=m+1}^{K} \frac{n_i\gamma_{th}(\bar{\alpha}_{s,r_i} + \delta_s w)}{\hat{\Omega}_{sr_i}\lambda_Q(1-\kappa_{s,r}^2\gamma_{th})}\right), \ \text{for } W > Q_{sp}, \quad (4.45)$$

with $\lambda_P = P/N_0$, $\lambda_Q = Q/N_0$, $\delta_s = 1 + \kappa_{ts}^2$, $\alpha_{s,r_m} = (1+\kappa_{s,r}^2)\sigma_{e,sr_m}^2$, $\bar{\alpha}_{s,r_m} = \lambda_Q\alpha_{s,r_m} + \sigma_{e,sp}^2\delta_s$, and $Q_{sp} = \frac{Q}{P\delta_s} - \sigma_{e,sp}^2$.

Proof. Please refer to Appendix C. ∎

From the derived result in Lemma 7, it is important to note that the HIs impose the undesirable constraint on γ_{th} which restricts the decoding of received signals at the relays in the first phase beyond a certain rate requirement. This is clearly reflected by the fact that the conditional decoding probability in (4.43) reduces to zero for $\gamma_{\mathrm{th}} \geq 1/\kappa_{s,r}^2$.

Next, the conditional probability $\Pr[\Lambda_{sd} < \gamma_{\rm th}|W]$ can be expressed as

$$\Pr[\Lambda_{sd} < \gamma_{\rm th}|W] = \begin{cases} \Phi_{sd}(\gamma_{\rm th}, w), \text{ for } \gamma_{\rm th} < 1/\kappa_{s,d}^2, \\ 1, \text{ for } \gamma_{\rm th} \geq 1/\kappa_{s,d}^2, \end{cases} \tag{4.46}$$

where the function $\Phi_{sd}(\gamma_{\rm th}, w)$ is given by

$$\Phi_{sd}(\gamma_{\rm th}, w) = \Pr\left[\frac{P_s|\hat{h}_{sd}|^2}{P_s\kappa_{s,d}^2|\hat{h}_{sd}|^2 + P_s\sigma_{e,sd}^2(1+\kappa_{s,d}^2) + N_0} < \gamma_{\rm th}|W\right]. \tag{4.47}$$

By substituting (4.34) into (4.47) and evaluating the resultant expression, $\Phi_{sd}(\gamma_{\rm th}, w)$ can be obtained as

$$\Phi_{sd}(\gamma_{\rm th}, w) = \begin{cases} 1 - \exp\left(\frac{-\gamma_{\rm th}(\alpha_{s,d}\lambda_P+1)}{\hat{\Omega}_{sd}\lambda_P(1-\kappa_{s,d}^2\gamma_{\rm th})}\right), \text{ for } W \leq Q_{sp}, \\ 1 - \exp\left(\frac{-\gamma_{\rm th}(\tilde{\alpha}_{s,d}+\delta_s w)}{\hat{\Omega}_{sd}\lambda_Q(1-\kappa_{s,d}^2\gamma_{\rm th})}\right), \text{ for } W > Q_{sp}, \end{cases} \tag{4.48}$$

with $\alpha_{s,d} = (1+\kappa_{s,d}^2)\sigma_{e,sd}^2$ and $\tilde{\alpha}_{s,d} = \lambda_Q\alpha_{s,d} + \sigma_{e,sp}^2\delta_s$.

Now, we need to derive the term $\Pr[\Lambda_{r_m d} < \gamma_{\rm th}|\mathcal{D}_m, W]$. For this, let R_m represent best selected[4] relay among the m relays in $\mathcal{D}_m$, which is based on the criterion

$$\Lambda_{r_m d} = \max_{\{\ell\in\mathcal{D}_m\}}\{\Lambda_{r_\ell d}\}. \tag{4.49}$$

Then, by applying concepts of order statistics, we have

$$\Pr[\Lambda_{r_m d} < \gamma_{\rm th}|\mathcal{D}_m, W] = \prod_{\ell=1}^{m}\Pr[\Lambda_{r_\ell d} < \gamma_{\rm th}|\mathcal{D}_m, W]. \tag{4.50}$$

Consequently, using (4.40), we can compute (4.50) as

$$\Pr[\Lambda_{r_m d} < \gamma_{\rm th}|\mathcal{D}_m, W] = \begin{cases} \prod_{\ell=1}^{m}\Phi_{r_\ell d}(\gamma_{\rm th}), \text{ for } \gamma_{\rm th} < 1/\kappa_{r,d}^2, \\ 1, \text{ for } \gamma_{\rm th} \geq 1/\kappa_{r,d}^2, \end{cases} \tag{4.51}$$

where the function $\Phi_{r_\ell d}(\gamma_{\rm th})$ is derived in the following lemma.

Lemma 8. *The function $\Phi_{r_\ell d}(\gamma_{th})$ in (4.51) can be derived as*

[4]We assume that the selection process is executed in a controller unit where all the information about channel estimates and statistics of the distortion noises are gathered and conveyed to the relays through feedback [119], [120].

$$\Phi_{r_\ell d}(\gamma_{th}) = 1 - \left[1 - exp\left(\frac{-Q_{r_\ell p}}{\hat{\Omega}_{r_\ell p}}\right)\right] exp\left(\frac{-\gamma_{th}(\alpha_{r_\ell,d}\lambda_P + 1)}{\hat{\Omega}_{r_\ell d}\lambda_P(1-\gamma_{th}\kappa_{r,d}^2)}\right) - exp\left(\frac{-\gamma_{th}\tilde{\alpha}_{r_\ell,d}}{\hat{\Omega}_{r_\ell d}\lambda_Q(1-\kappa_{r,d}^2\gamma_{th})}\right)$$
$$\times \left(1 + \frac{\hat{\Omega}_{r_\ell p}\gamma_{th}\delta_r}{\hat{\Omega}_{r_\ell d}\lambda_Q(1-\kappa_{r,d}^2\gamma_{th})}\right)^{-1} exp\left(-Q_{r_\ell p}\left(\frac{1}{\Omega_{r_\ell,p}} + \frac{\gamma_{th}\delta_r}{\Omega_{r_\ell d}\lambda_Q(1-\kappa_{r,d}^2\gamma_{th})}\right)\right), \quad (4.52)$$

with $\delta_r = 1 + \kappa_{tr}^2$, $\alpha_{r_\ell,d} = (1+\kappa_{r,d}^2)\sigma_{e,r_\ell d}^2$, $\tilde{\alpha}_{r_\ell,d} = \lambda_Q\alpha_{r_\ell,d} + \sigma_{e,r_\ell p}^2\delta_r$, *and* $Q_{r_\ell p} = \frac{Q}{P\delta_r} - \sigma_{e,r_\ell p}^2$.

Proof. Please refer to Appendix D. ∎

Hereby, on using the result from Lemma 8 in (4.51), one can infer that HIs restrict decoding of signals in second phase at the destination beyond a certain rate requirement as evident from the condition $\gamma_{\rm th} \geq 1/\kappa_{r,d}^2$. Now, using (4.43), (4.46), and (4.51), it is important to emphasize that the $\mathcal{P}_{\bar{\emptyset}}$ in (4.42) evaluates to different expressions depending on the impairment levels $\kappa_{s,d}^2$, $\kappa_{s,r}^2$, and $\kappa_{r,d}^2$. Consequently, plugging (4.43), (4.46), and (4.51) in (4.42), and then after performing the required integration, we obtain $\mathcal{P}_{\bar{\emptyset}}$ for all the possible cases as follows:

- When $\kappa_{s,d}^2 \leq \kappa_{r,d}^2 \leq \kappa_{s,r}^2$ or $\kappa_{r,d}^2 \leq \kappa_{s,d}^2 \leq \kappa_{s,r}^2$,

$$\mathcal{P}_{\bar{\emptyset}} = \begin{cases} \mathcal{P}_{\bar{\emptyset}1}, & \text{for } \gamma_{\rm th} < 1/\kappa_{s,r}^2, \\ 0, & \text{otherwise.} \end{cases} \quad (4.53)$$

- When $\kappa_{s,r}^2 \leq \kappa_{s,d}^2 \leq \kappa_{r,d}^2$,

$$\mathcal{P}_{\bar{\emptyset}} = \begin{cases} \mathcal{P}_{\bar{\emptyset}1}, & \text{for } \gamma_{\rm th} < 1/\kappa_{r,d}^2, \\ \mathcal{P}_{\bar{\emptyset}4}, & \text{for } 1/\kappa_{r,d}^2 \leq \gamma_{\rm th} < 1/\kappa_{s,d}^2, \\ \mathcal{P}_{\bar{\emptyset}3}, & \text{for } 1/\kappa_{s,d}^2 \leq \gamma_{\rm th} < 1/\kappa_{s,r}^2 \\ 0, & \text{otherwise.} \end{cases} \quad (4.54)$$

- When $\kappa_{s,d}^2 \leq \kappa_{s,r}^2 \leq \kappa_{r,d}^2$,

$$\mathcal{P}_{\bar{\emptyset}} = \begin{cases} \mathcal{P}_{\bar{\emptyset}1}, & \text{for } \gamma_{\rm th} < 1/\kappa_{r,d}^2, \\ \mathcal{P}_{\bar{\emptyset}4}, & \text{for } 1/\kappa_{r,d}^2 \leq \gamma_{\rm th} < 1/\kappa_{s,r}^2, \\ 0, & \text{otherwise.} \end{cases} \quad (4.55)$$

- When $\kappa_{r,d}^2 \leq \kappa_{s,r}^2 \leq \kappa_{s,d}^2$,

$$\mathcal{P}_{\bar{\emptyset}} = \begin{cases} \mathcal{P}_{\bar{\emptyset}1}, \text{ for } \gamma_{\text{th}} < 1/\kappa_{s,d}^2, \\ \mathcal{P}_{\bar{\emptyset}2}, \text{ for } 1/\kappa_{s,d}^2 \leq \gamma_{\text{th}} < 1/\kappa_{s,r}^2 \\ 0, \text{ otherwise.} \end{cases} \tag{4.56}$$

- When $\kappa_{s,r}^2 \leq \kappa_{r,d}^2 \leq \kappa_{s,d}^2$,

$$\mathcal{P}_{\bar{\emptyset}} = \begin{cases} \mathcal{P}_{\bar{\emptyset}1}, \text{ for } \gamma_{\text{th}} < 1/\kappa_{s,d}^2, \\ \mathcal{P}_{\bar{\emptyset}2}, \text{ for } 1/\kappa_{s,d}^2 \leq \gamma_{\text{th}} < 1/\kappa_{r,d}^2, \\ \mathcal{P}_{\bar{\emptyset}3}, \text{ for } 1/\kappa_{r,d}^2 \leq \gamma_{\text{th}} < 1/\kappa_{s,r}^2 \\ 0, \text{ otherwise.} \end{cases} \tag{4.57}$$

Now, we derive the expressions for the components $\mathcal{P}_{\bar{\emptyset}1}$, $\mathcal{P}_{\bar{\emptyset}2}$, $\mathcal{P}_{\bar{\emptyset}3}$, and $\mathcal{P}_{\bar{\emptyset}4}$ in the sequel. Firstly, $\mathcal{P}_{\bar{\emptyset}1}$ will be derived in the following lemma.

Lemma 9. *The component $\mathcal{P}_{\bar{\emptyset}1}$ is given as follows*

$$\begin{aligned}
\mathcal{P}_{\bar{\emptyset}1} =& \sum_{m=1}^{K}\sum_{n=0}^{1}\sum_{n_{m+1}=0}^{1}\cdots\sum_{n_K=0}^{1}\binom{K}{m}\left(\prod_{\ell=1}^{m}\Phi_{r_\ell d}(\gamma_{th})\right)(-1)^{n+\sum_{i=m+1}^{K}n_i} exp\left(\frac{-n\alpha_{s,d}\gamma_{th}}{\hat{\Omega}_{sd}(1-\kappa_{s,d}^2\gamma_{th})} - \sum_{\ell=1}^{m}\frac{\alpha_{s,r_\ell}\gamma_{th}}{\hat{\Omega}_{sr_\ell}(1-\kappa_{s,r}^2\gamma_{th})}\right. \\
&\left.-\sum_{i=m+1}^{K}\frac{n_i\alpha_{s,r_i}\gamma_{th}}{\hat{\Omega}_{sr_i}(1-\kappa_{s,r}^2\gamma_{th})}\right)\left[\left(1-exp\left(\frac{-Q_{sp}}{\hat{\Omega}_{sp}}\right)\right)exp\left(\frac{-n\gamma_{th}}{\hat{\Omega}_{sd}\lambda_P(1-\kappa_{s,d}^2\gamma_{th})} - \sum_{\ell=1}^{m}\frac{\gamma_{th}}{\hat{\Omega}_{sr_\ell}\lambda_P(1-\kappa_{s,r}^2\gamma_{th})} - \sum_{i=m+1}^{K}\right.\right. \\
&\left.\times\frac{n_i\gamma_{th}}{\hat{\Omega}_{sr_i}\lambda_P(1-\kappa_{s,r}^2\gamma_{th})}\right) + exp\left(\frac{-n\gamma_{th}\sigma_{e,sp}^2\delta_s}{\hat{\Omega}_{sd}\lambda_P(1-\kappa_{s,d}^2\gamma_{th})} - \sum_{\ell=1}^{m}\frac{\gamma_{th}\sigma_{e,sp}^2\delta_s}{\hat{\Omega}_{sr_\ell}\lambda_P(1-\kappa_{s,r}^2\gamma_{th})}\right) exp\left(\sum_{i=m+1}^{K}\frac{-n_i\gamma_{th}\sigma_{e,sp}^2\delta_s}{\hat{\Omega}_{sr_i}\lambda_P(1-\kappa_{s,r}^2\gamma_{th})}\right) \\
&\times\left(1+\hat{\Omega}_{sp}\left(\frac{n\gamma_{th}\delta_s}{\hat{\Omega}_{sd}\lambda_Q(1-\kappa_{s,d}^2\gamma_{th})} + \sum_{\ell=1}^{m}\frac{\gamma_{th}\delta_s}{\hat{\Omega}_{sr_\ell}\lambda_Q(1-\kappa_{s,r}^2\gamma_{th})} + \sum_{i=m+1}^{K}\frac{n_i\gamma_{th}\delta_s}{\hat{\Omega}_{sr_i}\lambda_Q(1-\kappa_{s,r}^2\gamma_{th})}\right)\right)^{-1} \\
&\left.\times\ exp\left(-Q_{sp}\left(\frac{1}{\hat{\Omega}_{sp}} + \frac{n\gamma_{th}\delta_s}{\hat{\Omega}_{sd}\lambda_Q(1-\kappa_{s,d}^2\gamma_{th})} + \sum_{\ell=1}^{m}\frac{\gamma_{th}\delta_s}{\hat{\Omega}_{sr_\ell}\lambda_Q(1-\kappa_{s,r}^2\gamma_{th})} + \sum_{i=m+1}^{K}\frac{n_i\gamma_{th}\delta_s}{\hat{\Omega}_{sr_i}\lambda_Q(1-\kappa_{s,r}^2\gamma_{th})}\right)\right)\right].
\end{aligned} \tag{4.58}$$

Proof. Please refer to Appendix E. ∎

On using the expression of $\mathcal{P}_{\bar{\emptyset}1}$ from Lemma 9 in (4.53)-(4.57), it is important to observe that $\mathcal{P}_{\bar{\emptyset}}$ equals to $\mathcal{P}_{\bar{\emptyset}1}$ for $\gamma_{\text{th}} < 1/\max(\kappa_{sr}^2, \kappa_{rd}^2, \kappa_{sd}^2)$. Based on this observation, it can be inferred that when the target threshold is sufficiently low, the effect of HIs does not inhibit the cooperation between direct and relaying links. However, the HIs may critically affect this cooperation when target threshold is increased, as we shall discuss at the end of this subsection.

Further, using (4.42), the component $\mathcal{P}_{\bar{\emptyset}2}$ can be expressed as

$$\mathcal{P}_{\bar{\emptyset}2} = \int_0^\infty \sum_{m=1}^{K}\sum_{\mathcal{D}_m} \Pr\left[\mathcal{D}_m|W\right]\Pr\left[\Lambda_{r_m d} < \gamma_{\text{th}}|\mathcal{D}_m, W\right] f_W(w)dw. \tag{4.59}$$

By following the similar steps as used for deriving $\mathcal{P}_{\bar{\emptyset}1}$ in Lemma 9, (4.59) can be solved to obtain $\mathcal{P}_{\bar{\emptyset}2}$ as given in (4.60).

$$\mathcal{P}_{\bar{\emptyset}2} = \sum_{m=1}^{K}\sum_{n_{m+1}=0}^{1}\cdots\sum_{n_K=0}^{1}\binom{K}{m}\left(\prod_{\ell=1}^{m}\Phi_{r_\ell d}(\gamma_{\rm th})\right)(-1)^{\sum_{i=m+1}^{K} n_i}\exp\left(\sum_{\ell=1}^{m}\frac{-\alpha_{s,r_\ell}\gamma_{\rm th}}{\hat{\Omega}_{sr_\ell}(1-\kappa_{s,r}^2\gamma_{\rm th})}-\sum_{i=m+1}^{K}\right.$$
$$\left.\times\frac{n_i\alpha_{s,r_i}\gamma_{\rm th}}{\hat{\Omega}_{sr_i}(1-\kappa_{s,r}^2\gamma_{\rm th})}\right)\left[\left[1-\exp\left(-\frac{Q_{sp}}{\hat{\Omega}_{sp}}\right)\right]\exp\left(\sum_{\ell=1}^{m}\frac{-\gamma_{\rm th}}{\hat{\Omega}_{sr_\ell}\lambda_P(1-\kappa_{s,r}^2\gamma_{\rm th})}-\sum_{i=m+1}^{K}\frac{n_i\gamma_{\rm th}}{\hat{\Omega}_{sr_i}\lambda_P(1-\kappa_{s,r}^2\gamma_{\rm th})}\right)\right.$$
$$+\exp\left(\sum_{\ell=1}^{m}\frac{-\gamma_{\rm th}\sigma_{e,sp}^2\delta_s}{\hat{\Omega}_{sr_\ell}\lambda_P(1-\kappa_{s,r}^2\gamma_{\rm th})}-\sum_{i=m+1}^{K}\frac{n_i\gamma_{\rm th}\sigma_{e,sp}^2\delta_s}{\hat{\Omega}_{sr_i}\lambda_P(1-\kappa_{s,r}^2\gamma_{\rm th})}\right)\exp\left(Q_{sp}\left(\frac{-1}{\hat{\Omega}_{sp}}+\sum_{\ell=1}^{m}\frac{-\gamma_{\rm th}\delta_s}{\hat{\Omega}_{sr_\ell}\lambda_Q(1-\kappa_{s,r}^2\gamma_{\rm th})}\right)\right)$$
$$\left.\times\exp\left(\sum_{i=m+1}^{K}\frac{-n_iQ(s,p)\gamma_{\rm th}\delta_s}{\hat{\Omega}_{sr_i}\lambda_Q(1-\kappa_{s,r}^2\gamma_{\rm th})}\right)\left(1+\hat{\Omega}_{sp}\left(\sum_{\ell=1}^{m}\frac{\gamma_{\rm th}\delta_s}{\hat{\Omega}_{sr_\ell}\lambda_Q(1-\kappa_{s,r}^2\gamma_{\rm th})}+\sum_{i=m+1}^{K}\frac{n_i\gamma_{\rm th}\delta_s}{\hat{\Omega}_{sr_i}\lambda_Q(1-\kappa_{s,r}^2\gamma_{\rm th})}\right)\right)^{-1}\right]. \tag{4.60}$$

Likewise, $\mathcal{P}_{\bar{\emptyset}3}$ and $\mathcal{P}_{\bar{\emptyset}4}$ can be derived, respectively, as

$$\mathcal{P}_{\bar{\emptyset}3} = \int_0^\infty \sum_{m=1}^{K}\sum_{\mathcal{D}_m}\Pr\left[\mathcal{D}_m|W\right]f_W(w)dw \tag{4.61}$$

$$\text{and}\quad \mathcal{P}_{\bar{\emptyset}4} = \int_0^\infty \sum_{m=1}^{K}\sum_{\mathcal{D}_m}\Pr\left[\Lambda_{sd}<\gamma_{\rm th}|W\right]\Pr\left[\mathcal{D}_m|W\right]f_W(w)dw. \tag{4.62}$$

On evaluating the integrals in (4.61) and (4.62), one can obtain the expressions of $\mathcal{P}_{\bar{\emptyset}3}$ and $\mathcal{P}_{\bar{\emptyset}4}$ which can be readily expressed in compact form as $\mathcal{P}_{\bar{\emptyset}3}=\mathcal{P}_{\bar{\emptyset}2}\Big/\left(\prod_{\ell=1}^{m}\phi_{r_\ell d}(\gamma_{\rm th})\right)$ and $\mathcal{P}_{\bar{\emptyset}4}=\mathcal{P}_{\bar{\emptyset}1}\Big/\left(\prod_{\ell=1}^{m}\phi_{r_\ell d}(\gamma_{\rm th})\right)$. On substituting the obtained expressions of $\mathcal{P}_{\bar{\emptyset}1}$, $\mathcal{P}_{\bar{\emptyset}2}$, $\mathcal{P}_{\bar{\emptyset}3}$, and $\mathcal{P}_{\bar{\emptyset}4}$ appropriately in (4.53)-(4.57), it can be observed that the cooperation between direct and relaying link transmissions ceases to exist beyond a certain threshold. This can be attested from the observation that component $\mathcal{P}_{\bar{\emptyset}}$ reduces to zero as $\gamma_{\rm th}\geq 1/\kappa_{s,r}^2$.

Computation of $\mathcal{P}_{\emptyset}$

The component $\mathcal{P}_{\emptyset}$ in (4.41) can be expressed, with the aid of (4.37), as

$$\mathcal{P}_{\emptyset} = \int_0^\infty \prod_{m=1}^{K}\Pr\left[\Lambda_{sr_m}<\gamma_{\rm th}|W\right]\Pr\left[\Lambda_{sd}<\gamma_{\rm th}|W\right]f_W(w)dw. \tag{4.63}$$

Based on the impairment levels $\kappa_{s,d}^2$ and $\kappa_{s,r}^2$, (4.63) yields different expressions. Thus, after plugging (C.4) and (4.46) in (4.63) and solving the required integral, $\mathcal{P}_{\emptyset}$ is obtained as follows:

- When $\kappa_{s,d}^2\leq\kappa_{s,r}^2$,

$$\mathcal{P}_{\emptyset} = \begin{cases}\mathcal{P}_{\emptyset1}, \text{ for } \gamma_{\rm th}<1/\kappa_{s,r}^2,\\ \mathcal{P}_{\emptyset2}, \text{ for } 1/\kappa_{s,r}^2\leq\gamma_{\rm th}<1/\kappa_{s,d}^2\\ 1, \text{otherwise}.\end{cases} \tag{4.64}$$

- When $\kappa_{s,d}^2 \geq \kappa_{s,r}^2$,

$$\mathcal{P}_{\emptyset} = \begin{cases} \mathcal{P}_{\emptyset 1}, \text{ for } \gamma_{\text{th}} < 1/\kappa_{s,d}^2, \\ \mathcal{P}_{\emptyset 3}, \text{ for } 1/\kappa_{s,d}^2 \leq \gamma_{\text{th}} < 1/\kappa_{s,r}^2 \\ 1, \text{otherwise.} \end{cases} \tag{4.65}$$

Here, component $\mathcal{P}_{\emptyset 1}$ can be evaluated by substituting (C.4) and (4.46) into (4.63), and solving the resultant integral to obtain

$$\begin{aligned}\mathcal{P}_{\emptyset 1} =& \sum_{n=0}^{1}\sum_{n_1=0}^{1}\cdots\sum_{n_K=0}^{1}(-1)^{n+\sum_{i=1}^{K}n_i}\exp\left(\frac{-n\gamma_{\text{th}}\alpha_{s,d}}{\hat{\Omega}_{sd}(1-\kappa_{s,d}^2\gamma_{\text{th}})}-\sum_{i=1}^{K}\frac{n_i\alpha_{s,r_i}\gamma_{\text{th}}}{\hat{\Omega}_{sr_i}(1-\kappa_{s,r}^2\gamma_{\text{th}})}\right)\left[\left[1-\exp\left(-\frac{Q_{sp}}{\hat{\Omega}_{sp}}\right)\right]\right.\\ &\times\exp\left(\frac{-n\gamma_{\text{th}}}{\hat{\Omega}_{sd}\lambda_P(1-\kappa_{s,d}^2\gamma_{\text{th}})}-\sum_{i=1}^{K}\frac{n_i\gamma_{\text{th}}}{\hat{\Omega}_{sr_i}\lambda_P(1-\kappa_{s,r}^2\gamma_{\text{th}})}\right)+\exp\left(\frac{-n\gamma_{\text{th}}\sigma_{e,sp}^2\delta_s}{\hat{\Omega}_{sd}\lambda_Q(1-\kappa_{s,d}^2\gamma_{\text{th}})}-\sum_{i=1}^{K}\right.\\ &\left.\times\frac{n_i\gamma_{\text{th}}\sigma_{e,sp}^2\delta_s}{\hat{\Omega}_{sr_i}\lambda_Q(1-\kappa_{s,r}^2\gamma_{\text{th}})}\right)\left(1+\hat{\Omega}_{sp}\left(\frac{n\gamma_{\text{th}}\delta_s}{\hat{\Omega}_{sd}\lambda_Q(1-\kappa_{s,d}^2\gamma_{\text{th}})}+\sum_{i=1}^{K}\frac{n_i\gamma_{\text{th}}\delta_s}{\hat{\Omega}_{sr_i}\lambda_Q(1-\kappa_{s,r}^2\gamma_{\text{th}})}\right)\right)^{-1}\\ &\left.\times\exp\left(-Q_{sp}\left(\frac{1}{\hat{\Omega}_{sp}}+\frac{n\gamma_{\text{th}}\delta_s}{\hat{\Omega}_{sd}\lambda_Q(1-\kappa_{s,d}^2\gamma_{\text{th}})}+\sum_{i=1}^{K}\frac{n_i\gamma_{\text{th}}\delta_s}{\hat{\Omega}_{sr_i}\lambda_Q(1-\kappa_{s,r}^2\gamma_{\text{th}})}\right)\right)\right].\end{aligned} \tag{4.66}$$

The components $\mathcal{P}_{\emptyset 2}$ and $\mathcal{P}_{\emptyset 3}$ are given by

$$\mathcal{P}_{\emptyset 2} = \int_0^\infty \prod_{m=1}^{K} \Pr\left[\Lambda_{sd} < \gamma_{\text{th}}|W\right] f_W(w)dw \tag{4.67}$$

$$\text{and} \quad \mathcal{P}_{\emptyset 3} = \int_0^\infty \prod_{m=1}^{K} \Pr\left[\Lambda_{sr_m} < \gamma_{\text{th}}|W\right] f_W(w)dw. \tag{4.68}$$

Evaluation of (4.67) and (4.68) yield $\mathcal{P}_{\emptyset 2}$ and $\mathcal{P}_{\emptyset 3}$ as given in (4.69) and (4.3.2), respectively.

$$\begin{aligned}\mathcal{P}_{\emptyset 2} =& \sum_{n=0}^{1}(-1)^n\exp\left(-\frac{n\gamma_{\text{th}}\alpha_{s,d}}{\hat{\Omega}_{sd}(1-\kappa_{s,d}^2\gamma_{\text{th}})}\right)\left[\left[1-\exp\left(-\frac{Q_{sp}}{\hat{\Omega}_{sp}}\right)\right]\exp\left(\frac{-n\gamma_{\text{th}}}{\hat{\Omega}_{sd}\lambda_P(1-\kappa_{s,d}^2\gamma_{\text{th}})}\right)\right.\\ &\left.+\exp\left(\frac{-n\gamma_{\text{th}}\sigma_{e,sp}^2\delta_s}{\hat{\Omega}_{sd}\lambda_Q(1-\kappa_{s,d}^2\gamma_{\text{th}})}\right)\left(1+\frac{n\gamma_{\text{th}}\delta_s\hat{\Omega}_{sp}}{\hat{\Omega}_{sd}\lambda_Q(1-\kappa_{s,d}^2\gamma_{\text{th}})}\right)^{-1}\exp\left(-Q_{sp}\left(\frac{1}{\hat{\Omega}_{sp}}+\frac{n\gamma_{\text{th}}\delta_s}{\hat{\Omega}_{sd}\lambda_Q(1-\kappa_{s,d}^2\gamma_{\text{th}})}\right)\right)\right].\end{aligned} \tag{4.69}$$

$$\begin{aligned}\text{and} \quad \mathcal{P}_{\emptyset 3} =& \sum_{n_1=0}^{1}\cdots\sum_{n_K=0}^{1}(-1)^{\sum_{i=1}^{K}n_i}\exp\left(\sum_{i=1}^{K}\frac{-n_i\alpha_{s,r_i}\gamma_{\text{th}}}{\hat{\Omega}_{sr_i}(1-\kappa_{s,r}^2\gamma_{\text{th}})}\right)\left[\left[1-\exp\left(\frac{-Q_{sp}}{\hat{\Omega}_{sp}}\right)\right]\right.\\ &\times\exp\left(-\sum_{i=1}^{K}\frac{n_i\gamma_{\text{th}}}{\hat{\Omega}_{sr_i}\lambda_P(1-\kappa_{s,r}^2\gamma_{\text{th}})}\right)+\left(1+\hat{\Omega}_{sp}\left(\sum_{i=1}^{K}\frac{n_i\gamma_{\text{th}}\delta_s}{\hat{\Omega}_{sr_i}\lambda_Q(1-\kappa_{s,r}^2\gamma_{\text{th}})}\right)\right)^{-1}\\ &\left.\times\exp\left(\sum_{i=1}^{K}\frac{-n_i\gamma_{\text{th}}\sigma_{e,sp}^2\delta_s}{\hat{\Omega}_{sr_i}\lambda_Q(1-\kappa_{s,r}^2\gamma_{\text{th}})}\right)\exp\left(-Q_{sp}\left(\frac{1}{\hat{\Omega}_{sp}}+\sum_{i=1}^{K}\frac{n_i\gamma_{\text{th}}\delta_s}{\hat{\Omega}_{sr_i}\lambda_Q(1-\kappa_{s,r}^2\gamma_{\text{th}})}\right)\right)\right].\end{aligned} \tag{4.70}$$

Finally, by substituting the obtained $\mathcal{P}_{\emptyset}$ and $\mathcal{P}_{\bar{\emptyset}}$ appropriately in (4.41), we compute the outage probability $\mathcal{P}_{\text{out}}(\gamma_{\text{th}})$ in the following proposition.

Proposition 1. *The outage probability $\mathcal{P}_{out}(\gamma_{th})$ of CMRN, for all the possible cases based on the impairments level $\kappa_{s,d}^2$, $\kappa_{s,r}^2$, and $\kappa_{r,d}^2$, can be given as follows:*
Case 1: For $\kappa_{s,d}^2 \leq \kappa_{r,d}^2 \leq \kappa_{s,r}^2$ or $\kappa_{r,d}^2 \leq \kappa_{s,d}^2 \leq \kappa_{s,r}^2$,

$$\mathcal{P}_{out}(\gamma_{th}) = \begin{cases} \mathcal{P}_{\bar{\emptyset}1} + \mathcal{P}_{\emptyset 1}, \ \text{for } \gamma_{th} < 1/\kappa_{s,r}^2, \\ \mathcal{P}_{\emptyset 2}, \ \text{for } 1/\kappa_{s,r}^2 \leq \gamma_{th} < 1/\kappa_{s,d}^2, \\ 1, \gamma_{th} \geq 1/\kappa_{s,d}^2. \end{cases} \tag{4.71}$$

Case 2: For $\kappa_{s,r}^2 \leq \kappa_{s,d}^2 \leq \kappa_{r,d}^2$ or $\kappa_{s,d}^2 \leq \kappa_{s,r}^2 \leq \kappa_{r,d}^2$,

$$\mathcal{P}_{out}(\gamma_{th}) = \begin{cases} \mathcal{P}_{\bar{\emptyset}1} + \mathcal{P}_{\emptyset 1}, \ \text{for } \gamma_{th} < 1/\kappa_{r,d}^2, \\ \mathcal{P}_{\emptyset 2}, \ \text{for } 1/\kappa_{r,d}^2 \leq \gamma_{th} < 1/\kappa_{s,d}^2, \\ 1, \gamma_{th} \geq 1/\kappa_{s,d}^2. \end{cases} \tag{4.72}$$

Case 3: For $\kappa_{r,d}^2 \leq \kappa_{s,r}^2 \leq \kappa_{s,d}^2$,

$$\mathcal{P}_{out}(\gamma_{th}) = \begin{cases} \mathcal{P}_{\bar{\emptyset}1} + \mathcal{P}_{\emptyset 1}, \ \text{for } \gamma_{th} < 1/\kappa_{s,d}^2, \\ \mathcal{P}_{\bar{\emptyset}2} + \mathcal{P}_{\emptyset 3}, \ \text{for } 1/\kappa_{s,d}^2 \leq \gamma_{th} < 1/\kappa_{s,r}^2, \\ 1, \gamma_{th} \geq 1/\kappa_{s,r}^2. \end{cases} \tag{4.73}$$

Case 4: For $\kappa_{s,r}^2 \leq \kappa_{r,d}^2 \leq \kappa_{s,d}^2$,

$$\mathcal{P}_{out}(\gamma_{th}) = \begin{cases} \mathcal{P}_{\bar{\emptyset}1} + \mathcal{P}_{\emptyset 1}, \ \text{for } \gamma_{th} < 1/\kappa_{s,d}^2, \\ \mathcal{P}_{\bar{\emptyset}2} + \mathcal{P}_{\emptyset 3}, \ \text{for } 1/\kappa_{s,d}^2 \leq \gamma_{th} < 1/\kappa_{r,d}^2, \\ 1, \gamma_{th} \geq 1/\kappa_{r,d}^2. \end{cases} \tag{4.74}$$

Proof. Please refer to Appendix F. ■

For the same hardware quality[5] at all the nodes[6] viz., $\kappa_{s,r}^2 = \kappa_{r,d}^2 = \kappa_{r,d}^2 = \kappa$, the $\mathcal{P}_{\text{out}}(\gamma_{\text{th}})$ can be obtained as

$$\mathcal{P}_{\text{out}}(\gamma_{\text{th}}) = \begin{cases} \mathcal{P}_{\bar{\emptyset}1} + \mathcal{P}_{\emptyset 1}, \ \text{for } \gamma_{\text{th}} < 1/\kappa^2, \\ 1, \gamma_{\text{th}} \geq 1/\kappa^2. \end{cases} \tag{4.75}$$

Now, based on the derived $\mathcal{P}_{\text{out}}(\gamma_{\text{th}})$ in Proposition 2 and (4.75), we discuss the important ceiling effects which influence the system's performance and prevail due to presence of HIs.

[5] A low-cost hardware usually has poor quality hardware, and thus has higher EVMs.

[6] Ideally, it would be better to have the same quality of hardware impairments at all the nodes for cost effective implementation and optimized performance [88].

Ceiling Effects

Herein, we discuss three ceiling effects namely relay cooperation ceiling (RCC), direct link ceiling (DLC), and overall system ceiling (OSC). RCC is said to occur in the system when relay ceases to cooperate the transmission of information from source to destination. This happens due to imposition of undesired constraint on γ_{th} essentially in the high-rate applications. To exemplify this, let us consider the *Case 1* when $\kappa_{s,d}^2 \leq \kappa_{r,d}^2 \leq \kappa_{s,r}^2$. From $\mathcal{P}_{\text{out}}(\gamma_{\text{th}})$ in (4.71), the first component $(\mathcal{P}_{\bar{\emptyset}1} + \mathcal{P}_{\emptyset 1})$ accounts for the cooperation between both relaying and direct links, whereas the second component $(\mathcal{P}_{\emptyset 2})$ arises from the direct transmission only. Thus, as γ_{th} exceeds $1/\kappa_{s,r}^2$, relay cooperation ceases and system has to rely on the direct link only. Importantly, direct link can partially compensate for RCC over the threshold range $1/\kappa_{s,r}^2 \leq \gamma_{\text{th}} < 1/\kappa_{s,d}^2$. But once the threshold exceeds $1/\kappa_{s,d}^2$, overall system goes in outage and this phenomenon is named as OSC. Similar observations can be made from *Case 2*, wherein the RCC occurs for $\gamma_{\text{th}} \geq 1/\kappa_{r,d}^2$. And, the direct link compensates for this RCC over the range $1/\kappa_{r,d}^2 \leq \gamma_{\text{th}} < 1/\kappa_{s,d}^2$. Considering now *Case 3*, the first component $(\mathcal{P}_{\bar{\emptyset}1} + \mathcal{P}_{\emptyset 1})$ in $\mathcal{P}_{\text{out}}(\gamma_{\text{th}})$ accounts for the cooperation between both relaying and direct links, whereas the second component $(\mathcal{P}_{\bar{\emptyset}2} + \mathcal{P}_{\emptyset 3})$ arises from the relaying link transmission only. In such case, as γ_{th} exceeds $1/\kappa_{s,d}^2$, direct link goes in outage and it is referred to as DLC. We note that, in this case, a relaying link can partially compensate for the DLC in the range $1/\kappa_{s,d}^2 \leq \gamma_{\text{th}} < 1/\kappa_{s,r}^2$ i.e., before occurrence of OSC $(\gamma_{\text{th}} \geq 1/\kappa_{s,r}^2)$. Likewise, in *Case 4*, the DLC occurs for $\gamma_{\text{th}} \geq 1/\kappa_{s,d}^2$. And, the relaying link compensates for this DLC over the threshold range $1/\kappa_{s,d}^2 \leq \gamma_{\text{th}} < 1/\kappa_{r,d}^2$ i.e., before occurrence of OSC $(\gamma_{\text{th}} \geq 1/\kappa_{r,d}^2)$. Moreover, from (4.75), we observe that for same hardware, the system directly experiences the OSC effect as $\gamma_{\text{th}} \geq 1/\kappa^2$.

Remarks:

In CMRN with HIs, RCC arises only when the transceiver hardware at the relay chain (either $\kappa_{s,r}$, $\kappa_{r,d}$ or both) is of inferior quality than the hardware of direct link chain $(\kappa_{s,d})$. In such cases (*Case 1* and *Case 2*), RCC effect occurs when $\gamma_{\text{th}} \geq \frac{1}{\max(\kappa_{s,r}^2, \kappa_{r,d}^2)}$. Note that the direct link can partially compensate for the incurred loss due to RCC. However, once the OSC effect occurs, system goes in outage. In contrast, when the hardware of direct link chain is of low quality than the relay chain (*Case 3* and *Case 4*), the DLC effect occurs when $\gamma_{\text{th}} \geq 1/\kappa_{s,d}^2$. In such cases, relaying link plays an important role in compensating the performance loss due to DLC before γ_{th} increases to OSC threshold. In general, the OSC effect occurs when $\gamma_{\text{th}} \geq \frac{1}{\min(\kappa_{s,d}^2, \max(\kappa_{s,r}^2, \kappa_{r,d}^2))}$, which limits the performance of system beyond a given target rate in high-rate applications. Based on these observations, it would be desirable to have $\min(\kappa_{s,d}^2, \max(\kappa_{s,r}^2, \kappa_{r,d}^2)) < \frac{1}{\gamma_{\text{th}}}$ while designing the practical systems for a given rate requirement. Also, for same hardware at all nodes, the OSC occurs when $\gamma_{\text{th}} \geq \frac{1}{\kappa^2}$. Thus, when hardware quality at all the transceivers are same, it would be suggested to have $\kappa^2 < \frac{1}{\gamma_{\text{th}}}$.

4.3.3 Asymptotic Outage Performance

In this section, we derive asymptotic outage expressions in the high-SNR regime (say $\gamma = \frac{1}{N_0} \to \infty$ [115]). Herein, without loss of generality, we assume independent and identically distributed channels such that $\Omega_{sr_m} = \Omega_{sr}$, $\Omega_{r_m d} = \Omega_{rd}$, $\Omega_{r_m p} = \Omega_{rp}$ $\forall\ m \in \{1, .., K\}$. Also, for getting better insights, we assume that $\kappa_{s,r}^2 = \kappa_{r,d}^2 = \kappa_{s,d}^2 = \kappa^2$. In what follows, we carry out the asymptotic analysis for imperfect CSI and perfect CSI scenarios.

Imperfect CSI

For imperfect CSI, let us consider $\sigma_{e,sp}^2 = \sigma_{e,sd}^2 = \sigma_{e,r_m p}^2 = \sigma_{e,r_m d}^2 = \sigma_{e,sr}^2 = \sigma_e^2$. Hereby, we apply $\mathrm{e}^{-x} \simeq 1 - x$ for small x in (C.4) to simplify

$$\Pr\left[\Lambda_{sr_m} < \gamma_{\text{th}} | W\right] \simeq \begin{cases} \tilde{\Phi}_{sr}(\gamma_{\text{th}}, w), \text{ for } \gamma_{\text{th}} < 1/\kappa^2, \\ 1, \text{ otherwise }, \end{cases} \tag{4.76}$$

where the function $\tilde{\Phi}_{sr}(\gamma_{\text{th}}, w)$ is given by

$$\tilde{\Phi}_{sr}(\gamma_{\text{th}}, w) = \begin{cases} 1 - \exp\left(\frac{-\gamma_{\text{th}}\alpha_{s,r}}{\hat{\Omega}_{sr}(1-\kappa^2\gamma_{\text{th}})}\right)\left(1 - \frac{\gamma_{\text{th}}}{\hat{\Omega}_{sr}P\gamma(1-\kappa^2\gamma_{\text{th}})}\right), \text{ for } W \leq Q_{sp}, \\ 1 - \exp\left(\frac{-\gamma_{\text{th}}\alpha_{s,r}}{\hat{\Omega}_{sr}(1-\kappa^2\gamma_{\text{th}})}\right)\left(1 - \frac{\gamma_{\text{th}}\delta_s(\sigma_e^2 + w)}{\hat{\Omega}_{sr}Q\gamma(1-\kappa^2\gamma_{\text{th}})}\right), \text{ for } W > Q_{sp}. \end{cases} \tag{4.77}$$

Likewise, simplifying $\Pr\left[\Lambda_{sd} < \gamma_{\text{th}} | W\right]$ in (4.46), we have

$$\Pr\left[\Lambda_{sd} < \gamma_{\text{th}} | W\right] \simeq \begin{cases} \tilde{\Phi}_{sd}(\gamma_{\text{th}}, w), \text{ for } \gamma_{\text{th}} < 1/\kappa^2, \\ 1, \text{ otherwise }, \end{cases} \tag{4.78}$$

where the function $\tilde{\Phi}_{sd}(\gamma_{\text{th}}, w)$ can be directly obtained by replacing $\alpha_{s,r}$ and $\hat{\Omega}_{sr}$ in (4.77) with $\alpha_{s,d}$ and $\hat{\Omega}_{sd}$, respectively. Further, applying the similar assumptions, we can subsequently simplify (4.51) as

$$\Pr\left[\Lambda_{r_\ell d} < \gamma_{\text{th}} | \mathcal{D}_m, W\right] \simeq \begin{cases} \left(\tilde{\Phi}_{rd}(\gamma_{\text{th}})\right)^m, \text{ for } \gamma_{\text{th}} < 1/\kappa^2, \\ 1, \text{ otherwise }, \end{cases} \tag{4.79}$$

where the function $\tilde{\Phi}_{rd}(\gamma_{\text{th}})$ can be obtained as

$$\tilde{\Phi}_{rd}(\gamma_{\text{th}}) = 1 - \left[1 - \exp\left(\frac{-Q_{rp}}{\hat{\Omega}_{rp}}\right)\right]\exp\left(\frac{-\gamma_{\text{th}}\alpha_{r,d}}{\hat{\Omega}_{rd}(1-\gamma_{\text{th}}\kappa^2)}\right)\left(1 - \frac{\gamma_{\text{th}}\alpha_{r,d}}{\hat{\Omega}_{rd}(1-\gamma_{\text{th}}\kappa^2)}\right) + \sum_{s=0}^{1}\sum_{\hat{s}=0}^{s} \times(-1)^{s+\hat{s}}\exp\left(\frac{-s\gamma_{\text{th}}\alpha_{r,d}}{\hat{\Omega}_{rd}(1-\kappa^2\gamma_{\text{th}})}\right)\left(\frac{\gamma_{\text{th}}\delta_r\hat{\Omega}_{rp}}{\hat{\Omega}_{rd}Q\gamma(1-\kappa^2\gamma_{\text{th}})}\right)^{\hat{s}}\left(1-\frac{\gamma_{\text{th}}\delta_r\sigma_e^2}{\hat{\Omega}_{rd}Q\gamma(1-\kappa^2\gamma_{\text{th}})}\right)^{s-\hat{s}}\Gamma\left(\hat{s}+1, \frac{Q_{rp}}{\hat{\Omega}_{rp}}\right). \tag{4.80}$$

Now, invoking (4.76) into (C.1), and the result alongwith (4.78) and (4.79) in (4.42), and then performing the required integration, we get $\mathcal{P}_{\bar{\emptyset}}$ at high-SNR as

$$\mathcal{P}_{\bar{\emptyset}} \simeq \begin{cases} \Theta(\gamma_{\text{th}}), \text{ for } \gamma_{\text{th}} < 1/\kappa^2, \\ 0, \text{ otherwise}, \end{cases} \tag{4.81}$$

where $\Theta(\gamma_{\text{th}})$ is given by

$$\Theta(\gamma_{\text{th}}) = \sum_{m=1}^{K}\sum_{l=0}^{K-m}\sum_{n=0}^{1}\binom{K-m}{l}\binom{K}{m}\left(\tilde{\Phi}_{rd}(\gamma_{\text{th}})\right)^m(-1)^{n+l}\exp\left(\frac{-n\gamma_{\text{th}}\alpha_{s,d}}{\hat{\Omega}_{sd}(1-\kappa^2\gamma_{\text{th}})} + \frac{(m+l)\gamma_{\text{th}}\alpha_{s,r}}{\hat{\Omega}_{sr}(1-\kappa^2\gamma_{\text{th}})}\right) \times\left[\left(1 - \frac{n\gamma_{\text{th}}}{\hat{\Omega}_{sd}P\gamma(1-\kappa^2\gamma_{\text{th}})}\right)\left[1 - \exp\left(-\frac{Q_{sp}}{\hat{\Omega}_{sp}}\right)\right]\left(1 - \frac{\gamma_{\text{th}}}{\hat{\Omega}_{sr}P\gamma(1-\kappa^2\gamma_{\text{th}})}\right)^{m+l} + \sum_{\hat{n}=0}^{n}\sum_{\hat{l}=0}^{l+m} \times\binom{l+m}{\hat{l}}(-1)^{\hat{n}+\hat{l}}\left(\frac{\hat{\Omega}_{sp}\gamma_{\text{th}}\delta_s}{\hat{\Omega}_{sd}Q\gamma(1-\kappa^2\gamma_{\text{th}})}\right)^{\hat{n}}\left(\frac{\hat{\Omega}_{sp}\gamma_{\text{th}}\delta_s}{\hat{\Omega}_{sr}Q\gamma(1-\kappa^2\gamma_{\text{th}})}\right)^{\hat{l}}\left(1 - \frac{\gamma_{\text{th}}\delta_s\sigma_e^2}{\hat{\Omega}_{sd}Q\gamma(1-\kappa^2\gamma_{\text{th}})}\right)^{n-\hat{n}} \times\left(1 - \frac{\gamma_{\text{th}}\delta_s\sigma_e^2}{\hat{\Omega}_{sr}Q\gamma(1-\kappa^2\gamma_{\text{th}})}\right)^{l+m-\hat{l}}\Gamma\left(\hat{n}+\hat{l}+1, \frac{Q_{sp}}{\hat{\Omega}_{sp}}\right)\right]. \tag{4.82}$$

Similarly, using (4.76) and (4.78) in (4.63), we can simplify $\mathcal{P}_{\emptyset}$ at high-SNR as

$$\mathcal{P}_{\emptyset} \simeq \begin{cases} \Upsilon(\gamma_{\text{th}}), \text{ for } \gamma_{\text{th}} < 1/\kappa^2, \\ 1, \text{ otherwise}, \end{cases} \tag{4.83}$$

where $\Upsilon(\gamma_{\text{th}})$ is given by

$$\Upsilon(\gamma_{\text{th}}) = \sum_{r=0}^{K}\sum_{n=0}^{1}\binom{K}{r}(-1)^{n+r}\exp\left(\frac{-n\gamma_{\text{th}}\alpha_{s,d}}{\hat{\Omega}_{sd}(1-\kappa^2\gamma_{\text{th}})} + \frac{r\gamma_{\text{th}}\alpha_{s,r}}{\hat{\Omega}_{sr}(1-\kappa^2\gamma_{\text{th}})}\right)\left[\left(1 - \frac{\gamma_{\text{th}}}{\hat{\Omega}_{sr}P\gamma(1-\kappa^2\gamma_{\text{th}})}\right)^r \times\left(1-\frac{n\gamma_{\text{th}}}{\hat{\Omega}_{sd}P\gamma(1-\kappa^2\gamma_{\text{th}})}\right)\left[1-\exp\left(-\frac{Q_{sp}}{\hat{\Omega}_{sp}}\right)\right] + \sum_{\hat{n}=0}^{n}\sum_{\hat{l}=0}^{r}\binom{r}{\hat{l}}(-1)^{\hat{n}+\hat{l}}\left(\frac{\hat{\Omega}_{sp}\gamma_{\text{th}}\delta_s}{\hat{\Omega}_{sd}Q\gamma(1-\kappa^2\gamma_{\text{th}})}\right)^{\hat{n}} \times\left(\frac{\hat{\Omega}_{sp}\gamma_{\text{th}}\delta_s}{\hat{\Omega}_{sr}Q\gamma(1-\kappa^2\gamma_{\text{th}})}\right)^{\hat{l}}\left(1-\frac{\gamma_{\text{th}}\delta_s\sigma_e^2}{\hat{\Omega}_{sd}Q\gamma(1-\kappa^2\gamma_{\text{th}})}\right)^{n-\hat{n}}\left(1-\frac{\gamma_{\text{th}}\delta_s\sigma_e^2}{\hat{\Omega}_{sr}Q\gamma(1-\kappa^2\gamma_{\text{th}})}\right)^{r-\hat{l}}\Gamma\left(\hat{n}+\hat{l}+1, \frac{Q_{sp}}{\hat{\Omega}_{sp}}\right)\right]. \tag{4.84}$$

Finally, using (4.81) and (4.83) in (4.41), we obtain $\mathcal{P}_{\text{out}}(\gamma_{\text{th}})$ at high-SNR as

$$\mathcal{P}_{\text{out}}(\gamma_{\text{th}}) \simeq \begin{cases} \Theta(\gamma_{\text{th}}) + \Upsilon(\gamma_{\text{th}}), \text{ for } \gamma_{\text{th}} < 1/\kappa^2, \\ 1, \text{ otherwise.} \end{cases} \tag{4.85}$$

Re-expressing $\mathcal{P}_{\text{out}}(\gamma_{\text{th}})$ as $(\mathcal{G}_c\varrho)^{-\mathcal{G}_d}$ [121], where $\mathcal{G}_c$ is the coding gain and $\mathcal{G}_d$ is the diversity order, one can infer that the diversity order $\mathcal{G}_d$ of the considered system is zero due to presence of CEEs. This zero diversity order eventually results in irreducible outage floors. Such outage floors imply that the outage probability of system cannot be further reduced by increasing the SNR γ. Thus, it can be deduced that the CEEs may potentially limit the system performance in the high-SNR region. Moreover, the CEEs pose critical impact on the coding gain $\mathcal{G}_c$, especially in the high-SNR regime, as illustrated through numerical results in Section 4.3.4.

Perfect CSI

For perfect CSI (i.e., $\sigma_e^2 = 0$) case, all error variances are substituted as zero in (4.76), (4.78), and (4.79). Then, following the similar lines of derivation as done for imperfect CSI, we can derive $\mathcal{P}_{\text{out}}(\gamma_{\text{th}})$ as

$$\mathcal{P}_{\text{out}}(\gamma_{\text{th}}) \simeq \begin{cases} \Psi(\gamma_{\text{th}}) \left(\frac{1}{\gamma}\right)^{K+1}, \text{ for } \gamma_{\text{th}} < 1/\kappa^2, \\ 1, \text{ otherwise,} \end{cases} \tag{4.86}$$

where $\Psi(\gamma_{\text{th}})$ is given in (4.87).

$$\begin{aligned}\Psi(\gamma_{\text{th}}) = &\sum_{m=1}^{K} \binom{K}{m} \left(\frac{\gamma_{\text{th}}}{1-\gamma_{\text{th}}\kappa^2}\right)^{K-m+1} \frac{1}{\Omega_{sd}} \left(\frac{1}{\Omega_{sr}}\right)^{K-m} \Bigg[\left(\frac{1}{P}\right)^{K-m+1} \left(1 - \exp\left(\frac{-Q}{P\delta_s\Omega_{sp}}\right)\right) \\ &+ \left(\frac{\Omega_{sp}\delta_s}{Q}\right)^{K-m+1} \Gamma\left(K-m+2, \frac{Q}{P\delta_r\Omega_{rp}}\right)\Bigg] \left(\frac{\gamma_{\text{th}}\left(1-\exp\left(\frac{-Q}{P\delta_r\Omega_{rp}}\right)\right)}{\Omega_{rd}P(1-\gamma_{\text{th}}\kappa^2)} + \frac{\gamma_{\text{th}}\delta_r\Omega_{rp}\Gamma\left(2, Q/(P\delta_r\Omega_{rp})\right)}{\Omega_{rd}Q(1-\gamma_{\text{th}}\kappa^2)}\right)^{m} \\ &+ \left(\frac{\gamma_{\text{th}}}{1-\gamma_{\text{th}}\kappa^2}\right)^{K+1} \frac{1}{\Omega_{sd}} \left(\frac{1}{\Omega_{sr}}\right)^{K} \left[\left(\frac{1}{P}\right)^{K+1} \left(1-\exp\left(\frac{-Q}{P\delta_s\Omega_{sp}}\right)\right) + \left(\frac{\delta_s}{Q}\right)^{K+1} \Omega_{sp}^{K+1}\Gamma\left(K+2, \frac{Q}{P\delta_r\Omega_{rp}}\right)\right].\end{aligned} \tag{4.87}$$

Herein, it can be observed that system achieves full diversity gain of $\mathcal{G}_d = K+1$ as long as the OSC phenomenon does not occur. Moreover, it can be deduced that HIs do not affect the diversity gain of the system but exert influence on the system's performance in terms of coding gain.

4.3.4 Numerical and Simulation Results

In this section, we perform numerical analysis of the considered CMRN and validate our derived results through Monte Carlo simulation. The Monte Carlo simulations are performed on the popular computing software MATLAB, while the analytical results are obtained using the MATHEMATICA software. For obtaining the numerical results, we adopt a two-dimensional (2-D) network topology, where the network nodes S, $\{R_m\}_{m=1}^{K}$, D, and T_p are located at coordinates $(0,0)$, $(0.5,0)$, $(1,0)$, and $(0.5,0.5)$, respectively. Following path-loss model, the parameter Ω_{ij} of the channel gains are obtained by $\Omega_{ij} = d_{ij}^{-\alpha}$, where d_{ij} is the distance between the two arbitrary nodes i and j, with path-loss exponent α equals to 4. We set error variances $\sigma_{e,sp}^2 = \sigma_{e,sr}^2 = \sigma_{e,r_md}^2 = \sigma_{e,r_mp}^2 = \sigma_e^2$. We also set $\kappa_{ts} = \kappa_{rd} = \kappa_{tr_m} = \kappa_{rr_m} = \kappa_o$ such that $\kappa_{s,d} = \kappa_{r,d} = \kappa_{s,r} = \kappa = \sqrt{2}\kappa_o$. Note that, for a fair comparison, the outage expression for an ideal system (without HIs and CEEs) can be readily obtained by substituting $\kappa_o = 0$ and $\sigma_e^2 = 0$ in $\mathcal{P}_{\text{out}}(\gamma_{\text{th}}) = \mathcal{P}_{\bar{\emptyset}1} + \mathcal{P}_{\emptyset 1}$ in (4.71)-(4.75).

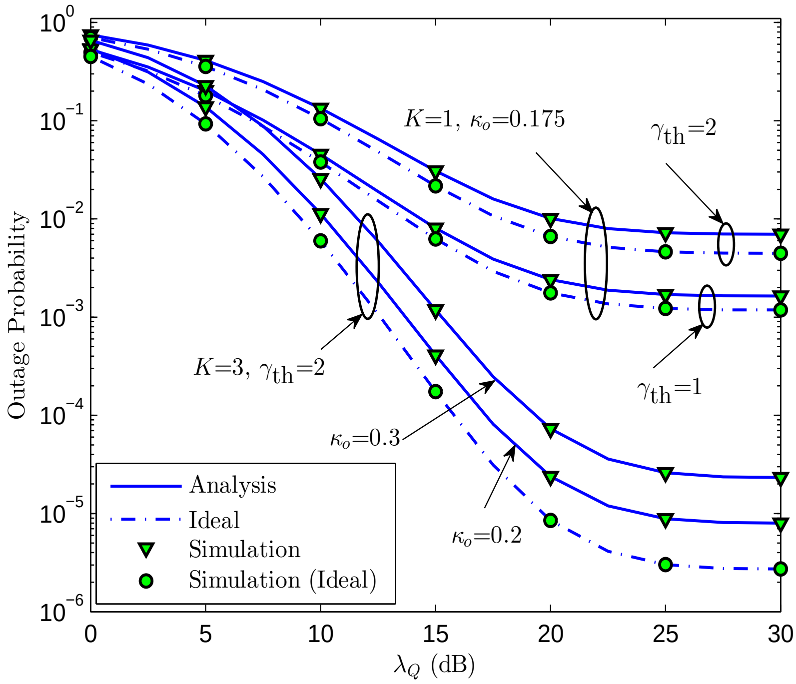

Figure 4.5: Impact of γ_{th} and HIs on the outage performance of the system.

In Fig. 4.5, we plot the outage probability curves versus λ_Q to illustrate the impact of γ_{th} and HIs on the considered CMRN. Herein, we set $\sigma_e^2 = 0.01$ and $\lambda_P = 10$ dB. For effective demonstration, we ensure that γ_{th} lies below all the ceilings' threshold points. Note that the analytical curves are in good agreement with the simulation results. From the respective curves, we can clearly see that for a fixed κ_o, as γ_{th} increases, the performance of the system degrades. There exists a performance gap between ideal and impaired systems, which tends to expand with increase in γ_{th} (see curves for γ_{th}= 1, 2). This can be associated with the fact that as γ_{th} increases, system approaches towards its ceiling threshold, and as a result, the deviation from the ideal system increases. Moreover, when HIs level κ_o increases from 0.2 to 0.3, the system's performance deteriorates significantly.

In Fig. 4.6, we plot the outage probability curves versus γ to depict the impact of CEEs on the outage performance and diversity gain of the system. We set $\gamma_{\text{th}}= 1$, $\lambda_P = \lambda_Q = 10$ dB, and $\kappa_o= 0.175$. It can be seen that asymptotic curves follow the analytical curves at high γ. We observe that presence of CEEs reduces the diversity gain of the system to zero which can be witnessed from the irreducible outage floors in the high γ regime. Further, as the σ_e^2 increases from 0.01 to 0.05, the outage performance deteriorates, especially in the high γ regime, owing to effect on the coding gain. Furthermore, for perfect CSI (i.e., $\sigma_e^2= 0$), the system exploits full diversity order of $K+1$ (evident from the various pertinent curves for $K = 1, 2, 3$).

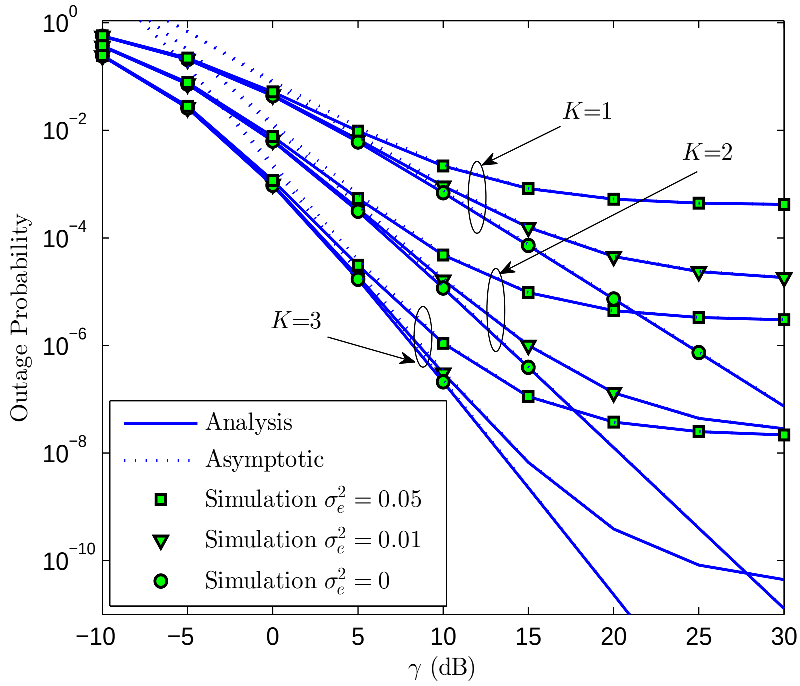

Figure 4.6: Impact of CEEs on the outage performance and diversity of the system.

In Fig. 4.7, we demonstrate the impact of ceiling effects RCC and OSC by plotting the outage curves against γ_{th}. Here, we fix $\sigma_e^2= 0.01$ and $\lambda_Q = \lambda_P = 20$ dB. For instance, if $\kappa_{s,d} = \kappa_{r,d} = 0.20, \kappa_{s,r} = 0.35$, the RCC and OSC effects occur at the threshold of ≈ 9 dB $\left(\gamma_{\text{th}} > \frac{1}{\max(\kappa_{s,r}^2,\kappa_{r,d}^2)}\right)$ and ≈ 13 dB $\left(\gamma_{\text{th}} > \frac{1}{\min(\kappa_{s,d}^2,\max(\kappa_{s,r}^2,\kappa_{r,d}^2))}\right)$, respectively. It can be manifestly observed from the curves that as γ_{th} crosses the RCC threshold, the system's performance converges to that of a pure direct link. Apparently, the direct link partially compensates for RCC (in the threshold range

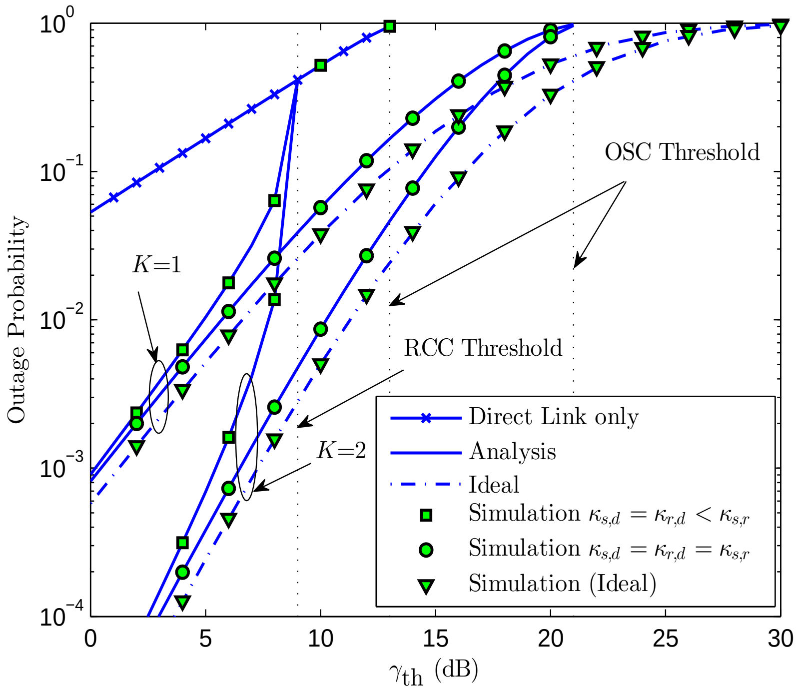

Figure 4.7: Impact of RCC and OSC on the outage performance of the system.

9 dB $\leq \gamma_{\text{th}} < 13$ dB) until the occurrence of OSC. Afterwards, when γ_{th} further increases to OSC threshold, the system outage probability approaches to unity. In another instance, when $\kappa_{s,d} = \kappa_{r,d} = \kappa_{s,r} = 0.08$, the OSC occurs at a threshold of ≈ 21 dB.

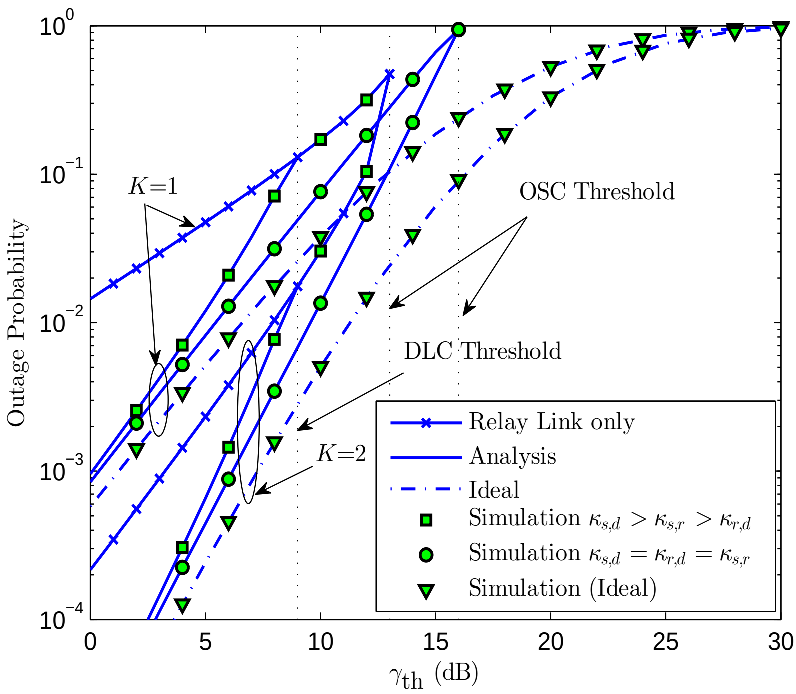

Figure 4.8: Impact of DLC and OSC on the outage performance of the system.

Similarly, the impact of DLC and OSC is shown in Fig. 4.8. For example, when $\kappa_{s,d} = 0.35, \kappa_{s,r} = 0.20, \kappa_{r,d} = 0.15$, the DLC and OSC effects occur at the threshold of ≈ 9 dB $\left(\gamma_{\text{th}} > \frac{1}{\kappa_{s,d}^2}\right)$ and ≈ 13 dB $\left(\gamma_{\text{th}} > \frac{1}{\min(\kappa_{s,d}^2, \max(\kappa_{s,r}^2, \kappa_{r,d}^2))}\right)$, respectively. Herein, as γ_{th} crosses the DLC threshold, the system's performance converges to that of a pure relaying link. As such, the relaying link partially compensates for DLC (in the threshold range 9 dB $\leq \gamma_{\text{th}} <$ 13 dB) until the occurrence of OSC. Thus, we can conclude that HIs are detrimental for considered system to sustain its performance standards in high-rate applications.

In a 3-D plot of Fig. 4.9, we illustrate the joint impact of HIs and CEEs on the outage performance of CMRN. It can be observed that outage probability attains its minimum value i.e., $\mathcal{P}_{\text{out}}(\gamma_{\text{th}}) = 0.00120$, when both HIs and CEEs are minimum ($\kappa_o < 0.1, \sigma_e^2 < 0.1$). Whereas, when both HIs and CEEs are maximum ($\kappa_o > 0.8, \sigma_e^2 > 0.8$), the $\mathcal{P}_{\text{out}}(\gamma_{\text{th}}) = 0.5609$. From these values, it can be deduced that the combined effect of HIs and CEEs dramatically degrade the system's performance.

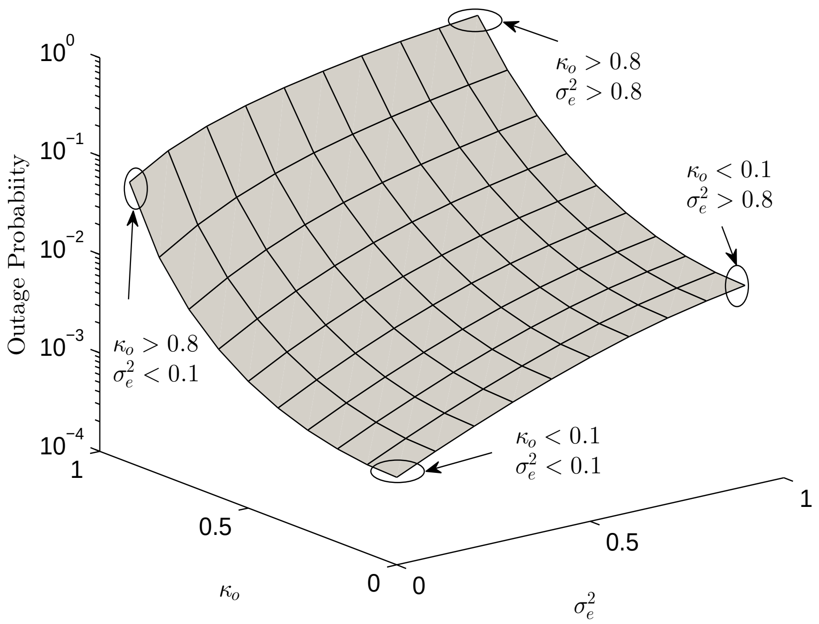

Figure 4.9: Joint impact of HIs and CEEs on the outage performance of the system.

In Fig. 4.10 and Fig. 4.11, we plot the outage probability curves against λ_Q and λ_P, respectively. From Fig. 4.10, it can be seen that for a fixed λ_P, the outage probability curves get saturated at high λ_Q. However, the performance improves when λ_P increases. Similar observations can be made for fixed λ_Q in Fig. 4.11. Further, for a fixed λ_Q, the saturation in outage curves reached quickly (curves in

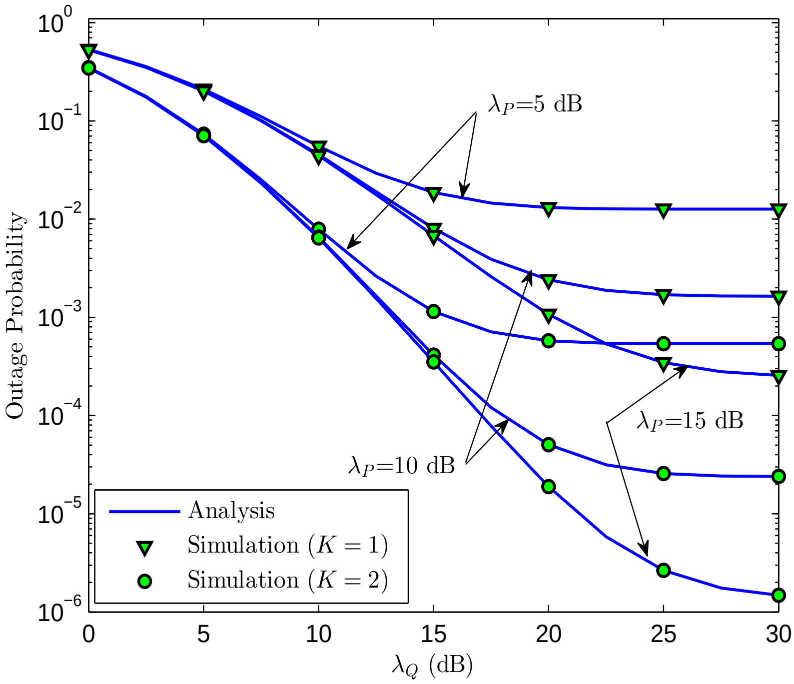

Figure 4.10: Outage performance of the system against λ_Q for different values of λ_P.

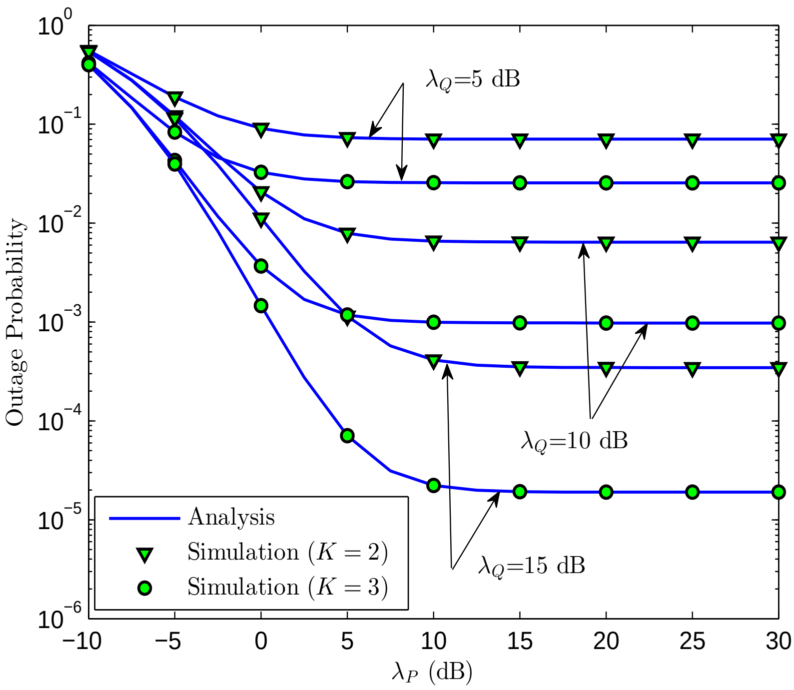

Figure 4.11: Outage performance of the system against λ_P for different values of λ_Q.

Fig. 4.11) as compared to the saturation for fixed λ_P (curves in Fig. 4.10). This is owing to the fact that when λ_Q is fixed, the powers of the SUs are only governed by maximum available power to them i.e., P. In contrast, when λ_P is fixed, the powers at SUs are governed by not only interference threshold Q but also by HIs and CEEs. For instance, when $\lambda_P = 15$ dB remains fixed and $K = 2$ (in Fig. 4.10), the outage probability saturates at $\mathcal{P}_{\text{out}}(\gamma_{\text{th}}) \approx 1.4 \times 10^{-6}$. While, for fixed $\lambda_Q = 15$ dB and $K = 2$ (in Fig. 4.11), the outage probability saturates at $\mathcal{P}_{\text{out}}(\gamma_{\text{th}}) \approx 3.4 \times 10^{-4}$.

4.3.5 Summary

We conducted performance analysis of a CMRN with direct link under the joint impact of hardware and channel imperfections. We considered the two classical relaying schemes, viz., AF relaying and DF relaying for the performance assessment. Based on the analysis, we discussed various ceiling effects invoked by HIs i.e., RCC, DLC, and OSC. These detrimental ceiling effects are found to limit the performance of system, especially when high target rates are anticipated. Specifically, it is found that RCC ceases the cooperation of relaying link, DLC inhibits the direct link transmission, whereas the OSC causes the overall system outage. However, it was shown that a potential direct link and a relaying link can partially compensate for the incurred performance losses due to RCC and DLC, respectively. To further delve into the system's performance, we also derived the asymptotic behaviour of outage probability in the high-SNR regime. It is observed that, due to CEEs, the system could not exploit the diversity, resulting in irreducible outage floors. In contrast, it is illustrated that HIs do not affect the diversity gain of the system. Above all, we deduced that the combined effect of HIs and CEEs poses critical impact on the system's performance. Besides, it is shown that the power constraints viz., maximum tolerable interference and maximum transmit power, may also cause the saturation in outage curves.

CHAPTER 5

EFFECT OF PU's INTERFERENCE ON COGNITIVE RELAY NETWORKS WITH HARDWARE AND CHANNEL IMPERFECTIONS

In the previous works, the effect of interference from the PUs has not been incorporated for the performance assessment of CRNs with HIs and CEEs. However, there may be instances when the existence of mutual interference between the SUs and PUs is inevitable [122]. Therefore, investigation of the PUs' interference on the performance of secondary network is also important. Hence, in this chapter, we investigate the performance of a DF relaying based CMRN with a direct link in the presence of HIs, CEEs, and interference from multiple PUs over Nakagami-m fading channels. Moreover, considering underlay spectrum sharing, the transmit powers at the SUs are adjusted in such a way that the stipulated QoS requirement of the PUs is satisfied. Further, we adopt Nakagami-m fading model that provides more degrees-of-freedom to characterize the realistic propagation environments [88]. Thus, the given analytical framework makes the performance analysis complicated and challenging but at the same time more general and practical. We also perform a comparative study to inspect the robustness of AF and DF relaying schemes against the HIs.

The rest of the chapter is organized as follows. In Section 5.1, we describe the signal models that take into account HIs, CEEs, and interference and subsequently present the descriptions of the designed analytical system in Section 5.2. In Section 5.3, we study the power allocation of SUs. In Section 5.4, we analyze the outage performance of considered system. In Section 5.5, we compare the performance of AF and DF relaying against HIs. Numerical and simulation results are provided in

Section 5.6, and finally, summary of the chapter is presented in Section 5.7.

5.1 Signal Model with HIs, CEEs, and Interference

Let $h_{\imath\jmath}$ be the channel coefficient between two arbitrary secondary nodes $\imath$ and $\jmath$, and $h_{c_i\jmath}$ be the channel coefficient between a primary node T_{c_i} and a secondary node $\jmath$. Then, considering MMSE channel estimation model, we have $h_{\imath\jmath} = \hat{h}_{\imath\jmath} + e_{h_{\imath\jmath}}$, where $\hat{h}_{\imath\jmath}$ and $e_{h_{\imath\jmath}}$ denote, respectively, the estimate and the estimation error for the channel $h_{\imath\jmath}$, and are mutually independent and orthogonal. As such, $h_{\imath\jmath} \sim \mathcal{CN}(0, \Omega_{\imath\jmath})$ and $e_{h_{\imath\jmath}} \sim \mathcal{CN}(0, \sigma^2_{e,\imath\jmath})$, where $\sigma^2_{e,\imath\jmath} = \mathbb{E}\{|h_{\imath\jmath}|^2\} - \mathbb{E}\{|\hat{h}_{\imath\jmath}|^2\}$ implies the quality of estimation and is chosen appropriately based on the estimation schemes [28]. Hence, we have $\hat{h}_{\imath\jmath} \sim \mathcal{CN}(0, \hat{\Omega}_{\imath\jmath})$, where $\hat{\Omega}_{\imath\jmath} = \Omega_{\imath\jmath} - \sigma^2_{e,\imath\jmath}$. Further, referring to HIs model[1] in [88], let x_s be the transmitted signal (with unit energy) over the channel $h_{\imath\jmath}$, then the signal at the receiving node $\jmath$ can be expressed as

$$y_\jmath = \sqrt{P_s}(\hat{h}_{\imath\jmath} + e_{h_{\imath\jmath}})(x_s + \eta_{t\imath}) + \eta_{r\jmath} + \sqrt{P_c}\sum_{i=1}^{L} h_{c_i\jmath}x_{c_i} + \eta_{c\jmath} + \nu_\jmath, \tag{5.1}$$

where P_s and P_c are the respective transmit powers at the nodes $\imath$ and T_{c_i}, $\nu_\jmath \sim \mathcal{CN}(0, N_0)$ denotes additive white Gaussian noise (AWGN), $\eta_{t\imath} \sim \mathcal{CN}(0, \kappa^2_{t\imath})$ represents distortion noise at the transmitter, whereas $\eta_{r\jmath} \sim \mathcal{CN}(0, \kappa^2_{r\jmath}P_s(|\hat{h}_{\imath\jmath}|^2 + \sigma^2_{e,\imath\jmath}))$ and $\eta_{c\jmath} \sim \mathcal{CN}(0, \kappa^2_{r\jmath}P_c\sum_{i=1}^{L}|h_{c_i\jmath}|^2)$ represent distortion noises at the receiver. The term $\sqrt{P_c}\sum_{i=1}^{L} h_{c_i\jmath}x_{c_i}$ represents the total interference due to primary transmissions, where x_{c_i} be the transmitted signal (with unit energy) from T_{c_i}. Hereby, the parameters $\kappa_{t\imath}$, $\kappa_{r\jmath} \geq 0$ quantify the level of impairments and are measured experimentally as EVMs. From (5.1), we can represent the aggregate power of the distortion noises at the receiver as

$$\mathbb{E}\{|\sqrt{P_s}(\hat{h}_{\imath\jmath} + e_{h_{\imath\jmath}})\eta_{t\imath} + \eta_{r\jmath}|^2\} = P_s(|\hat{h}_{\imath\jmath}|^2 + \sigma^2_{e,\imath\jmath})(\kappa^2_{t\imath} + \kappa^2_{r\jmath}). \tag{5.2}$$

Using (5.2), one can re-express (5.1) as

$$y_\jmath = \sqrt{P_s}(\hat{h}_{\imath\jmath} + e_{h_{\imath\jmath}})(x_s + \eta_{\imath,\jmath}) + \sqrt{P_c}\sum_{i=1}^{L} h_{c_i\jmath}x_{c_i} + \eta_{c\jmath} + \nu_\jmath, \tag{5.3}$$

[1] As such, our present work primarily focuses on analyzing the aggregate effect from many impairments that can be modeled as additive distortion noises, as also considered in many previous works [107], [123], [124]. However, the effect of HIs can also be modeled as a multiplicative factor [125] which can be viewed as an important direction for the future research.

where the distortion noise $\eta_{\imath,\jmath} \sim \mathcal{CN}(0, \kappa_{\imath,\jmath}^2)$ with $\kappa_{\imath,\jmath} = \sqrt{\kappa_{t\imath}^2 + \kappa_{r\jmath}^2}$. Hereafter, without loss of generality, we use the characterization in (5.3) for the subsequent analysis.

5.2 System Descriptions

As shown in Fig. 5.1, we consider a DF relaying based CMRN wherein a secondary network coexists with a primary network. The primary network consists of L pairs of PU transmitters and receivers, $\{T_{c_i} - T_{p_i}\}_{i=1}^{L}$. Let the bandwidth of B Hz is divided equally amongst all the primary links such that each primary link gets a bandwidth of B/L Hz. On the other hand, the secondary network comprises one secondary source S which communicates with one secondary destination D using the cooperation of K secondary relays $\{R_m\}_{m=1}^{K}$. It has been assumed that the

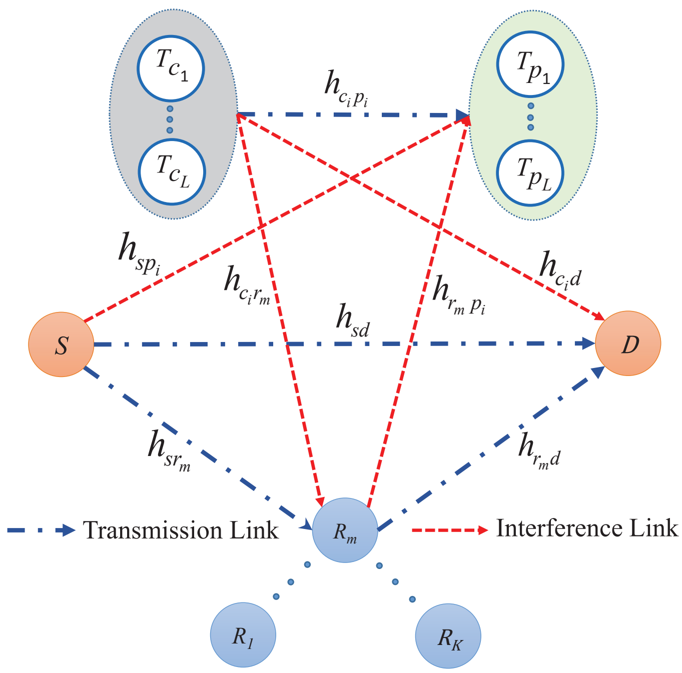

Figure 5.1: System model for CMRN with Interference.

direct link between the nodes S and D also exists. The intuitive reason for this is as follows. In the considered underlay spectrum sharing network, the power at the SU transmitter is constrained depending upon the QoS requirement of the PUs. Consequently, improving the performance of SUs in presence of such power constraint becomes challenging. To prevail over this, the relays are employed even for the shorter communication distance between source and destination nodes. Hence, the presence of a direct link can not be overlooked in such networks. In 5G cellular systems, the SUs may correspond to the femtocell users underlaying in a macrocell [76], [111]. Herein, all the secondary nodes (i.e., S, D, and R_m) are susceptible to HIs. As in most of the earlier works [100]-[104], we assume the hardware at the PUs to be ideal. Further, all the channels are assumed to follow block fading so that they remain constant during a packet transmission but changes independently during the next packet transmission [70], [71]. Let $h_{c_ip_i}$, h_{c_id}, $h_{c_ir_m}$, h_{sd}, h_{sr_m}, h_{sp_i}, h_{r_md}, and $h_{r_mp_i}$ denote the channel coefficients for the links $T_{c_i}-T_{p_i}$, $T_{c_i}-D$, $T_{c_i}-R_m$, $S-D$, $S-R_m$, $S-T_{p_i}$, R_m-D, and $R_m-T_{p_i}$ respectively, with $i=1,...,L$ and $m=1,...,K$. All the links are subject to independent Nakagami-m fading.

In considered CMRN, the overall communication in secondary network takes place in two time phases. In the first phase, the SU source node S transmits its signal x_s to SU destination node D and to all the relays. Consequently, the received signals at D and R_m can be given, respectively, by

$$y_{d,1} = \sqrt{P_s}(\hat{h}_{sd} + e_{h_{sd}})(x_s + \eta_{s,d}) + \sqrt{P_c}\sum_{i=1}^{L} h_{c_id}x_{c_i} + \eta_{cd} + \nu_{d,1} \tag{5.4}$$

and $$y_{r_m} = \sqrt{P_s}(\hat{h}_{sr_m} + e_{h_{sr_m}})(x_s + \eta_{s,r_m}) + \sqrt{P_c}\sum_{i=1}^{L} h_{c_ir_m}x_{c_i} + \eta_{cr_m} + \nu_{r_m}, \tag{5.5}$$

where P_s is the transmit power at node S, $\nu_{d,1}$ and ν_{r_m} represent AWGNs at the respective nodes, while $\eta_{s,d} \sim \mathcal{CN}(0, \kappa_{s,d}^2)$, $\eta_{cd} \sim \mathcal{CN}(0, \kappa_{rd}^2 P_c \sum_{i=1}^{L} |h_{c_id}|^2)$, $\eta_{s,r_m} \sim \mathcal{CN}(0, \kappa_{s,r_m}^2)$, and $\eta_{cr_m} \sim \mathcal{CN}(0, \kappa_{rr_m}^2 P_c \sum_{i=1}^{L} |h_{c_ir_m}|^2)$ represent distortion noises. Using (5.4) and (5.5), and considering the availability of the channel estimates, the resultant SNDRs at D and R_m in the first phase can be given, respectively, as[2]

$$\Lambda_{sd} = \frac{P_s|\hat{h}_{sd}|^2}{P_s\kappa_{s,d}^2|\hat{h}_{sd}|^2 + P_s\sigma_{e,sd}^2\delta_{s,d} + \sum_{i=1}^{L} P_c|h_{c_id}|^2\delta_{rd} + N_o} \tag{5.6}$$

and $$\Lambda_{sr_m} = \frac{P_s|\hat{h}_{sr_m}|^2}{P_s\kappa_{s,r_m}^2|\hat{h}_{sr_m}|^2 + P_s\sigma_{e,sr}^2\delta_{s,r} + \sum_{i=1}^{L} P_c|h_{c_ir_m}|^2\delta_{rr} + N_o}, \tag{5.7}$$

where $\delta_{s,d} = 1 + \kappa_{s,d}^2$, $\delta_{rd} = 1 + \kappa_{rd}^2$, $\delta_{s,r} = 1 + \kappa_{s,r_m}^2$, and $\delta_{rr} = 1 + \kappa_{rr_m}^2$.

In the second phase, the relays $\{R_m\}$ first attempt to decode the signal received from source S. Let $\mathcal{D}_m$ denotes the set of relays that can successfully decode the signal received in first phase. With a given target rate $\mathcal{R}_s$ of the system, the decoding

[2]Since we assume the scenario wherein the SU receiver nodes have access to only imperfect channel estimates, the SNDR expressions are obtained based on these estimates [28].

set $\mathcal{D}_m$ can be obtained as

$$\mathcal{D}_m = \{R_m | \Lambda_{sr_m} \geq \gamma_{\text{th}}, m \in \{1, ..., K\}\}, \tag{5.8}$$

where $\gamma_{\text{th}} = 2^{2\mathcal{R}_s} - 1$. Amongst all the relays in $\mathcal{D}_m$, the best relay (say mth relay) is selected in a reactive manner to forward the re-encoded signal x_r (satisfying $\mathbb{E}\{|x_r|^2\} = 1$) to SU destination D. Another possible way of selecting the relay is proactive relay selection in which the best relay is selected based on max-min criterion [119]. However, this proactive selection requires much larger feedback overhead to obtain CSI of all the links [116]. Therefore, we resort to the reactive relay selection which will be discussed in next section. As such, the received signal at D (via relay R_m) can be expressed as

$$y_{d,2} = \sqrt{P_r}(\hat{h}_{r_m d} + e_{h_{r_m d}})(x_r + \eta_{r_m,d}) + \sqrt{P_c}\sum_{i=1}^{L} h_{c_i d} x_{c_i} + \eta_{cd} + \nu_{d,2}, \tag{5.9}$$

where P_r is transmit power at node R_m, $\nu_{d,2}$ represents AWGN at D in the second phase and $\eta_{r_m,d} \sim \mathcal{CN}(0, \kappa^2_{r_m,d})$. Using (5.9), the SNDR at D via relaying link transmission in second phase can be written as

$$\Lambda_{r_m d} = \frac{P_r |\hat{h}_{r_m d}|^2}{P_r \kappa^2_{r_m,d} |\hat{h}_{r_m d}|^2 + P_r \sigma^2_{e,rd} \delta_{r,d} + \sum_{i=1}^{L} P_c |h_{c_i d}|^2 \delta_{rd} + N_o}, \tag{5.10}$$

where $\delta_{r,d} = 1 + \kappa^2_{r_m,d}$.

Hereafter, for simplicity, the links $T_{c_i} - T_{p_i}$ and multiple links over the same hop are assumed to be identically distributed by considering the cluster-based location of multiple nodes. As such, the channel gains $|h_{\imath\jmath}|^2$ and $|\hat{h}_{\imath\jmath}|^2$ follow gamma distribution with fading severity parameter $m_{\imath\jmath}$ and mean power $\Omega_{\imath\jmath}$ and $\hat{\Omega}_{\imath\jmath} = \Omega_{\imath\jmath} - \sigma^2_{e,\imath\jmath}$, respectively, where $\imath \in \{s, r_m\}$, $\jmath \in \{d, r_m\}$, and $\imath \neq \jmath$. The channels $|h_{c_i p}|^2$, $|h_{c_i d}|^2$, $|h_{c_i r_m}|^2$, $|h_{sp_i}|^2$, and $|h_{r_m p_i}|^2$ have severity parameters as m_{cp}, m_{cd}, m_{cr}, m_{sp}, and m_{rp}, respectively, and the corresponding mean powers are Ω_{cp}, Ω_{cd}, Ω_{cr}, Ω_{sp}, and Ω_{rp} respectively. In general, the PDF and CDF of a gamma random variable V with severity parameter m and mean Ω are given, respectively, by

$$f_V(v) = \frac{1}{\Gamma(m)} \left(\frac{m}{\Omega}\right)^m v^{m-1} e^{-\frac{mv}{\Omega}} \tag{5.11}$$

$$\text{and} \quad F_V(v) = \frac{1}{\Gamma(m)} \Upsilon\left(m, \frac{mv}{\Omega}\right). \tag{5.12}$$

Further, as in previous works [103], [104], [117], we consider $\kappa^2_{s,r_m} = \kappa^2_{s,r}$, $\kappa^2_{r_m,d} = \kappa^2_{r,d}$, $\kappa^2_{tr_m} = \kappa^2_{tr}$, $\kappa^2_{rr_m} = \kappa^2_{rr}$ for similar hardware of relays.

5.3 Power Allocation of SUs

In the primary network of considered CMRN, the ith transmitter T_{c_i} transmits its signal x_{c_i} to the corresponding ith receiver T_{p_i}. Consequently, after the first phase of transmissions, the signal received at T_{p_i} can be given as

$$y_{p_i,1} = \sqrt{P_c} h_{c_i p_i} x_{c_i} + \sqrt{P_s} h_{sp_i}(x_s + \eta_{ts}) + \nu_{p_i,1}, \tag{5.13}$$

where $\nu_{p_i,1}$ is the AWGN. Using (5.13), the SNDR at primary node T_{p_i} can be written as[3]

$$\Lambda_{p_i,1} = \frac{P_c |h_{c_i p_i}|^2}{P_s |h_{sp_i}|^2 + \kappa^2_{ts} P_s |h_{sp_i}|^2 + N_o}. \tag{5.14}$$

As discussed earlier, in the considered underlay spectrum sharing, the powers at the secondary transmitters viz., S and R_m, are governed by the stipulated QoS requirement of the PUs. To quantify the QoS requirement of PUs, the outage probability of each of the primary transmission shall be kept below a pre-defined threshold ξ_{th}. Consequently, following (5.14), we can express the outage probability for ith primary link, after the first phase, as

$$\mathcal{P}^{\text{pri},i}_{\text{out},1} = \Pr\left[\frac{B}{L}\log_2\left(1 + \Lambda_{p_i,1}\right) < \mathcal{R}_p\right] \leq \xi_{\text{th}}, \tag{5.15}$$

where $\mathcal{R}_p$ is the transmission rate for each primary link. Since there are L transmission links in primary network, we must ensure the QoS requirement of the link having worst SNDR. Therefore, we can write the primary outage constraint in first phase as

$$\mathcal{P}^{\text{pri}}_{\text{out},1} = \Pr\left[\min_{i=1,2,\ldots,L} \mathcal{P}^{\text{pri},i}_{\text{out},1}\right] \leq \xi_{\text{th}}, \tag{5.16}$$

which can be further expressed, after applying order statistics [118], as

$$\mathcal{P}^{\text{pri}}_{\text{out},1} = 1 - \prod_{i=1}^{L}\left(1 - \Pr\left[\Lambda_{p_i} < \varrho_{\text{th}}\right]\right) \leq \xi_{\text{th}}. \tag{5.17}$$

[3]Note that the objective of this chapter is to investigate the performance of the secondary system. Hence, we assume that the primary receivers may have knowledge of the true channel.

Lemma 10. *The primary outage probability $\mathcal{P}_{out,1}^{pri}$ in (5.17) can be evaluated as*

$$\mathcal{P}_{out,1}^{pri} = 1 - \left(\sum_{j=0}^{m_{cp}-1} \sum_{\hat{j}=0}^{j} \binom{j}{\hat{j}} \frac{\Gamma(\hat{j}+m_{sp})}{j!\Gamma(m_{sp})} \frac{(P_s\delta_{ts})^{\hat{j}}}{(N_o)^{\hat{j}-j}} e^{-\frac{m_{cp}\varrho_{th}N_o}{\Omega_{cp}P_c}} \left(\frac{m_{sp}}{\Omega_{sp}}\right)^{m_{sp}} \right.$$
$$\left. \times \left(\frac{m_{cp}\varrho_{th}}{\Omega_{cp}P_c}\right)^{j} \left(\frac{m_{sp}}{\Omega_{sp}} + \frac{m_{cp}\delta_{ts}\varrho_{th}P_s}{\Omega_{cp}P_c}\right)^{-(j+m_{sp})} \right)^{L} \leq \xi_{th}, \tag{5.18}$$

with $\delta_{ts} = 1 + \kappa_{ts}^2$ and $\varrho_{th} = 2^{\frac{L\mathcal{R}_p}{B}} - 1$.

Proof. Please refer to Appendix G. ∎

For a fixed ξ_{th}, the power P_s at SU node S can be obtained numerically by evaluating (5.18) with respect to P_s. Similarly, one can obtain the transmit power P_r at R_m by solving the primary outage constraint in the second phase as given below

$$\mathcal{P}_{\text{out},2}^{\text{pri}} = 1 - \left(\sum_{k=0}^{m_{cp}-1} \sum_{\hat{k}=0}^{k} \binom{k}{\hat{k}} \frac{\Gamma(\hat{k}+m_{rp})}{k!\Gamma(m_{rp})} \frac{(P_r\delta_{tr})^{\hat{j}}}{(N_o)^{\hat{k}-k}} e^{-\frac{m_{cp}\varrho_{\text{th}}N_o}{\Omega_{cp}P_c}} \left(\frac{m_{rp}}{\Omega_{rp}}\right)^{m_{rp}} \right.$$
$$\left. \times \left(\frac{m_{cp}\varrho_{\text{th}}}{\Omega_{cp}P_c}\right)^{k} \left(\frac{m_{rp}}{\Omega_{rp}} + \frac{m_{cp}\delta_{tr}\varrho_{\text{th}}P_r}{\Omega_{cp}P_c}\right)^{-(j+m_{rp})} \right)^{L} \leq \xi_{\text{th}}, \tag{5.19}$$

where (5.19) is obtained by following the same lines of derivation as done in Lemma 10, with $\delta_{tr} = 1 + \kappa_{tr}^2$.

For a special case when $m_{cp} = m_{sp} = m_{rp} = 1$, P_s and P_r can be obtained, respectively, as

$$P_s = \frac{P_c\Omega_{cp}}{\varrho_{\text{th}}\Omega_{sp}\delta_{ts}} \left(\frac{e^{-\frac{m_{cp}\varrho_{\text{th}}N_o}{\Omega_{cp}P_c}}}{(1-\xi_{\text{th}})^{1/L}} - 1 \right)^{+} \tag{5.20}$$

$$\text{and} \quad P_r = \frac{P_c\Omega_{cp}}{\varrho_{\text{th}}\Omega_{rp}\delta_{tr}} \left(\frac{e^{-\frac{m_{cp}\varrho_{\text{th}}N_o}{\Omega_{cp}P_c}}}{(1-\xi_{\text{th}})^{1/L}} - 1 \right)^{+}, \tag{5.21}$$

where $(\beta)^{+} = \max(0, \beta)$.

Note that, in such power adoption, the SUs only require the average channel gains of the link from itself to the PUs viz., $S - T_{p_i}$, $R_m - T_{p_i}$. In contrast to instantaneous channel gains, the average channel gains are relatively stable and can save the feedback channel resources [56], [126], [127]. Moreover, the average gains seem more viable as they can be obtained by using the transmission distance, frequency of radio waves, etc.

5.4 Outage Performance of Secondary Network

In this section, we conduct outage performance analysis of the considered CMRN. For a given threshold γ_{th}, the outage probability of the CMRN can be formulated using total probability theorem [118] as

$$\mathcal{P}_{\text{out}}^{\text{sec}}(\gamma_{\text{th}}) = \overbrace{\Pr\left[\Lambda_{sd} < \gamma_{\text{th}}, \mathcal{D}_m = \emptyset\right]}^{\mathcal{P}_{\emptyset}} + \overbrace{\sum_{m=1}^{K} \sum_{\mathcal{D}_m} \Pr\left[\Lambda_{sd} < \gamma_{\text{th}}, \Lambda_{r_m d} < \gamma_{\text{th}}, \mathcal{D}_m\right]}^{\mathcal{P}_{\bar{\emptyset}}}. \quad (5.22)$$

In (5.22), the first component $\mathcal{P}_{\emptyset}$ accounts for the case when no relay can successfully decode the signal received in the first phase, i.e., $\mathcal{D}_m$ is empty, and hence, system has to rely on the transmission from direct link only. Whereas, the other component $\mathcal{P}_{\bar{\emptyset}}$ corresponds to the case when $\mathcal{D}_m$ is non-empty, i.e, at least one relay is able to decode the signal successfully, and consequently, the destination D applies the selection cooperation to combine the signals received from direct link and best relaying link. The internal sum in $\mathcal{P}_{\bar{\emptyset}}$ spans over all $\binom{K}{m}$ possible decoding sets $\mathcal{D}_m$ of size m from the set of K candidate relays. On observing (5.6) and (5.10), we notice that $\mathcal{P}_{\bar{\emptyset}}$ in (5.22) involves joint events that are statistically dependent due to presence of a common random variable $W = \sum_{i=1}^{L} |h_{c_i d}|^2$. Therefore, this component can not be evaluated using conventional analysis. Hereby, we proficiently apply the conditioning approach to obtain $\mathcal{P}_{\bar{\emptyset}}$ and $\mathcal{P}_{\emptyset}$ in the following subsections.

Computation of $\mathcal{P}_{\bar{\emptyset}}$

Using (5.22), we obtain the component $\mathcal{P}_{\bar{\emptyset}}$ by first conditioning on W and then taking the expectation over W as

$$\mathcal{P}_{\bar{\emptyset}} = \int_{0}^{\infty} \sum_{m=1}^{K} \sum_{\mathcal{D}_m} \Pr\left[\Lambda_{sd} < \gamma_{\text{th}} | W\right] \Pr\left[\mathcal{D}_m\right] \Pr\left[\Lambda_{r_m d} < \gamma_{\text{th}} | \mathcal{D}_m, W\right] f_W(w) dw, \quad (5.23)$$

where $f_W(w)$ is the PDF of W that can be represented as [128]

$$f_W(w) = \left(\frac{m_{cd}}{\Omega_{cd}}\right)^{m_{cd}L} \frac{1}{\Gamma(m_{cd}L)} w^{m_{cd}L-1} e^{-\frac{m_{cd}}{\Omega_{cd}} w}. \quad (5.24)$$

Now, to compute the integral in (5.23), we require the expressions of probability terms $\Pr\left[\Lambda_{sd} < \gamma_{\text{th}} | W\right]$, $\Pr\left[\mathcal{D}_m\right]$, and $\Pr\left[\Lambda_{r_m d} < \gamma_{\text{th}} | \mathcal{D}_m, W\right]$. Firstly, let us begin with the derivation of $\Pr[\mathcal{D}_m]$ in the following lemma.

Lemma 11. *The decoding probability $Pr[\mathcal{D}_m]$ in (5.23) can be derived as*

$$Pr[\mathcal{D}_m] = \begin{cases} \Xi_m(\gamma_{th}), \; \textit{for } \gamma_{th} < 1/\kappa_{s,r}^2, \\ 0, \; \textit{for } \gamma_{th} \geq 1/\kappa_{s,r}^2, \end{cases} \tag{5.25}$$

where $\Xi_m(\gamma_{th})$ is given by

$$\Xi_m(\gamma_{th}) = \sum_{\mu=0}^{K-m} \binom{K-m}{\mu} (-1)^{\mu} \left(\sum_{t=0}^{m_{sr}-1} \sum_{\hat{t}=0}^{t} \binom{t}{\hat{t}} \frac{\Gamma(\hat{t}+m_{cr}L)}{t!\Gamma(m_{cr}L)} \frac{(\delta_{rr}P_c)^{\hat{t}}}{(\alpha_{s,r})^{\hat{t}-t}} e^{-\frac{m_{sr}\gamma_{th}\alpha_{s,r}}{\hat{\Omega}_{sr}P_s(1-\gamma_{th}\kappa_{s,r}^2)}} \left(\frac{m_{cr}}{\Omega_{cr}}\right)^{m_{cr}L} \right.$$
$$\left. \times \left(\frac{m_{sr}\gamma_{th}}{\hat{\Omega}_{sr}P_s(1-\gamma_{th}\kappa_{s,r}^2)} \right)^{t} \left(\frac{m_{cr}}{\Omega_{cr}} + \frac{m_{sr}\gamma_{th}P_c\delta_{rr}}{\hat{\Omega}_{sr}(1-\gamma_{th}\kappa_{s,r}^2)} \right)^{-(\hat{t}+m_{cr}L)} \right)^{m+\mu}, \tag{5.26}$$

Proof. Please refer to Appendix H. ∎

From (5.25), it is worth noticing that the HIs impose the undesirable constraint on γ_{th} which restricts the decoding of received signals at the relays in the first phase beyond a certain rate requirement. This can be witnessed from the fact that the decoding probability in (5.25) reduces to zero for $\gamma_{\text{th}} \geq 1/\kappa_{s,r}^2$.

Next, the conditional probability $\Pr[\Lambda_{sd} < \gamma_{\text{th}}|W]$ can be expressed, using (5.6), as

$$\Pr[\Lambda_{sd} < \gamma_{\text{th}}|W] = \Pr\left[|\hat{h}_{sd}|^2 < \frac{\gamma_{\text{th}}(P_s\sigma_{e,sd}^2\delta_{s,d} + \delta_{rd}P_c w + N_o)}{P_s(1-\gamma_{\text{th}}\kappa_{s,d}^2)} \Big| W \right], \tag{5.27}$$

which can be evaluated as

$$\Pr[\Lambda_{sd} < \gamma_{\text{th}}|W] = \begin{cases} \Phi_{sd}(\gamma_{\text{th}}, w), \; \text{for } \gamma_{\text{th}} < 1/\kappa_{s,d}^2, \\ 1, \; \text{for } \gamma_{\text{th}} \geq 1/\kappa_{s,d}^2, \end{cases} \tag{5.28}$$

where the function $\Phi_{sd}(\gamma_{\text{th}}, w)$ is given by

$$\Phi_{sd}(\gamma_{\text{th}}, w) = 1 - \sum_{l=0}^{m_{sd}-1} \sum_{\hat{l}=0}^{l} \binom{l}{\hat{l}} (\delta_{rd}P_c w)^{\hat{l}} (\alpha_{s,d})^{l-\hat{l}} e^{-\frac{m_{sd}\gamma_{\text{th}}(\delta_{rd}P_c w + \alpha_{s,d})}{\hat{\Omega}_{sd}P_s(1-\gamma_{\text{th}}\kappa_{s,d}^2)}}$$
$$\times \left(\frac{m_{sd}\gamma_{\text{th}}}{\hat{\Omega}_{sd}P_s(1-\gamma_{\text{th}}\kappa_{s,d}^2)} \right)^{l}, \tag{5.29}$$

with $\alpha_{s,d} = P_s(1+\kappa_{s,d}^2)\sigma_{e,sd}^2 + N_o$. Apparently, the probability term $\Pr[\Lambda_{sd} < \gamma_{\text{th}}|W]$ in (5.28) converges to unity for $\gamma_{\text{th}} \geq 1/\kappa_{s,d}^2$. This implies that the direct communication link will also be in outage beyond a certain rate due to presence of HIs.

Now, we derive the conditional probability term $\Pr\left[\Lambda_{r_m d} < \gamma_{\text{th}} | \mathcal{D}_m, W\right]$. For this, let R_m represents the best selected relay amongst the m relays in decoding set $\mathcal{D}_m$, which is based on the criterion

$$\Lambda_{r_m d} = \max_{\{\ell \in \mathcal{D}_m\}} \{\Lambda_{r_\ell d}\}. \tag{5.30}$$

Hereby, it has been assumed that the selection process is executed in a controller unit where all the information about channel estimates and statistics of the distortion noises are gathered and conveyed to the relays through feedback [119], [120]. As such, we apply the concepts of order statistics to express

$$\Pr\left[\Lambda_{r_m d} < \gamma_{\text{th}} | \mathcal{D}_m, W\right] = \prod_{\ell=1}^{m} \Pr\left[\Lambda_{r_\ell d} < \gamma_{\text{th}} | \mathcal{D}_m, W\right]. \tag{5.31}$$

Consequently, invoking (5.10) and then performing some involved manipulations with the aid of binomial and multinomial expansions [49, eq. 0.314], we can compute (5.31) as

$$\Pr\left[\Lambda_{r_m d} < \gamma_{\text{th}} | \mathcal{D}_m, W\right] = \begin{cases} \Phi_{rd}(\gamma_{\text{th}}, w), \text{ for } \gamma_{\text{th}} < 1/\kappa_{r,d}^2, \\ 1, \text{ for } \gamma_{\text{th}} \geq 1/\kappa_{r,d}^2, \end{cases} \tag{5.32}$$

where the function $\Phi_{rd}(\gamma_{\text{th}}, w)$ is given by

$$\begin{aligned} \Phi_{rd}(\gamma_{\text{th}}, w) &= \sum_{v=0}^{m} \sum_{g=0}^{v(m_{rd}-1)} \sum_{\hat{g}=0}^{g} \binom{m}{v} \binom{g}{\hat{g}} (-1)^v \omega_g^v (\alpha_{r,d})^{g-\hat{g}} \\ &\times (\delta_{rd} P_c w)^{\hat{g}} e^{-\frac{v m_{rd} \gamma_{\text{th}} (\delta_{rd} P_c w + \alpha_{r,d})}{\hat{\Omega}_{rd} P_r (1 - \gamma_{\text{th}} \kappa_{r,d}^2)}} \left(\frac{m_{rd} \gamma_{\text{th}}}{\hat{\Omega}_{rd} P_r (1 - \gamma_{\text{th}} \kappa_{r,d}^2)} \right)^g, \end{aligned} \tag{5.33}$$

with $\alpha_{r,d} = P_r(1 + \kappa_{r,d}^2)\sigma_{e,rd}^2 + N_o$, and the coefficients ω_g^v, for $0 \leq g \leq v(m_{rd} - 1)$, can be calculated recursively (with $\varepsilon_g = \frac{1}{g!}$) as $\omega_0^v = (\varepsilon_0)^v$, $\omega_1^v = v(\varepsilon_1)$, $\omega_{v(m_{rd}-1)}^v = (\varepsilon_{m_{rd}-1})^v$, $\omega_g^v = \frac{1}{g\varepsilon_0} \sum_{q=1}^{g} (qv - g + q) \varepsilon_q \omega_{g-q}^v$ for $2 \leq g \leq m_{rd} - 1$, and $\omega_g^v = \frac{1}{g\varepsilon_0} \sum_{q=1}^{m_{rd}-1} (qv - g + q) \varepsilon_q \omega_{g-q}^v$ for $m_{rd} \leq g < v(m_{rd} - 1)$. Hereby, the HIs restrict the decoding of signals (in second phase) at the destination beyond a certain rate requirement as evident from the condition $\gamma_{\text{th}} \geq 1/\kappa_{r,d}^2$ in (5.32). Now, by following (5.25), (5.28), and (5.32), it is worth remarking that the probability $\mathcal{P}_{\bar{\emptyset}}$ in (5.23) evaluates to different expressions depending on the impairment levels $\kappa_{s,d}^2$, $\kappa_{s,r}^2$, and $\kappa_{r,d}^2$. Consequently, plugging (5.25), (5.28), and (5.32) in (5.23), we obtain $\mathcal{P}_{\bar{\emptyset}}$ for all the possible cases as follows:

- When $\kappa_{s,d}^2 \leq \kappa_{r,d}^2 \leq \kappa_{s,r}^2$ or $\kappa_{r,d}^2 \leq \kappa_{s,d}^2 \leq \kappa_{s,r}^2$,

$$\mathcal{P}_{\bar{\emptyset}} = \begin{cases} \mathcal{P}_{\bar{\emptyset}1}, \text{ for } \gamma_{\text{th}} < 1/\kappa_{s,r}^2, \\ 0, \text{ otherwise.} \end{cases} \tag{5.34}$$

- When $\kappa_{s,r}^2 \leq \kappa_{s,d}^2 \leq \kappa_{r,d}^2$,

$$\mathcal{P}_{\bar{\emptyset}} = \begin{cases} \mathcal{P}_{\bar{\emptyset}1}, \text{ for } \gamma_{\text{th}} < 1/\kappa_{r,d}^2, \\ \mathcal{P}_{\bar{\emptyset}4}, \text{ for } 1/\kappa_{r,d}^2 \leq \gamma_{\text{th}} < 1/\kappa_{s,d}^2, \\ \mathcal{P}_{\bar{\emptyset}3}, \text{ for } 1/\kappa_{s,d}^2 \leq \gamma_{\text{th}} < 1/\kappa_{s,r}^2, \\ 0, \text{ otherwise.} \end{cases} \tag{5.35}$$

- When $\kappa_{s,d}^2 \leq \kappa_{s,r}^2 \leq \kappa_{r,d}^2$,

$$\mathcal{P}_{\bar{\emptyset}} = \begin{cases} \mathcal{P}_{\bar{\emptyset}1}, \text{ for } \gamma_{\text{th}} < 1/\kappa_{r,d}^2, \\ \mathcal{P}_{\bar{\emptyset}4}, \text{ for } 1/\kappa_{r,d}^2 \leq \gamma_{\text{th}} < 1/\kappa_{s,r}^2, \\ 0, \text{ otherwise.} \end{cases} \tag{5.36}$$

- When $\kappa_{r,d}^2 \leq \kappa_{s,r}^2 \leq \kappa_{s,d}^2$,

$$\mathcal{P}_{\bar{\emptyset}} = \begin{cases} \mathcal{P}_{\bar{\emptyset}1}, \text{ for } \gamma_{\text{th}} < 1/\kappa_{s,d}^2, \\ \mathcal{P}_{\bar{\emptyset}2}, \text{ for } 1/\kappa_{s,d}^2 \leq \gamma_{\text{th}} < 1/\kappa_{s,r}^2, \\ 0, \text{ otherwise.} \end{cases} \tag{5.37}$$

- When $\kappa_{s,r}^2 \leq \kappa_{r,d}^2 \leq \kappa_{s,d}^2$,

$$\mathcal{P}_{\bar{\emptyset}} = \begin{cases} \mathcal{P}_{\bar{\emptyset}1}, \text{ for } \gamma_{\text{th}} < 1/\kappa_{s,d}^2, \\ \mathcal{P}_{\bar{\emptyset}2}, \text{ for } 1/\kappa_{s,d}^2 \leq \gamma_{\text{th}} < 1/\kappa_{r,d}^2, \\ \mathcal{P}_{\bar{\emptyset}3}, \text{ for } 1/\kappa_{r,d}^2 \leq \gamma_{\text{th}} < 1/\kappa_{s,r}^2, \\ 0, \text{ otherwise.} \end{cases} \tag{5.38}$$

Hereby, the expressions for components $\mathcal{P}_{\bar{\emptyset}1}$, $\mathcal{P}_{\bar{\emptyset}2}$, $\mathcal{P}_{\bar{\emptyset}3}$, and $\mathcal{P}_{\bar{\emptyset}4}$ are derived in the sequel. Firstly, the component $\mathcal{P}_{\bar{\emptyset}1}$ can be expressed using (5.23) as

$$\mathcal{P}_{\bar{\emptyset}1} = \int_0^\infty \sum_{m=1}^{K} \binom{K}{m} \Phi_{sd}(\gamma_{\text{th}}, w) \Xi_m(\gamma_{\text{th}}) \Phi_{rd}(\gamma_{\text{th}}, w) f_W(w) dw. \tag{5.39}$$

On substituting $\Xi_m(\gamma_{\text{th}})$, $\Phi_{sd}(\gamma_{\text{th}}, w)$, and $\Phi_{rd}(\gamma_{\text{th}}, w)$ from (5.26), (5.29), and (5.33), respectively, in (5.39) and then solving the integral using the PDF from (5.24), we get $\mathcal{P}_{\bar{\emptyset}1}$ as

$$\mathcal{P}_{\bar{\emptyset}1} = \sum_{m=1}^{K}\sum_{v=0}^{m}\sum_{g=0}^{v(m_{rd}-1)}\sum_{\hat{g}=0}^{g}\binom{K}{m}\binom{m}{v}\binom{g}{\hat{g}}\Xi_m(\gamma_{\text{th}})\frac{(-1)^v\omega_g^v(\delta_{rd}P_c)^{\hat{g}}}{(\alpha_{r,d})^{\hat{g}-g}\Gamma(m_{cd}L)}\left(\frac{m_{cd}}{\Omega_{cd}}\right)^{m_{cd}L}e^{-\frac{vm_{rd}\gamma_{\text{th}}\alpha_{r,d}}{\hat{\Omega}_{rd}P_r(1-\gamma_{\text{th}}\kappa_{r,d}^2)}}$$
$$\times\left(\frac{m_{rd}\gamma_{\text{th}}}{\hat{\Omega}_{rd}P_r(1-\gamma_{\text{th}}\kappa_{r,d}^2)}\right)^g\left[\Gamma(\hat{g}+m_{cd}L)\left(\frac{m_{cd}}{\Omega_{cd}}+\frac{vm_{rd}\gamma_{\text{th}}P_c\delta_{rd}}{\hat{\Omega}_{rd}P_r(1-\gamma_{\text{th}}\kappa_{r,d}^2)}\right)^{-(\hat{g}+m_{cd}L)}-\sum_{l=0}^{m_{sd}-1}\sum_{\hat{l}=0}^{l}\binom{l}{\hat{l}}\right.$$
$$\times\frac{1}{l!}(\alpha_{s,d})^{l-\hat{l}}(\delta_{rd}P_c)^{\hat{l}}e^{-\frac{m_{sd}\gamma_{\text{th}}\alpha_{s,d}}{\hat{\Omega}_{sd}P_s(1-\gamma_{\text{th}}\kappa_{s,d}^2)}}\left(\frac{m_{sd}\gamma_{\text{th}}}{\hat{\Omega}_{sd}P_s(1-\gamma_{\text{th}}\kappa_{s,d}^2)}\right)^l\Gamma(\hat{l}+\hat{g}+m_{cd}L)$$
$$\left.\times\left(\frac{m_{cd}}{\Omega_{cd}}+\frac{m_{sd}\gamma_{\text{th}}P_c\delta_{rd}}{\hat{\Omega}_{sd}P_s(1-\gamma_{\text{th}}\kappa_{s,d}^2)}+\frac{vm_{rd}\gamma_{\text{th}}P_c\delta_{rd}}{\hat{\Omega}_{rd}P_r(1-\gamma_{\text{th}}\kappa_{r,d}^2)}\right)^{-(\hat{l}+\hat{g}+m_{cd}L)}\right]. \tag{5.40}$$

Next, the component $\mathcal{P}_{\bar{\emptyset}2}$ in (5.37) and (5.38) can be expressed using (5.23) as

$$\mathcal{P}_{\bar{\emptyset}2} = \int_0^\infty\sum_{m=1}^{K}\sum_{\mathcal{D}_m}\Pr[\mathcal{D}_m]\Pr[\Lambda_{r_m d}<\gamma_{\text{th}}|\mathcal{D}_m,W]f_W(w)dw. \tag{5.41}$$

By following the similar steps as used for deriving $\mathcal{P}_{\bar{\emptyset}1}$, (5.41) can be solved to obtain $\mathcal{P}_{\bar{\emptyset}2}$ as given by

$$\mathcal{P}_{\bar{\emptyset}2} = \sum_{m=1}^{K}\sum_{v=0}^{m}\sum_{g=0}^{v(m_{rd}-1)}\sum_{\hat{g}=0}^{g}\binom{K}{m}\binom{m}{v}\binom{g}{\hat{g}}\Xi_m(\gamma_{\text{th}})\frac{(-1)^v\omega_g^v(\delta_{rd}P_c)^{\hat{g}}}{(\alpha_{r,d})^{\hat{g}-g}\Gamma(m_{cd}L)}\left(\frac{m_{cd}}{\Omega_{cd}}\right)^{m_{cd}L}e^{-\frac{vm_{rd}\gamma_{\text{th}}\alpha_{r,d}}{\hat{\Omega}_{rd}P_r(1-\gamma_{\text{th}}\kappa_{r,d}^2)}}$$
$$\times\left(\frac{m_{rd}\gamma_{\text{th}}}{\hat{\Omega}_{rd}P_r(1-\gamma_{\text{th}}\kappa_{r,d}^2)}\right)^g\Gamma(\hat{g}+m_{cd}L)\left(\frac{m_{cd}}{\Omega_{cd}}+\frac{vm_{rd}\gamma_{\text{th}}P_c\delta_{rd}}{\hat{\Omega}_{rd}P_r(1-\gamma_{\text{th}}\kappa_{r,d}^2)}\right)^{-(\hat{g}+m_{cd}L)}. \tag{5.42}$$

Likewise, $\mathcal{P}_{\bar{\emptyset}3}$ can be obtained as

$$\mathcal{P}_{\bar{\emptyset}3} = \int_0^\infty\sum_{m=1}^{K}\sum_{\mathcal{D}_m}\Pr[\mathcal{D}_m]f_W(w)dw = \sum_{m=1}^{K}\binom{K}{m}\Xi_m(\gamma_{\text{th}}). \tag{5.43}$$

Lastly, $\mathcal{P}_{\bar{\emptyset}4}$ can be derived as

$$\mathcal{P}_{\bar{\emptyset}4} = \int_0^\infty\sum_{m=1}^{K}\sum_{\mathcal{D}_m}\Pr[\Lambda_{sd}<\gamma_{\text{th}}|W]\Pr[\mathcal{D}_m]f_W(w)dw, \tag{5.44}$$

which can be evaluated further to obtain the expression as given by

$$\mathcal{P}_{\bar{\emptyset}4} = \sum_{m=1}^{K}\binom{K}{m}\Xi_m(\gamma_{\text{th}})\left[1-\sum_{l=0}^{m_{sd}-1}\sum_{\hat{l}=0}^{l}\binom{l}{\hat{l}}\frac{1}{l!\Gamma(m_{cd}L)}(\alpha_{s,d})^{l-\hat{l}}(\delta_{rd}P_c)^{\hat{l}}e^{-\frac{m_{sd}\gamma_{\text{th}}\alpha_{s,d}}{\hat{\Omega}_{sd}P_s(1-\gamma_{\text{th}}\kappa_{s,d}^2)}}\Gamma(\hat{l}+m_{cd}L)\right.$$
$$\left.\times\left(\frac{m_{cd}}{\Omega_{cd}}\right)^{m_{cd}L}\left(\frac{m_{sd}\gamma_{\text{th}}}{\hat{\Omega}_{sd}P_s(1-\gamma_{\text{th}}\kappa_{s,d}^2)}\right)^l\left(\frac{m_{cd}}{\Omega_{cd}}+\frac{m_{sd}\gamma_{\text{th}}P_c\delta_{rd}}{\hat{\Omega}_{sd}P_s(1-\gamma_{\text{th}}\kappa_{s,d}^2)}\right)^{-(\hat{l}+m_{cd}L)}\right]. \tag{5.45}$$

It is worthwhile to recall that $\mathcal{P}_{\bar{\emptyset}}$ accounts for the selection cooperation between direct and relaying links. From (5.34)-(5.38), it can be deduced that this cooperative transmission ceases to exist beyond a certain threshold. This fact can be attested from the observation that probability $\mathcal{P}_{\bar{\emptyset}}$ reduces to zero as $\gamma_{\rm th} \geq 1/\kappa_{s,r}^2$.

Computation of $\mathcal{P}_{\emptyset}$

The component $\mathcal{P}_{\emptyset}$ in (5.22) can be expressed in an integral form with the aid of (5.8) as

$$\mathcal{P}_{\emptyset} = \int_0^{\infty} \prod_{m=1}^{K} \Pr\left[\Lambda_{sr_m} < \gamma_{\rm th} | W\right] \Pr\left[\Lambda_{sd} < \gamma_{\rm th} | W\right] f_W(w) dw. \tag{5.46}$$

Based on the impairment levels $\kappa_{s,d}^2$ and $\kappa_{s,r}^2$, (5.46) yields different expressions. Thus, after plugging (H.4) and (5.28) in (5.46) along with PDF $f_W(w)$ from (5.24), and then solving the resultant integral, $\mathcal{P}_{\emptyset}$ is obtained as follows:

- When $\kappa_{s,d}^2 \leq \kappa_{s,r}^2$,

$$\mathcal{P}_{\emptyset} = \begin{cases} \mathcal{P}_{\emptyset 1}, \text{ for } \gamma_{\rm th} < 1/\kappa_{s,r}^2, \\ \mathcal{P}_{\emptyset 2}, \text{ for } 1/\kappa_{s,r}^2 \leq \gamma_{\rm th} < 1/\kappa_{s,d}^2, \\ 1, \text{otherwise}. \end{cases} \tag{5.47}$$

- When $\kappa_{s,d}^2 \geq \kappa_{s,r}^2$,

$$\mathcal{P}_{\emptyset} = \begin{cases} \mathcal{P}_{\emptyset 1}, \text{ for } \gamma_{\rm th} < 1/\kappa_{s,d}^2, \\ \mathcal{P}_{\emptyset 3}, \text{ for } 1/\kappa_{s,d}^2 \leq \gamma_{\rm th} < 1/\kappa_{s,r}^2, \\ 1, \text{otherwise}. \end{cases} \tag{5.48}$$

Hereby, the component $\mathcal{P}_{\emptyset 1}$ can be evaluated by substituting (5.28) and (H.4) into (5.46), and computing the required integral to obtain

$$\begin{aligned}\mathcal{P}_{\emptyset 1} = &\Bigg(\Bigg(1 - \sum_{t=0}^{m_{sr}-1} \sum_{\hat{t}=0}^{t} \binom{t}{\hat{t}} \frac{\Gamma(\hat{t}+m_{cr}L)}{t!\Gamma(m_{cr}L)} \frac{(\delta_{rr}P_c)^{\hat{t}}}{(\alpha_{s,r})^{\hat{t}-t}} e^{-\frac{m_{sr}\gamma_{\rm th}\alpha_{s,r}}{\hat{\Omega}_{sr}P_s(1-\gamma_{\rm th}\kappa_{s,r}^2)}} \left(\frac{m_{cr}}{\Omega_{cr}}\right)^{m_{cr}L} \left(\frac{m_{sr}\gamma_{\rm th}}{\hat{\Omega}_{sr}P_s(1-\gamma_{\rm th}\kappa_{s,r}^2)}\right)^{t} \\ &\times \left(\frac{m_{cr}}{\Omega_{cr}} + \frac{m_{sr}\gamma_{\rm th}P_c\delta_{rr}}{\hat{\Omega}_{sr}(1-\gamma_{\rm th}\kappa_{s,r}^2)}\right)^{-(\hat{t}+m_{cr}L)}\Bigg)^{K} \Bigg(1 - \sum_{l=0}^{m_{sd}-1} \sum_{\hat{l}=0}^{l} \binom{l}{\hat{l}} \frac{1}{l!\Gamma(m_{cd}L)} (\alpha_{s,d})^{l-\hat{l}} (\delta_{rd}P_c)^{\hat{l}} e^{-\frac{m_{sd}\gamma_{\rm th}\alpha_{s,d}}{\hat{\Omega}_{sd}P_s(1-\gamma_{\rm th}\kappa_{s,d}^2)}} \\ &\times \Gamma(\hat{l}+m_{cd}L) \left(\frac{m_{cd}}{\Omega_{cd}}\right)^{m_{cd}L} \left(\frac{m_{sd}\gamma_{\rm th}}{\hat{\Omega}_{sd}P_s(1-\gamma_{\rm th}\kappa_{s,d}^2)}\right)^{l} \left(\frac{m_{cd}}{\Omega_{cd}} + \frac{m_{sd}\gamma_{\rm th}P_c\delta_{rd}}{\hat{\Omega}_{sd}P_s(1-\gamma_{\rm th}\kappa_{s,d}^2)}\right)^{-(\hat{l}+m_{cd}L)}\Bigg). \end{aligned} \tag{5.49}$$

Whereas, the components $\mathcal{P}_{\emptyset 2}$ and $\mathcal{P}_{\emptyset 3}$ in (5.47) and (5.48), respectively, are given by

$$\mathcal{P}_{\emptyset 2} = \int_0^\infty \prod_{m=1}^{K} \Pr\left[\Lambda_{sd} < \gamma_{\text{th}} | W\right] f_W(w) dw \tag{5.50}$$

and

$$\mathcal{P}_{\emptyset 3} = \int_0^\infty \prod_{m=1}^{K} \Pr\left[\Lambda_{sr_m} < \gamma_{\text{th}} | W\right] f_W(w) dw. \tag{5.51}$$

Evaluation of (5.50) and (5.51) yields $\mathcal{P}_{\emptyset 2}$ and $\mathcal{P}_{\emptyset 3}$ as given, respectively, by

$$\begin{aligned}\mathcal{P}_{\emptyset 2} = 1 - \sum_{l=0}^{m_{sd}-1} \sum_{\hat{l}=0}^{l} \binom{l}{\hat{l}} \frac{1}{l!\Gamma(m_{cd}L)} (\alpha_{s,d})^{l-\hat{l}} (\delta_{rd} P_c)^{\hat{l}} e^{-\frac{m_{sd}\gamma_{\text{th}}\alpha_{s,d}}{\hat{\Omega}_{sd} P_s (1-\gamma_{\text{th}}\kappa_{s,d}^2)}} \Gamma(\hat{l} + m_{cd}L) \\ \times \left(\frac{m_{cd}}{\Omega_{cd}}\right)^{m_{cd}L} \left(\frac{m_{sd}\gamma_{\text{th}}}{\hat{\Omega}_{sd} P_s (1-\gamma_{\text{th}}\kappa_{s,d}^2)}\right)^{l} \left(\frac{m_{cd}}{\Omega_{cd}} + \frac{m_{sd}\gamma_{\text{th}} P_c \delta_{rd}}{\hat{\Omega}_{sd} P_s (1-\gamma_{\text{th}}\kappa_{s,d}^2)}\right)^{-(\hat{l}+m_{cd}L)}\end{aligned} \tag{5.52}$$

and $$\begin{aligned}\mathcal{P}_{\emptyset 3} = \left(1 - \sum_{t=0}^{m_{sr}-1} \sum_{\hat{t}=0}^{t} \binom{t}{\hat{t}} \frac{\Gamma(\hat{t} + m_{cr}L)}{t!\Gamma(m_{cr}L)} \frac{(\delta_{rr} P_c)^{\hat{t}}}{(\alpha_{s,r})^{\hat{t}-t}} e^{-\frac{m_{sr}\gamma_{\text{th}}\alpha_{s,r}}{\hat{\Omega}_{sr} P_s (1-\gamma_{\text{th}}\kappa_{s,r}^2)}} \left(\frac{m_{cr}}{\Omega_{cr}}\right)^{m_{cr}L} \right. \\ \left. \times \left(\frac{m_{sr}\gamma_{\text{th}}}{\hat{\Omega}_{sr} P_s (1-\gamma_{\text{th}}\kappa_{s,r}^2)}\right)^{t} \left(\frac{m_{cr}}{\Omega_{cr}} + \frac{m_{sr}\gamma_{\text{th}} P_c \delta_{rr}}{\hat{\Omega}_{sr} (1-\gamma_{\text{th}}\kappa_{s,r}^2)}\right)^{-(\hat{t}+m_{cr}L)} \right)^{K}.\end{aligned} \tag{5.53}$$

Finally, by substituting the obtained $\mathcal{P}_{\emptyset}$ and $\mathcal{P}_{\bar{\emptyset}}$ appropriately in (5.22), we express the outage probability $\mathcal{P}_{\text{out}}^{\text{sec}}(\gamma_{\text{th}})$ in the following proposition.

Proposition 2. *The outage probability $\mathcal{P}_{out}^{sec}(\gamma_{th})$ of considered CMRN, for all the possible cases depending upon the impairments level $\kappa_{s,d}^2$, $\kappa_{s,r}^2$, and $\kappa_{r,d}^2$, can be given as follows:*

Case 1: For $\kappa_{s,d}^2 \le \kappa_{r,d}^2 \le \kappa_{s,r}^2$ or $\kappa_{r,d}^2 \le \kappa_{s,d}^2 \le \kappa_{s,r}^2$,

$$\mathcal{P}_{out}^{sec}(\gamma_{th}) = \begin{cases} \mathcal{P}_{\bar{\emptyset}1} + \mathcal{P}_{\emptyset 1}, \ \textit{for } \gamma_{th} < 1/\kappa_{s,r}^2, \\ \mathcal{P}_{\emptyset 2}, \ \textit{for } 1/\kappa_{s,r}^2 \le \gamma_{th} < 1/\kappa_{s,d}^2, \\ 1, \gamma_{th} \ge 1/\kappa_{s,d}^2. \end{cases} \tag{5.54}$$

Case 2: For $\kappa_{s,r}^2 \le \kappa_{s,d}^2 \le \kappa_{r,d}^2$ or $\kappa_{s,d}^2 \le \kappa_{s,r}^2 \le \kappa_{r,d}^2$,

$$\mathcal{P}_{out}^{sec}(\gamma_{th}) = \begin{cases} \mathcal{P}_{\bar{\emptyset}1} + \mathcal{P}_{\emptyset 1}, \ \textit{for } \gamma_{th} < 1/\kappa_{r,d}^2, \\ \mathcal{P}_{\emptyset 2}, \ \textit{for } 1/\kappa_{r,d}^2 \le \gamma_{th} < 1/\kappa_{s,d}^2, \\ 1, \gamma_{th} \ge 1/\kappa_{s,d}^2. \end{cases} \tag{5.55}$$

Case 3: For $\kappa_{r,d}^2 \leq \kappa_{s,r}^2 \leq \kappa_{s,d}^2$,

$$\mathcal{P}_{out}^{sec}(\gamma_{th}) = \begin{cases} \mathcal{P}_{\bar{\emptyset}1} + \mathcal{P}_{\emptyset 1}, \; for \; \gamma_{th} < 1/\kappa_{s,d}^2, \\ \mathcal{P}_{\bar{\emptyset}2} + \mathcal{P}_{\emptyset 3}, \; for \; 1/\kappa_{s,d}^2 \leq \gamma_{th} < 1/\kappa_{s,r}^2, \\ 1, \gamma_{th} \geq 1/\kappa_{s,r}^2. \end{cases} \tag{5.56}$$

Case 4: For $\kappa_{s,r}^2 \leq \kappa_{r,d}^2 \leq \kappa_{s,d}^2$,

$$\mathcal{P}_{out}^{sec}(\gamma_{th}) = \begin{cases} \mathcal{P}_{\bar{\emptyset}1} + \mathcal{P}_{\emptyset 1}, \; for \; \gamma_{th} < 1/\kappa_{s,d}^2, \\ \mathcal{P}_{\bar{\emptyset}2} + \mathcal{P}_{\emptyset 3}, \; for \; 1/\kappa_{s,d}^2 \leq \gamma_{th} < 1/\kappa_{r,d}^2, \\ 1, \gamma_{th} \geq 1/\kappa_{r,d}^2. \end{cases} \tag{5.57}$$

Proof. Please refer to Appendix I. ■

For the same hardware quality at all the nodes viz., $\kappa_{s,r}^2 = \kappa_{r,d}^2 = \kappa_{r,d}^2 = \kappa$, the $\mathcal{P}_{\mathrm{out}}^{\mathrm{sec}}(\gamma_{\mathrm{th}})$ can be obtained as

$$\mathcal{P}_{\mathrm{out}}^{\mathrm{sec}}(\gamma_{\mathrm{th}}) = \begin{cases} \mathcal{P}_{\bar{\emptyset}1} + \mathcal{P}_{\emptyset 1}, \; \text{for } \gamma_{\mathrm{th}} < 1/\kappa^2, \\ 1, \gamma_{\mathrm{th}} \geq 1/\kappa^2. \end{cases} \tag{5.58}$$

Now, based on the derived $\mathcal{P}_{\mathrm{out}}^{\mathrm{sec}}(\gamma_{\mathrm{th}})$ in (5.54)-(5.58), we discuss the important ceiling effects that can adversely affect the system's performance and prevail due to presence of HIs.

Discussion on Ceiling Effects

In this subsection, we discuss three important ceiling effects invoked due to presence of HIs and their deleterious impact on the system performance. These effects are RCC, DLC, and OSC. The RCC effect is said to occur in the system when relay ceases to cooperate the transmission of information from source to destination. This happens as a consequence to imposition of undesired constraint on γ_{th} by HIs. For better understanding, let us exemplify this by first considering the *Case 1* when $\kappa_{s,d}^2 \leq \kappa_{r,d}^2 \leq \kappa_{s,r}^2$. In $\mathcal{P}_{\mathrm{out}}^{\mathrm{sec}}(\gamma_{\mathrm{th}})$ of (5.54), the first component ($\mathcal{P}_{\bar{\emptyset}1} + \mathcal{P}_{\emptyset 1}$) accounts for the cooperation between direct and relaying links, whereas the second component ($\mathcal{P}_{\emptyset 2}$) corresponds to the transmission from direct link only. Thus, as γ_{th} exceeds $1/\kappa_{s,r}^2$, relay cooperation ceases and system has to rely on the direct link only. Importantly, direct link can partially compensate for RCC over the threshold range $1/\kappa_{s,r}^2 \leq \gamma_{\mathrm{th}} < 1/\kappa_{s,d}^2$. But once the threshold exceeds $1/\kappa_{s,d}^2$, overall system goes in outage and this phenomenon is named as OSC. Similar observations can be made from the *Case 2*, wherein the RCC occurs for $\gamma_{\text{th}} \geq 1/\kappa_{r,d}^2$. And, the direct link compensates for this RCC over the range $1/\kappa_{r,d}^2 \leq \gamma_{\text{th}} < 1/\kappa_{s,d}^2$. Considering now *Case 3*, the first component $(\mathcal{P}_{\bar{\emptyset}1} + \mathcal{P}_{\emptyset 1})$ in $\mathcal{P}_{\text{out}}^{\text{sec}}(\gamma_{\text{th}})$ accounts for the cooperation between direct and relaying links, whereas the second component $(\mathcal{P}_{\bar{\emptyset}2} + \mathcal{P}_{\emptyset 3})$ corresponds to the transmission from relaying link only. In such a case, as γ_{th} exceeds $1/\kappa_{s,d}^2$, direct link goes in outage and it is referred to as DLC. We note that, in this case, a relaying link can partially compensate for the DLC in the range $1/\kappa_{s,d}^2 \leq \gamma_{\text{th}} < 1/\kappa_{s,r}^2$ i.e., before occurrence of OSC $(\gamma_{\text{th}} \geq 1/\kappa_{s,r}^2)$. Likewise, in *Case 4*, the DLC occurs for $\gamma_{\text{th}} \geq 1/\kappa_{s,d}^2$. And, the relaying link compensates for this DLC over the threshold range $1/\kappa_{s,d}^2 \leq \gamma_{\text{th}} < 1/\kappa_{r,d}^2$ i.e., before occurrence of OSC $(\gamma_{\text{th}} \geq 1/\kappa_{r,d}^2)$. Moreover, from (5.58), we observe that for the same hardware at all the transceiver nodes, the system directly experiences the OSC effect as $\gamma_{\text{th}} \geq 1/\kappa^2$.

From the aforementioned discussion, following concluding remarks can be obtained:

- In a CMRN inflicted with HIs, the RCC effect arises when the transceiver hardware at the relay chain (either $\kappa_{s,r}$, $\kappa_{r,d}$ or both) is of inferior quality than the hardware of direct link chain $(\kappa_{s,d})$. In such cases (*Case 1* and *Case 2*), RCC effect occurs when $\gamma_{\text{th}} \geq \frac{1}{\max(\kappa_{s,r}^2, \kappa_{r,d}^2)}$. Note that the direct link can partially compensate for the incurred loss due to RCC. However, once the OSC effect occurs, system goes in outage.

- On the other hand, when the hardware of direct link chain is of low quality than the relay chain (*Case 3* and *Case 4*), the DLC effect occurs as $\gamma_{\text{th}} \geq 1/\kappa_{s,d}^2$. In such cases, relaying link plays an important role in compensating the performance loss due to DLC before γ_{th} increases to OSC threshold.

- In general, the OSC effect occurs when $\gamma_{\text{th}} \geq \frac{1}{\min(\kappa_{s,d}^2, \max(\kappa_{s,r}^2, \kappa_{r,d}^2))}$, which limits the performance of system beyond a given target rate, especially in high-rate applications.

- Based on above observations, it would be desirable to have $\min(\kappa_{s,d}^2, \max(\kappa_{s,r}^2, \kappa_{r,d}^2)) < \frac{1}{\gamma_{\text{th}}}$ while designing the practical systems for a given rate requirement. Also, for the same hardware at all the nodes, the OSC effect occurs when $\gamma_{\text{th}} \geq \frac{1}{\kappa^2}$. Therefore, when hardware quality at all the transceivers are same, it would be suggested to have $\kappa^2 < \frac{1}{\gamma_{\text{th}}}$.

5.5 AF Relaying Versus DF Relaying Against HIs

In this section, we inspect the robustness of AF relaying and DF relaying against the HIs. As disclosed in the previous section, HIs cause the ceiling effects which eventually cap the fundamental capacity of system beyond a certain target rate. For AF relaying, using (4.22), we observe that first ceiling effect, i.e., RCC, arises when $\gamma_{\text{th}} \geq \frac{1}{\kappa_{s,r}^2+\kappa_{r,d}^2+\kappa_{s,r}^2\kappa_{r,d}^2}$, while OSC occurs when $\gamma_{\text{th}} \geq \frac{1}{\kappa_{s,d}^2}$. Whereas, for DF relaying, first ceiling effect, i.e., RCC or DLC, arises when $\gamma_{\text{th}} \geq \frac{1}{\max(\kappa_{s,r}^2,\kappa_{r,d}^2)}$ or $\gamma_{\text{th}} \geq \frac{1}{\kappa_{s,d}^2}$, while OSC occurs when $\gamma_{\text{th}} \geq \frac{1}{\min(\kappa_{s,d}^2,\max(\kappa_{s,r}^2,\kappa_{r,d}^2))}$. On carefully observing these threshold limits, one can infer that DF relaying can support higher data rate than the AF relaying before any ceiling phenomenon comes into play. To further exemplify this, let us consider the instance when $\kappa_{s,r}^2 = \kappa_{r,d}^2 = \kappa_{s,d}^2 = 0.2$. For these values of HIs level, the RCC in AF relaying occurs when $\gamma_{\text{th}} \geq 12.254 \approx 11$dB. And, for DF relaying, RCC/DLC arises when $\gamma_{\text{th}} \geq 25 \approx 14$dB. Thus, it can be concluded that DF is more resilient and robust against HIs since it can support higher data rate than its AF counterpart.

5.6 Numerical and Simulation Results

In this section, numerical results for the performance of considered CMRN are presented. Monte Carlo simulations are performed for the veracity of derived analytical results. Herein, we set the several system parameters, unless otherwise specified, as $\Omega_{sd} = 1$, $\Omega_{sr} = 1$, $\Omega_{rd} = 1$, $\Omega_{cp} = 1$, $\Omega_{cd} = 0.1$, $\Omega_{cr} = 0.2$, $\Omega_{sp} = 0.1$, $\Omega_{rp} = 0.2$, $m_{sd} = 1$, $m_{sr} = 2$, $m_{rd} = 1$, $m_{cp} = 1$, $m_{cd} = 1$, $m_{cr} = 2$, $m_{sp} = 1$, $m_{rp} = 1$, $N_o = 1$, $\mathcal{R}_p = 0.5$ bps/Hz, $\mathcal{R}_s = 0.4$ bps/Hz, $B = 1$ Hz, $\xi_{\text{th}} = 0.4$. We set error variances $\sigma_{e,sp}^2 = \sigma_{e,sr}^2 = \sigma_{e,rd}^2 = \sigma_{e,rp}^2 = \sigma_e^2 = 0.01$. We also set $\kappa_{ts} = \kappa_{rd} = \kappa_{tr} = \kappa_{rr} = \kappa_o = 0.175$ such that $\kappa_{s,d} = \kappa_{r,d} = \kappa_{s,r} = \kappa = \sqrt{2}\kappa_o$.

In Fig. 5.2, we plot the outage probability curves versus primary system's outage probability threshold ξ_{th} to illustrate the impact of number of relays K on the outage performance of the secondary system. Herein, we set $P_c/N_o = 20$ dB and number of PUs $L = 1$. For effective demonstration, we ensure that γ_{th} lies below all the ceilings' threshold points. Note that the analytical curves are in well agreement with the simulation results. From the respective curves, we can clearly see that as ξ_{th} increases, the outage probability of secondary system improves. This is due to the fact that the increase in ξ_{th} allows the SUs to transmit with higher powers which

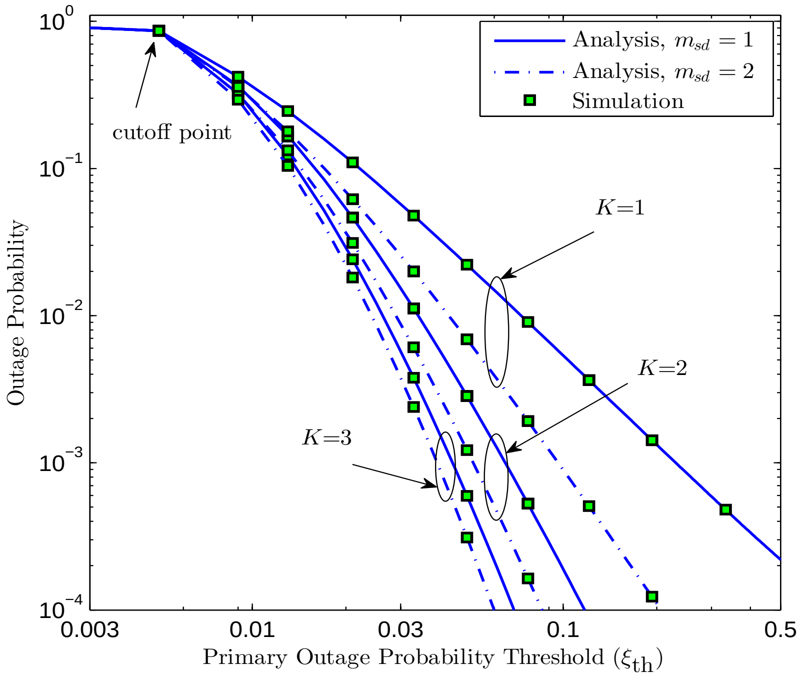

Figure 5.2: Impact of number of relays K on the outage performance of the secondary system.

eventually improves the SNDR at relay R_m and at secondary destination D, and hence, improves the performance of secondary system. Moreover, it is apparent that there exists a cutoff point below which the outage probability of secondary system is unity. It is associated with the fact that below this cutoff point, the QoS requirement of the PUs is so stringent that it would not allow the SUs to transmit. Furthermore, as expected, the performance of secondary system improves significantly with the increase in K and/or increase in fading parameter m_{sd} of the direct link.

In Fig. 5.3, we plot the outage probability curves versus P_c/N_o to depict the impact of number of PUs L and CEEs on the outage performance of secondary system. We set $K = 2$ and $m_{sd} = m_{rd} = 1$. From various curves, we observe that as the number of PUs rises, the performance of system deteriorates due to increased interference on the SUs. Moreover, there exists a cutoff point for $L = 2$ and $L = 3$ below which secondary system remains in outage. This is attributed to the more stringent QoS requirements from multiple PUs. It can also be seen that for higher P_c/N_o, system exhibits an outage floor which is primarily owing to the dominance of interference from PUs. Furthermore, the performance of system degrades with increase in CEEs as evident from various curves pertaining to different values of σ_e^2.

In Fig. 5.4, we plot the outage probability curves versus λ_Q to illustrate the

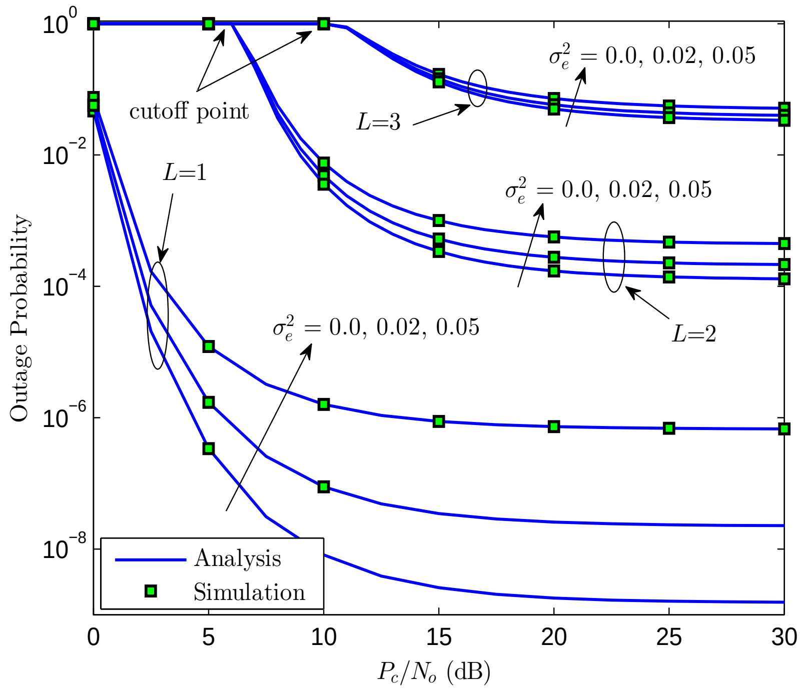

Figure 5.3: Impact of number of PUs L and CEEs on the outage performance of the secondary system.

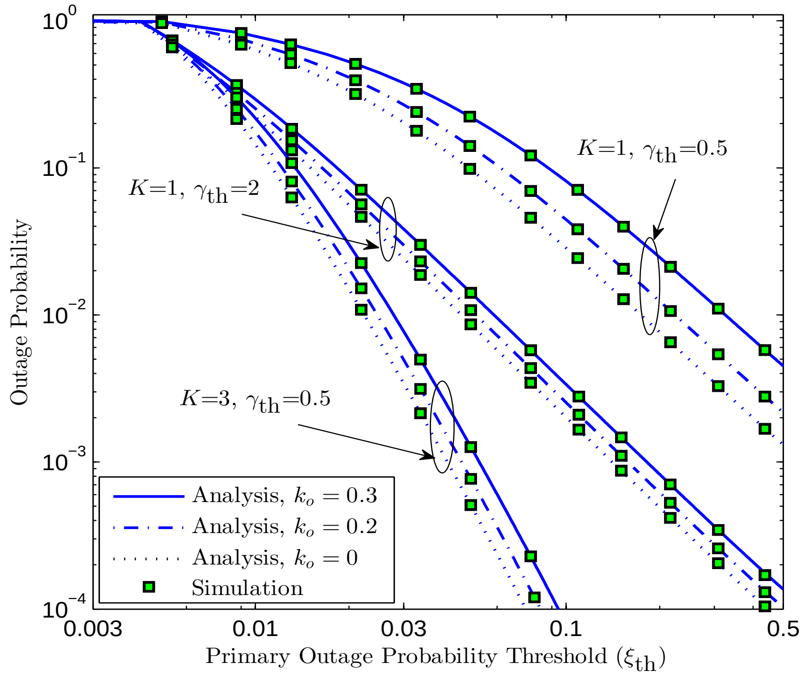

Figure 5.4: Impact of γ_{th} and HIs on the outage performance of secondary system.

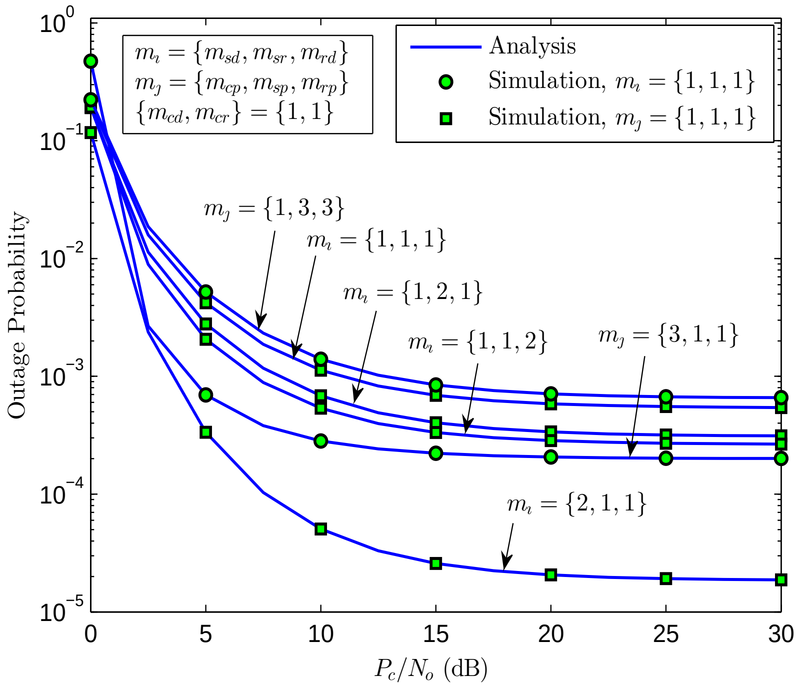

Figure 5.5: Outage performance of secondary system versus P_c for various fading severity parameters.

impact of γ_{th} and HIs on the considered CMRN. For this, we fix $L = 1$ and $P_c/N_o = 20$ dB. From the respective curves, we can clearly see that for a fixed κ_o, as γ_{th} increases, the performance of the system degrades due to high-rate requirements. Moreover, when HIs level κ_o increases, the outage performance of secondary system deteriorates significantly (see the curves corresponding to $\kappa_o = 0, 0.2, 0.3$).

In Fig. 5.5, the effect of various fading severity parameters on the performance of CMRN is depicted. As apparent from the curves, when $m_\jmath = \{1, 1, 1\}$, the outage performance improves with the increase in $m_\imath$. This is attributed to the fact that an increase in $m_\imath$ provides better channel condition for transmissions of secondary system, which eventually leads to its performance enhancement. For instance, see the corresponding curves when $m_\imath$ changes from $\{1, 1, 1\}$ to $\{1, 2, 1\}$ or $\{2, 1, 1\}$. Further, when $\{m_{sp}, m_{rp}\}$ increases from $\{1, 1\}$ to $\{3, 3\}$, the performance of system degrades. And when m_{cp} changes from 1 to 3, the performance of system improves. These two inferences are associated with the fact that when performance of primary system improves, the SUs are allowed to transmit with higher powers, which consequently improves the performance of secondary system. When $\{m_{sp}, m_{rp}\}$ increases, the interference on the primary receiver increases and hence its performance deteriorates. On the contrary, when m_{cp} increases, the channel condition for primary

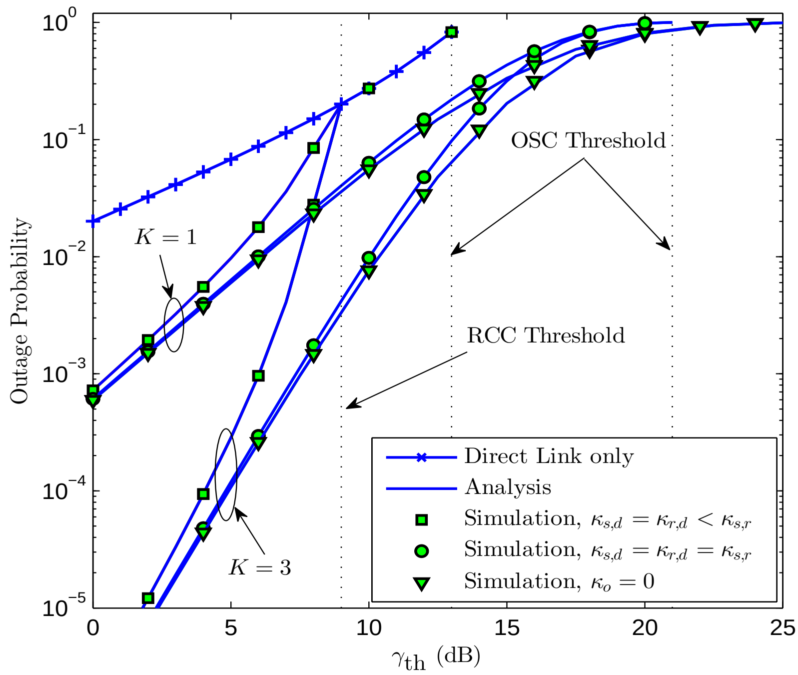

Figure 5.6: Impact of RCC and OSC on the outage performance of the secondary system.

transmission gets better and hence its performance improves.

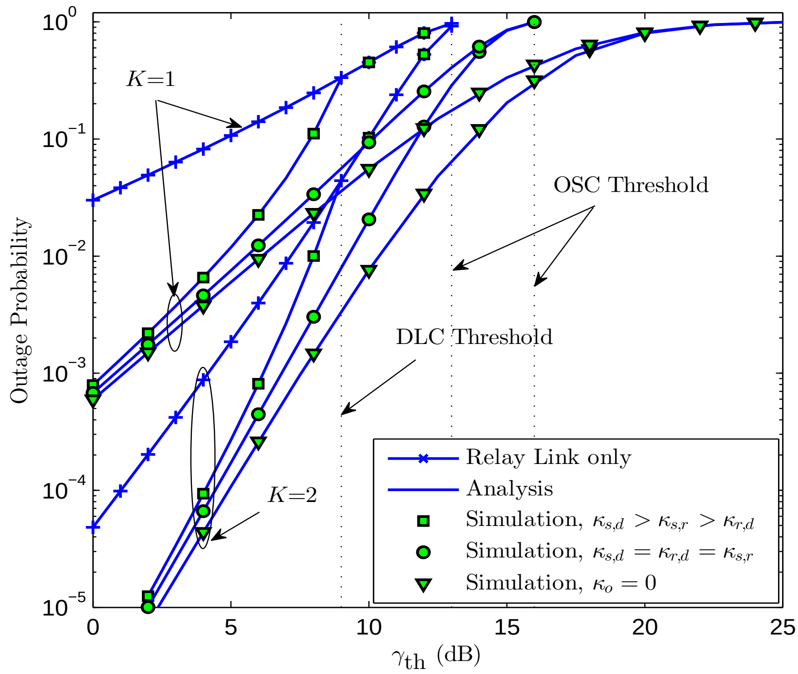

Figure 5.7: Impact of DLC and OSC on the outage performance of the secondary system.

In Fig. 5.6, we demonstrate the impact of ceiling effects RCC and OSC by plotting the outage curves against γ_{th}. For instance, if $\kappa_{s,d} = \kappa_{r,d} = 0.20, \kappa_{s,r} = 0.35$,

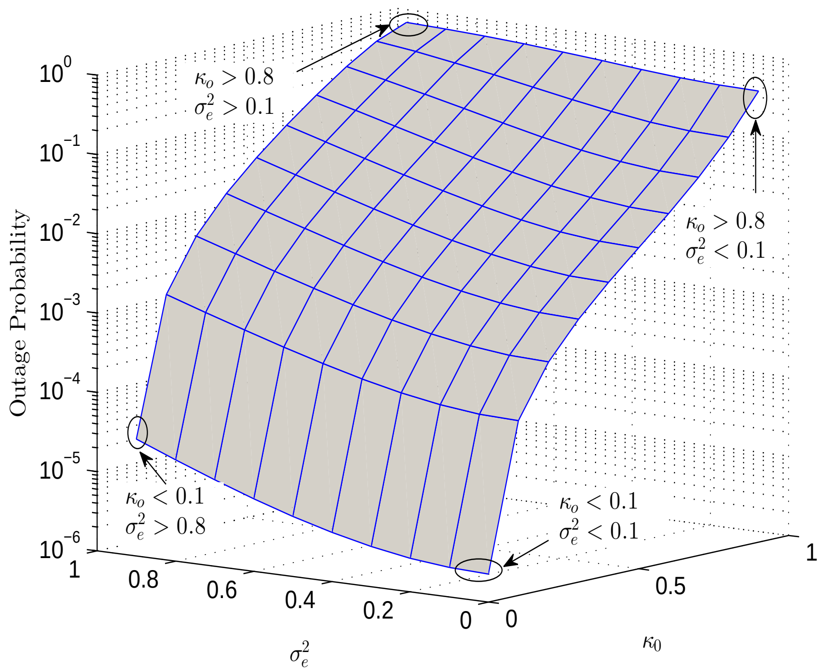

Figure 5.8: Joint impact of HIs and CEEs on the outage performance of the system.

the RCC and OSC effects occur at the threshold of ≈ 9 dB $\left(\gamma_{\text{th}} > \frac{1}{\max(\kappa_{s,r}^2, \kappa_{r,d}^2)}\right)$ and ≈ 13 dB $\left(\gamma_{\text{th}} > \frac{1}{\min(\kappa_{s,d}^2, \max(\kappa_{s,r}^2, \kappa_{r,d}^2))}\right)$, respectively. It can be manifestly observed from the curves that as γ_{th} crosses the RCC threshold, the system's performance converges to that of a pure direct link. Apparently, the direct link partially compensates for RCC (in the threshold range 9 dB $\leq \gamma_{\text{th}} <$ 13 dB) until the occurrence of OSC. Afterwards, when γ_{th} further increases to OSC threshold, the system outage probability approaches to unity. In another instance, when $\kappa_{s,d} = \kappa_{r,d} = \kappa_{s,r} = 0.08$, the OSC occurs at a threshold of ≈ 21 dB.

Similarly, the impact of DLC and OSC is illustrated in Fig. 5.7. For example, when $\kappa_{s,d} = 0.35, \kappa_{s,r} = 0.20, \kappa_{r,d} = 0.15$, the DLC and OSC effects occur at the threshold of ≈ 9 dB $\left(\gamma_{\text{th}} > \frac{1}{\kappa_{s,d}^2}\right)$ and ≈ 13 dB $\left(\gamma_{\text{th}} > \frac{1}{\min(\kappa_{s,d}^2, \max(\kappa_{s,r}^2, \kappa_{r,d}^2))}\right)$, respectively. Herein, as γ_{th} crosses the DLC threshold, the system's performance converges to that of a pure relaying link. As such, the relaying link partially compensates for DLC (in the threshold range 9 dB $\leq \gamma_{\text{th}} <$ 13 dB) until the occurrence of OSC. Thus, we can conclude that HIs are detrimental for the considered system to sustain its performance standards in high-rate applications.

In a 3-D plot of Fig. 5.8, we illustrate the joint impact of HIs and CEEs on the outage performance of considered CMRN. It can be observed that outage probability attains its minimum value i.e., $\mathcal{P}_{\text{out}}^{\text{sec}}(\gamma_{\text{th}}) = 2.25 \times 10^{-6}$, when both HIs and

CEEs are minimum ($\kappa_o < 0.1, \sigma_e^2 < 0.1$). Whereas, when both HIs and CEEs are maximum ($\kappa_o > 0.8, \sigma_e^2 > 0.8$), the $\mathcal{P}_{\text{out}}^{\text{sec}}(\gamma_{\text{th}}) = 0.9406$. From these values, it can be deduced that the combined effect of HIs and CEEs dramatically degrade the system's performance.

5.7 Summary

We investigated the performance of an underlay CMRN with direct link in the presence of HIs, CEEs, and interference from multiple PUs over Nakagami-m fading channels. Based on the derived outage expressions, we elucidated various ceiling effects viz., RCC, DLC, and OSC, which are induced in the system due to presence of HIs. It is illustrated that RCC ceases the cooperation of relaying link, DLC inhibits the direct link transmission, while the OSC causes the overall system outage. Interestingly, it is found that the direct link is essential in partially compensating for the incurred performance loss due to RCC, whereas the relaying link is useful to partially compensate for the performance loss due to DLC. Moreover, these deleterious effects predominantly affect the system, and may engender the OSC, especially when a high target rate is anticipated. Further, our results illuminated the joint impact of HIs and CEEs on the system performance. It was shown that there exists a cutoff point below which the outage probability of secondary system is unity. Such behavior is associated with the fact that below this cutoff point, the QoS requirement of the PUs is so stringent that it would not allow the SUs to transmit, driving consequently the system in outage. In addition, the increased PUs' interference and/or CEEs can lead to an outage floor. Above all, a comparative study revealed that DF relaying is more resilient and robust to HIs since it can support higher data rate than its AF counterpart.

CHAPTER 6

RF ENERGY HARVESTING IN COGNITIVE RELAY NETWORKS

Energy efficiency and spectrum efficiency are two important design objectives for future wireless networks, i.e., 5G and beyond [14]. Recently, EH has emerged as a promising technology for the design of energy-efficient systems. The key idea is to efficiently power the network nodes without having to replace the batteries periodically. This will significantly bring down the operational cost for future ultra-dense networks and IoT. As such, energy can be harvested from the surrounding environment using the various traditional sources viz., wind, solar, thermal, etc. However, EH from these conventional sources relies heavily on the different climatic conditions and, therefore, are not suitable for the incessant and ubiquitous energy supply. To this end, the simultaneous wireless information and power transfer (SWIPT) scheme has been regarded as an effective approach to scavenge the energy from the ambient RF signals [13]. The SWIPT scheme is based on the fact that energy and information can be simultaneously carried through RF signals. In this, the EH node gathers the transmitted energy (RF radiation) and stores it in a battery by converting it into the direct current (DC) using appropriate circuitry. However, it is difficult for a receiver to concurrently process the information and harvest energy from the received RF signals. For this, two practical receiver architectures viz., time-switching (TS) and power-splitting (PS), have been introduced in [129] and [130]. In the TS-based receiver architecture, time is switched between information processing (IP) and EH. While in the PS-based architecture, a part of the received power is used for the EH and the remaining one for the IP [131].

On another front, to accommodate the larger number of users in the ultra-dense networks and to interconnect various IoT devices, the efficient use of available scarce spectrum is crucial. In this context, cognitive radio technology has been envisioned as a potential candidate to dramatically improve the spectrum efficiency.

More recently, RF-EH and cognitive radio technologies have been integrated with each other for an energy and spectrum efficient system design. Various research works have incorporated the EH concept in cognitive radio networks to cater for the demands of future wireless networks. For instance, researches in [30]-[35] have focused on the use of EH techniques in underlay spectrum sharing networks. In [30], the authors proposed an EH scheme for a relay-assisted SU in spectrum sharing systems and examined its outage probability. The authors in [31] studied SWIPT for underlay cognitive radio networks, whereby statistical information for the channel of the primary link was employed in order to control the power at the secondary transmitter. In [32], Liu *et al.* proposed a new EH protocol while considering multiple primary transceivers. Three different power constraints on the SU were imposed to derive the outage probability and throughput of the system. On the other hand, in [33], the authors imposed two power constraints, i.e., primary outage constraint and peak power constraint, to control the power at the SUs. The authors in [34] analyzed the throughput of a CRN by considering a wireless powered relay. An improved TS protocol had been proposed wherein the energy was transmitted in the subslots to charge the relay node. Zhi *et al.* in [35] analyzed the outage probability of the EH-based underlay cognitive radio networks in which spatially random distributed network nodes for the performance assessment were considered. Note that, in underlay cognitive radio networks, SUs have to limit their transmit power in anticipation for the interference temperature limit stipulated by the PUs. Consequently, the performance of the secondary system is significantly affected. On the contrary, in the overlay cognitive radio, there is no such restriction over the transmit power at the SUs. In the overlay approach, spectrum sharing can be facilitated by incentivizing PUs through the cooperation of SUs [132]. In fact, the authors in [133] have compared the sum throughput of both overlay and underlay models in RF-EH networks. In such a study, they have shown that the overlay approach outperforms the underlay approach. This was primarily due to the imposition of stringent restrictions over the maximum transmit powers of the SUs in the underlay model. Owing to the potential benefits of the overlay model, some researches [36]-[41] have focused on this paradigm of spectrum sharing. For instance, the authors in [36] investigated the cooperation between primary and secondary networks in which the secondary transmitter was assumed to be an energy-constrained source that harvests energy from the primary transmission. In [37], Yin *et al.* studied the optimized cooperation strategy of the SUs to assist the PUs and to decide the EH time. The authors in [38] considered the selection of the best secondary transmitter to relay the PU's data. In [39], a PU was assumed to be an energy-constrained node which harvests energy from a SU as well as from an access point and then transfers the data using the cooperation from a SU. In a similar way, the authors in [40] considered the EH scheme at a cooperative SU node using a PU's signal as well as using a dedicated hybrid access point. In [41], the authors studied the joint power allocation and route selection to minimize the outage probability of the EH-based multihop cognitive radio networks.

Common to all the aforementioned works is that they have considered a linear EH model, i.e., the harvested energy at the node linearly varies with the received power. However, since the EH circuit consists of various non-linear elements viz., capacitors, inductors, and diodes, the conventional linear model of EH is not practical. In fact, the harvested energy should vary non-linearly with respect to the received power [134]-[138]. Motivated by the preceding discussion, in this chapter, we examine the outage performance of a non-linear EH-based multi-user overlay CRN (EHMCRN) system. Herein, a battery-enabled secondary node harvests energy from a RF signal of the PU and then utilizes this energy to relay the PU's data along with its own information. We employ a distributed user selection policy to select the best user amongst multiple PUs in an effort to extract the benefits of multiuser diversity. In the considered analytical framework, we attempt to harness the combined advantages of multiuser diversity and cooperative diversity to improve the performance of primary network. We highlight the importance of direct link for the performance of primary network in the considered system. In addition to the inherent benefit of cooperative diversity, we identify that when the cooperation from the secondary node ceases to exist beyond a certain rate, the primary network can rely on the potential direct links for its information transmission. Further, we analyze the impact of decoding primary's information at the secondary receiver on the performance of secondary network. Importantly, we propose an improved EH-based relaying scheme which makes the efficient use of available degrees of freedom and thereby enhances the performance of both primary and secondary networks significantly. For this analytical framework, we derive the expressions of outage probability for both primary and secondary networks. Numerical and simulation results are obtained to extract various useful insights and to validate our theoretical developments.

The remainder of the chapter is structured as follows. In Section 6.1, detailed descriptions of the considered EHMCRN system are presented along with discussions of the adopted EH and IP strategies. In Section 6.2, the performance of EHMCRN system is investigated by deriving the outage probability for the primary network while, in Section 6.3, the outage probability of secondary network is examined. Section 6.4 proposes an improved EH-based relaying scheme and then analyze its outage performance for both primary and secondary networks. Numerical and simulation results are provided in Section 6.5 and, finally, summary of the chapter is presented in Section 6.6.

6.1 System Descriptions

As shown in Fig. 6.1, we consider an EHMCRN system consisting of primary and secondary networks. The primary network includes a transmitter T_c and the corresponding multiple receivers $\{T_{p_n}\}_{n=1}^{N}$ while the secondary network comprises an energy-constrained transmitter S and a receiver D. Hereby, the primary transmitter T_c intends to establish a communication with one out of T_{p_n} receivers. Though the direct links are assumed to exist between T_c and T_{p_n}, the primary transmitter may still seek cooperation from the nearby secondary transmitter S to harness the benefits of diversity. As a reward for the benign cooperation towards the primary network, the secondary network gets access to primary's licensed spectrum. However, being an energy-constrained node, the secondary transmitter S first harvests energy from the received RF signal of T_c and then splits the harvested power to relay the primary data and to transmit its own data intended for its corresponding secondary receiver D. To harvest energy at the node S, we adopt a TS-based receiver architecture in which a transmission block duration is split into two time phases. The first phase is an EH phase wherein S harvests energy using the received signal from T_c and then utilizes this energy for broadcasting the combined signal (primary and secondary data) in the second phase. The second phase is further subdivided into two IP phases to realize the overall communication between T_c &

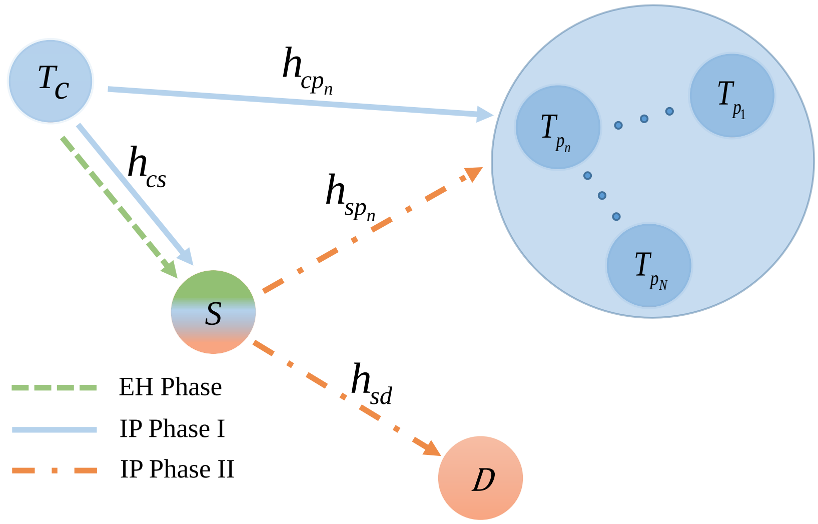

Figure 6.1: System model for EHMCRN.

T_{p_n} and S & D. The EH and IP will be discussed in detail in the subsequent subsections. In the considered analytical framework, we assume that all the network nodes are half-duplex and single-antenna devices. We also assume that all the channels follow the block fading so that they remain constant for a block duration (EH and IP phases) but changes independently in the next block transmission. Thermal noise at each receiver is modeled as AWGN variable with $\mathcal{CN}(0, \sigma^2)$. We denote the channel coefficients for the links $T_c - T_{p_n}$, $T_c - S$, $S - T_{p_n}$, and $S - D$ as h_{cp_n}, h_{cs}, h_{sp_n}, and h_{sd}, respectively. Further, we assume that all the channel coefficients experience Rayleigh flat fading such that the channel gains $|h_{\imath\jmath}|^2$ follow exponential distribution, where $\imath \in \{c, s\}$, $\jmath \in \{s, p_n, d\}$, and $\imath \neq \jmath$. We also assume that multiple links over the same hop are independent and identically distributed by considering a cluster-based placement of multiple nodes. The channels h_{cp_n}, h_{cs}, h_{sp_n}, and h_{sd} have average powers Ω_{cp}, Ω_{cs}, Ω_{sp}, and Ω_{sd}, respectively. In general, the CDF and the PDF for an exponentially distributed random variable W with mean $\Omega_{\imath\jmath}$ are given by $F_W(w) = 1 - \exp\left(-\frac{w}{\Omega_{\imath\jmath}}\right)$ and $f_W(w) = \frac{1}{\Omega_{\imath\jmath}}\exp\left(-\frac{w}{\Omega_{\imath\jmath}}\right)$, respectively, where $w \geq 0$.

EH Architecture

In the secondary network, the source S is an energy-constrained node and is equipped with a rechargeable battery. As shown in Fig. 6.2, the node S employs a harvest-then-transmit strategy. More specifically, we adopt a TS approach for the EH procedure [130] wherein a transmission block of duration T is split into two time phases i.e., αT and $(1-\alpha)T$. Here, α represents the fraction of time for which the node

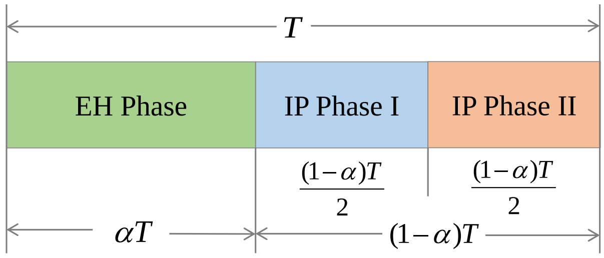

Figure 6.2: An illustration for TS-based EH.

S harvests the energy, with $0 < \alpha < 1$. In the first phase, S harvests energy from the RF signal transmitted by T_c for a duration of αT. In the second phase, the remaining $(1-\alpha)T$ is utilized for the IP and signaling which is further subdivided into two equal phases. To harvest energy, two EH models have been studied in the literature i.e., linear [130] and non-linear [134]. As the EH circuit, in general, comprises various non-linear electronic devices, the traditional linear model may not comprehend the actual harvested energy and, therefore, the non-linear model of EH is deemed more practical. In fact, as we shall observe later in Section VI, the linear model may provide very misleading results for the design of future networks. However, dealing with the accurate non-linear model is rather complex for analytical purposes. Consequently, we hereby adopt a simplified non-linear model [135]-[138] which closely follows the true behavior of the practical EH circuits. Following this, the transmit power at node S can be expressed as

$$P_{H,s} = \begin{cases} \frac{2\eta\alpha P_{E,R}}{1-\alpha}, & \text{if } P_c|h_{cs}|^2 \leq \zeta_{\text{th}}, \\ \frac{2\eta\alpha\zeta_{\text{th}}}{1-\alpha}, & \text{if } P_c|h_{cs}|^2 > \zeta_{\text{th}}, \end{cases} \tag{6.1}$$

where $P_{E,R} = P_c|h_{cs}|^2$, $0 < \eta \leq 1$ is the energy conversion efficiency, P_c is the transmit power at the node T_c, and ζ_{th} is the saturation threshold. In (6.1), the linear term ($P_{H,s} \propto P_{E,R}$) stands for the linear-regime operation of the RF-DC (direct current) conversion curves of the EH circuit, whereas, the constant term corresponds to the saturation-regime operation.

Information Processing

After the EH phase, the overall communication in the considered EHMCRN system takes place in two IP phases. In the first IP phase, the primary transmitter T_c transmits its unit energy symbol x_c, such that $\mathbb{E}\{|x_c|^2\} = 1$, to T_{p_n} and to the cooperative secondary node S. Consequently, the signals received at T_{p_n} and S can be expressed, respectively, as

$$y_{p_n,1} = \sqrt{P_c} h_{cp_n} x_c + n_{p_n,1} \tag{6.2}$$

$$\text{and} \quad y_{s,1} = \sqrt{P_c} h_{cs} x_c + n_{s,1}, \tag{6.3}$$

where $n_{p_n,1}$ and $n_{s,1}$ denote AWGN terms at T_{p_n} and S, respectively. As such, the resulting SNR at T_{p_n} via direct link in the first phase can be written, using (6.2), as

$$\Lambda_{p_n,1} = \frac{P_c |h_{cp_n}|^2}{\sigma^2}. \tag{6.4}$$

In the second IP phase, the node S superimposes the received primary signal along with its own information symbol x_s to obtain a combined signal as $x_{c,s} = \mathcal{G} y_{s,1} + \sqrt{(1-\xi) P_{H,s}} x_s$, where $\mathcal{G} = \sqrt{\frac{\xi P_{H,s}}{P_c |h_{cs}|^2 + \sigma^2}} \approx \sqrt{\frac{\xi P_{H,s}}{P_c |h_{cs}|^2}}$ [139]. This approximation is found to yield tight results over the entire SNR regime. Note that the secondary cooperative node S utilizes a fraction of the harvested power, denoted by $\xi P_{H,s}$, to transmit the primary's data and the remaining $(1-\xi)P_{H,s}$ for its own transmission, where $\xi \in [0,1]$ is referred to as a spectrum sharing factor since it facilitates the spectrum sharing between PUs and SUs. Consequently, after the second IP phase, the received signals at nodes T_{p_n} and D can be expressed, respectively, as

$$y_{p_n,2} = h_{sp_n} \left(\mathcal{G} y_{s,1} + \sqrt{(1-\xi) P_{H,s}} x_s \right) + n_{p_n,2} \tag{6.5}$$

$$\text{and} \quad y_{d,2} = h_{sd} \left(\mathcal{G} y_{s,1} + \sqrt{(1-\xi) P_{H,s}} x_s \right) + n_{d,2}, \tag{6.6}$$

where $n_{p_n,2}$ and $n_{d,2}$ denote AWGN terms at T_{p_n} and D, respectively, in the second IP phase. On substituting $\mathcal{G}$ along with $y_{s,1}$ from (6.3) in (6.5), the resulting SNR at node T_{p_n}, after the second phase, can be written as

$$\Lambda_{p_n,2} = \frac{\xi P_{H,s} P_c |h_{cs}|^2 |h_{sp_n}|^2}{\xi P_{H,s} |h_{sp_n}|^2 \sigma^2 + (1-\xi) P_{H,s} P_c |h_{cs}|^2 |h_{sp_n}|^2 + P_c |h_{cs}|^2 \sigma^2}. \tag{6.7}$$

Similarly, the SNR at D, after the second phase, can be expressed as

$$\Lambda_{d,2} = \frac{(1-\xi) P_{H,s} P_c |h_{cs}|^2 |h_{sd}|^2}{\xi P_{H,s} P_c |h_{cs}|^2 |h_{sd}|^2 + \xi P_{H,s} |h_{sd}|^2 \sigma^2 + P_c |h_{cs}|^2 \sigma^2}. \tag{6.8}$$

Best User Selection Policy

As discussed, the primary transmitter T_c intends to establish a communication link with one out of T_{p_n} receivers. As such, the best user amongst multiple N receivers can be opportunistically selected as

$$n^* = \arg \max_{n=1,\ldots,N} (\Lambda_{p_n,1}). \tag{6.9}$$

Herein, we assume that the user selection process is executed using distributed timer technique [141] based on the CSI of the direct links.
In the subsequent sections, we present the performance analysis for the primary and secondary networks.

6.2 Performance Analysis of Primary Network

In this section, we assess the performance of the primary network in the considered EHMCRN system.

Outage Probability

The primary system is said to be in outage if the instantaneous SNR at T_{p_n} falls below a fixed target rate $r_{\rm th}$. As such, the outage probability, with the application of selection combining, can be formulated as

$$\mathcal{P}_{\rm out}^{\rm Pri}(\gamma_{\rm th}) = \Pr\left[\max\left(\max_n(\Lambda_{p_n,1}), \Lambda_{p_{n^*},2}\right) < \gamma_{\rm th}\right], \tag{6.10}$$

where $\gamma_{\rm th} = 2^{\frac{2r_{\rm th}}{1-\alpha}} - 1$. Since the direct links and relaying links are independent, the outage expression in (6.10) can be reformulated as

$$\mathcal{P}_{\rm out}^{\rm Pri}(\gamma_{\rm th}) = \underbrace{\Pr\left[\max_n(\Lambda_{p_n,1}) < \gamma_{\rm th}\right]}_{\mathcal{P}_1} \underbrace{\Pr\left[\Lambda_{p_{n^*},2} < \gamma_{\rm th}\right]}_{\mathcal{P}_2}, \tag{6.11}$$

where the probability term $\mathcal{P}_1$ can be obtained as

$$\begin{aligned}\mathcal{P}_1 &= \prod_{n=1}^{N} \Pr\left[\Lambda_{p_n,1} < \gamma_{\rm th}\right] \\ &= \sum_{a=0}^{N} \binom{N}{a} (-1)^a \exp\left(-\frac{a\gamma_{\rm th}}{\varrho\Omega_{cp}}\right),\end{aligned} \tag{6.12}$$

with $\varrho = \frac{P_c}{\sigma^2}$. By utilizing the concepts of total probability theorem [118], the other probability term $\mathcal{P}_2$ in (6.11) can be obtained, using (6.7), as

$$\begin{aligned}\mathcal{P}_2 &= \Pr[\Lambda_{p_{n^*},2} < \gamma_{\rm th}] \\ &= \sum_{n=1}^{N} \Pr[n^* = n] \Pr\left[\frac{\xi P_{H,s}\varrho|h_{cs}|^2|h_{sp_n}|^2}{\xi P_{H,s}|h_{sp_n}|^2 + (1-\xi)P_{H,s}\varrho|h_{cs}|^2|h_{sp_n}|^2 + P_c|h_{cs}|^2} < \gamma_{\rm th}\right].\end{aligned} \tag{6.13}$$

On substituting $P_{H,s}$ from (6.1) into (6.13), we can express $\mathcal{P}_2$ as

$$\mathcal{P}_2 = \sum_{n=1}^{N} \Pr[n^* = n] \Bigg\{ \underbrace{\Pr\left[\frac{\xi\varrho|h_{cs}|^2|h_{sp_n}|^2}{\xi|h_{sp_n}|^2+(1-\xi)\varrho|h_{cs}|^2|h_{sp_n}|^2+\frac{1-\alpha}{2\eta\alpha}} < \gamma_{\rm th},\ P_c|h_{cs}|^2 \le \zeta_{\rm th}\right]}_{\mathcal{P}_{21}}$$

$$+ \underbrace{\Pr\left[\frac{\xi\varrho|h_{cs}|^2|h_{sp_n}|^2}{\xi|h_{sp_n}|^2+(1-\xi)\varrho|h_{cs}|^2|h_{sp_n}|^2+\frac{1-\alpha}{2\eta\alpha\zeta_{\rm th}}P_c|h_{cs}|^2} < \gamma_{\rm th},\ P_c|h_{cs}|^2 > \zeta_{\rm th}\right]}_{\mathcal{P}_{22}} \Bigg\}. \tag{6.14}$$

Hereby, firstly, $\mathcal{P}_{21}$ in (6.14) is derived in the following lemma.

Lemma 12. *The probability $\mathcal{P}_{21}$ in (6.14) can be expressed as*

$$\mathcal{P}_{21} = \begin{cases} 1-\exp\left(\frac{-\zeta_{th}}{P_c\Omega_{cs}}\right), & \textit{for } \gamma_{th} \ge \frac{\xi}{1-\xi}, \\ 1-\exp\left(\frac{-\zeta_{th}}{P_c\Omega_{cs}}\right), & \textit{for } \gamma_{th} < \frac{\xi}{1-\xi}\ \&\ \frac{\zeta_{th}}{P_c} \le \frac{\xi\gamma_{th}}{\mathcal{B}}, \\ \Psi(\gamma_{th}), & \textit{for } \gamma_{th} < \frac{\xi}{1-\xi}\ \&\ \frac{\zeta_{th}}{P_c} > \frac{\xi\gamma_{th}}{\mathcal{B}}, \end{cases} \tag{6.15}$$

where $\Psi(\gamma_{th})$ is given by

$$\Psi(\gamma_{th}) = \sum_{\ell=0}^{1}(-1)^{\ell}\exp\left(\frac{-\ell\xi\gamma_{th}}{\mathcal{B}\Omega_{cs}}\right) + \exp\left(\frac{-\gamma_{th}\xi}{\mathcal{B}\Omega_{cs}}\right) - \exp\left(\frac{-\zeta_{th}}{P_c\Omega_{cs}}\right) - \sum_{k=0}^{\infty}\frac{(-1)^k}{k!}$$
$$\times \exp\left(\frac{-\psi}{2}\right)\left(\frac{\mathcal{A}}{\mathcal{B}\Omega_{cs}\Omega_{sp}}\right)^{k+1}\exp\left(\frac{-\gamma_{th}\xi}{\mathcal{B}\Omega_{cs}}\right)\psi^{-\frac{k+2}{2}}\mathcal{W}_{-\frac{k+2}{2},-\frac{k+1}{2}}(\psi), \tag{6.16}$$

with $\mathcal{A} = \frac{\gamma_{th}(1-\alpha)}{2\eta\alpha}$, $\mathcal{B} = (\xi - \gamma_{th}(1-\xi))\varrho$, and $\psi = \mathcal{A}/\Omega_{sp}\left(\frac{\mathcal{B}\zeta_{th}}{P_c} - \gamma_{th}\xi\right)$.

Proof. See Appendix J. ■

Following the same lines of derivation used for obtaining $\mathcal{P}_{21}$, we can derive $\mathcal{P}_{22}$ in (6.14) as

$$\mathcal{P}_{22} = \begin{cases} \exp\left(\frac{-\zeta_{\rm th}}{P_c\Omega_{cs}}\right), & \text{for } \gamma_{\rm th} \ge \frac{\xi}{1-\xi}, \\ \mathcal{I}_1 + \Phi(\gamma_{\rm th}), & \text{for } \gamma_{\rm th} < \frac{\xi}{1-\xi}\ \&\ \frac{\zeta_{\rm th}}{P_c} < \frac{\xi\gamma_{\rm th}}{\mathcal{B}}, \\ \Phi(\gamma_{\rm th}), & \text{for } \gamma_{\rm th} < \frac{\xi}{1-\xi}\ \&\ \frac{\zeta_{\rm th}}{P_c} \ge \frac{\xi\gamma_{\rm th}}{\mathcal{B}}, \end{cases} \tag{6.17}$$

where $\mathcal{I}_1 = \exp\left(\frac{-\zeta_{\rm th}}{P_c\Omega_{cs}}\right) - \exp\left(\frac{-\xi\gamma_{\rm th}}{\mathcal{B}\Omega_{cs}}\right)$ and $\Phi(\gamma_{\rm th})$ is given by

$$\Phi(\gamma_{\rm th}) = \exp\left(\frac{-1}{\Omega_{cs}}\max\left(\frac{\xi\gamma_{\rm th}}{\mathcal{B}}, \frac{\zeta_{\rm th}}{P_c}\right)\right) - \sum_{m=0}^{\infty}\frac{(-1)^m}{m!}\left(\frac{1}{\mathcal{B}\Omega_{cs}}\right)^m \exp\left(\frac{-\mathcal{A}P_c}{\mathcal{B}\zeta_{\rm th}\Omega_{sp}} - \frac{\gamma_{\rm th}\xi}{\mathcal{B}\Omega_{cs}}\right)$$
$$\times \left(\frac{\gamma_{\rm th}\xi\mathcal{A}P_c}{\mathcal{B}\Omega_{sp}\zeta_{\rm th}}\right)^m \left(\frac{\phi}{\mathcal{B}\Omega_{cs}}\right)^{-\frac{m}{2}} \exp\left(\frac{-\phi}{2\mathcal{B}\Omega_{cs}}\right)\mathcal{W}_{-\frac{m}{2},\frac{1-m}{2}}\left(\frac{\phi}{\mathcal{B}\Omega_{cs}}\right), \tag{6.18}$$

with $\phi = \mathcal{B}\max\left(\frac{\xi\gamma_{\text{th}}}{\mathcal{B}}, \frac{\zeta_{\text{th}}}{P_c}\right)$. Next, the probability $\Pr[n^* = n]$ in (6.14) can be obtained as [142]

$$\Pr[n^* = n] = \Pr\left[\bigcap_{\substack{m=1\\m\neq n}}^{N}(\Lambda_{p_n,1} > \Lambda_{p_m,1})\right] = \int_0^\infty \prod_{\substack{m=1\\m\neq n}}^{N} \Pr\left[\Lambda_{p_m,1} < y\right] f_{\Lambda_{p_n,1}}(y)dy$$
$$= \sum_{b=0}^{N-1}\binom{N-1}{b}\frac{N(-1)^b}{(b+1)}. \tag{6.19}$$

On substituting (6.19) in (6.14) and the resultant expression along with (6.12) in (6.11), we can obtain the outage probability of primary network as

$$\mathcal{P}_{\text{out}}^{\text{Pri}}(\gamma_{\text{th}}) = \sum_{a=0}^{N}\sum_{b=0}^{N-1}\binom{N}{a}\binom{N-1}{b}\frac{N(-1)^{a+b}}{(b+1)}\exp\left(-\frac{a\gamma_{\text{th}}}{\varrho\Omega_{cp}}\right)(\mathcal{P}_{21}+\mathcal{P}_{22}), \tag{6.20}$$

where $\mathcal{P}_{21}$ and $\mathcal{P}_{22}$ are given in (6.15) and (6.17), respectively.

Remarks: From (6.15) and (6.17), it can be observed that, for the condition $\gamma_{\text{th}} \geq \frac{\xi}{1-\xi}$, the cooperative transmission via secondary node ceases to exist, since $\mathcal{P}_{21} + \mathcal{P}_{22}$ becomes unity. Nevertheless, the primary network still has the availability of potential direct links to carry out the information transmission. From this observation, it is worth remarking that the value of spectrum sharing factor ξ is crucial and should be appropriately chosen for harnessing the benefits of cooperative diversity.

6.3 Performance Analysis of Secondary Network

In this section, we assess the performance of the secondary network in the considered EHMCRN system. Hereby, we consider two different cases i.e., when the SU node D is either able or unable to successfully decode the PU's signal received in the first IP phase.

When SU is unable to decode the PU's signal

Firstly, we consider the case when secondary node D is unable to decode the PU's signal in the first IP phase.

Outage Probability

The outage probability of secondary network in the considered EHMCRN system can be formulated, using (6.8), as

$$\mathcal{P}_{\text{out}}^{\text{Sec}}(\gamma_{\text{th}}) = \Pr[\Lambda_{d,2} < \gamma_{\text{th}}] = \left[\frac{(1-\xi)\varrho P_{H,s}|h_{cs}|^2|h_{sd}|^2}{\xi\varrho P_{H,s}|h_{cs}|^2|h_{sd}|^2 + \xi P_{H,s}|h_{sd}|^2 + P_c|h_{cs}|^2} < \gamma_{\text{th}}\right]. \tag{6.21}$$

On invoking $P_{H,s}$ from (6.1) in (6.21), we obtain

$$\mathcal{P}_{\text{out}}^{\text{Sec}}(\gamma_{\text{th}}) = \underbrace{\Pr\left[\frac{(1-\xi)\varrho XZ}{\xi Z + \xi\varrho XZ + \frac{1-\alpha}{2\eta\alpha}} < \gamma_{\text{th}},\ X \leq \frac{\zeta_{\text{th}}}{P_c}\right]}_{\mathcal{S}_1}$$
$$+ \underbrace{\Pr\left[\frac{(1-\xi)\varrho XZ}{\xi Z + \xi\varrho XZ + \frac{1-\alpha}{2\eta\alpha\zeta_{\text{th}}}P_c X} < \gamma_{\text{th}},\ X > \frac{\zeta_{\text{th}}}{P_c}\right]}_{\mathcal{S}_2}, \tag{6.22}$$

where $X = |h_{cs}|^2, Z = |h_{sd}|^2$. Hereby, $\mathcal{S}_1$ can be re-expressed as

$$\mathcal{S}_1 = \Pr\left[Z < \frac{\mathcal{A}}{\mathcal{C}X - \xi\gamma_{\text{th}}},\ X \leq \frac{\zeta_{\text{th}}}{P_c}\right], \tag{6.23}$$

with $\mathcal{C} = ((1-\xi) - \gamma_{\text{th}}\xi)\varrho$. Further, based on the limits of γ_{th}, (6.23) is obtained as

$$\mathcal{S}_1 = \begin{cases} 1 - \exp\left(\frac{-\zeta_{\text{th}}}{P_c\Omega_{cs}}\right), & \text{for } \gamma_{\text{th}} \geq \frac{\xi}{1-\xi}, \\ 1 - \exp\left(\frac{-\zeta_{\text{th}}}{P_c\Omega_{cs}}\right), & \text{for } \gamma_{\text{th}} < \frac{\xi}{1-\xi}\ \&\ \frac{\zeta_{\text{th}}}{P_c} \leq \frac{\xi\gamma_{\text{th}}}{\mathcal{B}}, \\ \Xi(\gamma_{\text{th}}), & \text{for } \gamma_{\text{th}} < \frac{\xi}{1-\xi}\ \&\ \frac{\zeta_{\text{th}}}{P_c} > \frac{\xi\gamma_{\text{th}}}{\mathcal{B}}, \end{cases} \tag{6.24}$$

where $\Xi(\gamma_{\text{th}})$ can be evaluated as

$$\Xi(\gamma_{\text{th}}) = \int_{x=0}^{\frac{\xi\gamma_{\text{th}}}{\mathcal{C}}} f_X(x)dx + \int_{x=\frac{\xi\gamma_{\text{th}}}{\mathcal{C}}}^{\frac{\zeta_{\text{th}}}{P_c}} F_Z\left(\frac{\mathcal{A}}{\mathcal{C}x - \gamma_{\text{th}}\xi}\right) f_X(x)dx. \tag{6.25}$$

After computing the involved integration in (6.25), one can obtain $\Xi(\gamma_{\text{th}})$ as

$$\Xi(\gamma_{\text{th}}) = \sum_{p=0}^{1}(-1)^p \exp\left(\frac{-p\xi\gamma_{\text{th}}}{\mathcal{C}\Omega_{cs}}\right) + \exp\left(\frac{-\gamma_{\text{th}}\xi}{\mathcal{C}\Omega_{cs}}\right) - \exp\left(\frac{-\zeta_{\text{th}}}{P_c\Omega_{cs}}\right) - \sum_{q=0}^{\infty}\frac{(-1)^q}{q!}$$
$$\times \left(\frac{\mathcal{A}}{\mathcal{C}\Omega_{cs}\Omega_{sd}}\right)^{q+1} \exp\left(\frac{-\gamma_{\text{th}}\xi}{\mathcal{C}\Omega_{cs}}\right) \varphi^{-\frac{q+2}{2}} \exp\left(\frac{-\varphi}{2}\right) \mathcal{W}_{-\frac{q+2}{2}, -\frac{q+1}{2}}(\varphi), \tag{6.26}$$

with $\varphi = \mathcal{A}/\Omega_{sd}\left(\frac{\mathcal{C}\zeta_{\text{th}}}{P_c} - \gamma_{\text{th}}\xi\right)$. In a similar way, $\mathcal{S}_2$ can be obtained as

$$\mathcal{S}_2 = \begin{cases} \exp\left(\frac{-\zeta_{\text{th}}}{P_c\Omega_{cs}}\right), & \text{for } \gamma_{\text{th}} \geq \frac{\xi}{1-\xi}, \\ \mathcal{I}_1 + \Theta(\gamma_{\text{th}}), & \text{for } \gamma_{\text{th}} < \frac{\xi}{1-\xi}\ \&\ \frac{\zeta_{\text{th}}}{P_c} < \frac{\xi\gamma_{\text{th}}}{\mathcal{C}}, \\ \Theta(\gamma_{\text{th}}), & \text{for } \gamma_{\text{th}} < \frac{\xi}{1-\xi}\ \&\ \frac{\zeta_{\text{th}}}{P_c} \geq \frac{\xi\gamma_{\text{th}}}{\mathcal{C}}, \end{cases} \tag{6.27}$$

where $\Theta(\gamma_{\text{th}})$ is given by

$$\Theta(\gamma_{\text{th}}) = \exp\left(\frac{-\chi}{\mathcal{C}\Omega_{cs}}\right) - \sum_{r=0}^{\infty} \frac{(-1)^r}{r!} \left(\frac{1}{\mathcal{C}\Omega_{cs}}\right)^r \left(\frac{\chi}{\mathcal{C}\Omega_{cs}}\right)^{-\frac{r}{2}} \exp\left(\frac{-\mathcal{A}P_c}{\mathcal{C}\zeta_{\text{th}}\Omega_{sd}} - \frac{\gamma_{\text{th}}\xi}{\mathcal{C}\Omega_{cs}}\right)$$
$$\times \left(\frac{\gamma_{\text{th}}\xi\mathcal{A}P_c}{\mathcal{C}\Omega_{sd}\zeta_{\text{th}}}\right)^r \exp\left(\frac{-\chi}{2\mathcal{C}\Omega_{cs}}\right) \mathcal{W}_{-\frac{r}{2},\frac{1-r}{2}}\left(\frac{\chi}{\mathcal{C}\Omega_{cs}}\right), \tag{6.28}$$

with $\chi = \mathcal{C}\max\left(\frac{\xi\gamma_{\text{th}}}{\mathcal{C}}, \frac{\zeta_{\text{th}}}{P_c}\right)$. Substituting the expressions from (6.24) and (6.27) in (6.22), one can obtain the outage probability of the secondary network. By carefully observing $\mathcal{S}_1$ and $\mathcal{S}_2$, one can note that $\mathcal{P}_{\text{out}}^{\text{Sec}}(\gamma_{\text{th}})$ becomes unity for $\gamma_{\text{th}} \geq \frac{\xi}{1-\xi}$. Thus, the values of spectrum sharing factor ξ should be judiciously chosen to avoid the outage of secondary network.

When SU is able to decode the PU's signal

Next, we consider the case when the SU node D can successfully decode the PU's signal in the first phase. Consequently, D can eliminate the interference from primary signal in the second IP phase. With this, the resultant SNR at D, in the second IP phase, can be expressed as

$$\Lambda_{d,2}^{d} = \frac{(1-\xi)P_{H,s}\varrho|h_{cs}|^2|h_{sd}|^2}{\xi P_{H,s}|h_{sd}|^2 + P_c|h_{cs}|^2}. \tag{6.29}$$

Outage Probability

The outage probability for this case can be formulated, using (6.29), as

$$\mathcal{P}_{\text{out},d}^{\text{Sec}}(\gamma_{\text{th}}) = \Pr[\Lambda_{d,2}^{d} < \gamma_{\text{th}}] = \left[\frac{(1-\xi)\varrho P_{H,s}|h_{cs}|^2|h_{sd}|^2}{\xi P_{H,s}|h_{sd}|^2 + P_c|h_{cs}|^2} < \gamma_{\text{th}}\right]. \tag{6.30}$$

On substituting $P_{H,s}$ from (6.1) in (6.30), we obtain

$$\mathcal{P}_{\text{out},d}^{\text{Sec}}(\gamma_{\text{th}}) = \underbrace{\Pr\left[\frac{(1-\xi)\varrho XZ}{\xi Z + \frac{1-\alpha}{2\eta\alpha}} < \gamma_{\text{th}},\ X \leq \frac{\zeta_{\text{th}}}{P_c}\right]}_{\mathcal{D}_1}$$
$$+ \underbrace{\Pr\left[\frac{(1-\xi)\varrho XZ}{\xi Z + \frac{1-\alpha}{2\eta\alpha\zeta_{\text{th}}}P_c X} < \gamma_{\text{th}},\ X > \frac{\zeta_{\text{th}}}{P_c}\right]}_{\mathcal{D}_2}. \tag{6.31}$$

Hereby, $\mathcal{D}_1$ can be obtained as

$$\mathcal{D}_1 = \begin{cases} 1 - \exp\left(\frac{-\zeta_{\text{th}}}{P_c\Omega_{cs}}\right), & \text{for } \frac{\zeta_{\text{th}}}{P_c} \leq \frac{\xi\gamma_{\text{th}}}{(1-\xi)\varrho}, \\ \Upsilon(\gamma_{\text{th}}), & \text{for } \frac{\zeta_{\text{th}}}{P_c} > \frac{\xi\gamma_{\text{th}}}{(1-\xi)\varrho}, \end{cases} \tag{6.32}$$

where $\Upsilon(\gamma_{\text{th}})$ is given by

$$\Upsilon(\gamma_{\text{th}}) = \sum_{t=0}^{1}(-1)^t \exp\left(\frac{-t\zeta_{\text{th}}}{P_c\Omega_{cs}}\right) - \sum_{u=0}^{\infty}\frac{(-1)^u}{u!}\left(\frac{\mathcal{A}}{\mathcal{Q}\Omega_{sd}}\right)^{-\frac{u+2}{2}}\left(\frac{\mathcal{A}}{(1-\xi)\varrho\Omega_{cs}\Omega_{sd}}\right)^{u+1}$$
$$\times \exp\left(\frac{-\gamma_{\text{th}}\xi}{(1-\xi)\varrho\Omega_{cs}}\right)\exp\left(\frac{-\mathcal{A}}{2\mathcal{Q}\Omega_{sd}}\right)\mathcal{W}_{-\frac{u+2}{2},-\frac{u+1}{2}}\left(\frac{\mathcal{A}}{\mathcal{Q}\Omega_{sd}}\right), \tag{6.33}$$

with $\mathcal{Q} = \frac{(1-\xi)\varrho\zeta_{\text{th}}}{P_c} - \gamma_{\text{th}}\xi$. Similarly, $\mathcal{D}_2$ in (6.22) can be obtained as

$$\mathcal{D}_2 = \begin{cases} \mathcal{I}_2 + \mathcal{Z}(\gamma_{\text{th}}), & \text{for } \frac{\zeta_{\text{th}}}{P_c} < \frac{\xi\gamma_{\text{th}}}{(1-\xi)\varrho}, \\ \mathcal{Z}(\gamma_{\text{th}}), & \text{for } \frac{\zeta_{\text{th}}}{P_c} \geq \frac{\xi\gamma_{\text{th}}}{(1-\xi)\varrho}, \end{cases} \tag{6.34}$$

where $\mathcal{I}_2 = \exp\left(\frac{-\zeta_{\text{th}}}{P_c\Omega_{cs}}\right) - \exp\left(\frac{-\xi\gamma_{\text{th}}}{(1-\xi)\varrho\Omega_{cs}}\right)$ and $\mathcal{Z}(\gamma_{\text{th}})$ is given by

$$\mathcal{Z}(\gamma_{\text{th}}) = \exp\left(\frac{-\mathcal{F}}{\Omega_{cs}}\right) - \sum_{v=0}^{\infty}\frac{1}{v!}\exp\left(\frac{-\mathcal{A}P_c}{(1-\xi)\varrho\zeta_{\text{th}}\Omega_{sd}} - \frac{\gamma_{\text{th}}\xi}{(1-\xi)\varrho\Omega_{cs}} - \frac{\mathcal{F}}{2\Omega_{cs}}\right)$$
$$\times\left(\frac{-1}{(1-\xi)\varrho\Omega_{cs}}\right)^v\left(\frac{\mathcal{F}}{\Omega_{cs}}\right)^{-\frac{v}{2}}\left(\frac{\gamma_{\text{th}}\xi\mathcal{A}P_c}{(1-\xi)\varrho\Omega_{sd}\zeta_{\text{th}}}\right)^v\mathcal{W}_{-\frac{v}{2},\frac{1-v}{2}}\left(\frac{\mathcal{F}}{\Omega_{cs}}\right), \tag{6.35}$$

with $\mathcal{F} = \max\left(\frac{\xi\gamma_{\text{th}}}{(1-\xi)\varrho}, \frac{\zeta_{\text{th}}}{P_c}\right)$. Substituting the expressions from (6.32) and (6.34) in (6.31), one can obtain the outage probability of the secondary network. It is worth remarking that, unlike the previous case, the constraint on the spectrum sharing factor ξ is relaxed when SU node is able to decode the PU's signal. Thus, it can be inferred that when the SU node has the ability to successfully decode the PU's signal, the performance of secondary system can be significantly improved as we shall observe later in Section 6.5 through the numerical results.

6.4 An Improved Energy Harvesting-Based Relaying Scheme

In this section, we propose another relaying scheme for overlay spectrum sharing systems which improves the performance of both primary and secondary networks compared with the conventional fixed relaying scheme. In this scheme, the primary network invokes the relaying cooperation only when its direct transmission fails. Specifically, the first phase is dedicated for EH at the cooperative SU and for the information transfer of the PU. In particular, S harvests energy from the RF signal transmitted by T_c for a duration of αT and simultaneously T_c also transmits its information to its intended receiver T_{p_n}. Depending on the success/failure of the direct primary's transmission ($T_c \to T_{p_n}$), the relaying transmission is invoked. Thus, the mutual information of the direct primary transmission can be given as

$$\mathcal{I}_{cp_n} = \alpha \log_2 (1 + \Lambda_{p_n,1}). \tag{6.36}$$

If T_{p_n} is able to successfully decode the information signal from T_c, i.e., if $\mathcal{I}_{cp_n} > r_{\text{th}}$, it sends an error-free one-bit feedback[1] to the cooperative node S indicating that the relaying cooperation is not needed. For this case, the remaining $(1-\alpha)T$ period is utilized for the information transmission of $S \to D$, as shown in Fig. 6.3. As such, the received signal at T_{p_n}, after the IP phase I, is as given in (6.2). On the other hand, the signal received at D, after the IP phase II, can be written as

$$y_{d,2}^{\text{IR}} = h_{sd}\sqrt{P_{H,s}^{\text{IR}}} x_s + n_{d,2}, \tag{6.37}$$

where $P_{H,s}^{\text{IR}}$ is the harvested power at the node S. Based on (6.37), the corresponding SNR at D is given by

$$\Lambda_{d,2}^{\text{IR}} = \frac{P_{H,s}^{\text{IR}}|h_{sd}|^2}{\sigma^2}. \tag{6.38}$$

It is important to note here that node S can utilize all the harvested power for its information transfer which is in contrast to the fixed relaying protocol wherein S has to split the total harvested power for the transmission of primary's information as well. Hereby, the transmitted power $P_{H,s}^{\text{IR}}$ at S can be expressed as

$$P_{H,s}^{\text{IR}} = \begin{cases} \frac{\eta\alpha P_c|h_{cs}|^2}{1-\alpha}, & \text{if } P_c|h_{cs}|^2 \le \zeta_{\text{th}}, \\ \frac{\eta\alpha\zeta_{\text{th}}}{1-\alpha}, & \text{if } P_c|h_{cs}|^2 > \zeta_{\text{th}}. \end{cases} \tag{6.39}$$

On the other hand, if T_{p_n} is unable to decode the signal from T_c in the first phase, i.e., if $\mathcal{I}_{cp_n} < r_{\text{th}}$, it sends a negative feedback to T_c and S. Consequently, the relaying cooperation is invoked and further information exchange operation will remain the same as of fixed relaying. For this case, the remaining $(1-\alpha)T$ period is subdivided into two equal IP phases of duration $\frac{(1-\alpha)T}{2}$ each, as shown in Fig. 6.4.

In the following sections, we assess the performance of primary and secondary networks for the proposed improved relaying protocol.

[1]Hereby, it is assumed that the feedback/acknowledge time is negligible compared to the information processing time [111].

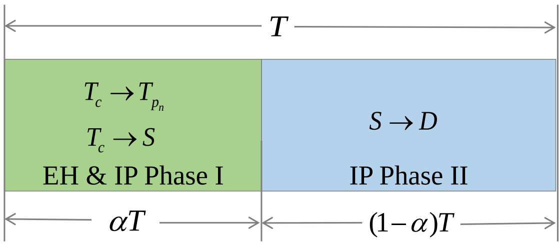

Figure 6.3: Time frame for successful primary's direct transmission.

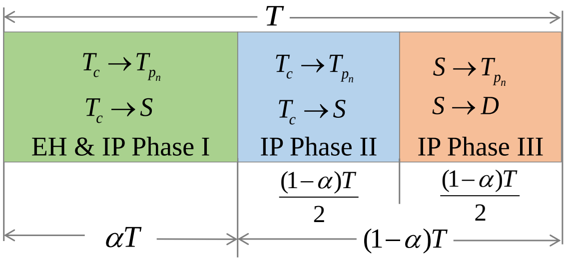

Figure 6.4: Time frame for unsuccessful primary's direct transmission.

6.4.1 Outage Probability of Primary Network

The outage probability of the primary network for the proposed relaying scheme can be formulated as

$$\begin{aligned}\mathcal{P}_{\text{out}}^{\text{Pri,IR}}(\gamma_{\text{th}}) &= \Pr\left[\max\left(\max_n(\Lambda_{p_n,1}), \Lambda_{p_{n^*},2}\right) < \gamma_{\text{th}}, \max_n(\Lambda_{p_n,1}) < \gamma_{\text{th}}^{\text{IR}}\right] \\ &= \Pr\left[\max_n(\Lambda_{p_n,1}) < \gamma_{\text{th}}, \Lambda_{p_{n^*},2} < \gamma_{\text{th}}, \max_n(\Lambda_{p_n,1}) < \gamma_{\text{th}}^{\text{IR}}\right] \\ &= \Pr\left[\max_n(\Lambda_{p_n,1}) < \min\left(\gamma_{\text{th}}, \gamma_{\text{th}}^{\text{IR}}\right), \Lambda_{p_{n^*},2} < \gamma_{\text{th}}\right], \end{aligned} \tag{6.40}$$

where $\gamma_{\text{th}}^{\text{IR}} = 2^{\frac{r_{\text{th}}}{\alpha}} - 1$. Owing to the independence between the two events in (6.40), we can express

$$\mathcal{P}_{\text{out}}^{\text{Pri,IR}}(\gamma_{\text{th}}) = \underbrace{\Pr\left[\max_n(\Lambda_{p_n,1}) < \min\left(\gamma_{\text{th}}, \gamma_{\text{th}}^{\text{IR}}\right)\right]}_{\mathcal{P}_1^{\text{IR}}} \underbrace{\Pr\left[\Lambda_{p_{n^*},2} < \gamma_{\text{th}}\right]}_{\mathcal{P}_2}, \tag{6.41}$$

where $\mathcal{P}_1^{\text{IR}}$ can be readily obtained by replacing γ_{th} with $\min\left(\gamma_{\text{th}}, \gamma_{\text{th}}^{\text{IR}}\right)$ in (6.12) and $\mathcal{P}_2$ is the same as obtained in (6.13).

6.4.2 Outage Probability of Secondary Network

The outage probability of secondary network for the proposed improved relaying scheme in the considered EHMCRN system can be formulated as

$$\mathcal{P}_{\text{out}}^{\text{Sec,IR}}(\gamma_{\text{th}}) = \underbrace{\Pr\left[\Lambda_{d,2}^{d} < \gamma_{\text{th}}, \max_{n}(\Lambda_{p_n,1}) < \gamma_{\text{th}}^{\text{IR}}\right]}_{\mathcal{L}_1} + \underbrace{\Pr\left[\Lambda_{d,2}^{\text{IR}} < \hat{\gamma}_{\text{th}}, \max_{n}(\Lambda_{p_n,1}) \geq \gamma_{\text{th}}^{\text{IR}}\right]}_{\mathcal{L}_2}, \tag{6.42}$$

where $\hat{\gamma}_{\text{th}} = 2^{\frac{r_{\text{th}}}{1-\alpha}} - 1$. In (6.42), the term $\mathcal{L}_1$ accounts for the case when the direct primary transmission is not successful while the other term $\mathcal{L}_2$ captures the event when direct primary transmission is successful. At first, we re-express $\mathcal{L}_1$ to obtain

$$\mathcal{L}_1 = \underbrace{\Pr\left[\Lambda_{d,2}^{d} < \gamma_{\text{th}}\right]}_{\mathcal{L}_{11}} \underbrace{\Pr\left[\max_{n}(\Lambda_{p_n,1}) < \gamma_{\text{th}}^{\text{IR}}\right]}_{\mathcal{L}_{12}}. \tag{6.43}$$

It is worth noting that $\mathcal{L}_{11}$ is given by (6.30) while $\mathcal{L}_{12}$ can be readily obtained by replacing γ_{th} with $\gamma_{\text{th}}^{\text{IR}}$ in (6.12). Next, $\mathcal{L}_2$ in (6.42) can be expressed, due to underlying independence, as

$$\mathcal{L}_2 = \underbrace{\Pr\left[\Lambda_{d,2}^{\text{IR}} < \hat{\gamma}_{\text{th}}\right]}_{\mathcal{L}_{21}} \underbrace{\Pr\left[\max_{n}(\Lambda_{p_n,1}) \geq \gamma_{\text{th}}^{\text{IR}}\right]}_{\mathcal{L}_{22}}, \tag{6.44}$$

where $\mathcal{L}_{21}$ can be written, using (6.38), as

$$\mathcal{L}_{21} = \Pr\left[\frac{P_{H,s}^{\text{IR}}|h_{sd}|^2}{\sigma^2} < \hat{\gamma}_{\text{th}}\right]. \tag{6.45}$$

On substituting $P_{H,s}^{\text{IR}}$ from (6.39) in (6.45) and after performing various manipulations, we obtain $\mathcal{L}_{21}$ as

$$\begin{aligned}\mathcal{L}_{21} = &\sum_{w=0}^{1}(-1)^{w}\exp\left(\frac{-2w\hat{\gamma}_{\text{th}}\mathcal{A}\sigma^2}{\gamma_{\text{th}}\Omega_{sd}\zeta_{\text{th}}} - \frac{w\zeta_{\text{th}}}{P_c\Omega_{cs}}\right) - \sum_{\nu=0}^{\infty}\frac{(-1)^{\nu}}{\nu!}\left(\frac{2\hat{\gamma}_{\text{th}}\mathcal{A}\sigma^2}{\gamma_{\text{th}}\Omega_{sd}\zeta_{\text{th}}}\right)^{-\frac{\nu+2}{2}} \\ &\times\left(\frac{2\hat{\gamma}_{\text{th}}\mathcal{A}}{\gamma_{\text{th}}\varrho\Omega_{cs}\Omega_{sd}}\right)^{\nu+1}\exp\left(\frac{-\hat{\gamma}_{\text{th}}\mathcal{A}\sigma^2}{\gamma_{\text{th}}\zeta_{\text{th}}\Omega_{sd}}\right)\mathcal{W}_{-\frac{u+2}{2},-\frac{u+1}{2}}\left(\frac{2\hat{\gamma}_{\text{th}}\mathcal{A}\sigma^2}{\hat{\gamma}_{\text{th}}\zeta_{\text{th}}\Omega_{sd}}\right).\end{aligned} \tag{6.46}$$

The other probability term $\mathcal{L}_{22}$ in (6.44) can be obtained as $\mathcal{L}_{22} = \left[\exp\left(-\frac{\gamma_{\text{th}}^{\text{IR}}}{\varrho\Omega_{cp}}\right)\right]^{N}$. Finally, substituting (6.43) and (6.44) in (6.42), we can obtain the outage probability for the secondary network.

Remarks: The proposed improved relaying scheme has two main advantages: 1) This scheme makes the efficient use of available degrees of freedom and thereby improves the performance of primary network significantly. 2) When primary network does not invoke relaying cooperation, the secondary node can exploit all the harvested power for its own information transmission and eventually the performance of secondary improves substantially.

6.5 Numerical and Simulation Results

In this section, representative numerical results for the performance of considered EHMCRN system are presented. Monte Carlo simulations are performed to corroborate the derived expressions. All the analytical curves are drawn after truncating the infinite series up to the initial seven terms to achieve a sufficient level of accuracy. Herein, we set several system parameters, unless otherwise specified, as $\Omega_{\imath\jmath} = 1$, $T = 1$ sec, $\zeta_{\text{th}} = 0$ dB, $r_{\text{th}} = 0.01$, and $\sigma^2 = 1$.

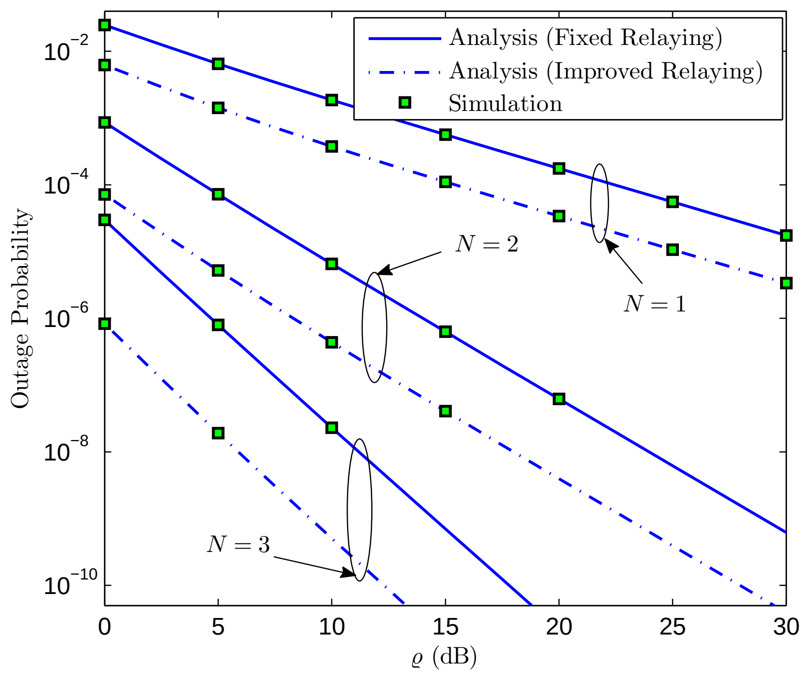

Figure 6.5: Outage probability curves of primary network for various N.

In Fig. 6.5, we plot the outage probability curves of primary network against ϱ for varying number of PUs N. For this, we set $\alpha = 0.6$, $\eta = 0.1$, and $\xi = 0.2$. It can be clearly seen that the performance of primary network improves drastically as N increases. This performance improvement can be attributed to the exploitation of multiuser diversity gain. Further, we have also shown that the proposed improved relaying scheme delivers significantly better performance as compared with the conventional fixed relaying scheme as it makes the efficient use of available degrees of freedom for the information transmission.

In Fig. 6.6, we plot the outage probability curves of primary network against ϱ for different values of energy conversion efficiency η. It can be observed that the

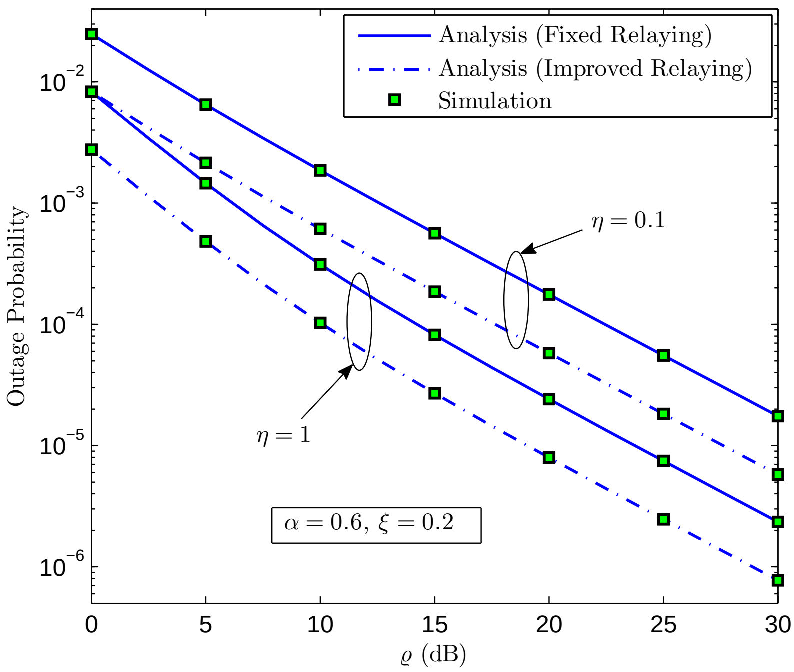

Figure 6.6: Outage probability curves of primary network for different η.

performance of primary network improves with increase in η, since higher η renders more harvested power at the cooperative secondary node. And this effect remains the same for both the considered relaying schemes.

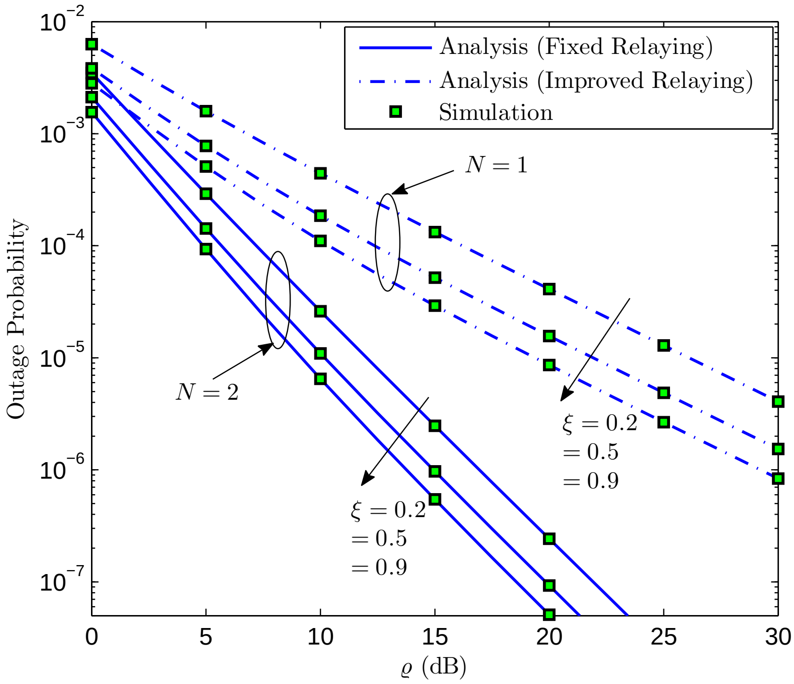

Figure 6.7: Outage probability curves of primary network for various ξ.

In Fig. 6.7, we analyze the impact of spectrum sharing factor ξ on the performance of primary network by plotting the outage probability curves against ϱ. For the curves, we set $\alpha = 0.6$ and $\eta = 0.2$. From the plots, it can be observed that as ξ increases the performance of primary network improves for both the relaying schemes (see the curves corresponding to $N = 1$ for improved relaying and $N = 2$ for fixed relaying). This is due to the fact that higher values of ξ allocate more power for the primary transmission and hence results in better performance.

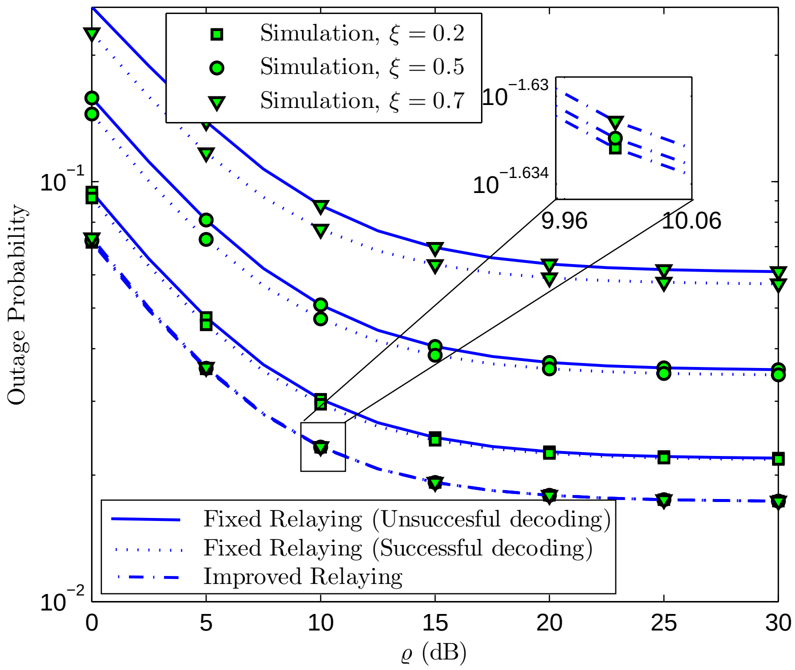

Figure 6.8: Outage probability curves of secondary network for various ξ.

In Fig. 6.8, we plot the outage probability curves of the secondary network against ϱ and assuming $\alpha = 0.5$ and $\eta = 0.8$. Herein, we compare the performance of three different scenarios viz., when SU is unsuccessful in decoding the PU's signal, when SU is successful in decoding the PU's signal, and for the proposed improved relaying. As shown in the curves, when SU is able to decode the PU's signal, the performance of secondary network gets better since the SU can remove the interference of primary's signal. It can also be observed that the proposed improved relaying scheme performs substantially better than the other two cases of fixed relaying scheme. It can be seen from the various curves that the outage performance degrades with the increase in ξ, which is in contrast to the performance of primary network. As such, this is due to low power allocation towards the secondary transmission at high ξ. Note that the increase in ξ has nominal effect on the performance of the improved relaying scheme.

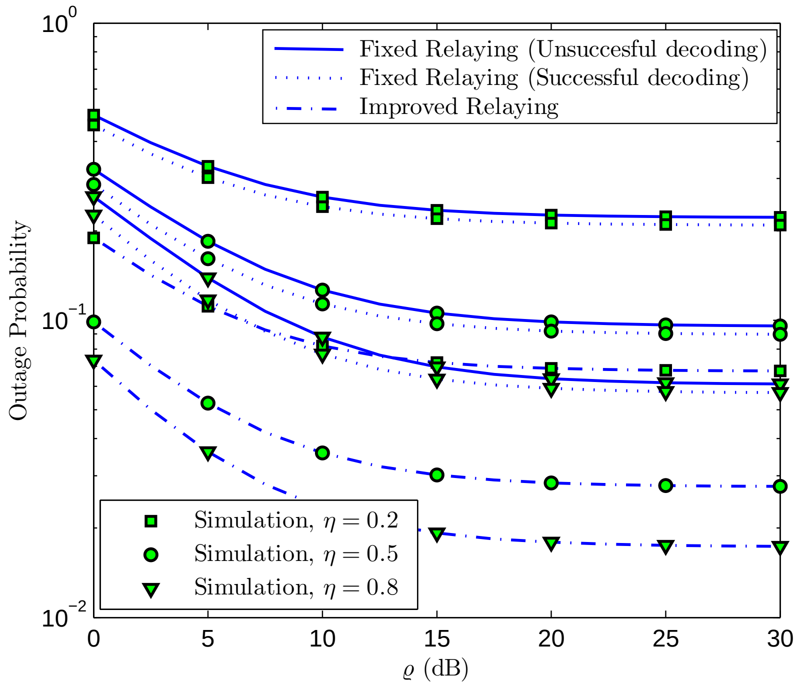

Figure 6.9: Outage probability curves of secondary network for various η.

In Fig. 6.9, we plot the outage probability curves of secondary network against ϱ for different values of energy conversion efficiency η and by setting $\alpha = 0.5$ and $\xi = 0.7$. From the corresponding curves, it can be observed that the performance of secondary network improves with an increase in η. This is associated with the fact that higher η implies more harvested power at the cooperative secondary node and thus better performance.

Lastly, in Fig. 6.10 and Fig. 6.11, we demonstrate a comparison between the conventional linear model and considered non-linear model of EH for primary and secondary networks, respectively. Here, we obtain the numerical results for the linear EH model using the simulations. Clearly, there exists a significant performance gap between these two models for both primary and secondary networks. In particular, it can be observed that the performance gap between the two models becomes wider with an increase in the ϱ, showing that the linear model is accurate only in the low power regions. In addition, it can also be witnessed that as the saturation threshold ζ_{th} increases, the performance of non-linear model converges towards the performance of linear model. For instance, see the curves corresponding to $\zeta_{\text{th}} = -5$ dB and $\zeta_{\text{th}} = 5$ dB. Though impractical, the conventional model of EH gives a better performance. From this observation, it can be concluded that the conventional linear model of EH is not appropriate to provide the useful results.

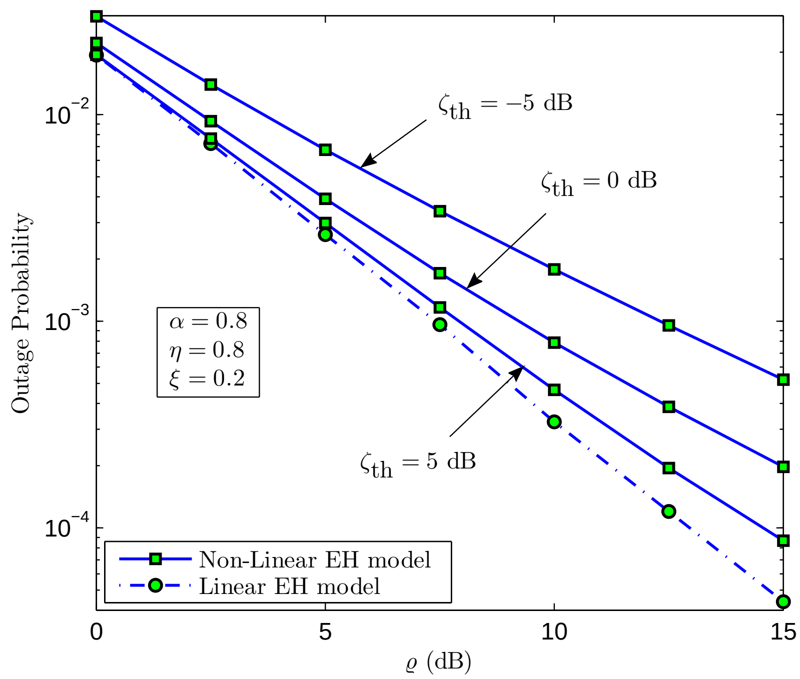

Figure 6.10: Performance comparison between linear and non-linear EH models for primary network.

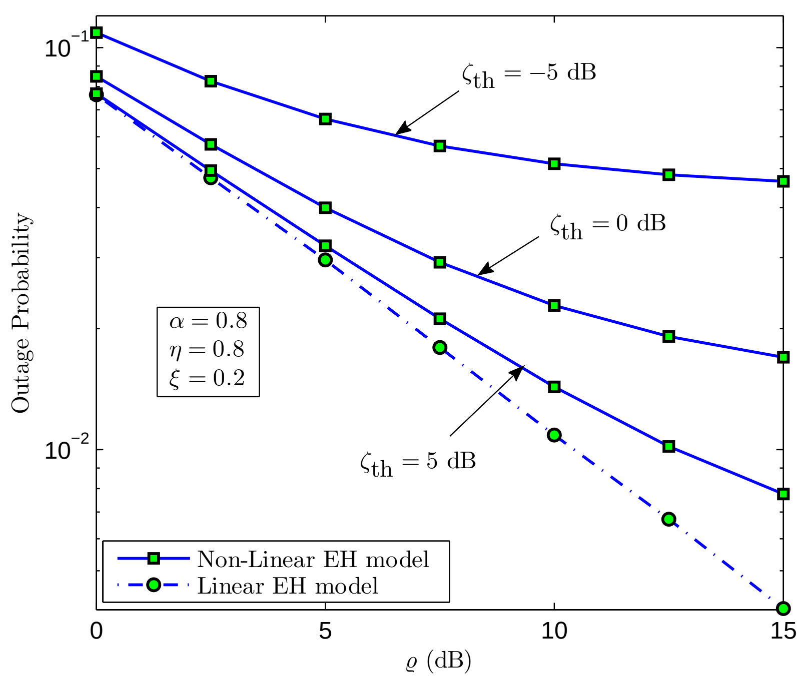

Figure 6.11: Performance comparison between linear and non-linear EH models for secondary network.

Finally, from Figs. 6.5-6.11, note that all the analytical curves are in perfect agreement with the simulation results. This validates the accuracy of all the derived expressions.

6.6 Summary

In this chapter, we have examined the outage performance of a non-linear EHMCRN system over Rayleigh fading channels. Specifically, an energy-constrained SU node has been assumed to cooperate with the PU's transmission while simultaneously transmitting its own information. We have considered a non-linear EH model which relies on the TS-based receiver architecture. We have shown that the spectrum sharing factor should be judiciously chosen to avoid the outage of secondary network. In addition, it has also been reported that the direct link can be quite useful for significantly enhancing the performance of primary network. Furthermore, we have proposed an improved relaying scheme which has been shown to substantially enhance the performance of both primary and secondary networks as compared to conventional fixed relaying. In particular, the proposed scheme has made the efficient use of available degrees of freedom to improvise the performance of primary network. On the other hand, when primary network did not invoke the cooperation, the secondary node got to utilize all the harvested power for its own information transmission which eventually enhanced the performance of secondary network considerably. We have also concluded that the conventional linear model of EH can provide very misleading results for the deployment of future networks.

CHAPTER 7

CONCLUSIONS AND FUTURE WORKS

In this chapter, we present the conclusions derived from the work in this thesis and provide the possible directions for the future works.

7.1 Conclusions

This thesis presented a comprehensive performance analysis of the CRNs with spectral- and energy-efficient schemes. The primary objective of the thesis was to provide various system designs for the future networks which can efficiently utilize the precious spectrum and energy resources. Firstly, we have explored the possibility of resource sharing for the two-way CRNs and investigated its performance to offer various design insights. Specifically, our study showed that, leveraging two-way relaying for primary communications, the proposed system design offers higher spectral efficiency. In addition, it is found that by exploiting the multi-user cooperation, reliability of SU communication is significantly improved. Further, we examined the performance of two-way CRNs with direct link in the presence of PU's interference. We studied an efficient scheme that can exploit both direct and relay links with appropriate diversity combining methods to improve the performance of SUs. Our results revealed that the full diversity for secondary system can be achieved as long as the primary interference remains limited, otherwise the performance remarkably deteriorates. We also studied an incremental relaying scheme and found that it outperforms fixed relaying scheme and hence could be a promising candidate for deployment in future wireless systems. Further, we analyzed the impact of hardware and channel imperfections on the performance of CRNs. In this analysis, we highlighted the detrimental impact of the HIs on the system's performance and eventually provided useful insights into the endurable level of HIs for designing the practical systems. We highlighted the importance of both direct link and relaying link in CRN with HIs. Specifically, we manifested that direct link is essential in partially compensating for the incurred performance loss due to RCC whereas relaying link is useful to partially compensate the performance loss due to DLC. In addition, the increased PUs' interference and/or CEEs can lead to an outage floor. We also compared the robustness of AF and DF relaying schemes against the HIs and found that DF relaying is more resilient to HIs and, therefore, preferable when the nodes are impaired. Lastly, we investigated the performance of a non-linear EH-based multiuser CRN in which an energy-constrained secondary node acts as a cooperative relay to assist the transmission of PU. We also proposed an improved EH-based relaying scheme which makes the efficient use of available degrees of freedom and thereby enhances the performance of both primary and secondary networks significantly. In this study, it has been reported that the direct link can be quite useful for significantly enhancing the performance of primary network. We have shown that the spectrum sharing factor should be judiciously chosen to avoid the outage of secondary network in the considered CRN. From this study, we have concluded that the conventional linear model of EH can provide very misleading results for the deployment of future networks.

In essence, we have comprehensively investigated the performance of CRNs to offer useful insights into the practical design. We have proposed various schemes and strategies which can improve the spectral efficiency, energy efficiency, and reliability of the CRNs and eventually facilitate their deployment for the next-generation wireless systems.

7.2 Future Works

The work in this thesis opens up various research problems that can be further explored. Some future prospects for the research work are given in the sequel.

Since spectrum efficiency (SE) and energy efficiency (EE) are key objectives for the future networks, their analysis has gained significant research attention. Though SE gives an idea about how efficiently a given spectrum band is utilized, it does not account for how efficiently power is consumed. Unfortunately, optimizing SE and EE cannot go hand-in-hand and may even conflict sometimes. Therefore, study of an existing trade-off between SE and EE is worth pursuing in context of CRNs.

To further increase the spectral efficiency and throughput of the CRNs, exploiting multiple-input-multiple-output (MIMO) technology can be viewed as an important direction. In MIMO systems, multiple antennas are employed at the transceiver nodes to provide the high data rate. Moreover, non-orthogonal multiple access (NOMA) capabilities can be incorporated with concepts of CRNs for a more spectral-efficient system design, since both NOMA and CRNs target efficient spectrum utilization. In NOMA, spectrum sharing is facilitated among multiple users by adjusting the power levels at different users. Hence, NOMA-enabled CRNs could offer an intelligent spectrum sharing in a constructive way to enhance the spectrum utilization.

In addition, due to coexistence of PUs and SUs together, the CRNs are susceptible to security threats. Consequently, it would be important and interesting to develop the strategies for the physical layer security of the CRNs. Dealing with the security breaches is of paramount importance and also one of the main challenges for designing the 5G networks.

Besides, in this thesis work, the impact of HIs and CEEs was analyzed for the underlay CRN. One can also perform this investigation for the overlay CRN. Further, one can also study the resource allocation in the CRNs based on the optimization of the performance metric. For instance, it would be interesting and challenging to find an optimal value of time switching factor α for the EHCRN. Moreover, studying the beamforming techniques to power the energy-constrained nodes would also be an interesting direction for future work.

With the above mentioned prospects, the existing body of knowledge in the design of CRNs can be further expanded.

APPENDIX A

DERIVATION OF (3.19)

The probability $\mathcal{P}_{\mathrm{MRC}}^{\mathrm{FR}}(\gamma_{\mathrm{th}})$ in (3.13) can be expressed using the SINRs from (3.3), (3.4), and (3.8) as

$$\mathcal{P}_{\mathrm{MRC}}^{\mathrm{FR}}(\gamma_{\mathrm{th}})=\Pr\Big[\lambda_Q^{ap}\frac{g_{ab}}{X}+\lambda_Q^{rp}\frac{g_{rb}}{X}<\gamma_{\mathrm{th}},\lambda_Q^{ap}\frac{g_{ar}}{Y}\geq\gamma_{\mathrm{th}},\lambda_Q^{bp}\frac{g_{br}}{Y}<\gamma_{\mathrm{th}}\Big]. \tag{A.1}$$

As the exact evaluation of (A.1) is cumbersome due to underlying dependence, we can simplify this as [22]

$$\mathcal{P}_{\mathrm{MRC}}^{\mathrm{FR}}(\gamma_{\mathrm{th}})\approx\int_0^\infty\int_0^\infty\Bigg[F_{g_{ab}|X}\left(\frac{\gamma_{\mathrm{th}}x}{\lambda_Q^{ap}}\right)F_{g_{rb}|X}\left(\frac{1}{2}\frac{\gamma_{\mathrm{th}}x}{\lambda_Q^{rp}}\right)+F_{g_{ab}|X}\left(\frac{1}{2}\frac{\gamma_{\mathrm{th}}x}{\lambda_Q^{ap}}\right)F_{g_{rb}|X}\left(\frac{\gamma_{\mathrm{th}}x}{\lambda_Q^{rp}}\right)$$
$$-F_{g_{ab}|X}\left(\frac{1}{2}\frac{\gamma_{\mathrm{th}}x}{\lambda_Q^{ap}}\right)F_{g_{rb}|X}\left(\frac{1}{2}\frac{\gamma_{\mathrm{th}}x}{\lambda_Q^{rp}}\right)\Bigg]\overline{F}_{g_{ar}|Y}\left(\frac{\gamma_{\mathrm{th}}y}{\lambda_Q^{ap}}\right)F_{g_{br}|Y}\left(\frac{\gamma_{\mathrm{th}}y}{\lambda_Q^{bp}}\right)f_X(x)f_Y(y)dxdy, \tag{A.2}$$

where $\overline{F}_{g_{ar}|Y}(\cdot)=1-F_{g_{ar}|Y}(\cdot)$. Further, by realizing the symmetry of the three terms inside the square brackets in (A.2), we define a function $\Xi(\alpha,\beta;\gamma_{\mathrm{th}})$ as

$$\Xi(\alpha,\beta;\gamma_{\mathrm{th}})=\overbrace{\int_0^\infty F_{g_{ab}|X}\left(\alpha\frac{\gamma_{\mathrm{th}}x}{\lambda_Q^{ap}}\right)F_{g_{rb}|X}\left(\beta\frac{\gamma_{\mathrm{th}}x}{\lambda_Q^{rp}}\right)f_X(x)dx}^{\Theta(\alpha,\beta;\gamma_{\mathrm{th}})}$$
$$\times\int_0^\infty\overline{F}_{g_{ar}|Y}\left(\frac{\gamma_{\mathrm{th}}y}{\lambda_Q^{ap}}\right)F_{g_{br}|Y}\left(\frac{\gamma_{\mathrm{th}}y}{\lambda_Q^{bp}}\right)f_Y(y)dy, \tag{A.3}$$

with

$$\Theta(\alpha,\beta;\gamma_{\mathrm{th}})=\int_1^\infty\sum_{n=0}^{m_{cb}-1}\mathcal{C}_n^{m_{cb}-1}\frac{(-1)^{m_{cb}-n-1}e^{\frac{m_{cb}}{\Omega_{cb}\lambda_c}}}{\Gamma(m_{cb})\Gamma(m_{ab})\Gamma(m_{rb})}\left(\frac{m_{cb}}{\Omega_{cb}\lambda_c}\right)^{m_{cb}}$$
$$\times\Upsilon\left(m_{ab},\frac{\alpha m_{ab}\gamma_{\mathrm{th}}}{\Omega_{ab}\lambda_Q^{ap}}x\right)\Upsilon\left(m_{rb},\frac{\beta m_{rb}\gamma_{\mathrm{th}}}{\Omega_{rb}\lambda_Q^{rp}}x\right)x^n e^{-\frac{m_{cb}}{\Omega_{cb}\lambda_c}x}dx, \tag{A.4}$$

which can be solved using [49, 3.351.2] to arrive at (3.21). Similarly, solving the other integral in (A.3), we can get (3.20).

APPENDIX B

DERIVATION OF (3.32)

From (3.31), $\mathcal{P}_{\mathrm{MRC}}^{\mathrm{IR}}$ can be represented as

$$\mathcal{P}_{\mathrm{MRC}}^{\mathrm{IR}} = \Pr\Big[\lambda_Q^{ap}\frac{g_{ab}}{X} + \lambda_Q^{rp}\frac{g_{rb}}{X} < \gamma_{\mathrm{th}}, \lambda_Q^{ap}\frac{g_{ab}}{X} < \gamma_{\mathrm{th}}^{\mathrm{d}}, \lambda_Q^{ap}\frac{g_{ar}}{Y} \geq \gamma_{\mathrm{th}}, \lambda_Q^{bp}\frac{g_{br}}{Y} < \gamma_{\mathrm{th}}\Big], \tag{B.1}$$

which further, owing to the independence between last two and other terms, can be written as

$$\mathcal{P}_{\mathrm{MRC}}^{\mathrm{IR}} = \underbrace{\Pr\Big[g_{ab} < \min\left(\frac{\gamma_{\mathrm{th}}^{\mathrm{d}}X}{\lambda_Q^{ap}}, \frac{\gamma_{\mathrm{th}}X}{\lambda_Q^{ap}} - \frac{\lambda_Q^{rp}g_{rb}}{\lambda_Q^{ap}}\right)\Big]}_{\mathcal{I}_1} \underbrace{\Pr\Big[\lambda_Q^{ap}\frac{g_{ar}}{Y} \geq \gamma_{\mathrm{th}}, \lambda_Q^{bp}\frac{g_{br}}{Y} < \gamma_{\mathrm{th}}\Big]}_{\mathcal{I}_2}. \tag{B.2}$$

Here, $\mathcal{I}_1$ can be re-expressed as

$$\begin{aligned}\mathcal{I}_1 = {} & \underbrace{\Pr\Big[g_{ab} < \frac{\gamma_{\mathrm{th}}^{\mathrm{d}}X}{\lambda_Q^{ap}}, \frac{\gamma_{\mathrm{th}}^{\mathrm{d}}X}{\lambda_Q^{ap}} < \frac{\gamma_{\mathrm{th}}X}{\lambda_Q^{ap}} - \frac{\lambda_Q^{rp}g_{rb}}{\lambda_Q^{ap}}\Big]}_{\mathcal{I}_{11}} \\ & + \underbrace{\Pr\Big[g_{ab} < \frac{\gamma_{\mathrm{th}}X}{\lambda_Q^{ap}} - \frac{\lambda_Q^{rp}g_{rb}}{\lambda_Q^{ap}}, \frac{\gamma_{\mathrm{th}}^{\mathrm{d}}X}{\lambda_Q^{ap}} > \frac{\gamma_{\mathrm{th}}X}{\lambda_Q^{ap}} - \frac{\lambda_Q^{rp}g_{rb}}{\lambda_Q^{ap}}\Big]}_{\mathcal{I}_{12}},\end{aligned} \tag{B.3}$$

where

$$\mathcal{I}_{11} = \int_{x=1}^{\infty}\int_{w=0}^{\frac{x(\gamma_{\mathrm{th}}-\gamma_{\mathrm{th}}^{\mathrm{d}})}{\lambda_Q^{rp}}} F_{g_{ab}|X}\left(\frac{x\gamma_{\mathrm{th}}^{\mathrm{d}}}{\lambda_Q^{ap}}\right) f_{g_{rb}}(w) f_X(x)\,dw\,dx, \tag{B.4}$$

and

$$\mathcal{I}_{12} = \int_{x=1}^{\infty} \int_{w=\frac{x(\gamma_{\text{th}}-\gamma_{\text{th}}^{\text{d}})}{\lambda_Q^{rp}}}^{\frac{x\gamma_{\text{th}}}{\lambda_Q^{rp}}} F_{g_{ab}|g_{rb},X}\left(\frac{x\gamma_{\text{th}}^{\text{d}}}{\lambda_Q^{ap}} - \frac{\lambda_Q^{rp} w}{\lambda_Q^{ap}}\right) f_{g_{rb}}(w) f_X(x) dw dx, \tag{B.5}$$

can be solved using [49, eqs. 3.351.2, 2.321.2].

Next, $\mathcal{I}_2$ in (J.1) is obtained by

$$\mathcal{I}_2 = \int_0^{\infty} \overline{F}_{g_{ar}|Y}\left(\frac{zy}{\lambda_Q^{ap}}\right) F_{g_{br}|Y}\left(\frac{zy}{\lambda_Q^{bp}}\right) f_Y(y) dy, \tag{B.6}$$

which, on solving, yields the expression that can be directly obtained from (3.20), and is given by $\frac{\Xi(1,1,;\gamma_{\text{th}})}{\Theta(1,1,;\gamma_{\text{th}})}$. Finally, invoking the obtained $\mathcal{I}_1$ and $\mathcal{I}_2$ into (J.1), one can arrive at (3.32).

APPENDIX C

DERIVATION OF (4.43)

Let there be m relays which have successfully decoded the received signal in first phase, then for $|\mathcal{D}_m| = m$, we can write the conditional decoding probability, using (4.37), as

$$\Pr\left[\mathcal{D}_m|W\right] = \prod_{\ell \in \mathcal{D}_m} \Pr\left[\Lambda_{sr_\ell} \geq \gamma_{\text{th}}|W\right] \prod_{n \notin \mathcal{D}_m} \Pr\left[\Lambda_{sr_n} < \gamma_{\text{th}}|W\right]. \tag{C.1}$$

Using (4.36), we can evaluate $\Pr\left[\Lambda_{sr_m} < \gamma_{\text{th}}|W\right]$ as

$$\Pr\left[\Lambda_{sr_m} < \gamma_{\text{th}}|W\right] = \Pr\left[\frac{P_s|\hat{h}_{sr_m}|^2}{P_s\kappa_{s,r}^2|\hat{h}_{sr_m}|^2 + P_s\alpha_{s,r_m} + N_0} < \gamma_{\text{th}}|W\right]. \tag{C.2}$$

From (4.34), P_s can be given by

$$P_s = \begin{cases} P, \text{ for } W \leq Q_{sp}, \\ \frac{Q}{(|\hat{h}_{sp}|^2 + \sigma_{e,sp}^2)(1+\kappa_{ts}^2)}, \text{ for } W > Q_{sp}. \end{cases} \tag{C.3}$$

On substituting (C.3) in (C.2) and evaluating the resultant expression, one can obtain $\Pr\left[\Lambda_{sr_m} < \gamma_{\text{th}}|W\right]$ as

$$\Pr\left[\Lambda_{sr_m} < \gamma_{\text{th}}|W\right] = \begin{cases} \Phi_{sr_m}(\gamma_{\text{th}}, w), \text{ for } \gamma_{\text{th}} < 1/\kappa_{s,r}^2, \\ 1, \text{ for } \gamma_{\text{th}} \geq 1/\kappa_{s,r}^2, \end{cases} \tag{C.4}$$

where $\Phi_{sr_m}(\gamma_{\text{th}}, w)$ is given by

$$\Phi_{sr_m}(\gamma_{\text{th}}, w) = \begin{cases} 1-\exp\left(\frac{-\gamma_{\text{th}}(\alpha_{s,r_m}\lambda_P+1)}{\hat{\Omega}_{sr_m}\lambda_P(1-\kappa_{s,r}^2\gamma_{\text{th}})}\right), \text{ for } W \leq Q_{sp}, \\ 1-\exp\left(\frac{-\gamma_{\text{th}}(\tilde{\alpha}_{s,r_m}+\delta_s w)}{\hat{\Omega}_{sr_m}\lambda_Q(1-\kappa_{s,r}^2\gamma_{\text{th}})}\right), \text{ for } W > Q_{sp}. \end{cases} \tag{C.5}$$

Thus, by using (C.4) in (C.1), $\Pr\left[\mathcal{D}_m|W\right]$ can be obtained as given in (4.43).

APPENDIX D

DERIVATION OF (4.52)

The function $\Phi_{r_\ell d}(\gamma_{\rm th})$ in (4.52) can be obtained as

$$\Phi_{r_\ell d}(\gamma_{\rm th}) = \Pr\left[\Lambda_{r_\ell d} < \gamma_{\rm th}\right]. \tag{D.1}$$

Using (4.40) in (D.1), we can write

$$\Phi_{r_\ell d}(\gamma_{\rm th}) = \Pr\left[\frac{P_{r_\ell}|\hat{h}_{r_\ell d}|^2}{P_{r_\ell}\kappa_{r,d}^2|\hat{h}_{r_\ell d}|^2 + P_{r_\ell}\alpha_{r_\ell,d} + N_0} < \gamma_{\rm th}\right]. \tag{D.2}$$

Invoking (4.39) in (D.2) and by conditioning $Y = |\hat{h}_{r_\ell p}|^2$, we have

$$\begin{aligned}\Phi_{r_\ell d}(\gamma_{\rm th}) = &\int_{y=0}^{Q_{r_\ell p}} F_{|\hat{h}_{r_\ell d}|^2}\left(\frac{\gamma_{\rm th}(\alpha_{r_\ell,d}\lambda_P + 1)}{\lambda_P(1-\kappa_{r,d}^2\gamma_{\rm th})}\Big|Y\right) f_Y(y)dy \\ &+ \int_{y=Q_{r_\ell p}}^{\infty} F_{|\hat{h}_{r_\ell d}|^2}\left(\frac{\gamma_{\rm th}(\tilde{\alpha}_{r_\ell,d} + \delta_r y)}{\lambda_Q(1-\kappa_{r,d}^2\gamma_{\rm th})}\Big|Y\right) f_Y(y)dy. \end{aligned} \tag{D.3}$$

Substituting for the corresponding CDF and PDF and computing the required integration (after some manipulations) with the aid of [49, eq. 3.310], one can arrive at (4.52).

APPENDIX E

DERIVATION OF (4.58)

From (4.42), using (4.34), we can write

$$\mathcal{P}_{\bar{\emptyset}1} = \int_{w=0}^{Q_{sp}} \sum_{m=1}^{K} \binom{K}{m} \Pr\left[\Lambda_{sd} < \gamma_{\text{th}} | W\right] \Pr\left[\mathcal{D}_m | W\right] \Pr\left[\Lambda_{r_m d} < \gamma_{\text{th}} | \mathcal{D}_m, W\right] f_W(w) dw$$
$$+ \int_{w=Q_{sp}}^{\infty} \sum_{m=1}^{K} \binom{K}{m} \Pr\left[\Lambda_{sd} < \gamma_{\text{th}} | W\right] \Pr\left[\mathcal{D}_m | W\right] \Pr\left[\Lambda_{r_m d} < \gamma_{\text{th}} | \mathcal{D}_m, W\right] f_W(w) dw. \tag{E.1}$$

On substituting $[\Lambda_{sd} < \gamma_{\text{th}}|W]$, $\Pr[\mathcal{D}_m|W]$, and $\Pr[\Lambda_{r_m d} < \gamma_{\text{th}}|\mathcal{D}_m, W]$ from (4.46), (4.43), and (4.51), respectively, in (4.42) and then solving the resultant integration alongwith PDF of W (with tedious manipulations after applying binomial theorem [49, eq. 1.111]), we get $\mathcal{P}_{\bar{\emptyset}1}$ as given in (4.58).

APPENDIX F

PROOF OF PROPOSITION 1

On carefully substituting the components $\mathcal{P}_{\bar{\emptyset}}$ from (4.53)-(4.57) and $\mathcal{P}_{\emptyset}$ from (4.64)-(4.65) into (4.41), we obtain the outage probability for different possible cases as follows:

Case 1: For $\kappa_{s,d}^2 \leq \kappa_{r,d}^2 \leq \kappa_{s,r}^2$ or $\kappa_{r,d}^2 \leq \kappa_{s,d}^2 \leq \kappa_{s,r}^2$,

$$\mathcal{P}_{\text{out}}(\gamma_{\text{th}}) = \begin{cases} \mathcal{P}_{\bar{\emptyset}1} + \mathcal{P}_{\emptyset 1}, \text{ for } \gamma_{\text{th}} < 1/\kappa_{s,r}^2, \\ \mathcal{P}_{\emptyset 2}, \text{ for } 1/\kappa_{s,r}^2 \leq \gamma_{\text{th}} < 1/\kappa_{s,d}^2, \\ 1, \gamma_{\text{th}} \geq 1/\kappa_{s,d}^2. \end{cases} \tag{F.1}$$

Case 2: For $\kappa_{s,r}^2 \leq \kappa_{s,d}^2 \leq \kappa_{r,d}^2$,

$$\mathcal{P}_{\text{out}}(\gamma_{\text{th}}) = \begin{cases} \mathcal{P}_{\bar{\emptyset}1} + \mathcal{P}_{\emptyset 1}, \text{ for } \gamma_{\text{th}} < 1/\kappa_{r,d}^2, \\ \mathcal{P}_{\bar{\emptyset}4} + \mathcal{P}_{\emptyset 1}, \text{ for } 1/\kappa_{r,d}^2 \leq \gamma_{\text{th}} < 1/\kappa_{s,d}^2, \\ \mathcal{P}_{\bar{\emptyset}3} + \mathcal{P}_{\emptyset 3}, \text{ for } 1/\kappa_{s,d}^2 \leq \gamma_{\text{th}} < 1/\kappa_{s,r}^2, \\ 1, \gamma_{\text{th}} \geq 1/\kappa_{s,r}^2. \end{cases} \tag{F.2}$$

Case 3: For $\kappa_{s,d}^2 \leq \kappa_{s,r}^2 \leq \kappa_{r,d}^2$,

$$\mathcal{P}_{\text{out}}(\gamma_{\text{th}}) = \begin{cases} \mathcal{P}_{\bar{\emptyset}1} + \mathcal{P}_{\emptyset 1}, \text{ for } \gamma_{\text{th}} < 1/\kappa_{r,d}^2, \\ \mathcal{P}_{\bar{\emptyset}4} + \mathcal{P}_{\emptyset 1}, \text{ for } 1/\kappa_{r,d}^2 \leq \gamma_{\text{th}} < 1/\kappa_{s,r}^2, \\ \mathcal{P}_{\emptyset 2}, \text{ for } 1/\kappa_{s,r}^2 \leq \gamma_{\text{th}} < 1/\kappa_{s,d}^2, \\ 1, \gamma_{\text{th}} \geq 1/\kappa_{s,d}^2. \end{cases} \tag{F.3}$$

Case 4: For $\kappa_{r,d}^2 \leq \kappa_{s,r}^2 \leq \kappa_{s,d}^2$,

$$\mathcal{P}_{\text{out}}(\gamma_{\text{th}}) = \begin{cases} \mathcal{P}_{\bar{\emptyset}1} + \mathcal{P}_{\emptyset 1}, \text{ for } \gamma_{\text{th}} < 1/\kappa_{s,d}^2, \\ \mathcal{P}_{\bar{\emptyset}2} + \mathcal{P}_{\emptyset 3}, \text{ for } 1/\kappa_{s,d}^2 \leq \gamma_{\text{th}} < 1/\kappa_{s,r}^2, \\ 1, \gamma_{\text{th}} \geq 1/\kappa_{s,r}^2. \end{cases} \tag{F.4}$$

Case 5: For $\kappa_{s,r}^2 \leq \kappa_{r,d}^2 \leq \kappa_{s,d}^2$,

$$\mathcal{P}_{\text{out}}(\gamma_{\text{th}}) = \begin{cases} \mathcal{P}_{\bar{\emptyset}1} + \mathcal{P}_{\emptyset 1}, \text{ for } \gamma_{\text{th}} < 1/\kappa_{s,d}^2, \\ \mathcal{P}_{\bar{\emptyset}2} + \mathcal{P}_{\emptyset 3}, \text{ for } 1/\kappa_{s,d}^2 \leq \gamma_{\text{th}} < 1/\kappa_{r,d}^2, \\ \mathcal{P}_{\bar{\emptyset}3} + \mathcal{P}_{\emptyset 3}, \text{ for } 1/\kappa_{r,d}^2 \leq \gamma_{\text{th}} < 1/\kappa_{s,r}^2, \\ 1, \gamma_{\text{th}} \geq 1/\kappa_{s,r}^2. \end{cases} \tag{F.5}$$

In (F.2) and (F.5), the probability component $\mathcal{P}_{\bar{\emptyset}3}+\mathcal{P}_{\emptyset 3}$ can be expressed, using total probability theorem, as

$$\begin{aligned} \mathcal{P}_{\bar{\emptyset}3}+\mathcal{P}_{\emptyset 3} = & \int_0^\infty \sum_{m=1}^{K} \sum_{\mathcal{D}_m} \Pr\left[\mathcal{D}_m | W\right] f_W(w) dw \\ & + \int_0^\infty \prod_{m=1}^{K} \Pr\left[\Lambda_{sr_m} < \gamma_{\text{th}} | W\right] f_W(w) dw = 1. \end{aligned} \tag{F.6}$$

And, the probability component $\mathcal{P}_{\bar{\emptyset}4}+\mathcal{P}_{\emptyset 1}$ in (F.2) and (F.3) can be expressed as

$$\begin{aligned} \mathcal{P}_{\bar{\emptyset}4}+\mathcal{P}_{\emptyset 1} = & \int_0^\infty \left(\sum_{m=1}^{K} \sum_{\mathcal{D}_m} \Pr\left[\mathcal{D}_m | W\right] + \prod_{m=1}^{K} \Pr\left[\Lambda_{sr_m} < \gamma_{\text{th}} | W\right] \right) \\ & \times \Pr\left[\Lambda_{sd} < \gamma_{\text{th}} | W\right] f_W(w) dw = \mathcal{P}_{\emptyset 2}. \end{aligned} \tag{F.7}$$

Substituting (F.6) in (F.5) and (F.2), and (F.7) in (F.2) and (F.3), the outage probability can be expressed as given in Proposition 1.

APPENDIX G

DERIVATION OF (4.105)

Using (5.14), $\Pr[\Lambda_{p_i} < \varrho_{\text{th}}]$ in (5.17) can be written as

$$\Pr[\Lambda_{p_i} < \varrho_{\text{th}}] = \Pr\left[\frac{P_c|h_{c_ip_i}|^2}{P_s|h_{sp_i}|^2 + \kappa_{ts}^2 P_s|h_{sp_i}|^2 + N_o} < \varrho_{\text{th}}\right], \tag{G.1}$$

which can be evaluated as

$$\Pr[\Lambda_{p_i} < \varrho_{\text{th}}] = \int_0^\infty \frac{1}{m_{cp}} \Upsilon\left(m_{cp}, \frac{m_{cp}\varrho_{\text{th}}(\delta_s P_s x + N_o)}{\Omega_{cp}P_c}\right) \times f_{|h_{sp_i}|^2}(x)dx, \tag{G.2}$$

where PDF $f_{|h_{sp_i}|^2}(x)$ is of the form given by (5.11). Using this PDF along with the series expansion of incomplete gamma function [49, eq. 8.352.1]) in (G.2), and then solving the resultant integral, we obtain $\Pr[\Lambda_{p_i} < \varrho_{\text{th}}]$. On substituting the obtained $\Pr[\Lambda_{p_i} < \varrho_{\text{th}}]$ in (5.17), one can arrive at (5.18).

APPENDIX H

DERIVATION OF (4.112)

Let there be m relays that have successfully decoded the received signal in first phase, then for $|\mathcal{D}_m| = m$, we can write the conditional decoding probability, using (5.8), as

$$\Pr\left[\mathcal{D}_m\right] = \prod_{\ell\in\mathcal{D}_m} \Pr\left[\Lambda_{sr_\ell} \geq \gamma_{\text{th}}\right] \prod_{n\notin\mathcal{D}_m} \Pr\left[\Lambda_{sr_n} < \gamma_{\text{th}}\right], \tag{H.1}$$

where the probability $\Pr\left[\Lambda_{sr_\ell} \geq \gamma_{\text{th}}\right] = 1-\Pr\left[\Lambda_{sr_\ell} < \gamma_{\text{th}}\right]$. As such, to obtain $\Pr\left[\mathcal{D}_m\right]$ in (H.1), we evaluate $\Pr\left[\Lambda_{sr_m} < \gamma_{\text{th}}\right]$, using (5.7), as

$$\Pr\left[\Lambda_{sr_m} < \gamma_{\text{th}}\right] = \Pr\left[\frac{P_s|\hat{h}_{sr_m}|^2}{P_s\kappa^2_{s,r_m}|\hat{h}_{sr_m}|^2+P_s\sigma^2_{e,sr_m}\delta_{s,r}+\delta_{rr}P_cY+N_o} < \gamma_{\text{th}}\right], \tag{H.2}$$

where $Y = \sum_{i=1}^{L}|h_{c_ir_m}|^2$. We can further solve (H.2) as

$$\Pr\left[\Lambda_{sr_m} < \gamma_{\text{th}}\right] = \int_0^\infty \frac{1}{\Gamma(m_{sr})}\Upsilon\left(m_{sr}, \frac{m_{sr}\gamma_{\text{th}}(\delta_{rr}P_cy+\alpha_{s,r})}{\hat{\Omega}_{sr}(1-\gamma_{\text{th}}\kappa^2_{s,r})}\right) f_Y(y)dy, \tag{H.3}$$

where the PDF $f_Y(y)$ is of the same form as given in (5.24). Thus, invoking the PDF $f_Y(y)$ in (H.3) and using the series expansion of incomplete gamma function [49, eq. 8.352.1]), and then evaluating the resultant integral after applying binomial theorem [49, eq. 1.111]), one can obtain

$$\Pr\left[\Lambda_{sr_m} < \gamma_{\text{th}}\right] = \begin{cases} \Phi_{sr_m}(\gamma_{\text{th}}), \text{ for } \gamma_{\text{th}} < 1/\kappa^2_{s,r}, \\ 1, \text{ for } \gamma_{\text{th}} \geq 1/\kappa^2_{s,r}, \end{cases} \tag{H.4}$$

where $\Phi_{sr_m}(\gamma_{\rm th})$ is as follows

$$\Phi_{sr_m}(\gamma_{\rm th}) = 1 - \sum_{t=0}^{m_{sr}-1} \sum_{\hat{t}=0}^{t} \binom{t}{\hat{t}} \frac{\Gamma(\hat{t}+m_{cr}L)}{t!\Gamma(m_{cr}L)} \frac{(\delta_{rr}P_c)^{\hat{t}}}{(\alpha_{s,r})^{\hat{t}-t}} e^{-\frac{m_{sr}\gamma_{\rm th}\alpha_{s,r}}{\hat{\Omega}_{sr}P_s(1-\gamma_{\rm th}\kappa_{s,r}^2)}} \left(\frac{m_{cr}}{\Omega_{cr}}\right)^{m_{cr}L}$$
$$\times \left(\frac{m_{sr}\gamma_{\rm th}}{\hat{\Omega}_{sr}P_s(1-\gamma_{\rm th}\kappa_{s,r}^2)}\right)^{t} \left(\frac{m_{cr}}{\Omega_{cr}} + \frac{m_{sr}\gamma_{\rm th}P_c\delta_{rr}}{\hat{\Omega}_{sr}(1-\gamma_{\rm th}\kappa_{s,r}^2)}\right)^{-(\hat{t}+m_{cr}L)}. \qquad \text{(H.5)}$$

Finally, by using (H.4) in (H.1), $\Pr[\mathcal{D}_m]$ can be obtained as given in (5.25).

APPENDIX I

PROOF OF PROPOSITION 2

On carefully substituting the components $\mathcal{P}_{\bar{\emptyset}}$ from (5.34)-(5.38) and $\mathcal{P}_{\emptyset}$ from (5.47)-(5.48) into (5.22), we obtain the outage probability for different possible cases as follows:

Case 1: For $\kappa_{s,d}^2 \leq \kappa_{r,d}^2 \leq \kappa_{s,r}^2$ or $\kappa_{r,d}^2 \leq \kappa_{s,d}^2 \leq \kappa_{s,r}^2$,

$$\mathcal{P}_{\text{out}}^{\text{sec}}(\gamma_{\text{th}}) = \begin{cases} \mathcal{P}_{\bar{\emptyset}1} + \mathcal{P}_{\emptyset 1}, \text{ for } \gamma_{\text{th}} < 1/\kappa_{s,r}^2, \\ \mathcal{P}_{\emptyset 2}, \text{ for } 1/\kappa_{s,r}^2 \leq \gamma_{\text{th}} < 1/\kappa_{s,d}^2, \\ 1, \gamma_{\text{th}} \geq 1/\kappa_{s,d}^2. \end{cases} \tag{I.1}$$

Case 2: For $\kappa_{s,r}^2 \leq \kappa_{s,d}^2 \leq \kappa_{r,d}^2$,

$$\mathcal{P}_{\text{out}}^{\text{sec}}(\gamma_{\text{th}}) = \begin{cases} \mathcal{P}_{\bar{\emptyset}1} + \mathcal{P}_{\emptyset 1}, \text{ for } \gamma_{\text{th}} < 1/\kappa_{r,d}^2, \\ \mathcal{P}_{\bar{\emptyset}4} + \mathcal{P}_{\emptyset 1}, \text{ for } 1/\kappa_{r,d}^2 \leq \gamma_{\text{th}} < 1/\kappa_{s,d}^2, \\ \mathcal{P}_{\bar{\emptyset}3} + \mathcal{P}_{\emptyset 3}, \text{ for } 1/\kappa_{s,d}^2 \leq \gamma_{\text{th}} < 1/\kappa_{s,r}^2, \\ 1, \gamma_{\text{th}} \geq 1/\kappa_{s,r}^2. \end{cases} \tag{I.2}$$

Case 3: For $\kappa_{s,d}^2 \leq \kappa_{s,r}^2 \leq \kappa_{r,d}^2$,

$$\mathcal{P}_{\text{out}}^{\text{sec}}(\gamma_{\text{th}}) = \begin{cases} \mathcal{P}_{\bar{\emptyset}1} + \mathcal{P}_{\emptyset 1}, \text{ for } \gamma_{\text{th}} < 1/\kappa_{r,d}^2, \\ \mathcal{P}_{\bar{\emptyset}4} + \mathcal{P}_{\emptyset 1}, \text{ for } 1/\kappa_{r,d}^2 \leq \gamma_{\text{th}} < 1/\kappa_{s,r}^2, \\ \mathcal{P}_{\emptyset 2}, \text{ for } 1/\kappa_{s,r}^2 \leq \gamma_{\text{th}} < 1/\kappa_{s,d}^2, \\ 1, \gamma_{\text{th}} \geq 1/\kappa_{s,d}^2. \end{cases} \tag{I.3}$$

Case 4: For $\kappa_{r,d}^2 \leq \kappa_{s,r}^2 \leq \kappa_{s,d}^2$,

$$\mathcal{P}_{\text{out}}^{\text{sec}}(\gamma_{\text{th}}) = \begin{cases} \mathcal{P}_{\bar{\emptyset}1} + \mathcal{P}_{\emptyset 1}, \text{ for } \gamma_{\text{th}} < 1/\kappa_{s,d}^2, \\ \mathcal{P}_{\bar{\emptyset}2}+\mathcal{P}_{\emptyset 3}, \text{ for } 1/\kappa_{s,d}^2 \leq \gamma_{\text{th}} < 1/\kappa_{s,r}^2, \\ 1, \gamma_{\text{th}} \geq 1/\kappa_{s,r}^2. \end{cases} \tag{I.4}$$

Case 5: For $\kappa_{s,r}^2 \leq \kappa_{r,d}^2 \leq \kappa_{s,d}^2$,

$$\mathcal{P}_{\text{out}}^{\text{sec}}(\gamma_{\text{th}}) = \begin{cases} \mathcal{P}_{\bar{\emptyset}1} + \mathcal{P}_{\emptyset 1}, \text{ for } \gamma_{\text{th}} < 1/\kappa_{s,d}^2, \\ \mathcal{P}_{\bar{\emptyset}2}+\mathcal{P}_{\emptyset 3}, \text{ for } 1/\kappa_{s,d}^2 \leq \gamma_{\text{th}} < 1/\kappa_{r,d}^2, \\ \mathcal{P}_{\bar{\emptyset}3}+\mathcal{P}_{\emptyset 3}, \text{ for } 1/\kappa_{r,d}^2 \leq \gamma_{\text{th}} < 1/\kappa_{s,r}^2, \\ 1, \gamma_{\text{th}} \geq 1/\kappa_{s,r}^2. \end{cases} \tag{I.5}$$

In (I.2) and (I.5), the probability component $\mathcal{P}_{\bar{\emptyset}3}+\mathcal{P}_{\emptyset 3}$ can be expressed, using total probability theorem, as

$$\begin{aligned} \mathcal{P}_{\bar{\emptyset}3}+\mathcal{P}_{\emptyset 3} &= \int_0^\infty \sum_{m=1}^{K} \sum_{\mathcal{D}_m} \Pr\left[\mathcal{D}_m\right] f_W(w)dw + \int_0^\infty \prod_{m=1}^{K} \Pr\left[\Lambda_{sr_m} < \gamma_{\text{th}} | W\right] f_W(w)dw \\ &= 1. \end{aligned} \tag{I.6}$$

And, the probability component $\mathcal{P}_{\bar{\emptyset}4}+\mathcal{P}_{\emptyset 1}$ in (I.2) and (I.3) can be expressed as

$$\begin{aligned} \mathcal{P}_{\bar{\emptyset}4}+\mathcal{P}_{\emptyset 1} &= \int_0^\infty \left(\sum_{m=1}^{K} \sum_{\mathcal{D}_m} \Pr\left[\mathcal{D}_m\right] + \prod_{m=1}^{K} \Pr\left[\Lambda_{sr_m} < \gamma_{\text{th}} | W\right] \right) \\ &\qquad \times \Pr\left[\Lambda_{sd} < \gamma_{\text{th}} | W\right] f_W(w)dw \\ &= \mathcal{P}_{\emptyset 2}. \end{aligned} \tag{I.7}$$

After substituting (I.6) in (I.5) and (I.2), and (I.7) in (I.2) and (I.3), the outage probability can be expressed as given in Proposition 2.

APPENDIX J

PROOF OF LEMMA 12

Using (6.14), we can write $\mathcal{P}_{21}$ as

$$\begin{aligned}\mathcal{P}_{21} &= \Pr\left[\frac{\xi\varrho XY}{\xi Y + (1-\xi)\varrho XY + \frac{1-\alpha}{2\eta\alpha}} < \gamma_{\text{th}},\ \ P_c X \leq \zeta_{\text{th}}\right] \\ &= \Pr\left[Y < \frac{\mathcal{A}}{\mathcal{B}X - \xi\gamma_{\text{th}}},\ \ X \leq \frac{\zeta_{\text{th}}}{P_c}\right], \end{aligned} \tag{J.1}$$

where $X = |h_{cs}|^2, Y = |h_{sp_n}|^2$ for notational simplicity. Further, based on the values of ξ, we can express (J.1) as

$$\mathcal{P}_{21} = \begin{cases} \int_{x=0}^{\frac{\zeta_{\text{th}}}{P_c}} f_X(x)dx, & \text{for } \gamma_{\text{th}} \geq \frac{\xi}{1-\xi}, \\ \int_{x=0}^{\frac{\zeta_{\text{th}}}{P_c}} f_X(x)dx, & \text{for } \gamma_{\text{th}} < \frac{\xi}{1-\xi} \ \&\ \frac{\zeta_{\text{th}}}{P_c} \leq \frac{\xi\gamma_{\text{th}}}{\mathcal{B}}, \\ \Psi(\gamma_{\text{th}}), & \text{for } \gamma_{\text{th}} < \frac{\xi}{1-\xi} \ \&\ \frac{\zeta_{\text{th}}}{P_c} > \frac{\xi\gamma_{\text{th}}}{\mathcal{B}}, \end{cases} \tag{J.2}$$

where $\Psi(\gamma_{\text{th}})$ can be derived as

$$\Psi(\gamma_{\text{th}}) = \underbrace{\int_{x=0}^{\frac{\xi\gamma_{\text{th}}}{\mathcal{B}}} f_X(x)dx}_{\mathcal{J}_1} + \underbrace{\int_{x=\frac{\xi\gamma_{\text{th}}}{\mathcal{B}}}^{\frac{\zeta_{\text{th}}}{P_c}} F_Y\left(\frac{\mathcal{A}}{\mathcal{B}x - \gamma_{\text{th}}\xi}\right) f_X(x)dx}_{\mathcal{J}_2}. \tag{J.3}$$

Now $\mathcal{J}_1$ can be evaluated as $\mathcal{J}_1 = 1 - \exp\left(-\frac{\xi\gamma_{\text{th}}}{\mathcal{B}\Omega_{cs}}\right)$. To evaluate $\mathcal{J}_2$, we perform the appropriate substitutions followed by some manipulations to obtain

$$\begin{aligned}\mathcal{J}_2 = F_X\left(\frac{\zeta_{\text{th}}}{P_c}\right) - F_X\left(\frac{\xi\gamma_{\text{th}}}{\mathcal{B}}\right) - \frac{1}{\mathcal{B}\Omega_{cs}}\exp\left(-\frac{\xi\gamma_{\text{th}}}{\mathcal{B}\Omega_{cs}}\right) \\ \times \int_{t=0}^{\frac{\mathcal{B}\zeta_{\text{th}}}{P_c} - \gamma_{\text{th}}\xi} \exp\left(-\frac{\mathcal{A}}{\Omega_{sp}t} - \frac{t}{\mathcal{B}\Omega_{cs}}\right) dt. \end{aligned} \tag{J.4}$$

It can be observed that the integral form in (J.4) is intractable. Therefore, relying on the Maclaurin series expansion [143] of the term $\exp\left(-\frac{t}{\mathcal{B}\Omega_{cs}}\right)$ and then solving the resultant integral with the aid of [49, eq. 3.381.6], we can derive the analytical expression of $\Psi(\gamma_{\mathrm{th}})$, after performing various algebric manipulations, as given in (6.16).

REFERENCES

[1] "Spectrum Policy Task Force Report," *Federal Commun. Comm.*, Washington, DC, ET Docket No. 02-135, Nov. 2002.

[2] S. Haykin, "Cognitive Radio: Brain-empowered wireless communications," *IEEE J. Sel. Areas Communi.*, vol. 23, no. 2, pp. 201-220, Feb. 2005.

[3] J. Laneman, D. Tse, and G. Wornell, "Cooperative diversity in wireless networks: Efficient protocols and outage behavior," *IEEE Trans. Inf. Theory*, vol. 50, no. 12, pp. 3062-3080, Dec. 2004.

[4] J. Mitola III, "Cognitive radio: making software radios more personal," *IEEE Pers. Commun.*, vol. 6, no. 4, pp. 13-18, Aug. 1999.

[5] A. Goldsmith, S. A. Jafar, I. Maric, and S. Srinivasa, "Breaking spectrum gridlock and cognitive radios: An information theoretic perspective," *Proc. IEEE*, vol. 97, no. 5, pp. 894-914, May 2009.

[6] G. C. C. Stevenson, L. Zhongding, H. Wendong, S. J. Shellhammer, and W. Caldwell, "IEEE 802.22: The first cognitive radio wireless regional area network standard," *IEEE Commun. Mag.*, vol. 47, no. 1, pp. 130-138, Jan. 2009.

[7] A. B. Flores, R. E. Guerra, and E. W. Knightly, "IEEE 802.11af: A standard for TV white space spectrum sharing," *IEEE Commun. Mag.*, vol. 51, no. 10, pp. 92-100, Oct. 2013.

[8] *Air Interface for Broadband Wireless Access Systems-Amendment 1: Multihop Relay Specification,* IEEE Std. 802.16j-2009, Jun. 2009.

[9] C. Hoymann *et al.*, "LTE release 14 outlook," *IEEE Commun. Mag.*, vol. 54, no. 6, pp. 44-49, Jun. 2016.

[10] *Air Interface for Fixed and Mobile Broadband Wireless Access Systems Amendment 2: Physical and Medium Access Control Layers for Combined Fixed and Mobile Operation in Licensed Bands and Corrigendum 1,* IEEE Std 802.16e-2005, Feb. 2006.

[11] I. Krikidis, "Relay selection for two-way relay channels with MABC DF: A diversity perspective," *IEEE Trans. Veh. Technol.*, vol. 59, no. 9, pp. 4620-4628, Nov. 2010.

[12] X. Xia, D. Zhang, K. Xu, and Y. Xu, "Interference-limited two-way relaying: Symbol-error-rate analysis and comparison," *IEEE Trans. Veh. Technol.*, vol. 63, no. 7, pp. 3474-3480, Sep. 2014.

[13] L. R. Varshney, "Transporting information and energy simultaneously," in *Proc. IEEE ISIT*, Toronto, Canada, Jul. 2008.

[14] Y. Liu, Y. Zhang, R. Yu, and S. Xie, "Integrated energy and spectrum harvesting for 5G wireless communications," *IEEE Network*, vol. 29, no. 3, pp. 75-81, Jun. 2015.

[15] O. Simeone, J. Gambini, Y. B. Ness, and U. Spagnolini, "Cooperation and cognitive radio," in *Proc. IEEE ICC*, pp. 6511-6515, Glasgow, UK, June 2007.

[16] Y. Han, A. Pandharipande, and S. H. Ting, "Cooperative decode-and-forward relaying for secondary spectrum access," *IEEE Trans. Wireless Commun.*, vol. 8, no. 10, pp. 4945-4950, Oct. 2009.

[17] M. Hafeez, and J. M. H. Elmirghani, "Analysis of dynamic spectrum leasing for coded bi-directional communication," *IEEE J. Sel. Areas Commun.*, vol. 30, no. 8, pp. 1500-1512, Sept. 2012.

[18] Q. Li, S. H. Ting, A. Pandharipande, and Y. Han, "Cognitive spectrum sharing with two-way relaying systems," *IEEE Trans. Veh. Technol.*, vol. 60, no. 3, pp. 1233-1240, Mar. 2011.

[19] T. Q. Duong, V. N. Q. Bao, G. C. Alexandropoulos, and H.-J. Zepernick, "Outage and diversity of cognitive relaying systems under spectrum sharing environment in Nakagami-m fading," *IEEE Commun. Lett.*, vol. 16, no. 12, pp. 2075-2078, Dec. 2012.

[20] S. Sagong, J. Lee, and D. Hong, "Capacity of reactive DF scheme in cognitive relay networks," *IEEE Trans. Wireless Commun.*, vol. 10, no. 10, pp. 3133-3138, Oct. 2011.

[21] C. Zhong, T. Ratnarajah, and K. K. Wong, "Outage analysis of decode-and-forward cognitive dual-hop systems with interference constraint in Nakagami-m fading channels," *IEEE Trans. Veh. Technol.*, vol. 60, no. 6, pp. 2875-2879, July 2011.

[22] P. K. Sharma, S. Solanki, and P. K. Upadhyay, "Outage analysis of cognitive opportunistic relay networks with direct link in Nakagami-m fading," *IEEE Commun. Lett.*, vol. 19, no. 5, pp. 875-878, May 2015.

[23] P. Ubaidulla and S. Aissa, "Optimal relay selection and power allocation for cognitive two-way relaying network," *IEEE Wireless Commun. Lett.*, vol. 1, no. 3, pp. 225-228, June 2012.

[24] W. Jaafar, W. Ajib, and D. Haccoun, "A novel relay-aided transmission scheme in cognitive radio networks," in *Proc. IEEE Globecom*, pp. 1-6, Houston, Texas, USA, Dec. 2011.

[25] T. M. C. Chu, H. Phan, and H.-J. Zepernick, "Amplify-and-forward relay assisting both primary and secondary transmissions in cognitive radio networks over Nakagami-m fading," in *Proc. IEEE PIMRC*, pp. 932-937, Sydney, Australia, Sep. 2012.

[26] D. Li, “Amplify-and-forward relay sharing for both primary and cognitive users,” *IEEE Trans. Veh. Technol.*, vol. PP, no. 99, Apr. 2015.

[27] T. Schenk, *RF Imperfections in High-Rate Wireless Systems: Impact and Digital Compensation.*, Springer 2008.

[28] S. Han, S. Ahn, E. Oh, and D. Hong, “Effect of channel estimation error on BER performance in cooperative transmission,” *IEEE Trans. Veh. Technol.*, vol. 58, no. 4, pp. 2083-2088, May 2009.

[29] N. Abuzainab and A. Ephremides, “Energy efficiency of cooperative relaying over a wireless link,” *IEEE Trans. Wireless Commun.*, vol. 11, no. 6, pp. 2076-2083, Nov. 2012.

[30] S. A. Mousavifar, Y. Liu, C. Leung, M. Elkashlan, and T. Q. Duong, “Wireless energy harvesting and spectrum sharing in cognitive radio,” in *Proc. IEEE Veh. Technol. Conf. (VTC)*, Vancouver, BC, Canada, Sep. 2014.

[31] L. Sibomana, H.-J. Zepernick, and H. Tran, “Wireless information and power transfer in an underlay cognitive radio network,” in *Proc. Int. Conf. Sig. Process. Commun. Syst. (ICSPCS)*, Gold Coast, QLD, Australia, Dec. 2014.

[32] Y. Liu, S. A. Mousavifar, Y. Deng, C. Leung, and M. Elkashlan, “Wireless energy harvesting in a cognitive relay network,” *IEEE Trans. Wireless Commun.*, vol. 15, no. 4, pp. 2498-2508, Apr. 2016.

[33] S. S. Kalamkar and A. Banerjee, “Interference-aided energy harvesting: Cognitive relaying with multiple primary transceivers,” *IEEE Trans. Cogn. Commun. Netw.*, vol. 3, no. 3, pp. 313-327, Sep. 2017.

[34] K. Janghel and S. Prakriya, “Throughput of underlay cognitive energy harvesting relay networks with an improved time-switching protocol,” *IEEE Trans. Cogn. Commun. Netw.*, vol. 4, no. 1, pp. 66-81, Mar. 2018.

[35] Z. Yan, S. Chen, X. Zhang, and H.-L. Liu, “Outage performance analysis of

wireless energy harvesting relay-assisted random underlay cognitive networks," *IEEE Internet Things J.*, vol. 5, no. 4, pp. 2691-2699, Aug. 2018.

[36] G. Zheng, Z. Ho, E. A. Jorswieck, and B. Ottersten, "Information and energy cooperation in cognitive radio networks," *IEEE Trans. Signal Process.*, vol. 62, no. 9, pp. 2290-2303, May 2014.

[37] S. Yin, E. Zhang, Z. Qu, L. Yin, and S. Li, "Optimal cooperation strategy in cognitive radio systems with energy harvesting," *IEEE Trans. Wireless Commun.*, vol. 13, no. 9, pp. 4693-4707, Sep. 2014.

[38] P. M. Quang, T. T. Duy, and V. N. Q. Bao, "Energy harvesting-based spectrum access model in overlay cognitive radio," in *Proc. Int. Conf. Adv. Tech. Commun.*, Ho Chi Minh City, Vietnam, Oct. 2015.

[39] C. Zhai, J. Liu, and L. Zheng, "Cooperative spectrum sharing with wireless energy harvesting in cognitive radio networks," *IEEE Trans. Veh. Technol.*, vol. 65, no. 7, pp. 5303-5316, Jul. 2016.

[40] S. Kalamkar, J. P. Jeyaraj, A. Banerjee, and K. Rajawat, "Resource allocation and fairness in wireless powered cooperative cognitive radio networks," *IEEE Trans. Commun.*, vol. 64, no. 8, pp. 3246-3261, Aug. 2016.

[41] A. Banerjee, A. Paul, and S. P. Maity, "Joint power allocation and route selection for outage minimization in multihop cognitive radio networks with energy harvesting," *IEEE Trans. Cogn. Commun. Netw.*, vol. 4, no. 1, pp. 82-92, Mar. 2018.

[42] R. Pabst *et al.*, "Relay-based deployment concepts for wireless and mobile broadband radio," *IEEE Commun. Mag.*, vol. 42, no. 9, pp. 80-89, Sep. 2004.

[43] M. Xia, C. Xing, Y.-C. Wu, and S. Aissa, "Exact performance analysis of dual-hop semi-blind AF relaying over arbitrary Nakagami-m fading channels," *IEEE Trans. Wireless Commun.*, vol. 10, no. 10, pp. 3449-3459, Oct. 2011.

[44] M. Xia, Y.-C. Wu, and S. Aissa, "Exact outage probability of dual-hop CSI-assisted AF relaying over Nakagami-m fading channels," *IEEE Trans. Signal Processing*, vol. 60, no. 10, pp. 5578-5583, Oct. 2012.

[45] H. Xiao and S. Ouyang, "Power allocation for a hybrid decode-amplify-forward cooperative communication system with two source-destination pairs under outage probability constraint," *IEEE Systems J.*, vol. 9, no. 3, pp. 797-804, Sep. 2015.

[46] P. K. Sharma and P. K. Upadhyay, "Overlay spectrum sharing with multiuser two-way relaying using TDBC in Nakagami-m fading," in *Proc. IEEE VTC-Spring*, pp. 1-5, Glasgow, UK, May 2015.

[47] C. Gong, G. Yue, and X. Wang, "Transmission protocol for a cognitive bidirectional shared relay system," *IEEE J. Sel. Top. Sig. Process.*, vol. 5, no. 1, pp. 160-170, Feb. 2011.

[48] Y. Li, H. Long, M. Peng, and W. Wang, "Spectrum sharing with analog network coding," *IEEE Trans. Veh. Technol.*, vol. 63, no. 4, pp. 1703-1716, May 2014.

[49] I. S. Gradshteyn and I. M. Ryzhik, *Tables of Integrals, Series and Products*, 6th ed. New York: Academic Press, 2000.

[50] J. A. Hussain, S. S. Ikki, S. Boussakta, C. C. Tsimenidis, and J. Chambers, "Performance analysis of a multi-hop UCRN with co-channel interference," *IEEE Trans. Commun.*, vol. 64, no. 10, pp. 4346-4364, Oct. 2016.

[51] X. Zhang, Y. Zhang, Z. Yan, J. Xing, and W. Wang, "Performance analysis of cognitive relay networks over Nakagami-m fading channels," *IEEE J. Sel. Areas Commun.*, vol. 33, no. 5, pp. 865-877, May 2015

[52] D. C. Gonzalez, D. B. da Costa, and J. C. S. S. Filho, "Distributed suboptimal schemes for TAS/SC and TAS/LS in fixed-gain AF relaying systems," *IEEE Trans. Wireless Commun.*, vol. 13, no. 11, pp. 6041-6053, Nov. 2014

[53] Q. Li, M. Yu, A. Pandharipande, and X. Ge, "Outage analysis of co-operative two-path relay channels," *IEEE Trans. Wireless Commun.*, vol. 15, no. 5, pp. 3157-3169, May 2016.

[54] A. M. Akhtar, X. Wang, and L. Hanzo, "Synergistic spectrum sharing in 5G HetNets: A harmonized SDN-enabled approach," *IEEE Commun. Mag.*, vol. 54, no. 1, pp. 40-47, Jan. 2016.

[55] H. A. Suraweera, P. J. Smith, and M. Shafi, "Capacity limits and performance analysis of cognitive radio with imperfect channel knowledge," *IEEE Trans. Veh. Technol.*, vol. 59, no. 4, pp. 1811-1822, May 2010.

[56] Y. Zou, J. Zhu, B. Zheng, and Y. Yao, "An adaptive cooperation diversity scheme with best-relay selection in cognitive radio networks," *IEEE Trans. Signal Process.*, vol. 58, no. 10, pp. 5438-5445, Oct. 2010.

[57] T. Q. Duong, V. N. Q. Bao, G. C. Alexandropoulos, and H.-J. Zepernick, "Outage and diversity of cognitive relaying systems under spectrum sharing environment in Nakagami-m fading," *IEEE Commun. Lett.*, vol. 16, no. 12, pp. 2075-2078, Dec. 2012.

[58] S. Sagong, J. Lee, and D. Hong, "Capacity of reactive DF scheme in cognitive relay networks," *IEEE Trans. Wireless Commun.*, vol. 10, no. 10, pp. 3133-3138, Oct. 2011.

[59] C. Zhong, T. Ratnarajah, and K. K. Wong, "Outage analysis of decode-and-forward cognitive dual-hop systems with interference constraint in Nakagami-m fading channels," *IEEE Trans. Veh. Technol.*, vol. 60, no. 6, pp. 2875-2879, July 2011.

[60] P. Yang, L. Luo, and J. Qin, "Outage performance of cognitive relay networks with interference from primary user," *IEEE Commun. Lett.*, vol. 16, no. 10, pp. 1695-1698, Oct. 2012.

[61] T. Q. Duong, P. L. Yeoh, V. N. Q. Bao, M. Elkashlan, and N. Yang, "Cognitive

relay networks with multiple primary transceivers under spectrum sharing," *IEEE Signal Process. Lett.*, vol. 19, no. 11, pp. 741-744, Nov. 2012.

[62] W. Jaafar, W. Ajib, and D. Haccoun, "Incremental relaying transmissions with relay selection in cognitive radio networks," *Proc. IEEE GLOBECOM*, Anaheim, CA, USA, Dec. 2012, pp. 1230-1235.

[63] K. Tourki, K. A. Qaraqe, and M. -S. Alouini, "Outage analysis for underlay cognitive networks using incremental regenerative relaying," *IEEE Trans. Veh. Technol.*, vol. 62, no. 2, pp. 721-734, Feb. 2013.

[64] H. Huang, Z. Li, J. Si and R. Gao, "Outage analysis of underlay cognitive multiple relays networks with a direct link," *IEEE Commun. Lett.*, vol. 17, no. 8, pp. 1600-1603, Aug. 2013.

[65] P. Das and N. B. Mehta, "Revisiting incremental relaying and relay selection for underlay cognitive radio," *Proc. IEEE GLOBECOM*, San Diego, CA, USA, Dec. 2015, pp. 1-6.

[66] X. Guan, W. Yang, and Y. Cai, "Outage performance of statistical CSI assited cognitive relay with interference from primary user," *IEEE Commun. Lett.*, vol. 17, no. 7, pp. 1416-1419, July 2013.

[67] P. Das, N. B. Mehta, and G. Singh "Novel relay relection rules for average interference-constrained cognitive AF relay networks," *IEEE Trans. Wireless Commun.*, vol. 14, no. 8, pp. 4304-4315, Aug. 2015.

[68] G. Wang, Y. Zou, J. Lu, and C. Tellambura, "Cognitive transmission and performance analysis of amplify-and-forward two-way relay networks," *Proc. IEEE ICC*, Sydney, Australia, June 2014, pp. 5843-5848.

[69] P. Liu, S. Gazor, and I.-M. Kim, "Opportunistic relaying with time-division broadcast in bidirectional cooperative networks," *Proc. IEEE GLOBECOM*, Anaheim, CA, USA, Dec. 2012, pp. 4102-4107.

[70] T. T. Duy and H. Y. Kong, "Exact outage probability of cognitive two-way relaying scheme with opportunistic relay selection under interference constraint," *IET Commun.*, vol. 6, no. 16, pp. 2750-2759, Nov. 2012.

[71] X. Zhang, Z. Zhang, J. Xing, R. Yu, P. Zhang, and W. Wang, "Exact outage analysis in cognitive two-way relay networks with opportunistic relay selection under primary user's interference," *IEEE Trans. Veh. Technol.*, vol. 64, no. 6, pp. 2502-2511, June 2015.

[72] H. H. Hong, L. Xiao, Y. Yan, X. Xu, and J. Wang, "Outage performance for cognitive two-way relaying networks with underlay spectrum sharing," *Proc. IEEE VTC-Spring*, Seoul, Korea, May 2014, pp. 1-5.

[73] Q. Li, S. H. Ting, A. Pandharipande, and Y. Han, "Cognitive spectrum sharing with two-way relaying systems," *IEEE Trans. Veh. Technol.*, vol. 60, no. 3, pp. 1233-1240, Mar. 2011.

[74] A. Hyadi, E. M. Driouch, W. Ajib, and M.-S. Alouini, "Overlay cognitive radio systems with adaptive two-way relaying," *Proc. IEEE GLOBECOM*, Atlanta, GA, USA, Dec. 2013, pp. 937-942.

[75] P. K. Sharma and P. K. Upadhyay, "Cooperative spectrum sharing in two-way multi-user multi-relay networks," *IET Communications*, vol. 10, no. 1, pp. 111-121, Feb. 2016.

[76] M. Xia and S. Aissa, "Modeling and analysis of cooperative relaying in spectrum-sharing cellular systems," *IEEE Trans. Veh. Technol.*, vol. 65, no. 11, pp. 9112-9122, Nov. 2016.

[77] B. Zhong and Z. Zhang, "Opportunistic two-way full-duplex relay selection in underlay cognitive networks," *IEEE Systems Journal*, vol. 12, no. 1, pp. 725-734, Mar. 2018.

[78] H. Ding, J. Ge, D. B. da Costa, and Z. Jiang, "Two birds with one stone: Exploiting direct links for multiuser two-way relaying systems," *IEEE Trans. Wireless Commun.*, vol. 11, no. 1, pp. 54-59, Jan. 2012

[79] H. Tran, T. Q. Duong, H.-J. Zepernick, "Performance of a spectrum sharing system over Nakagami-m fading channels," *Proc. IEEE ICSPCS*, Gold Coast, Australia, Dec. 2010, pp. 1-6.

[80] F. Khan, K. Tourki, M.-S. Alouini, and K. Qaraqe, "Delay performance of a broadcast spectrum sharing network in Nakagami-m fading," *IEEE Trans. Veh. Technol.*, vol. 63, no. 3, pp. 1350-1364, Mar. 2014.

[81] I. Stanojev, O. Simeone, Y. B.-Ness, and C. You, "Performance of multi-relay collaborative hybrid-ARQ protocols over fading channels," *IEEE Commun. Lett.*, vol. 10, no. 7, pp. 522-524, Jul. 2006.

[82] N. B. Mehta, V. Sharma, and G. Bansal, "Performance analysis of a cooperative system with rateless codes and buffered relays," *IEEE Trans. Wireless Commun.*, vol. 10, no. 4, pp. 1069-1081, Apr. 2011.

[83] J. Lee, H. Wang, J. G. Andrews, and D. Hong, "Outage probability of cognitive relay networks with interference constraints," *IEEE Trans. Wireless Commun.*, vol. 10, no. 2, pp. 390-395, Feb. 2011.

[84] L. Luo, P. Zhang, G. Zhang, and J. Qin, "Outage performance for cognitive relay networks with underlay spectrum sharing," *IEEE Commun. Lett.*, vol. 15, no. 7, pp. 710-712, July 2011.

[85] V. N. Q. Bao, T. Q. Duong, D. B. da Costa, G. C. Alexandropoulos, and A. Nallanathan, "Cognitive amplify-and-forward relaying with best relay selection in non-identical Rayleigh fading," *IEEE Commun. Lett.*, vol. 17, no. 3, pp. 475-478, Mar. 2013.

[86] J. M. Moualeu, W. Hamouda, and F. Takawira, "Performance of AF relay selection with outdated channel estimates in spectrum-sharing systems," *IEEE Commun. Lett.*, vol. 20, no. 9, pp. 1844-1847, Sep. 2016.

[87] J. Hussein, S. Ikki, S. Boussakta, and C. Tsimenidis, "Performance analysis of opportunistic scheduling in dual-hop multiuser underlay cognitive network

in the presence of co-channel interference," *IEEE Trans. Veh. Technol.*, vol. 65, no. 10, pp. 8163-8176, Oct. 2016.

[88] E. Björnson, M. Matthaiou, and M. Debbah, "A new look on dual-hop relaying: Performance limits with hardware impairments," *IEEE Trans. Commun.*, vol. 61, no. 11, pp. 4512-4525, Nov. 2013.

[89] M. Matthaiou, A. Papadogiannis, E. Bjornson, and M. Debbah, "Two-way relaying under the presence of relay transceiver hardware impairments," *IEEE Commun. Lett.*, vol. 17, no. 6, pp. 1136-1139, June 2013.

[90] M. Mokhtar, A.-A. A. Boulogeorgos, G. K. Karagiannidis, and N. Al-Dhahir, "OFDM opportunistic relaying under joint transmit/receive I/Q imbalance," *IEEE Trans. Commun.*, vol. 62, no. 5, pp. 1458-1478, May 2014.

[91] J. Li, M. Matthaiou, and T. Svensson, "I/Q imbalance in two-way AF relaying," *IEEE Trans. Commun.*, vol. 62, no. 7, pp. 2271-2285, July 2014.

[92] A. Z.-Ghasabeh, A. Tarighat, and B. Daneshrad, "Cyclo-stationary sensing of OFDM waveforms in the presence of receiver RF impairments," in *Proc. IEEE Wireless Commun. Netw. Conf.*, Sydney, Australia, Apr. 2010, pp. 1-6.

[93] J. V.-Chenet, J. Renard, J.-M. Dricot, P. D. Doncker, and F. Horlin, "Sensitivity of spectrum sensing techniques to RF impairments," in *Proc. IEEE 71st Veh. Tech. Conf.*, Taipei, Taiwan, May 2010, pp. 1-5.

[94] O. Semiari, B. Maham, and C. Yuen, "Effect of I/Q imbalance on blind spectrum sensing for OFDMA overlay cognitive radio," in *Proc. IEEE Int. Conf. Commun. China*, Beijing, China, Aug. 2012, pp. 433-437.

[95] A. ElSamadouny, A. Gomaa, and N. Al-Dhahir, "Likelihood-based spectrum sensing of OFDM signals in the presence of Tx/Rx I/Q imbalance," *IEEE Global Commun. Conf.*, Anaheim, CA, USA, Dec. 2012, pp. 3616-3621.

[96] A. Gokceoglu, S. Dikmese, M. Valkama, and M. Renfors, "Energy detection under IQ imbalance with single- and multi-channel direct-conversion receiver:

Analysis and mitigation," *IEEE J. Sel. Areas Commun.*, vol. 32, no. 3, pp. 411-424, Mar. 2014.

[97] A.-A. A. Boulogeorgos, N. D. Chatzidiamantis, and G. K. Karagiannidis, "Energy detection spectrum sensing under RF imperfections," *IEEE Trans. Commun.*, vol. 64, no. 7, pp. 2754-2766, July 2016.

[98] A.-A. A. Boulogeorgos, H. A. B. Salameh, and G. K. Karagiannidis, "Spectrum sensing in full-duplex cognitive radio networks under hardware imperfections," *IEEE Trans. Veh. Technol.*, vol. 66, no. 3, pp. 2072-2084, Mar. 2017.

[99] G. Zheng, I. Krikidis, and B. Ottersten, "Full-duplex cooperative cognitive radio with transmit imperfections," *IEEE Trans. Wireless Commun.*, vol. 12, no. 5, pp. 2498-2511, May 2013.

[100] D. K. Nguyen and H. Ochi, "Transceiver impairments in DF/AF dual-hop cognitive relay networks: Outage performance and throughput analysis," in *Proc. IEEE 81st Veh. Tech. Conf.*, Glasgow, UK, May 2015, pp. 1-5.

[101] N. I. Miridakis, D. D. Vergados, and A. Michalas, "Cooperative relaying in underlay cognitive systems with TAS/MRC, spatial correlation and hardware impairments," in *Proc. IEEE 82nd Veh. Tech. Conf.*, Boston, MA, USA, Sep. 2015, pp. 1-5.

[102] P. T. D. Ngoc, T. T. Duy, V. N. Q. Bao, and K. H-Van, "Performance enhancement for underlay cognitive radio with partial relay selection methods under impact of hardware impairment," in *Proc. Int. Conf. on Advan. Technol. for Commun.*, Ho Chi Minh City, Vietnam, Oct. 2015, pp. 645-650.

[103] H. Huang, Z. Li, B. Ai, G. Wang, and M. S. Obaidat, "Impact of hardware impairment on spectrum underlay cognitive multiple relays network," in *Proc. IEEE Int. Conf. on Commun.*, Kuala Lumpur, Malaysia, May 2016, pp. 1-6.

[104] P. K. Sharma and P. K. Upadhyay, "Cognitive relaying with transceiver hardware impairments under interference constraints," *IEEE Commun. Lett.*, vol. 20, no. 4, pp. 820-823, Apr. 2016.

[105] H. V. Khuong, "Exact outage analysis of modified partial relay selection in cooperative cognitive networks under channel estimation errors," *IET Commun.*, vol. 10, no. 2, pp. 219-226, Feb. 2016.

[106] A. M. Salhab and S. A. Zummo, "Cognitive DF generalized order relay selection networks with imperfect channel estimation and interference from primary user," in *Proc. IEEE Global Commun. Conf.*, Austin, TX, USA, Dec. 2014, pp. 4137-4142.

[107] N. I. Miridakis, T. A. Tsiftsis, and C. Rowell, "Distributed spatial multiplexing systems with hardware impairments and imperfect channel estimation under rank-1 Rician fading channels," *IEEE Trans. Veh. Technol.*, vol. 66, no. 6, pp. 5122-5133, June 2017.

[108] A. K. Mishra, D. Mallick, and P. Singh, "Combined effect of RF impairment and CEE on the performance of dual-hop fixed-gain AF relaying," *IEEE Commun. Lett.*, vol. 20, no. 9, pp. 1725-1728, Sep. 2016.

[109] A. Bouhlel, S. G. Domouchtsidis, S. S. Ikki, and A. Sakly, "Performance of OFDM-IM under joint hardware impairments and channel estimation errors over correlated fading channels," *IEEE Access*, vol. 5, pp. 25342-25352, Dec. 2017.

[110] "8 Hints for making and interpreting EVM measurements," *Tech. Rep., Agilent Technologies*, 2005.

[111] S. Solanki, P. K. Sharma, and P. K. Upadhyay, "Adaptive link utilization in two-way spectrum sharing relay systems under average interference-constraints," *IEEE Systems Journal*, vol. 12, no. 4, pp. 3461-3472, Dec. 2018.

[112] X. Kang, Y.-C. Liang, and A. Nallanathan, "Optimal power allocation for fading channels in cognitive radio networks: Delay-limited capacity and outage capacity," in *Proc. IEEE 67th Veh. Tech. Conf.*, Singapore, Singapore, May 2008, pp. 1-5.

[113] A. Hyadi, M. Benjillali, M.-S. Alouini, and D. B. da Costa, "Performance analysis of underlay cognitive multihop regenerative relaying systems with multiple primary receivers," *IEEE Trans. Wireless Commun.*, vol. 12, no. 12, pp. 6418-6429, Dec. 2013.

[114] H. Huang, Z. Li, J. Si, and R. Gao, "Outage analysis of underlay cognitive multiple relays networks with a direct link," *IEEE Commun. Lett.*, vol. 17, no. 8, pp. 1600-1603, Aug. 2013.

[115] F. R. V. Guimarães, D. B. da Costa, T. A. Tsiftsis, C. C. Cavalcante, and G. K. Karagiannidis, "Multiuser and multirelay cognitive radio networks under spectrum-sharing constraints," *IEEE Trans. Veh. Technol.*, vol. 63, no. 1, pp. 433-439, Jan. 2014.

[116] S. Sagong, J. Lee, and D. Hong, "Capacity of reactive DF scheme in cognitive relay networks," *IEEE Trans. Wireless Commun.*, vol. 10, no. 10, pp. 3133-3138, Oct. 2011.

[117] T. T. Duy, T. Q. Duong, D. B. da Costa, V. N. Q. Bao, and M. Elkashlan, "Proactive relay selection with joint impact of hardware impairment and co-channel interference," *IEEE Trans. Commun.*, vol. 63, no. 5, pp. 1594-1606, May 2015.

[118] A. Papoulis and S. U. Pillai, *Probability, Random Variables, and Stochastic Processes*, Tata McGraw-Hill Education, 2002.

[119] A. Bletsas, H. Shin and M. Z. Win, "Cooperative communications with outage-optimal opportunistic relaying," *IEEE Trans. Wireless Commun.*, vol. 6, no. 9, pp. 3450-3460, Sep. 2007.

[120] E. Beres and R. Adve, "Selection cooperation in multi-source cooperative networks," *IEEE Trans. Wireless Commun.*, vol. 7, no. 1, pp. 118-127, Jan. 2008.

[121] Z. Wang and G. B. Giannakis, "A simple and general parameterization quantifying performance in fading channels," *IEEE Trans. Commun.*, vol. 51, no. 8, pp. 1389-1398, Aug. 2003.

[122] Y. Huang, F. A.-Qahtani, Q. Wu, C. Zhong, J. Wang, and H. Alnuweiri, "Outage analysis of spectrum sharing relay systems with multiple secondary destinations under primary user's interference," *IEEE Trans. Veh. Technol.*, vol. 63, no. 7, pp. 3456-3463, Sep. 2014.

[123] N. I. Miridakis and T. A. Tsiftsis, "On the joint impact of hardware impairments and imperfect CSI on successive decoding," *IEEE Trans. Veh. Technol.*, vol. 66, no. 6, pp. 4810-4822, June 2017.

[124] A. K. Papazafeiropoulos, S. K. Sharma, T. Ratnarajah, and S. Chatzinotas, "Impact of residual additive transceiver hardware impairments on Rayleigh-product MIMO channels with linear receivers: Exact and asymptotic analyses," *IEEE Trans. Commun.*, vol. 66, no. 1, pp. 105-118, Jan. 2018.

[125] J. Zhang, Y. Wei, E. Björnson, Y. Han, and X. Li, "Spectral and energy efficiency of cell-free massive MIMO systems with hardware impairments," in *Proc. Wireless Commun. Signal Process.*, Nanjing, China, Dec. 2017, pp. 1-6.

[126] K. Ho-Van, "Outage analysis of opportunistic relay selection in underlay cooperative cognitive networks under general operation conditions," *IEEE Trans. Veh. Technol.*, vol. 65, no. 10, pp. 8145-8154, Oct. 2016.

[127] S. Hatamnia, S. Vahidian, S. Aissa, B. Champagne, and M. A. Attari, "Network-coded two-way relaying in spectrum sharing systems with quality-of-service requirements," *IEEE Trans. Veh. Technol.*, vol. 66, no. 2, pp. 1299-1312, Feb. 2017.

[128] J. A. Hussein, S. Boussakta, and S. S. Ikki, "Performance study of a UCRN over Nakagami-m fading channels in the presence of CCI," *IEEE Trans. Cogn. Commun. Netw.*, vol. 3, no. 4, pp. 752-765, Dec. 2017.

[129] X. Zhou, R. Zhang, and C. K. Ho, "Wireless information and power transfer: Architecture design and rate-energy tradeoff," *IEEE Trans. Commun.*, vol. 61, no. 11, pp. 4754-4767, Nov. 2013.

[130] A. A. Nasir, X. Zhou, S. Durrani, and R. A. Kennedy, "Wireless-powered relays in cooperative communications: Time-switching relaying protocols and throughput analysis," *IEEE Trans. Commun.*, vol. 63, no. 5, pp. 1607-1622, May 2015.

[131] U. Singh, S. Solanki, D. S. Gurjar, P. K. Upadhyay, and D. B. da Costa, "Wireless power transfer in two-way AF relaying with maximal-ratio combining under Nakagami-m fading," in *Proc. Inter. Wireless Commun. & Mob. Comp. Conf. (IWCMC)*, Limassol, Cyprus, Jun. 2018.

[132] P. K. Sharma and P. K. Upadhyay, "Performance analysis of cooperative spectrum sharing with multiuser two-way relaying over fading channels," *IEEE Trans. Veh. Technol.*, vol. 66, no. 2, pp. 1324-1333, Feb. 2017.

[133] S. Lee and R. Zhang, "Cognitive wireless powered network: Spectrum sharing models and throughput maximization," *IEEE Trans. Cogn. Commun. Netw.*, vol. 1, no. 3, pp. 335-346, Sep. 2015.

[134] E. Boshkovska, D. W. K. Ng, N. Zlatanov, and R. Schober, "Practical non-linear energy harvesting model and resource allocation for SWIPT systems," *IEEE Commun. Lett.*, vol. 19, no. 12, pp. 2082-2085, Dec. 2015.

[135] Y. Dong, M. J. Hossain, and J. Cheng, "Performance of wireless powered amplify and forward relaying over Nakagami-m fading channels with nonlinear energy harvester," *IEEE Commun. Lett.*, vol. 20, no. 4, pp. 672-675, Apr. 2016.

[136] J. Zhang and B. Pan, "Outage analysis of wireless-powered relaying MIMO systems with non-linear energy harvesters and imperfect CSI," *IEEE Access*, vol. 4, pp. 7046-7053, Oct. 2016.

[137] Y. Huang, T. Q. Duong, J. Wang, and P. Zhang, "Performance of multi-antenna wireless-powered communications with nonlinear energy harvester," in *Proc. IEEE Veh. Technol. Conf. (VTC)*, Toronto, ON, Canada, Sep. 2017.

[138] S. Pejoski, Z. H.-Velkov, and R. Schober, "Optimal power and time allocation for WPCNs with piece-wise linear EH model," *IEEE Wireless Commun. Lett.*, vol. 7, no. 3, pp. 364-367, Jun. 2018.

[139] X. Lei, L. Fan, D. S. Michalopoulos, P. Fan, and R. Q. Hu, "Outage probability of TDBC protocol in multiuser two-way relay systems with Nakagami-m fading," *IEEE Commun. Lett.*, vol. 17, no. 3, pp. 487-490, Mar. 2013.

[140] V. Singh, S. Solanki, and P. K. Upadhyay, "Cognitive relaying cooperation in satellite-terrestrial systems with multiuser diversity," *IEEE Access*, vol. 6, pp. 65539-65547, Oct. 2018.

[141] A. Bletsas, A. Khisti, D. P. Reed, and A. Lippman, "A simple cooperative diversity method based on the path selection," *IEEE J. Sel. Areas Commun.*, vol. 24, no. 3, pp. 659-672, Mar. 2006.

[142] H. Ding, J. Ge, D. B. da Costa, and Z. Jiang, "A new efficient low-complexity scheme for multi-source multi-relay cooperative networks," *IEEE Trans. Veh. Technol.*, vol. 60, no. 2, pp. 716-722, Feb. 2011.

[143] N. T. Do, D. B. da Costa, T. Q. Duong, V. N. Q. Bao, and B. An, "Exploiting direct links in multiuser multirelay SWIPT cooperative networks with opportunistic scheduling," *IEEE Trans. Wireless Commun.*, vol. 16, no. 8, pp. 5410-5427, Aug. 2017.

List of Publications

A. Publications from PhD Thesis Work

A1. In Refereed Journals

1. **S. Solanki**, P. K. Upadhyay, D. B. da Costa, H. Ding, and J. M. Moualeu, "Performance analysis of non-linear energy harvesting-based multiuser overlay spectrum sharing networks," ***IEEE Transactions on Wireless Communications***, under review.

2. **S. Solanki**, P. K. Sharma, and P. K. Upadhyay, "Adaptive link utilization in two-way spectrum sharing relay systems under average interference-constraints," ***IEEE Systems Journal***, vol. 12, no. 4, pp. 3461-3472, Dec. 2018.

3. **S. Solanki**, P. K. Upadhyay, D. B. da Costa, P. S. Bithas, A. G. Kanatas, and U. S. Dias, "Joint impact of RF hardware impairments and channel estimation errors in spectrum sharing multiple-relay networks," ***IEEE Transactions on Communications***, vol. 66, no. 9, pp. 3809-3824, Sep. 2018.

4. **S. Solanki**, P. K. Upadhyay, D. B. da Costa, P. S. Bithas, and A. G. Kanatas, "Performance analysis of cognitive relay networks with RF hardware impairments and CEEs in the presence of primary users' interference," ***IEEE Transactions on Cognitive Communications and Networking***, vol. 4, no. 2, pp. 406-421, June 2018.

5. **S. Solanki** and P. K. Upadhyay, "Performance analysis of cognitive relay sharing systems with bidirectional primary transmissions under Nakagami-m fading," ***IET Communications***, vol. 11, no. 8, pp. 1199-1206, June 2017.

A2. In Refereed Conferences

1. **S. Solanki**, P. K. Upadhyay, D. B. da Costa, H. Ding, and J. M. Moualeu, "Non-linear energy harvesting based cooperative spectrum sharing networks," ***International Symposium on Wireless Communication Systems (ISWCS)***, Oulu, Finland, Aug. 2019.

2. **S. Solanki**, P. K. Sharma, P. K. Upadhyay, D. B. da Costa, P. S. Bithas, and A. G. Kanatas, "Cognitive multi-relay networks with RF hardware impairments and channel estimation errors," in *Proc.* ***IEEE Global Communications Conference (GLOBECOM)***, Singapore, Dec. 2017.

3. **S. Solanki**, P. K. Sharma, and P. K. Upadhyay, "Cognitive relay sharing for two-way primary transmissions under Nakagami-m fading channels," in *Proc.* ***International Conference on Signal Processing and Communications (SPCOM)***, Indian Institute of Science (IISc) Bangalore, India, June 2016.

4. **S. Solanki**, P. K. Sharma, and P. K. Upadhyay, "Average interference-constrained cognitive two-way relaying with efficient link utilization," in *Proc.* ***IEEE International Conference on Communications (ICC)***, Kuala Lumpur, Malaysia, May 2016.

B. Other Publications During PhD

B1. In Refereed Journals

1. **S. Solanki**, V. Singh, and P. K. Upadhyay, "RF energy harvesting in hybrid two-way relaying systems with hardware impairments," ***IEEE Transactions on Vehicular technology***, under review.

2. V. Singh, **S. Solanki**, and P. K. Upadhyay, "Cognitive relaying cooperation in satellite-terrestrial systems with multiuser diversity," ***IEEE Access***, vol. 6, pp. 65539-65547, Oct. 2018.

B2. In Refereed Conferences

1. U. Singh, **S. Solanki**, D. S. Gurjar, P. K. Upadhyay, and D. B. da Costa, "Wireless power transfer in two-way AF relaying with maximal-ratio combining under Nakagami-m fading," in *Proc.* ***14th International Wireless Communications and Mobile Computing Conference (IWCMC)***, Limassol, Cyprus, June 2018.

2. **S. Solanki** and P. K. Upadhyay, "Secure underlay cognitive relay networks in presence of primary user's interference," in *Proc.* ***IEEE Vehicular Technology Conference (VTC)***, Sydney, Australia, June 2017.